



POLITECNICO DI MILANO

SCHOOL OF INDUSTRIAL AND INFORMATION ENGINEERING
Master of Science in Energy Engineering

Master Thesis

**Modeling system integration of variable renewable
energies for long-term climate objectives:
the role of electric grid and storage**

Thesis supervisor:

Prof. Massimo Tavoni

Co-supervisors:

Ph.D. Samuel Carrara

Prof. Evasio Lavagno

Authors::

Marco Marni

ID Num. 849985

Simone Prato

ID Num. 851306

Academic Year 2016-2017

Joint Acknowledgements

First, we would like to thank the two institutions that allowed the realization of this thesis work: Politecnico di Milano and Fondazione Eni Enrico Mattei. In particular, we are grateful to Professor Massimo Tavoni and Ph.D. Samuel Carrara for the opportunity they have offered us and the support received.

Thanks to Adriano and Marco for the help and the encouragements, and also to Laurent, Johannes, Soheil, Valentina and the other FEEM researchers that were always glad to solve our doubts and helpful with their questions and insights.

We are grateful to the people from our FEEM office: Cate, Susi, Teo e Fili, that made the days spent there nicer and fun.

Thanks to Alta Scuola Politecnica and in particular to Professor Lavagno for adding value to our work.

Finally, we are grateful to Robert Pietzcker from PIK and Nils Johnson from IIASA for their availability and their answers to our questions, and to JP and Anne-Perine from UC Berkeley for the help in retrieving SWITCH data and interpreting them correctly.

Acknowledgements (Marco Marni)

*“There is a driving force more powerful than steam,
electricity and nuclear power: the will.”*

Albert Einstein

A truly enriching journey has come to an end. All I learnt and experienced would not have been the same without all the fabulous people that I am lucky to have in my life. So, I would like to devote these lines to thank them from the bottom of my heart.

Firstly, I would like to thank my mother, my father and my sister Martina for the incredible love and support that give me every day. You are the pillar of my life without whom nothing I achieved would have been possible. Mamma grazie per il tuo amore e la tua gentilezza, Papà grazie perchè la tua umiltà e i tuoi valori sono ciò a cui mi ispiro ogni giorno, Marti grazie perchè sei un dono che ho ricevuto dalla vita.

I would also like to thank Francesca, with whom I had the privilege of spending the most of my university years and who has always been my inner companion of adventures and happiness. These years have been much sweeter with you by my side. Thank you for your unfailing support and love.

A special mention goes to my long-time friends of the Real Carmine: Baraz, Boni, Bose, Chino, Dane, Gui, Jack, Into, Maste, Miro, Prevo, Riz, Sprez. Your true friendship has been an anchor in the difficult moments. Being able to count on you, no matter what, has been a precious source of relief.

Then, I would like to thank the Tori: Carlo, Ciccio, Cla, Cox, Cresi, Dipo, Greg, Lofi, Mauro, Mba, Pippo, an inexhaustible source of laughs with whom I shared some of the best experiences of these last years.

Moreover, I am extremely grateful for having the possibility to share the most of my university path and the master thesis journey with a guy that I profoundly admire. Working with Simone made everything simpler and every day spent with him was a day full of laughs and jokes.

I also would like to thank Berti, a friend who has left me but whose presence I feel every day in my life.

There are many other people I would like to thank, a list follows below without a specific order, just as the names have come to my mind. For sure I am going to forget someone and I apologize for that. I am grateful to my elementary schools teacher Maestra Mariagrazia, who taught me the values of generosity and hard-work; my roommate Teone for having my back in the difficult moments and celebrating with me all my achievements; Bea, a long time friend who holds a place in my heart; Marco a long-lasting friend who truly knows me; my PNC friends Albe, Frezzi, Gabri, Nico for some of the craziest moments of my life, and all my other high school mates for being a true family. Sasaki, Benfo, Carli, Benni, Cri, Angelino, Asa, Lollone, Balla, Furlo, Ema, Greta, Ore, Flavio, Sofi, Rello Dario, Ori, Elia, Raffa, Mitra and all the other friends of Collegio di Milano who have been my second family in the last five years; le mie amiche di fatiche Ceci and Chiara and my mates Alfred, Andrea, Luca, Butta and Fuma with whom I shared the joy and pain that Politecnico gives; all my Erasmus adventure companions, in particular Ciccio and Fede for surviving with me in Farsta; Il Pres, Fra F., Fra S., Dile, Jack and all the other Alta Scuola Politecnica friends for all the great moments together and finally my high school teachers for caring for me and my education and allowing me to be prepared to face university.

Acknowledgements (Simone Prato)

πολλὰ τὰ δεινὰ κοῦδὲν ἀν-
θρώπου δεινότερον πέλει

Sofocle, Antigone; I Stasimo, vv.332-333

Ringraziare tutti coloro che hanno contribuito al raggiungimento di questo traguardo, e a ciò che simbolicamente rappresenta, è un'impresa tanto doverosa quanto difficilmente realizzabile. Mi limiterò a citare le persone verso le quali, al momento della stesura di queste righe, più sento di essere in debito, tentando di ripercorrere in ordine cronologico alcuni degli incontri che hanno segnato la mia vita.

Il primo ringraziamento va ai miei genitori, Giuliana e Aldo, che mi hanno amato, incoraggiato e supportato da quando ho mosso i primi passi a quando ho deciso di lasciare casa, per iniziare questa avventura a Milano, fino ad oggi. Con loro ringrazio anche zii e cugini, che fanno il tifo per me e che non vado a trovare mai abbastanza spesso. Farò tutto il possibile per rendervi orgogliosi di me, sempre.

Poi vengono i miei amici di infanzia Chri, Dani, Enri e Gian, a fianco ai quali sono cresciuto: compagni di mille avventure sotto il sole di Genova Borzoli, l'unico luogo che chiamerò sempre *casa*. La cosa più bella, ogni volta che li rivedo, è rendermi conto che dai vecchi tempi ad oggi, in fondo, tra noi non è cambiato nulla.

Durante gli anni della scuola media e del liceo ho avuto la fortuna di incontrare dei veri e propri maestri, prima che dei professori: Augias, Fabiano e Sanchioni. Mi hanno aiutato, ognuno a modo suo, a crescere e maturare, coltivando le mie passioni.

Grazie ai ragazzi del Liceo Classico Mazzini, con cui ho condiviso i (tanti) bei momenti e le difficoltà di quegli anni. In particolare ringrazio Clelia, Marco, Camilla, Federica e Martina, perché la nostra amicizia è andata ben oltre i banchi di scuola e non c'è stata distanza in grado di separarci davvero. Grazie a Ugo e Giulia.

Gli anni al Politecnico non sarebbero stati gli stessi senza gli *Amici di fatiche* e senza Pase ed Elena, amici e compagni di studio, di vacanze e di risate, capaci di iniziarmi, rispettivamente, alla cultura lombarda e napoletana.

Mi sento profondamente in debito con i ragazzi del Collegio di Milano, che sono stati la mia seconda famiglia negli ultimi quattro anni: in particolare con Andrea, Lollo, Sofia, Friso, Flavio DP, Fra D'Angelo, ASA, Dario, Oriella, Ema, Furlo, Teone, Benfo, Greta, Mari, Lucia, Albi, Simo A., Angelino, Benni, Saskia, Rubbo, Agnese, i Bros e il Running Club. Non posso non citare il gruppo dei Tori: Carlo, Claudio, Ciccio, Dipo, Cox, Pippo, Greg, Lofi, Mauro, Cresi e Mba. Modelli sotto molti punti di vista.

Grazie ad Alta Scuola Politecnica e in particolare ai ragazzi del gruppo *118*, Dile, Pietro, Alfre, Fra Fontana e Sara. Grazie a tutto il gruppo di Göteborg, che ha reso quell'esperienza indimenticabile, e in particolare ai miei Coinqui. Grazie agli straordinari ragazzi di Free2Change, con i quali porto avanti una missione che mi rende orgoglioso e dà molto più valore a ciò che ho studiato.

Ringrazio Rossella, che è stata la mia fonte di ispirazione negli ultimi due anni.

Per ultimo, ma non certo per importanza, ringrazio Marco, con cui ho condiviso molte delle esperienze degli ultimi anni. Molto più di un collegiale, di un collega e di un compagno di tesi: un amico vero di cui, anche adesso che una nuova pagina delle nostre vite sta per cominciare, non riuscirò a liberarmi facilmente. Per fortuna.

Abstract

Among the efforts towards climate change mitigation, the decarbonization of the power sector is a necessary step in order to meet the Paris Agreement target of keeping the temperature increase at the end of the current century well below 2°C with respect to pre-industrial levels. In this context, it is a shared opinion that Variable Renewable Energy (VRE) sources, mainly wind turbines and solar photovoltaics (PV), will play a key role. On the other hand, the variable and uncertain nature of VREs supply, especially at high shares in the electricity mix, introduces multiple challenges for modern energy systems. Working on the World Induced Technical Change Hybrid (WITCH) energy-economy-climate model, we aimed at evaluating the long-term contribution of VREs in climate constrained scenarios, by introducing in the model a more accurate representation of both electric grid and electricity storage technologies. The contribution of our work is as follows:

(1) among the main electricity storage technologies, identify which ones are more suitable for being included in long-term models; (2) investigate the effect of different climate policy scenarios on the diffusion of VRE sources, grid and storage technologies; (3) clarify how grid and storage technologies affect the electricity generation mix and their impact on economic growth and costs, in the context of VRE system integration; (4) individuate the cost and performance parameters that have the strongest impact on VRE, grid and storage diffusion; (5) understand how the new, more accurate representation of grid and storage affects the results, if compared to previous versions of the model. We address these research questions by providing an extensive literature review, designing analytic formulations of the studied dynamics and implementing them in the WITCH Integrated Assessment Model (IAM), running a set of policy scenarios and verifying the robustness of our results through a set of sensitivity analyses and comparisons with other models. The main conclusions can be summarized as follows. Imposing a global carbon tax in order to achieve the 2°C target, VREs become the most widespread technology options, accounting for 51% of global net electricity generation in 2100 (against 24% in Business As Usual case). This deployment requires higher investments in distribution, smartening and pooling of the grid. Concerning storage capacity, the introduction of a carbon tax benefits Compressed Air Storage and Lithium-ion batteries, that leverage on cost reductions from learning effect to become the dominant technologies. Conversely, results indicate that without the installation of storage capacity, it is not possible to reach high shares of VRE generation. Concerning grid parameters, grid cost and grid requirement per unit of generation capacity installed show a great influence on average grid investments. However, they do not show a significant impact on the installed generation capacity. As regards storage parameters, decreasing the capability of storage to provide flexibility and firm capacity dramatically affects both VRE share and storage investments. Moreover, the costs of storage technologies, both the initial and the minimum one they can achieve, are other two important drivers of VRE share growth and overall storage investments.

Keywords: Variable Renewable Energy Integration; Storage; Electric Grid; Climate Change Mitigation; Integrated Assessment Models.

Sommario

Nell'ambito degli sforzi globali per mitigare il cambiamento climatico, la decarbonizzazione del settore elettrico è un passaggio necessario per rispettare l'obiettivo, concordato nell'Accordo di Parigi, di mantenere l'aumento della temperatura al di sotto dei 2°C rispetto ai livelli pre-industriali. In questo contesto, è opinione condivisa che le Fonti Rinnovabili Non Programmabili (FRNP), in particolar modo fotovoltaico ed eolico, svolgeranno un ruolo chiave. D'altro canto, la variabilità e l'incertezza associate alla produzione da FRNP, specialmente ad alte quote nel mix di generazione, comportano molteplici complicazioni per i moderni sistemi energetici. Utilizzando il modello di valutazione integrata energia-economia-clima WITCH (World Induced Technical Change Hybrid), abbiamo introdotto una più accurata rappresentazione della rete elettrica, delle tecnologie di accumulo di energia elettrica e del loro ruolo nell'integrazione delle FRNP. Il contributo del nostro lavoro è il seguente: (1) fra le principali tecnologie di accumulo, identificare quali sono le più adatte ad essere modellate in WITCH; (2) investigare l'effetto di differenti scenari di politiche climatiche sull'installazione di FRNP, rete elettrica e tecnologie di accumulo; (3) analizzare l'impatto della rete e dell'accumulo di energia elettrica sul mix di generazione, e di conseguenza sulla crescita economica e sui costi associati all'integrazione delle FRNP; (4) individuare i parametri di costo e performance più rilevanti in termini di impatto sull'installazione di FRNP, rete e accumulo elettrico; (5) valutare come la nuova, più accurata rappresentazione di rete e accumulo elettrico condiziona i risultati, se paragonati alle precedenti versioni del modello WITCH. Affrontiamo queste domande di ricerca sintetizzando i risultati di un'approfondita ricerca bibliografica, sviluppando formulazioni analitiche dei fenomeni studiati e implementandole nel modello WITCH, esplorando diversi scenari di politiche climatiche e verificando la solidità dei nostri risultati tramite analisi di sensitività e paragoni con altri modelli. Le conclusioni principali possono essere così sintetizzate. Imponendo una carbon tax globale con l'obiettivo di rispettare l'aumento massimo di temperatura di 2°C, le FRNP diventano le tecnologie più utilizzate, rappresentando il 51% della produzione globale netta di energia elettrica nel 2100 (24% nello scenario Business As Usual). Riguardo l'accumulo elettrico, l'introduzione di una carbon tax favorisce l'installazione di accumulo ad aria compressa e di batterie agli ioni di litio, che, grazie alla riduzione nel loro costo di investimento per apprendimento, diventano le tecnologie dominanti. D'altra parte, i risultati del modello WITCH indicano che, senza l'installazione di capacità di accumulo elettrico, non sarà possibile raggiungere alte quote di generazione da FRNP. Riguardo la rete elettrica, il suo costo di installazione e il requisito di rete per unità di capacità di generazione installata presentano un impatto notevole sugli investimenti medi in rete, ma non sulla generazione elettrica. A proposito dei parametri caratterizzanti le tecnologie di accumulo, diminuire la loro capacità di fornire flessibilità e capacità continua impatta drasticamente sugli investimenti in FRNP e in tecnologie di accumulo. Inoltre, anche i costi di investimento delle tecnologie di accumulo, sia quello iniziale che quello minimo raggiungibile, mostrano di essere fattori chiave nel determinare gli investimenti totali in queste tecnologie.

Parole chiave: Fonti Rinnovabili Non Programmabili; Accumulo di Energia Elettrica; Rete Elettrica; Mitigazione del Cambiamento Climatico; Modelli di Valutazione Integrata

Extended Summary

Scope of the work

Climate change is acknowledged as one of the major challenges mankind will have to face in the 21st century, due to its potential effects on the delicate equilibrium of our planet. With the Paris Agreement, reached in 2015 during the Conference of Parties 21 (COP21), 195 countries have formally declared their willingness to pursue the ambitious target of keeping the temperature increase at the end of the current century well below 2°C with respect to pre-industrial levels, staying as close as possible to 1.5°C to limit climate impacts. This target, however, is everything but easy to be reached, not only due to the amount of international coordination it requires, but also because it entails both technological and economical fundamental transformations. As a matter of fact, state-of-the-art technical energy solutions with low or zero associated emissions require, overall, a higher expenditure with respect to the current energy system configuration, therefore mitigation comes at a higher present cost, even if it will reduce future costs of climate change.

The electric power sector accounts for the relative majority of global GHG emissions, but also presents a high potential for a deep decarbonization. Thanks to the diffusion of low carbon options such as renewable energy technologies, mainly wind turbines and solar photovoltaics (PV), the power sector is expected not only to reduce its carbon intensity, but also to play an important role in the decarbonization of other carbon-intensive sectors such as transportation and heating. Even though solar cells and wind turbines have witnessed a steep capital cost decrease over the last decades, there are some techno-economical barriers that limit their diffusion: besides capital and operational expenditures, these technologies entail further expenses so as to integrate them into the energy system, defined as “system integration costs”.

This is due to the inherent variability, uncertainty and site-specificity that characterize their supply and defines them as Variable Renewable Energy (VRE) sources. The variable and uncertain nature of renewable supply, especially at high shares in the electricity mix, introduces multiple challenges for modern energy systems, such as the capability to deal with steep and possibly unexpected ramp ups and downs of the residual load and the necessity to install expensive and underutilized flexible power plants to cover peak demand. Moreover, the number of transmission and distribution grid bottlenecks and congestions is likely to increase. Finally, decentralized VRE generation technologies (e.g. off-grid solar) are spreading, especially in developing countries, where the grid infrastructure is often lacking, unreliable or too expensive. This may put the existing infrastructure under considerable pressure and hinder further VRE expansion

for penetrations higher than 15-20%. These challenges can be overcome with several measures aimed at increasing grid flexibility. Smart grids will likely have a central role in dampening the challenges that VRE diffusion entails, allowing a better management and control of generation and demand side, ensuring power quality and grid stability. Also pooling VRE production over large geographical areas can help mitigate their inherent variability, related to weather conditions. This requires further investments for improving grid interconnections, at national and international level.

Electric storage is another valuable option to address the challenges introduced by high VRE shares. Due to its capability of accumulating energy, keeping it inside for a variable amount of time and then releasing it when needed, electricity storage can help VRE integration buffering and optimizing the output from VREs, mitigating short-term and seasonal output changes and filling both temporal and geographic gaps between supply and demand, to increase quality and value of the resource. Nevertheless, there is a number of caveats to consider when discussing the future diffusion of electricity storage technologies, whose uncertainty depends on both techno-economical and regulatory aspects.

Energy-economy-climate models have become standard tools for *ex ante* evaluation of low carbon policies, generating a wide array of multi decadal scenarios. These models forecast significant expansion of VRE technologies, but do not always feature options to manage the integration of the electrical system, at least if compared to short term dispatching models. Working on the World Induced Technical Change Hybrid (WITCH) energy-economy-climate model, we aimed at introducing a more accurate representation of electric grid, electricity storage technologies and their role in VRE integration in energy systems. This improves the accuracy and reliability of the scenarios produced, whose final objective is informing policy makers about economically-meaningful solutions to mitigate climate change.

The contribution of our work is the following: (1) among the main electricity storage technologies, identify which ones are more suitable for being included in long-term models; (2) investigate the effect of different climate policy scenarios on the diffusion of VRE sources, grid and storage technologies; (3) clarify how grid and storage technologies affect the electricity generation mix and their impact on economic growth and policy costs, in the context of VRE system integration; (4) individuate the cost and performance parameters that have the strongest impact on VRE, grid and storage diffusion; (5) understand how the new, more accurate representation of grid and storage affects the results if compared to previous versions of the model.

We believe that this thesis contributes to the climate change mitigation literature in two different yet intertwined ways. The first contribution regards the energy modelling for climate change, in particular the long term models. The improvements we introduce in WITCH make it, to our knowledge, the only Integrated Assessment Model among those of the ADVANCE modeling framework, and probably also worldwide, to introduce technological differentiation for both grid and storage technologies and endogenous global investments in short-term and seasonal storage that are driven by VRE-share dependent requirements for firm capacity and flexibility. This is expected to provide a more realistic representation of the role played by electric grid and storage in VRE system integration. Second, from the policy-making perspective, the technological differentiation we introduced, the results obtained running the model with different

policy scenarios and the sensitivity analyses on key cost and performance parameters represent, in our view, a good source of information to design climate policies aimed at increasing VREs penetration while minimizing the associated integration cost.

Structure

The sequence of the thesis is organized as follows. Chapter 1 introduces the context of climate change, the role of VRE, electric grid and storage. It is concluded by the definition of the main research questions and the work methodology. In Chapter 2 we introduce WITCH and we describe how the VRE system integration problem is tackled in other Integrated Assessment Models. Chapter 3 is intended to provide a detailed technical state of the art review of the main electric grid and electric energy storage technologies, with a particular focus on those implemented within the model. Technical information is instrumental in explaining and justifying our modeling choices in terms of selected technologies and their performance and cost parameters, which are therefore described in this chapter. Chapter 4 starts presenting the VRE system integration features that were already present in the WITCH model at the beginning of our work. After that, we introduce our new interpretation of an already existing part of the model, related to the VRE system integration. Then, the largest portion of the Chapter is devoted to the equations and modeling assumptions behind the new formulation of storage and grid we implemented in the model. Chapter 5 is dedicated to the results, with a particular attention towards their consistence through sensitivity analyses and comparison with results from other models. Finally, Chapter 6 summarizes the main conclusions and major findings of our work, including suggestions for some future developments.

Methodology

The tool we used in our research is the World Induced Technical Change Hybrid (WITCH) model, which is a dynamic optimization Integrated Assessment Model (IAM) designed to investigate climate change mitigation and adaptation policies and developed by Fondazione Eni Enrico Mattei (FEEM) and Centro Euro-Mediterraneo sui Cambiamenti Climatici (CMCC). IAMs power lies in their ability to schematize complex dynamics, such as the relationship between climate, energy and economy, allowing to derive a simple interpretation of multiple interdependent phenomena. WITCH, in particular, is a regionally disaggregated hybrid global model with top-down, simplified representation of the global economy and a bottom-up, detailed energy input component. The energy sector is particularly developed and hard-linked with economy, so energy investments and resources are chosen optimally considering trends of macroeconomic variables and policy-induced economical stimuli.

One of the major challenges encountered during our work concerned the lack of data in literature about key aspects of our formulation. In particular, we found considerable difficulties in assessing the projected future cost decrease of storage technologies and their overall potential in the different regions of the world. As regards the electric grid, a scarcity of data about overall installed transmission and distribution capacity and its

future projections was encountered. During our research, we retrieved the most recent data, focusing on the latest technical publications, and when data were missing we made our own assumptions, always verifying their technical consistence and coherence. Another difficult task, frequent in Integrated Assessment modelling, consisted in determining an acceptable trade-off between technical details and simplified representations fitting to the aggregated structure of the model.

The whole research work we conducted can be structured as follows:

1. Literature review: gathering and organization of information and data.
2. Design of model equations: raw data and concepts from literature are translated into a mathematical structure. The modeling choices about the characterizing costs and performance parameters have been performed.
3. Implementation in numerical form of the equations and translation in General Algebraic Modeling System (GAMS) language, that is WITCH's language. This phase required particular attention as our final implementation of the electric storage and grid sections, after the supervision of other researchers, are going to be used in the official version of the WITCH model.
4. Robustness check of the results: sensitivity analysis in two stages, first with a detailed analysis on all the possible variations of the key parameters values, then through a comparison with the results of models representing electric storage or grid in a more detailed way.
5. Analysis and discussion of the results.

In order to answer to the initial research questions, we introduced the following new features in the WITCH model:

- As regards the electric grid, we introduced the differentiation between transmission and distribution lines, distinguishing them in terms of costs, grid requirement per unit of installed power plant capacity and electricity losses, with regional differentiation of these parameters.
- We distinguished between generation technologies requiring both transmission and distribution capacity, and the ones requiring just one of the two types of line.
- We introduced the possibility, for the model, to invest in “grid smartening” options and international grid interconnections to pool VRE variability over large areas and minimize the negative effects of increasing VRE shares on transmission and distribution lines. These investments, proportional to regional VRE share and grid investments, reduce the need for flexibility of wind and solar technologies, especially at high shares.
- Concerning storage, two main electricity storage types are modeled in our work: short-term storage, aimed at dealing with the VRE supply-demand mismatch on a hourly-to-daily scale, and seasonal storage, that leverages the mismatch between yearly peaks in VRE supply and in electricity demand to store energy for long time periods (months) and re-inject it into the grid when needed.
- Both the storage types are characterized in terms of efficiency, power and energy capacity, energy-to-power ratio, full production hours and capability to provide firm capacity and flexibility to the power system. Where reasonable, we also introduced the opportunity for cost reduction through learning effect and different cost options to represent the uncertainty about future commercial development of storage technologies.

- As regards the energy input to storage, short-term storage technologies can store both energy coming from the short-term curtailment of excess VRE production and a fraction of non-curtailed VRE generation, while seasonal storage can store only electricity from seasonal VRE curtailment.

We are aware of the challenges introduced by the modeling of grid and storage investment choices in very aggregated IAMs, as these decisions normally require a detailed representation of local and short-term dynamics. For this reason, as further development of our work, we compared the results obtained from WITCH with other models, belonging to two categories. First models that share similar scope and structure with WITCH, to verify how our model behaves within its own framework, and then more accurate, temporally refined and geographically restricted models, as a form of validation of our results.

Results and conclusions

The three short-term storage technologies modeled are Pumped Hydro Energy Storage (PHES), Adiabatic Compressed Air Storage (A-CAES) and Lithium-ion batteries. They have been chosen based on these criteria: compatibility with the level of temporal detail captured by WITCH, technological and commercial maturity of the technologies, potential for future development, ability to complement each other in terms of performance and technology type. Moreover, the modeling of Li-ion batteries is very flexible and can be potentially adapted to represent also other battery technologies. As regards seasonal storage, the only technological solution modelled is the conversion of seasonal curtailment into hydrogen via alkaline electrolyser and its subsequent re-conversion into electricity via Polymeric Electrolyte Membrane Fuel Cells (PEMFCs). The reasons for this choice are analogous to those presented for short-term storage.

Raising the value of a global carbon tax to achieve increasingly ambitious temperature reduction targets has a positive effect both on the deployment of VRE technologies and of electricity storage technologies if compared to the Business As Usual (BAU) scenario, where no price on carbon emissions is set. As a matter of fact, while VRE technologies represent in 2100 just 24% of global net generation in the BAU scenario, if the tax is raised to achieve the 2°C target indicated by the Paris Agreement (CTAX2DEG), VREs become the most widespread technology options, accounting for 51% of global net electricity generation.

Yearly grid investments increase in time in all the scenarios from 2015 to 2100 and grow with increasing value of carbon tax: investments in transmission grid decrease from BAU to CTAX and CTAX2DEG, while investments in distribution, smartening and pooling of the grid behave the other way around, more than compensating the transmission reduction.

Concerning storage capacity, it grows with increasing carbon tax and with the share of VRE generation. PHES is the dominant technology in the BAU scenario, while the introduction of a carbon tax benefits CAES and batteries, that leverage on cost reductions from learning effect to become the dominant technologies. Considering the energy capacity, CAES is the dominant option in CTAX and CTAX2DEG, followed

by batteries, while if we consider the power capacity, a proxy for the number of single installation required, batteries are the most widespread technologies in both the scenarios, due to their lower energy-to-power ratio. Overall, A-CAES is the preferred short-term storage option in regions with very high VRE shares, due to its higher capability to provide firm capacity compared to batteries. Global yearly investments in short-term storage experience a considerable growth in time, particularly in presence of a carbon tax: at the end of the century investments they have the same order of magnitude of investments in transmission plus grid smartening and pooling.

Seasonal storage deployment is almost an order of magnitude lower than short-term one in the most favourable CTAX2DEG scenario (and so are yearly investments), slowed mostly by the high costs of electrolysers and fuel cells.

Interestingly, the model is able to reach a 100% renewable scenario if no investments towards nuclear and CCS are allowed (simulating social or political obstacles to the adoption of these technologies) and a 2°C target via carbon tax is imposed. This scenario entails a four-fold increase in installed CAES capacity, becoming the dominant storage option and responding to the high firm capacity and flexibility requirements of this electricity mix. The fully renewable scenario, however, requires higher expenditures in the energy sector than the normal 2°C scenario and this reflects on global economic growth, with an undiscounted GDP loss of 16 percentage points with respect to BAU in 2100 (the loss for the same scenario is lower if CCS and nuclear are available, around 10%).

WITCH results indicate that without the installation of storage capacity, it is not possible to reach high shares of VRE generation. In a counter-factual scenario in which storage technologies are not present in the model, the role of VREs is considerably undermined: world net VRE shares arrive at best just around 20% in 2100, even in presence of a high carbon tax aimed at achieving the 2°C target. The model compensates the limitation on VRE installing more biomass plants, CSP and CCS and decreasing global generation. This, in turn, affects economic growth, entailing, for the CTAX2DEG scenario, an additional 0.6% undiscounted GDP loss in 2100 with respect to BAU, equivalent to 1.8 trillion \$ of 2005. As regards the effect of grid, VRE plants that are closer to load centers are favoured, as they only necessitate distribution line investments and no transmission line. Concerning the requirements for VRE system integration, it can be said that the need for firm capacity has more influence on VRE and storage investment options than the flexibility requirement in the first years, while increasing the carbon tax entails a growing influence of the flexibility requirement, also in time.

As concerns the translation of storage and grid installation into integration costs, we have investigated the effect on the LCOE of VREs technologies. Taking Europe as an example, the impact becomes visible in 2050 with a LCOE increment of 1.5% for PV and 4% for wind plants. In 2100 the increase is the largest: 7% for PV and 17% for wind plants. Taking into account also the effect on LCOE of the shadow costs related to the VRE additional flexibility and firm capacity requirement, their impact on integration costs is much larger: LCOE of wind is increased by half in 2050 and almost tripled in 2100. Finally, results indicate that if a price on emissions is present, distribution grid and short-term storage (especially CAES and Li-ion battery) complement each other

from an economic point of view, meaning investments in both of them are necessary to increase VRE generation.

The sensitivity analysis on grid cost and grid requirement per unit of generation capacity installed shows that these parameters hold a great influence on average grid investments. However, they do not show a significant impact on the installed generation capacity. Concerning the pooling requirement coefficient, the analysis suggests that the choice of its value, even if subject to uncertainty, does not affect results in a relevant way.

As regards storage parameters, decreasing the capability of storage to provide flexibility and firm capacity (through the correspondent coefficients) dramatically affects both VRE share and storage investments. This confirms that, on the one hand, the satisfaction of flexibility and firm capacity requirements plays a central role in the diffusion of VRE technologies and, on the other hand, storage is instrumental in providing this flexibility and firm capacity to the system, benefiting wind and solar installations. The costs of short-term storage technologies, both the initial and the minimum one (floor cost) they can achieve through learning-induced cost reduction, are other two important drivers of VRE share growth and overall storage investments, while varying learning rate and storage efficiency (especially increasing them) does not influence much these two global variables. Looking at the impact of storage parameters on the single technologies, efficiency improvements may considerably enhance the diffusion of CAES, and higher values of Full Production Hours for both CAES and batteries technologies could play an important role as well, while their impact on PHES is minor.

The main effect of the more detailed representation of electric grid introduced in our work is an overall increase in VRE generation with respect to the previous grid modeling, across all policy scenarios. This is due to the fact that “near” VRE technologies require only investments in distribution line, and this decreases their integration cost with respect to the previous WITCH implementation. On the other side, the new storage modeling has the opposite effect on VREs, whose global generation decrease in all policy scenarios (while other technologies are not affected by these change). This is mainly due to the fact that we introduced an efficiency loss due to storage, previously absent, that penalizes net wind and solar generation. The combined effect of grid and storage yields different results according to the policy scenario considered. Overall, with the new formulation, the model is more responsive to price signals and technology availability options.

If we compare our new WITCH version with the old MASTER version, featuring a less detailed representation of system integration, grid and storage, it is clear that a better modeling VRE system integration challenges, together with detailed electric grid and storage formulations, compensates for the previous underestimation of VRE integration costs and entails a reduction of the global net VRE share of 4 percentage point in the CTAX2DEG scenario.

Finally, WITCH results for VRE share, grid investments and storage capacity have undergone comparison with other models. Within the ADVANCE IAM modeling framework, a group of six models (including WITCH) that feature similar structure, level

of aggregation and purpose, WITCH results for VRE share and storage installed capacity (all obtained under the same carbon tax policy scenario) place themselves near the ones from POLES. This is the only other ADVANCE IAM to feature a detailed technological representation of short-term and seasonal storage technologies, the same technological choice for them and also a better representation of VRE supply-load matching throughout the year, considered a very important piece of information for representing the typical dynamics of VRE integration, grid and storage investments. Moreover, storage results for the EU countries are analogous for the two models. Considering that investment and generation decisions for EU countries in POLES rely on a temporally and spatially detailed unit commitment and dispatch model (EUCAD), a matching between our and POLES results represents an important *ex post* validation of our work. As regards global grid investments, not present in POLES, they are in line with two out of the three IAMs considered in this comparison.

A further comparison has been performed with the SWITCH model application to the Chinese power sector. Thanks to its higher temporal and spatial resolution, its prediction about the development of the investment in grid projects can be considered a reliable term of comparison. Comparing the high VREs penetration scenario with the WITCH CTAX2DEG one, we found that the order of magnitude of the investments is similar, even if higher in the WITCH scenario due to the more detailed distribution lines and grid smartening-related investments. An additional result of the comparison with the SWITCH model has been the validation of the formulation we introduced regarding the storage capacity fed by non-curtailed VREs generation.

Possible future developments of our work include a more detailed representation of battery technology options, a possible learning spillover between utility-scale and automotive Li-ion batteries, a more rigorous assessment of compressed air storage geographical potential, the modeling of hydrogen as a secondary energy source that can affect also the transportation and CHP sectors, explicit representations of Demand Response and Vehicle-to-Grid options to complete the picture of VRE system integration.

Contents

List of Figures	XIX
List of Tables	XXIII
Acronyms	XXIX
1 Introduction and motivation	1
1.1 Climate change framework	1
1.1.1 Benefits and challenges of Variable Renewable Energy sources	2
1.1.2 The role of electric grid and storage in VRE integration	3
1.2 Main research questions and methodology	5
1.2.1 Research Methodology	6
1.2.2 Thesis structure	7
2 Model description	9
2.1 Integrated Assessment Models	9
2.2 WITCH	10
2.2.1 Economy	11
2.2.2 The CES framework	12
2.2.3 Energy sector	12
2.2.4 Climate	14
2.3 VRE system integration in IAMs	14
2.3.1 The ADVANCE modeling framework	16
2.4 VRE system integration in WITCH	16
2.4.1 Investment dynamics	16
2.4.2 Power system operation	19
2.4.3 Temporal matching of VRE and demand	20
2.4.4 Grid	20
2.4.5 Storage	20
3 Grid and Storage Technologies: State of the Art	21
3.1 Grid	21
3.1.1 Transmission and Distribution grid	21
3.1.2 Smart Grids	24
3.1.3 Choice of cost and performance parameters for grid	25
3.2 Storage technologies	28
3.2.1 Functioning principle and applications	28

3.2.2	Short-term storage	29
3.2.3	Choice of cost and performance parameters for short-term storage	36
3.2.4	Seasonal storage	43
3.2.5	Choice of cost and performance parameters for seasonal storage	51
4	WITCH Model Advancement	55
4.1	Pre-existing VRE integration modelling	55
4.1.1	Capacity Constraint Equation	56
4.1.2	VRE Curtailment	57
4.1.3	Flexibility Constraint Equation	59
4.1.4	Pre-existing Electric Grid Formulation	64
4.1.5	Pre-existing Electric Storage Formulation	64
4.2	New Interpretation of VRE Flexibility Coefficient	65
4.2.1	Behind the Calculation of VRE Marginal Flexibility Coefficients	66
4.2.2	Flexibility Coefficient Curve as Sum of Two Contributions . . .	67
4.3	New Electric Grid Modeling	67
4.3.1	Better Definition of Installed Grid Capacity	68
4.3.2	Distinction between Transmission and Distribution Lines	69
4.3.3	Refinement of the Grid Pooling modeling	70
4.3.4	Grid Losses	72
4.4	New Electric Storage Formulation	72
4.4.1	Short-Term Storage	73
4.4.2	Seasonal Storage	77
4.4.3	Effect of New Formulation on Pre-Existing Equations	79
5	Results and robustness analysis	83
5.1	Policy analysis	83
5.1.1	Policy impact on Electricity Generation	84
5.1.2	Policy impact on Grid and Storage	86
5.1.3	Policy impact on GHG Emissions and Economy	92
5.1.4	Policy impact and technology substitution: towards 100% renewable scenarios	93
5.2	Impact of Storage and Grid modeling on VRE System Integration . . .	97
5.2.1	Impact of Storage presence	97
5.2.2	Impact on VRE and Electricity LCOE	97
5.2.3	Interdependence of electricity storage and grid	100
5.2.4	Impact of flexibility and firm capacity constraints	101
5.3	Sensitivity analyses	102
5.3.1	Sensitivity on Grid parameters	102
5.3.2	Sensitivity on Storage parameters	103
5.3.3	Sensitivity on CAES and battery technologies	105
5.3.4	Fraction of VREs Non-Curtailed as Input to Short-Term Storage	108
5.4	Comparison with previous WITCH modeling	111
5.5	Comparison with other Models	114
5.5.1	ADVANCE IAMs	115
5.5.2	SWITCH China	119

6	Conclusions and future work	125
A	WITCH model description and other ADVANCE IAMs	133
A.1	The Economy	133
A.1.1	Welfare function	133
A.1.2	Utility function	133
A.1.3	Consumption	134
A.1.4	Output	134
A.1.5	Energy Services	135
A.2	The Energy sector	135
A.2.1	Energy supply	136
A.2.2	Electric energy technology sectors	136
A.2.3	Capital accumulation for electric energy technology sectors . . .	137
A.2.4	Additional constraints in the electric sector	137
B	Additional Graphs	139
C	RLDC approach for system integration	140
D	VRE System Integration: Additional Material	143
E	Datasheets	146
F	GAMS code	148

List of Figures

1.1	Correlation between temperature increase, sea level rise and GHG concentrations in the atmosphere since 1850. Source:[2]	2
2.1	Feedback loop between climate and energy-economy sections in WITCH Source:[25]	10
2.2	World divided into 13 regions in WITCH	11
2.3	The residual power supply time series over the year (left) is reshaped to represent the RLDC (right, solid line). The dashed line represents the actual LDC. Source:[9]	16
3.1	Transmission and distribution grid in the energy system. Source: [15]	22
3.2	European high voltage (220 kV and above) transmission grid. Higher voltage lines in blue, lower voltage lines in red. Source: ENTSO-E	23
3.3	Components of an energy storage system. Source: [50]	28
3.4	Working principle of a battery technology in discharge phase.	31
3.5	Main components of a Li-ion battery. Source: [54]	32
3.6	Temperature-entropy diagram for the two D-CAES plant: Huntorf (grey) and McIntosh (black). Starting point: air leaving the storage cavern. Source:[59]	33
3.7	Plant scheme of the McIntosh D-CAES facility (1991). Source:[59]	34
3.8	Plant scheme of a medium-temperature Adiabatic CAES configuration. Source:[59]	35
3.9	PHES plant layout. Source: Tennessee Valley Authority	36
3.10	Variable speed pump-turbine section 3D rendering. Source: GE Renewable Energy	36
3.11	Capital x technology risk vs level of commercial maturity for many storage technologies. Source:[20]	38
3.12	Mapping storage technologies according to discharge time at rated power and energy capacity. Source:PwC, (2015), following Sterner et al. (2014)	38
3.13	Mapping storage technologies according to discharge time at rated power and energy capacity. Source:PwC, (2015), following Sterner et al. (2014)	40
3.14	Annual time series of weekly averages that illustrate the seasonal correlation of load, wind and solar for U.S.A. Source: [34]	44
3.15	Traditional (left) and zero-gap (right) configurations for alkaline electrolyser. Source: [88]	46
3.16	Main potential hydrogen storage paths in the energy sector. Source: [68]	47
3.17	Components of a generic fuel cell. Source: [89]	49

3.18	Scheme of a PEM fuel cell. Source: [89]	50
3.19	PEMFC efficiency as a function of normalized operating power (left). Specific cost per unit of useful power as a function of fuel cell efficiency. Source: [89]	50
3.20	Typical components of a SOFC and main reactions occurring in each layer. Source: [96]	51
3.21	Number of pilot and demonstration projects of power-to-gas launched worldwide in the past decade. Source: [87]	52
4.1	Average capacity value of VRE technologies as a function of their gener- ation share before curtailment for the case of USA [37].	57
4.2	Average total curtailment as a function of the VRE share before curtail- ment in MESSAGE, for the USA case [37].	58
4.3	Short-term and seasonal curtailment representation in WITCH as a function of the VRE share before curtailment for the USA.	59
4.4	VRE Flexibility Coefficient curve derived from marginal VRE flexibility coefficient values in [37] for the USA case.	63
4.5	VRE alone FC 3 rd degree polynomial curve, grid pooling coefficient 2 rd degree polynomial curve and overall VRE FC curve resulting from the sum of the other two curves, all function of the VRE share before cur- tailment, for the USA case.	68
4.6	Comparison between the overall VRE FC 3 rd degree polynomial curve implemented in WITCH and 3 rd degree polynomial curve interpolated from the original MFCs values taken from Johnson et al. [37].	68
4.7	POOLING quadratic behaviour as a function of <i>SHARE_EL_VRE_BC</i> for the USA case.	71
5.1	Carbon tax and carbon tax for 2 degrees: growth in time.	84
5.2	Electricity generation (after storage) by technology type in BAU, CTAX and CTAX2DEG policy scenarios.	85
5.3	Regional electricity generation by technology type in BAU, CTAX and CTAX2DEG policy scenarios in 2100.	86
5.4	Yearly investments in grid and pooling [$\frac{T\$}{year}$] in BAU, CTAX and CTAX2DEG policy scenarios.	87
5.5	Installed grid length [km] for transmission and distribution grid in BAU, CTAX and CTAX2DEG policy scenarios.	88
5.6	Global short-term storage installed energy capacity [TWh] by technology type in BAU, CTAX and CTAX2DEG policy scenarios in 2100.	89
5.7	Global storage installed power capacity [TW] by technology type in BAU, CTAX and CTAX2DEG policy scenarios.	90
5.8	Global fuel cells installed capacity [TW] in CTAX and CTAX2DEG policy scenarios.	90
5.9	Seasonal and short-term curtailment destination in time for BAU, CTAX and CTAX2DEG policy scenarios. Stored curtailment in blue, wasted curtailment in red.	91

5.10	Regional storage installed energy capacity by technology type in BAU, CTAX and CTAX2DEG policy scenarios in 2100.	92
5.11	Global equivalent CO_2 emissions [Gton] in BAU, CTAX and CTAX2DEG policy scenarios.	93
5.12	Undiscounted GDP loss with respect to BAU scenario for CTAX and CTAX2DEG policies.	93
5.13	Electricity generation (after storage) by technology type in CTAX and CTAX2DEG policy scenarios, with and without the possibility to invest in nuclear and CCS.	95
5.14	Investments in electric grid divided by type in CTAX and CTAX2DEG policy scenarios, with and without the possibility to invest in nuclear and CCS.	95
5.15	Short-term storage technologies installed capacities in CTAX and CTAX2DEG policy scenarios, without the possibility to invest in nuclear and CCS.	96
5.16	Undiscounted GDP loss of CTAX_NOCCS and CTAX2DEG_NOCCS scenarios with respect to BAU of the base case.	96
5.17	Comparison of the electricity generation mix in some relevant years between the cases with and without storage technologies in the model.	98
5.18	Comparison of the world VRE share (after curtailment) over the years between the cases with and without storage technologies in the model.	98
5.19	Comparison of the world undiscounted GDP losses in the CTAX and CTAX2DEG scenarios (with respect to the BAU scenario) between the cases with and without storage technologies in the model.	99
5.20	PV LCOE [\$/MWh] trend in CTAX2DEG scenario in <i>oldeuro</i> and <i>usa</i> regions. Three different definitions: “only VRE” includes only the technology related costs, “w/ Storage and Pooling” involves the addition of the costs related to storage technologies and grid pooling, “w/ System Integration Constraints” takes into account also the effect of the shadow cost of the constraint equations.	100
5.21	Wind Onshore LCOE [\$/MWh] trend in CTAX2DEG scenario in <i>oldeuro</i> and <i>usa</i> regions. Three different definitions: “only VRE” includes only the technology related costs, “w/ Storage and Pooling” involves the addition of the costs related to storage technologies and grid pooling, “w/ System Integration Constraints” takes into account also the effect of the shadow cost of the constraint equations.	100
5.22	Global investments in transmission and distribution grid and short-term storage technologies (the latter multiplied by 10).	101
5.23	Sensitivity analysis on average 2015-2100 investments in grid [T\$/year], for CTAX (red) and CTAX2DEG (blue) scenarios: effect of the main parameters. Horizontal lines represent the results with the parameters default values.	103
5.24	Sensitivity analysis on 2100 VRE generation share before curtailment, for CTAX (red) and CTAX2DEG (blue) scenarios: effect of the storage main parameters. Horizontal lines represent the results with the parameters default values.	105

5.25	Sensitivity analysis on average 2015-2100 storage installed power capacity [TW], for CTAX (red) and CTAX2DEG (blue) scenarios: effect of the storage main parameters. Horizontal lines represent the results with the parameters default values.	106
5.26	Sensitivity analysis on average 2015-2100 CAES installed capacity [TW], for CTAX (red) and CTAX2DEG (blue) scenarios: effect of the storage main parameters. Horizontal lines represent the effect of default values.	107
5.27	Sensitivity analysis on average 2015-2100 battery installed capacity [TW], for CTAX (red) and CTAX2DEG (blue) scenarios: effect of the storage main parameters. Horizontal lines represent the effect of default values.	107
5.28	Destination of the world non-curtailed VRE generation along the years. The non stored portion meets directly the demand, while the stored one is fed to the storage capacity K_STOR_PEAK	109
5.29	Saturation level of the storable fraction of VRE non-curtailed generation for five different values of the allowed storable fraction.	109
5.30	Global electricity generation [TWh/year] by technology type in CTAX2DEG scenario, as a function of $fraction_vre_stored$ value.	110
5.31	Global short-term storage installed capacity by type in CTAX2DEG scenario, as a function of $fraction_vre_stored$ value.	111
5.32	Electricity generation (after storage) by technology type in 2100 for the comparison between WITCH model editions.	113
5.33	Installed overall storage capacity along the years for the comparison between WITCH model editions.	114
5.34	Overall yearly investments in grid for the comparison between WITCH model editions.	115
5.35	Global VRE share of electricity generation before curtailment (if modeled) in a CTAX30 policy scenario for the six ADVANCE IAMs. Source: ADVANCE database and own data.	116
5.36	EU VRE share of electricity generation before curtailment (if modeled) in a CTAX30 policy scenario for the six ADVANCE IAMs. Source: ADVANCE database and own data.	116
5.37	Global, total investments in grid [$\frac{bln\$}{year}$] in CTAX2DEG scenario, as a function of $fraction_vre_stored$ value. Source: ADVANCE database and own data.	117
5.38	Global short-term storage installed capacity by type in CTAX2DEG scenario, as a function of $fraction_vre_stored$ value. Source: ADVANCE database and own data.	119
5.39	EU short-term storage installed capacity by type in CTAX2DEG scenario, as a function of $fraction_vre_stored$ value. Source: ADVANCE database and own data.	119
5.40	Comparison of total investments in grid trend as a function of the VRE share (after curtailment for WITCH) for China between the SWITCH IPCC Scenario [108] and three WITCH scenarios.	121

5.41	Comparison of the trend of the ratio between the installed capacity of storage in GW and the installed capacity of VRE in GW as a function of the VRE share (after curtailment for WITCH) for China between the SWITCH IPCC Scenario [108] and three WITCH scenarios.	123
5.42	Comparison of the trend of the ratio between the installed capacity of storage in GW and the installed capacity of VRE in GW as a function of the VRE share (after curtailment for WITCH) for China. The comparison is made between the SWITCH IPCC scenario [108] with and without considering the installed capacity of CGT, and the WITCH CTAX2DEG scenario counting the overall storage capacity and only the <i>K_STOR_PEAK</i> one.	123
A.1	CES Production Function of WITCH	136
B.1	Installed capacity in TW by technology type (included storage) in 2100 for the comparison between WITCH model editions. Source: own graph.	139
C.1	The Load Duration Curve (LDC) (right) is derived by ranking the load curve points (left) in descending order. Source: [9]	140
C.2	The residual load curve time series (left) is obtained by subtracting the time series of VRE from the time series of the electric load. The RLDC (right) is obtained by ranking the residual load curve points in descending order. Source: [9]	141
C.3	RLDCs are able to represent three main challenges of the integration of VREs. Source: [9]	141
C.4	Installed capacity in TW by technology type (included storage) in 2100 for the comparison between WITCH model editions. Source: [9]	142

List of Tables

2.1	18 features of the fundamental dynamics and drivers of VRE system integration in ADVANCE IAMs, divided into 5 clusters. Source: [17]	17
2.2	Flexibility coefficients in the first implementation of flexibility and capacity constraints in WITCH [36]	19
2.3	Market growth rates for wind and solar PV technologies	19
3.1	Grid requirement values for all the WITCH regions. It stands for the km of transmission or distribution lines required per 1 TW on installed generation capacity on average.	26
3.2	Grid thermal losses as percentage of the overall electricity generation in the different WITCH regions.	27
3.3	Cost data for short-term storage technologies. Variable O&M costs are intended per unit of energy, while fix ones are per unit of power.	39
3.4	Short-term storage technologies:values of the parameters implemented in WITCH.	39
3.5	Cost data for seasonal storage technologies.	53
3.6	Seasonal storage technologies:values of the parameters implemented in WITCH.	54
4.1	Flexibility coefficient of load for the 13 regions of the WITCH model [37].	60
4.2	Marginal Flexibility Coefficients of VRE technologies for different ranges of VRE shares before curtailment for USA [37].	62
4.3	POOLING values in correspondence of three different VRE share BC for all the WITCH regions.	72
5.1	Generation technologies included in each macro category.	85
5.2	Legenda for sensitivity analysis on grid parameters.	103
5.3	Legend for sensitivity analysis on storage parameters.	104
5.4	Legenda for sensitivity analysis on CAES parameters.	106
5.5	Legenda for sensitivity analysis on battery parameters.	106
A.3	Main characteristics of the five IAMs that, together with WITCH, represent the ADVANCE modeling framework. Source: [17]	138
D.1	Firm requirement values for the different WITCH regions. It represents the peak load to be supplied as a multiple of the annual average load (equation 4.1). Values derived from [37] and then adapted to WITCH.	143

D.2	Short-term and seasonal curtailment values in WITCH as percentage of VRE generation before curtailment for the 13 WITCH regions	144
D.3	Marginal Flexibility Coefficients of VRE technologies for different ranges of VRE shares before curtailment, derived from [37] and adapted to WITCH regions	144
D.4	Coefficients of the 3 rd degree polynomial curves representing the flexibility coefficients of the VRE technologies alone for the different WITCH regions.	145
D.5	Coefficients of the 2 nd degree polynomial curves representing the grid pooling coefficients for the different WITCH regions	145
D.6	Coefficients of the 3 rd degree polynomial curves representing the overall flexibility coefficients of the VRE technologies, including the effect of grid pooling	145
E.1	PHES Initial installed capacity. Data gathered at national level from IRENA Renewable Energy Statistics [73] and then aggregated at regional level for the implementation in WITCH.	146
E.2	PHES full production hours. Data for the installed capacity and annual generation gathered at national level from IRENA Renewable Energy Statistics [73] and then averaged at regional level for the implementation in WITCH. For each region the annual minimum, average and maximum values (between 2005 and 2015) of PHES full production hours have been selected to perform a sensitivity analysis.	147
E.3	CAES and Li-B initial installed capacity in 2015. Data gathered at national level from insertire reference and then aggregated at regional level for the implementation in WITCH.	147

Acronyms

AC Alternate Current.

AEM Anion Exchange Membrane.

BC Before Curtailment.

CAES Compressed Air Energy Storage.

CC Capacity Coefficient.

CCS Carbon Capture and Storage.

CES Constant Elasticity of Substitution.

CGT Combustion Gas Turbine.

CHP Combined Heat and Power Generation.

CMCC Centro Euro-Mediterraneo sui Cambiamenti Climatici.

CRRA Constant Relative Risk Aversion.

CV Capacity Value of the single VRE technology.

DC Direct Current.

DSO Distribution System Operator.

EIA U.S. Energy Information and Administration.

EtoP Energy to Power Ratio.

EU European Union.

FC Flexibility Coefficient.

FEEM Fondazione ENI Enrico Mattei.

FPH Full Production Hours.

FRT Fault-Ride Through.

GAMS General Algebraic Modeling System.

GDP Gross Domestic Product.

GHG Green House Gas.

GLOBIOM Global Biosphere Management Model.

IAM Integrated Assessment Models.

ICT Information and Communication Technologies.

LDC Load Duration Curve.

LiB Lithium-ion Battery.

MAGICC Model for the Assessment of Greenhouse-gas Induced Climate Change.

MESSAGE Model for Energy Supply Strategy Alternatives and their General Environmental Impact.

MFC Marginal Flexibility Coefficient.

O&M Operation and Maintenance.

PHEM Pumped Hydro Energy Storage.

POOLING Grid Pooling Coefficient.

PV Photovoltaic.

RFB Redox Flow Batteries.

RLDC Residual Load Duration Curve.

RTE Round Trip Efficiency.

SOC State Of Charge.

STEST Short-Term Energy Storage Technology.

T&D Transmission and Distribution.

TSO Transmission System Operator.

VRE Variable Renewable Energy.

WITCH World Induced Technical Change Hybrid.

Chapter 1

Introduction and motivation

1.1 Climate change framework

Climate change is acknowledged as one of the major challenges mankind will have to face in the 21st century, due to its potential effects on the delicate equilibrium of our planet. In particular, the link between temperature increase and anthropogenic Greenhouse Gas (GHG) emissions is broadly recognized as true by the scientific community [1], [2]. Intergovernmental Panel on Climate Change declared that human activities, driven by economic and population growth, are “*extremely likely*” [3] to be the cause of this temperature increase since the mid twentieth century.

Human activities related to energy consumption and generation, such as transportation, industry, agriculture and power production release GHGs. Studies indicate that this phenomenon may induce irreversible damages in terms of extreme weather events, biodiversity loss, ocean acidification, sea level rise and many more [2] (see figure 1.1). These phenomena may negatively affect ecosystems and people with increasing severity and irreversible effects. The two ways to reduce potential climate-change induced damages are preventing climate change from worsening (defined as mitigation) or introduce modifications in everyday life (for instance moving far from the seaside, use air conditioning etc.) to minimize the negative effects of climate change (adaptation).

Worried by the costs (not only economic) of climate change, both governments and public opinion are today advocating for countermeasures to reduce this risk, in terms of mitigation and adaptation. The Paris Agreement, reached in 2015 during the Conference of Parties 21 (COP21), represented a turning point for international cooperation aimed at fighting climate change: 195 countries have formally declared their willingness to pursue the ambitious target of keeping the temperature increase at the end of the current century well below 2°C with respect to pre-industrial levels, staying as close as possible to 1.5°C to limit damages. This agreement has been translated into Intended Nationally Determined Contributions (INDCs), in which every country ratifying the protocol (170 on 195 as of November 2017) specifies which adaptation and mitigation measures is going to implement to contribute to this global goal [4].

This target, however, is everything but easy to be reached, not only due to the amount of international coordination it requires, but also because it entails both technological and economical challenges. As a matter of fact, state-of-the-art technical energy solutions with low or zero associated emissions require, overall, a higher expenditure

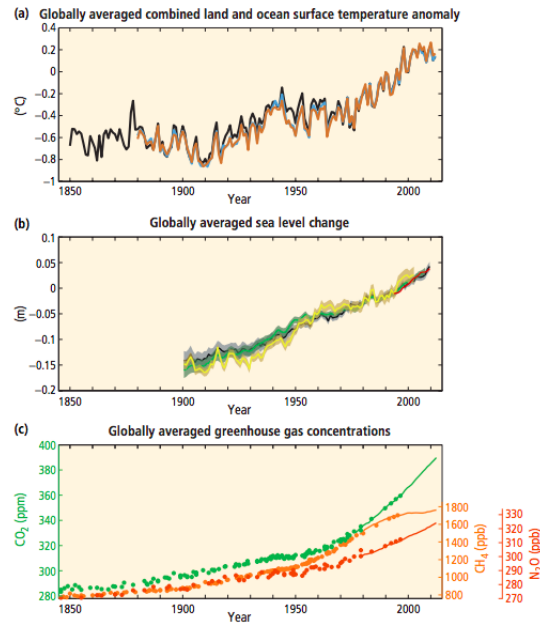


Figure 1.1: Correlation between temperature increase, sea level rise and GHG concentrations in the atmosphere since 1850. Source:[2]

with respect to the current energy system configuration, therefore mitigation comes at a higher present cost, even if it will reduce future cost of climate change [5]. Moreover many studies confirm that the best approach to deal with climate change mitigation and emission reductions is a diversified portfolio of low carbon technologies combined to improvements in energy efficiency to reduce final energy consumption and behavioural changes, aimed at reducing *per capita* consumption. Finally, the heat and power, agricultural, industrial, transportation and building sectors have a different impact on global GHG emissions and present different potential for decarbonization, therefore mitigation policies should take into account these differences and define coherent instruments to meet the temperature target.

1.1.1 Benefits and challenges of Variable Renewable Energy sources

The electric power sector accounts for the relative majority of global GHG emissions: 25% in 2010 [3]. Electricity production still occurs mainly by burning fossil fuels, with coal (the most carbon-intensive fossil fuel) representing 40% of the total electric energy production, and the figure grows to almost two thirds (65%) if we include also natural gas and oil. However, the power sector also presents high potential for a deep decarbonization. Renewable energy technologies such as wind turbines and solar photovoltaics (PV) are mainly present in the power sector as they normally produce electricity, an energy carrier that can be easily transported and used over long distances. Therefore the power sector is expected not only to reduce its carbon intensity, but also to play an important role in the decarbonisation of other carbon-intensive sectors such as transportation (with the diffusion of plug-in hybrid and full electric vehicles) and heating (though heat pumps) [6],[7], [8].

Nevertheless, even though solar cells and wind turbines have witnessed a steep capital

cost decrease over the last decades, there are some techno-economical barriers that limit their diffusion [9]. Besides occurring in direct capital and operational cost as the other generation technologies do, wind turbines and solar PVs entail further expenses so as to integrate them into the energy system, defined as “system integration costs”, “hidden costs” or “system-level cost”. These costs stem from the characteristics that distinguish wind and solar supply, as summarized by Hirt et al. [10]:

- **Variability:** instantaneous supply depends on weather conditions and cannot be regulated to balance energy demand, i.e. cannot be dispatched. For this reason, wind and solar are often referred to as Variable Renewable Energy (VRE). This entails costs, for instance in the form of investments in storage devices that can shift the output of VRE in time, or to remunerate dispatchable power plants that are ready to ramp up or down their production to balance this variability (ancillary services), or the opportunity cost of the amount of VRE supply that exceeds demand and, in absence of storage options, is just cut (curtailment).
- **Uncertainty:** in the electricity market, equilibrium between supply and demand, energy price, the consequent production and plant commitment decisions are made before physical delivery, therefore any deviation from the forecast VRE supply profile has to be balanced instantaneously, which entails further costs and affects the composition of the generation fleet.
- **Location-specificity:** for VRE, the primary energy carrier (solar radiation, wind) is present only in a specific geographical area and cannot be transported like other fuels. Areas with high density of renewable resources may be far from the load centers, hence further investments in electricity transmission and distribution grid are required.

The variable and uncertain nature of wind and solar supply, especially when it represents a high share in the electricity mix, introduces multiple challenges for modern energy systems, such as the capability to deal with steep and possibly unexpected ramp-ups and downs of the residual load (intended as the electricity demand that is not covered by VREs) and the necessity to install expensive and underutilized flexible power plants to cover peak demand [9]. Moreover, also the number of transmission and distribution grid bottlenecks is likely to increase, as they were not designed neither to transport peak VRE generation nor to deal with bi-directional energy fluxes, determined by the presence or absence of renewable generation [11]. Finally, decentralized VRE generation technologies (e.g. off-grid solar) are spreading, especially in developing countries, where the grid infrastructure is often lacking, unreliable or too expensive [12].

1.1.2 The role of electric grid and storage in VRE integration

Grid

Transmission and distribution electric grids are respectively the backbone and the ramifications of electric power systems, as they allow electricity to be transported from the place where it is physically generated to the place where it is consumed for final use [13].

The existing electric grid infrastructure is likely to face multiple challenges in the decades to come [14], for several reasons: the continuous growth in global and regional electricity demand, due to increasing final consumption but also to the electrification of other sectors, such as transportation and heating; the infrastructural aging, as transmission grids are long-lived assets that were mostly built forty or more years ago in the developing countries; the increasing attention to energy security and affordability and finally climate change, requiring a deep decarbonization of the power sector [15]. This last trend in global power systems has promoted the diffusion of VRE technologies in most of the world's regions, with the arousal of firm capacity and flexibility needs this entails (see chapter 3). VRE integration is related to a number of different technical issues, and traditional transmission and distribution grids may experience them at different levels: frequency and voltage regulation, thermal stress and management of bi-directional flows on traditionally uni-directional lines, especially in the case of decentralized VRE installations [16], are some examples. This may put the existing infrastructure under considerable pressure and hinder further VRE expansion when penetrations typically higher than 15-20% are reached [14]. This challenges can be overcome with several measures aimed at increasing the grid flexibility [16], such as:

- Allowing bi-directional electricity flows, not only from producers to consumers but also the other way around, given the growing interest towards small decentralized generation (we talk about “prosumers”) and the benefits this could potentially introduce in terms of grid stability.
- Establishing intelligent grid and demand-side management mechanisms, aimed at increasing demand flexibility while smoothing peak load.
- Improving national and international grid interconnection, aimed at increasing flexibility, stability and security of energy supply.

In this context, smart grids are considered enablers of the transformation necessary to accommodate larger shares of VRE generation in future electric power systems, [15] [16]. IEA defines a smart grid as “*an electricity network that uses digital and other advanced technologies to monitor and manage the transport of electricity from all generation sources to meet the varying electricity demands of end-users*” [15]. It is not a single or well defined number of devices, but rather an evolving set of technologies that will spread in different times and modes all around the world, depending on the economical, regulatory and technical context [14],[15], in an evolutionary context. As regards integration of VRE technologies, smart grids will likely have a central role in dampening the challenges VRE diffusion entails, allowing a better management and control of generation and demand side, ensuring power quality and grid stability.

Besides “smartening” and updating existing grids, also pooling VRE production over large geographical areas can help mitigate their inherent variability, related to weather conditions [17]. Grid pooling requires further investments for improving grid interconnections, at national and international level. This benefits the system stability, smoothing VRE generation and reducing gradients in the residual load, so that less flexibility is needed from the non-VRE power fleet. Pooling is in turn favoured by the introduction of ICT and smart control systems at transmission and distribution level [14], which may ease national and international cooperation in balancing operations [17].

Electricity storage

A growing number of studies and company reports ([18],[19], [20],[21],[22],[23], [24]) indicate that also storage is a valuable option to address the challenges introduced by high VRE shares.

Due to its capability of accumulating energy, keeping it inside for a variable amount of time (largely depending on the technology type) and then releasing it when needed, electricity storage can help VRE integration buffering and optimizing the output from VREs, mitigating short-term and seasonal output changes and filling both temporal and geographic gaps between supply and demand, to increase quality and value of the resource.

Nevertheless, there is a number of caveats to consider when discussing the future diffusion of electricity storage technologies, whose uncertainty depends on both techno-economical and regulatory aspects.

As regards techno-economical issues, the main point of concern is the commercial maturity of storage technologies, which is directly related to the technology cost and performance, especially in terms of efficiency and durability [19]. On the other hand, regulatory concerns regard the general absence of an energy market regulation that: acknowledges storage as a separate asset class and encourages investments; recognizes that storing electricity is not equivalent to final consumption, so it should not be subject to final-consumption or discriminatory fees; defines conditions for the participation of storage into ancillary service markets; clarifies to which extent TSOs and DSOs can own and operate storage facilities or should rely on private services [22].

1.2 Main research questions and methodology

The tool we used in our research is the World Induced Technical Change Hybrid (WITCH) model, which is an optimization Integrated Assessment Model (IAM) designed to investigate climate change mitigation and adaptation policies and developed by Fondazione ENI Enrico Mattei (FEEM) and Centro Euro-Mediterraneo per i Cambiamenti Climatici (CMCC) [25]. IAMs power relies on their ability to capture complex dynamics, such as the relationship between climate, energy and economy, allowing to derive a simple interpretation of multiple interdependent phenomena. To achieve this, a high grade of simplification and aggregation is needed. As regards the power sector, this clashes with the high temporal and spatial dependence of VREs, thus inducing difficulties in obtaining a reliable representation of their integration challenges. Being electric storage and grid seen as possible solutions for the integration of VREs, a trustworthy representation in the IAMs is urged. On the other hand, being strictly related with VREs and so dependent on temporal load pattern and geographical locations, their modeling in this type of models presents significant difficulties.

The overarching goal of our thesis is introducing a more accurate representation of the electric grid and storage, and their role in VRE system integration, to improve the accuracy and reliability of the scenarios produced by the WITCH IAM, whose final objective is informing policy makers about cost-effective solutions to mitigate climate change.

Therefore, our research has proceeded along two interrelated directions. First, we carried out the modeling of electric grid and storage in the WITCH IAM, aimed at getting a reliable and technically consistent representation of their presence in the energy system. Second, we evaluated how grid and storage influence the diffusion of VRE sources and the effect this diffusion has on the system, in technological and economical terms. More specifically, the research questions we want to address with our work are the following ones:

1. Among the main electricity storage technologies, which ones are more suitable for being included in long-term models?
2. What is the effect of different climate policy scenarios on the diffusion of VRE technologies and on grid and storage technologies?
3. How do grid and storage technologies affect the electricity generation mix? How does this impact on economic growth and costs, in the context of VRE system integration?
4. Which of their cost and performance parameters have the strongest impact on VRE diffusion and on grid and storage investments?
5. What are the effects on results of the new, more accurate representation of grid and storage if compared to previous versions of the model?

We are aware of the challenges introduced by the modeling of grid and storage investment choices in very aggregated IAMs, as these decisions normally require a detailed representation of local and short-term dynamics, typical of short-term dispatching models. For this reason, as further development of our work, we compared the results obtained from WITCH with other models, belonging to two categories. Firstly, models that share similar scope and structure with WITCH, to verify how our model behaves within its own framework. Secondly, more accurate, temporally refined and geographically restricted models: one featuring unit commitment and dispatch decisions in the European Union, the other representing grid and power investments in China, as a form of validation of our results.

1.2.1 Research Methodology

One of the major challenges encountered during our work concerned the lack of data in literature about key aspects of our formulation. In particular, we found considerable difficulties in assessing the projected future cost decrease of storage technologies and their overall potential in the different regions of the world. As regards the electric grid, a scarcity of data about overall installed transmission and distribution capacity and its future projections was encountered. During our research, we focused on the most recent data, analyzing the latest technical publications, and when data were missing we made our own assumptions, always verifying their technical consistence and coherence. Another difficult task, frequent in Integrated Assessment modelling, consisted in determining an acceptable trade-off between technical details and simplified representations that could fit to the aggregated structure of the model.

The whole research work we conducted can be structured as follows:

1. Literature review: gathering and organization of information and data.

2. Design of model equations: raw data and concepts from literature are translated into a mathematical structure. The modeling choices about the characterizing costs and performance parameters have been performed.
3. Implementation in numerical form of the equations and translation in General Algebraic Modeling System (GAMS) language, the programming language of WITCH. This phase required particular attention, as our final implementation of the electric storage and grid sections, after the supervision of other researchers, are going to be used in the official version of the WITCH model.
4. Robustness check of the results: sensitivity analysis in two stages, first with a detailed analysis on all the possible variations of the key parameters values, then through a comparison with the results of models representing electric storage or grid in a more detailed way.
5. Analysis and discussion of the results.

1.2.2 Thesis structure

The sequence of chapters is organized as follows. In Chapter 2 we introduce WITCH and we describe how the VRE system integration problem is faced in other Integrated Assessment Models. Chapter 3 is intended to provide a detailed technical state of the art review of the main electric grid and electric energy storage technologies, with a particular focus on those implemented within the model. Technical information is instrumental in explaining and justifying our modeling choices in terms of selected technologies and their performance and cost parameters, which are therefore discussed in this chapter. Chapter 4 starts presenting the VRE system integration features that were already present in the WITCH model at the beginning of our work. After that, we introduce our new interpretation of an already existing part of the model, related to the VRE system integration. Then, the largest portion of the Chapter is devoted to the equations and modeling assumptions behind the new formulation of storage and grid we implemented in the model. Chapter 5 is dedicated to the results, with a particular attention towards their consistency through sensitivity analysis and comparison with results from other models. Finally, Chapter 6 summarizes the main conclusions and major findings of our work, including some future developments.

Chapter 2

Model description

In the previous Chapter, we clarify that the overarching goal of our work is contributing a more accurate representation of electric grid, electricity storage and system integration dynamics of VRE technologies, whose large scale diffusion in the future is regarded as a possible solution to cut GHG emissions and mitigate climate change [3]. Yet, climate change is a complex and multidimensional problem and reaching a deep level of understanding about its dynamics requires a simultaneous analysis of three dimensions, closely intertwined by non-linear positive and negative feedback loops: climate, energy and economy. This purpose can be served with the help of Integrated Assessment Models (IAMs), that combine information from different research fields and translate them into an analytic form. IAMs aim at approximating the mutual influences among fields and obtaining information about possible future scenarios by performing computer-based numerical analyses[26]. In the following sections, first we briefly describe the main features of IAMs for climate change in general, then we focus on the model used in our work, WITCH, and finally we examine how VRE system integration is represented in the IAM modeling framework, with particular attention to what had been implemented in WITCH before our work.

2.1 Integrated Assessment Models

Integrated Assessment is the process of using pieces of information from different branches of human knowledge and combining them to get meaningful insights on a certain topic [26]. When applied to climate change, the main branches involved are political science, economics, climate science, biochemistry and engineering, combined to understand how human activities (production of goods, consumption of energy, transportation, investment choices etc.) affect GHG emissions and, ultimately, temperature increase. The dynamics governing all the described phenomena and their interactions are described in a mathematical form and are synthesized in a numerical model, typically computer-based.

Given their capability to synthesize and provide a considerable amount of information about the problem as a whole, without focusing just on a narrow field of expertise, IAMs are particularly suitable for policy design and assessment [27]: they provide insights about the effects of policy measures on the entire economic system, reporting

also the detailed consequences on the modeled sectors. In evaluating the link between economic activity and GHG emissions, IAMs can follow two different approaches [28]: a top-down or aggregated approach, that represents reality starting from a low number of variables summarizing the relationships between sectors in a very condensed way, typical of macroeconomics and econometric studies (e.g. using a damage function to quantify the impact of climate change on economy with only one parameter); a bottom-up or dis-aggregated approach, that describes in detail the relevant sectors of the economy, such as energy, agriculture, transportation and, given their configuration, builds up the effects on both economy and environment.

Despite being regarded as the main tool to analyze the investment efforts required to meet climate change mitigation targets [17], IAMs present a number of limitations in predicting the exact influence of human activities on climate change, hereby summarized:

- Model uncertainty: there is a level of uncertainty associated to the response of temperature increase to growing concentrations of GHG in the atmosphere, represented by confidence intervals around the climate module estimations.
- Climate uncertainty: internal interactions among the main climate forcing elements (oceans, atmosphere, Earth's surface) inducing climate changes in hardly predictable ways and timings (e.g. hurricanes, El Nino).
- Parameter uncertainty: it is not possible to predict parameters such as the exact prices of energy technologies in the long term, especially if the technology is not commercially mature or it is just at an early stage of development. Some assumptions must be introduced.

2.2 WITCH

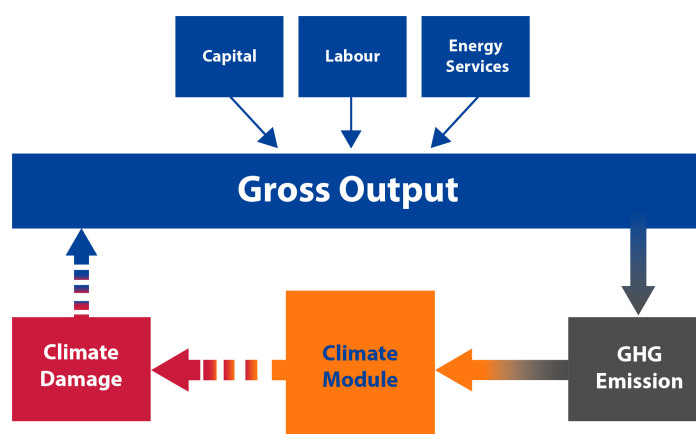


Figure 2.1: Feedback loop between climate and energy-economy sections in WITCH Source:[25]

WITCH (World Induced Technical Change Hybrid) is an IAM developed by Fondazione Eni Enrico Mattei (FEEM) and Centro Euro-Mediterraneo sui Cambiamenti Climatici (CMCC). It is a regionally disaggregated hybrid global model with a neoclas-

sical Ramsey-type optimal growth structure (top-down) and a detailed energy input component (bottom-up) [29]. The energy sector is particularly detailed and hard-linked with economy so energy investments and resources are chosen optimally considering the trend of macroeconomic variables and policy-induced economical stimuli. Instead land use mitigation and future climate are soft linked, so they are available through GLOBIOM and MAGICC that are respectively a land use and forestry model and a climate model. Technological change is accounted for endogenously, both via learning curves that influence the investment cost of new vintages of capital and via R&D investments. The model features the main economic and environmental policies in each world region as the outcome of a dynamic game. The reason why WITCH is an IAM lies in the fact that there is a continuous feedback loop among the economic part, generating GHG emissions affecting the climate module that, in turn, influences the economic output through a climate damage function, as shown in figure 2.1.

In its default configuration, the model is divided into 13 regions (see fig. 2.2, whose countries share similar economic situations, energy systems, climate policies and political strategies. It ranges a time frame going from 2005 to 2150. If regions are facing a global policy target, they can either behave independently or form coalitions: in the second case, coalitions of regions optimize their total welfare as a whole.

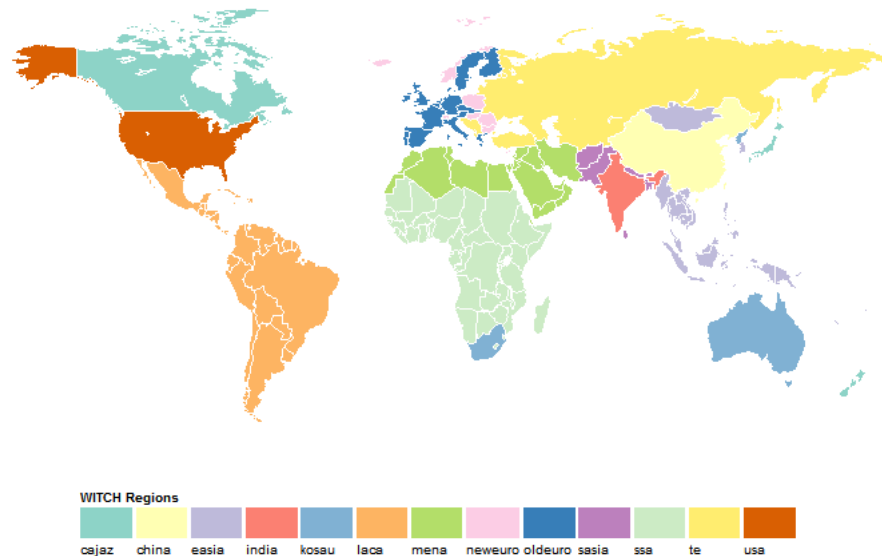


Figure 2.2: World divided into 13 regions in WITCH

2.2.1 Economy

In the model, a social planner (with perfect foresight) maximizes a utility function the sum of regional discounted utility of each coalition. The regional utility function at any point in time and each region is based on Constant Relative Risk Aversion (CRRA) utility function derived from consumption per capita (and log-shaped). If no coalitions are present, the model optimizes considering each region as a coalition.

Consumption, the argument of the utility function, is given by the budget constraint as the output of a single region, to which investments (in final good, energy and extraction sector, R&D, grid and adaptation), operation and maintenance costs (O&M) are subtracted, as they represent competing claims of the economy.

The economic output of each region is represented by a nested production function combining labour, capital (these two aggregated in a Cobb-Douglas function) and energy services in a Constant Elasticity of Substitution (CES) framework, plus the influence of a climate damage function, cost of fossil fuels and GHG emissions mitigation, reducing the output. All economic quantities are defined in 2005 United States Dollars. A more detailed description of the economic module is provided in Appendix A. Since the CES framework is particularly important to understand how investments in energy technologies are done, the following subsection provides a brief explanation of what a Constant Elasticity of Substitution function is and how it is applied to WITCH.

2.2.2 The CES framework

The Constant Elasticity of Substitution production function is a macroeconomic functional form that sees the output as a function of a number of inputs (inputs are just two in the original formulation [30]). The peculiarity of this function is that it accounts for the extent to which one input (e.g. labour) can be substituted by another one (e.g. capital) to produce the final output, through the concept of elasticity of substitution. Equation 2.1 represents a general two-variable CES production function.

$$Y = A[aX_1^\rho + (1 - a)X_2^\rho]^{\frac{1}{\rho}} \quad (2.1)$$

The output Y depends on the productivity A , on the two inputs X_1 and X_2 , on a , determining the optimal distribution of inputs, and on ρ , which is in turn a function of σ (the elasticity of substitution between the two outputs), as:

$$\sigma = \frac{1}{1 - \rho} \quad (2.2)$$

Therefore, if σ approaches infinity the CES function becomes linear and the two outputs become perfect substitutes (the two inputs can be used equivalently to generate the same output). The more σ approaches zero, the more the two outputs become complements, so a certain amount of both should always be provided to obtain the output, and the margin to substitute one source of input with another decreases [31]. Appendix A provides further information on how the CES structure is applied to WITCH's production function, especially for the energy sector [25].

2.2.3 Energy sector

Within the economic part of the model, the energy sector is the one described with the highest level of detail. This feature represents an exception in the IAM field and it is the origin of the "hybrid" nature of WITCH: on one hand, the economy is described in a very aggregated way (top-down), while on the other hand the level of detail allows to account for the different technologies and their performance, primary fuel requirements and pollutant emissions (bottom-up).

Energy Services are provided either with investments in efficiency improvements, that are endogenously accounted for, or via actual energy consumption, that is in turn a CES combination of electric and non-electric energy. The two sub-sectors are described in detail and decomposed to the level of the single technology: the choice among different energy production options is determined by the utility maximization, where a CES-tree structure (see Appendix A) determines substitutability and complementarity between technologies, to avoid a so called “bang-bang solution”, i.e. technological choice is purely based on cost minimization and all the investments are shifted towards the most economical option, without any inertia of the energy sector.

Electric sector includes both fossil-based plants, such as gas, coal and oil, and low carbon options such as wind, solar, biomass, Carbon Capture and Storage (CCS) and hydro, plus an electric backstop technology (representing a basket of promising technological options, far from commercialization). Non-electric demand regards transportation, industrial, commercial and residential sectors. Cost of production includes investments, O&M and fuel costs.

Investment costs in energy technologies are subject to two different types of learning, allowing for cost improvements in the future:

- Learning by doing: investment costs decrease proportionally to cumulative installed capacity, therefore endogenously. Before our work, the technologies benefiting from this type of learning were solar, wind and advanced biofuels. We also added storage technologies.
- Learning by researching: similarly to what is done for general energy intensity of the economy, it is possible to invest money and accumulate an R&D capital stock, whose growth determines a technology cost decrease. This is done for the two backstop technologies (electric and non-electric) and for energy efficiency improvements, that decrease the total energy demand at same output level.

The existing capital of generation technologies and grid undergoes depreciation, meaning that capital shrinks in time if no further investments are done. WITCH uses a standard exponential depreciation rule: the depreciation rate is calibrated based on a finite useful life of each technology, with a linear depreciation rate of 1% per year until the end of the lifetime and full depreciation thereafter. Based on realistic plant lifetimes, the exponential depreciation rate is found equalizing the integral of both depreciation schedules. Further information about depreciation of capital are available in Appendix A.

Operation and maintenance cost are constant in time for all the technologies, while the price of fossil fuels and exhaustible resources (oil, gas, coal and uranium) is determined by the marginal cost of extraction, which in turn depends on current and cumulative extraction [25]. A regional mark-up is added to mimic different regional costs including transportation costs. The regional fuel consumption takes into account the domestic extraction and fuel imports, to determine the fuel expenditure of each region.

The electric grid is schematically represented though dedicated capital stock investments and depreciation, see Section 4.1 for a better description of the grid implementation before our work. Finally, VRE system integration is accounted for with a number of constraint that will be dealt with in subsection 2.4.

2.2.4 Climate

GHG emissions are responsible for climate change, and can be generated by energy sector (power production, residential heating, transportation and industry) and land use. Emissions include Carbon Dioxide (CO_2), NitrousOxide (N_2O), Methane (CH_4) and Fluorinated gases (targets of Kyoto Protocol). The estimates of agriculture, forestry and bioenergy emissions are provided in input from Global Biosphere Management Model (GLOBIOM), a land-use model soft-linked with WITCH. As regards the relation between GHG concentration in the atmosphere and temperature increase, WITCH can internally convert regional emissions or can alternatively be soft-linked with a climate model (as done in our work): Model for the Assessment of Greenhouse-gas Induced Climate Change (MAGICC).

2.3 VRE system integration in IAMs

IAMs are useful instruments to understand the role of energy technologies in meeting long-term climate policy targets [3]. Representing the dynamics that lie behind the existence of VRE integration cost (see Chapter 1) is a challenge for IAMs, due to their high level of spatial and temporal aggregation [32]. The models have a broad scope, covering multiple sectors, embracing a centennial perspective to address a global problem. From the energy system perspective, investment decisions are made every 5-10 years, representing the temporal resolution of the model, and the main quantities (supply, demand, price, operating costs etc.) are present as annual averages. This hinders an accurate representation of the main features of VRE generation (described in Chapter 1), that can be captured just if the time resolution is refined to minutes - even seconds: an accuracy these models cannot reach due to numerical and complexity limits.

To compensate for this weakness, IAMs feature a stylized representation of these phenomena, with different levels of detail and accuracy [32]:

- Upper bounds to maximum VRE generation share: it is a simple yet rigid measure, that neither specific literature nor real-world experience indicate as reliable.
- Integration cost markups: often defined as a cost penalty per unit of VRE generation, growing with the VRE share. It is a less rigid approach but it does not capture the influence of high VRE share on other power plants, in terms of operation and installed capacity requirement.
- Fixed investments in specific integration options: they rise with VRE share and associate the diffusion of wind and solar with a change in the energy system mix (e.g. firm capacity from gas-fired power plants, electricity storage or transmission infrastructure). Nevertheless, the mitigation option to invest in is often only one, so the model is not left free to choose the most cost-effective integration option. Moreover, VRE integration entails multiple challenges (see section 1.1.1), that cannot be addressed by a single technical solution.
- Time slices: some models differentiate energy demand in time [17], [33], representing characteristic situations in the power sector with different and often co-existing

levels of temporal detail (seasonal variability, day/night, weekday/holiday). The goal is capturing demand variability with the lowest number of times slices possible, leveraging the regularity of load patterns in time, to minimize the model complexity. However, this approach does not allow to capture the correlation between load and solar/wind generation patterns, that requires a more accurate spatial and temporal definition, increasing both model complexity and computational time, besides requiring extensive regional-based studies [34].

- Flexibility and capacity constraints: some models [35],[36] try to incorporate the concept of reliability of electricity supply in the modeling framework, elaborating on the concept of adequacy. This feature is intended both as the capability of an electric power system (grid and generation fleet) to satisfy the expected peak demand, plus some extra reserves to face possible contingencies and outages (capacity requirement), and as the possibility to adjust generation over different time scales in response to foreseen and unforeseen demand variations (flexibility requirement). Both these requirements are accounted for in a stylized, parametric way: a capacity constraint equation, representing the fact that technologies are able to cover peak demand with different degrees of reliability (depending mostly on the availability of the primary resource); a flexibility requirement, indicating if each technology is capable of providing flexibility to the system or requires additional flexible generation and ultimately imposing a balance between flexible and non-flexible options. A more detailed description of the theoretical background and the actual implementation of these two equations is provided in Section 2.4.
- Application of RLDCs : this innovative approach stems from the model implementation of the so-called Residual Load Duration Curves (RLDCs) [32], [34], [37]. RLDCs represent the duration of electricity demand non satisfied by VRE generation within a geographical area, which must be satisfied by non-VRE power sources. They can be used to estimate the capacity value of VRE technologies, the fraction of VRE curtailment, and the impacts on capacity factors of non-VRE technologies with an increasing share of renewables. They are built starting from Load Duration Curves (LDCs), a representation of the instantaneous power demand (and supply, since they have to be continuously balanced) a certain load area experiences, ordered according to the number of hours this load condition is verified (see figure 2.3).

The shape of RLDCs changes with the VRE share in the region of interest: the higher the amount of VRE generation, the steeper the slope of the RLDC, that can even assume negative values for a small amount of hours per year, meaning that renewables production exceeds demand requirement, thus it is curtailed. The advantage of RLDCs is that they allow to capture key features of VRE sources, such as their low capacity credit, their effect on the reduced capacity factor of dispatchable power plants and possible VRE over-production. Nevertheless, this approach presents shortcomings as well: we lose information about the temporal sequence of demand and supply, so it is not possible to represent accurately features such as short-term storage or demand-side management, that are subject to fast dynamics. The way RLDCs are applied in WITCH is discussed in section 4.1, while further information on their physical meaning is available in Appendix C.

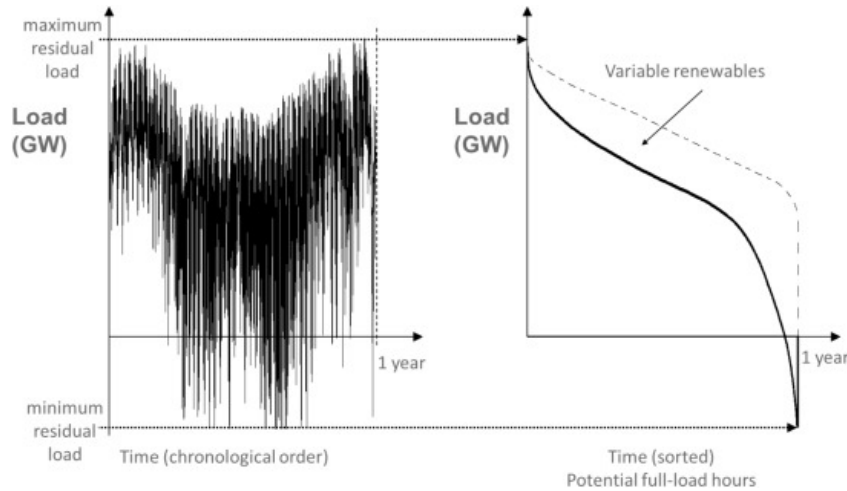


Figure 2.3: The residual power supply time series over the year (left) is reshaped to represent the RLDC (right, solid line). The dashed line represents the actual LDC. Source:[9]

2.3.1 The ADVANCE modeling framework

As said in subsection 2.3, several different approaches are followed to represent VRE system integration in IAMs. Therefore, it is useful to narrow the field of observation on the models that, compared to WITCH, present similar time and space boundaries, similar objective functions and consider the energy part of the economy with a similar level of detail, in order to make meaningful comparison among the different approaches and gain a better understanding of the starting point of our work. The EU FP7 ADVANCE project [38] gathers six state-of-the-art IAMs (including WITCH) that share the same characteristics (global models spanning the entire 21st century) and have recently developed new representations of the VRE integration challenges. Pietzcker et al. [17] offer a thorough overview of how system integration is accounted for in ADVANCE IAMs, providing, on the one hand, a framework of 18 features of the fundamental dynamics and drivers of VRE system integration, and on the other hand a quantitative performance evaluation of the models, compared among themselves. The 18 features are clustered in 5 categories, listed in table 2.1. These categories are then analyzed in the following section, with particular attention to the WITCH modeling choices done, the starting point of our work.

2.4 VRE system integration in WITCH

In this section, we examine the dynamics and drivers of VRE system integration featured in WITCH before our thesis work [36], following the clusterization suggested by Pietzcker et al. [17] and discussed above.

2.4.1 Investment dynamics

WITCH considers electricity as a homogeneous good, hence its value does not change in time. Electricity demand and supply are not time-dependent: they are considered only as annual averages.

To differentiate between baseload and peaking plants, the model introduces both a

<i>Investment dynamics</i>	Investment into dispatchable technologies differentiated by load band Investment into VRE Expansion dynamics Capital stock inertia and vintaging Structural shift of generation capacity mix Love of variety
<i>Power system operation</i>	Dispatch Flexibility and ramping Capacity adequacy Curtailment
<i>Temporal matching of VRE and demand</i>	Wind/solar complementarity Demand profile evolution
<i>Storage</i>	Short-term storage Seasonal storage Demand response
<i>Grid</i>	General transmission and distribution grid Grid expansion linked to VRE Pooling effect from grid expansion

Table 2.1: 18 features of the fundamental dynamics and drivers of VRE system integration in ADVANCE IAMs, divided into 5 clusters. Source: [17]

capacity and a flexibility constraint equation, representing the increasing flexibility demand and back-up firm capacity required when VRE share increases. Their structure is based on the methodology developed by of Sullivan et al. [35], implemented in WITCH by Carrara et al. (2017) [36] and described in detail. A more recent implementation of flexibility and capacity constraints (especially as far as the coefficients are concerned), based on the RLDC approach, is available at chapter 4 and it constitutes the starting point of our work. However, the description of the previous implementation as conceived in [36] will facilitate the rest of the explanation, so it is provided in the following:

- Capacity constraint: this equation ensures that sufficient firm capacity is built to cover peak demand and reliably face contingency events. The total firm capacity requirement is computed as approximately twice (the multiplying coefficient is $firm_req(n)$) the average annual load ($Q_{EL_TOT} / yearly_hours$), and non-VRE plants contribute with their full nameplate capacity K_{EL} to cover it, while storage contributes with 85% of it (see subsection 2.4.5). On the other hand, to account for their variability and unpredictability, VRE capacities are multiplied by their capacity factor CF (defined as the ratio between full production hours of a power plant over the number of hours in a year, 8760) and their capacity value CV : the latter represent the VRE capability of actually contributing to firm requirement and it decreases with the share of wind and solar penetration. The equation is written as follows:

$$\begin{aligned}
& \sum_{jel|non-VRE} K_EL(jel, t, n) + \sum_{jel|VRE} K_EL(jel, t, n) \times CF(jel, t, n) \\
& \quad \times CV(jel, t, n) + K_EL_{storage}(t, n) \times CC_{storage} \\
& \quad \geq firm_req(n) \times \frac{Q_EL_TOT(t, n)}{yearly_hours} \quad (2.3)
\end{aligned}$$

- Flexibility constraint: this equations ensures operational reliability in each modeled region, by assigning each generating technology a flexibility coefficient FC (constant over time and across regions) between -1 and 1, that multiplies the electricity generation of the specific technology (Q_EL). A positive flexibility coefficient means that specific technology is able to provide flexibility to the energy system (for instance rapidly ramping up or down its production to follow the load), while a negative coefficient stands for the flexibility required by an additional unit of generation from that technology. Storage is assumed as a “dummy” technology that provides energy at its nameplate capacity ($K_EL_{storage}$) for 2000 hours a year ($yearly_storage_hours$).

$$\begin{aligned}
& \sum_{jel} Q_EL(jel, t, n) \times FC(jel) + K_EL_{storage}(t, n) \times yearly_storage_hours \\
& \quad \times FC_{storage} + FC_{load} \times Q_EL_TOT(t, n) \geq 0 \quad (2.4)
\end{aligned}$$

The load has been assigned a negative coefficient of -0.1 (FC_{load}), to represent the fact that, even in absence of negative-FC technologies, some flexibility is still required to follow the load. All other coefficients have been computed via a unit-commitment model featuring a simplified six-nodes grid [39] : a number of scenarios with different levels of wind capacity penetrations have been run and the annual generation mix across scenarios compared, so as to extract a set of flexibility coefficients that could better approximate the observed behaviour. Coefficients of technologies that are not present in the model have been assumed (nuclear and PV). Table 2.2 shows the flexibility coefficient of generation technologies in WITCH:

As regard VRE expansion dynamics, WITCH uses hard constraints in the form of market growth rates, imposing an upper bound to the yearly growth of installed capacity for renewable technologies; this upper bound becomes less and less rigid in time, yet it is present until the final year of optimization. This representation also includes an offset to allow the installation of technologies with low-to-null initial installed capacity. Table 2.3 provides the values of market growth rates for VRE technologies:

Capital stock vintaging is expressed through exponential depreciation of the installed capacity each year, without keeping track of the building time. As regards the potential for a structural shift of the electric power system towards new generation technologies, the CES structure *per se* might represent an obstacle to technology substitution, nevertheless a medium elasticity of substitution of 5 between fossils and renewables

Technology	Flexibility coefficient
Load	-0.1
Wind	-0.08
PV	-0.05
Nuclear	0
CSP	0
Coal ST	0.15
IGCC	0.15
Coal CCS	0.15
Oil	0.3
Biomass	0.3
Combined cycle	0.5
Gas CCS	0.5
hydroelectric	0.5
Storage	1

Table 2.2: Flexibility coefficients in the first implementation of flexibility and capacity constraints in WITCH [36]

Years	Onshore wind	Offshore wind	Solar PV
2015-2020	0.03	0.01	0.15
2020-2030	0.06	0.06	0.15
2030-2050	0.15	0.15	0.15
2050 - onwards	0.20	0.20	0.20

Table 2.3: Market growth rates for wind and solar PV technologies

technologies (see Appendix A) leaves space to broad structural shifts [36]. This formulation also encourages love for variety, together with the above-mentioned market growth rates.

2.4.2 Power system operation

WITCH does not represent dispatch decisions, yet the flexibility and capacity constraint may indirectly force a lower electricity generation from traditional power plants as VRE share increases (see Appendix C) and represent the need for back-up and flexible capacity.

Curtailement, which is the need to cut VRE supply when it exceeds demand and cannot be stored, is only implicitly represented in WITCH: the introduction of a new VRE generation technology induces a less-than-linear increase of the production function with VRE output, without accounting for regional differences or demand-supply correlation.

A more recent implementation of WITCH features both short-term and seasonal VRE curtailment, as illustrated in chapter 4, and it constitutes the starting point of our work.

2.4.3 Temporal matching of VRE and demand

The model does not take into account the typical anti-correlation between wind and solar production (as wind typically blows stronger in the early and late hours of the day, while sun shines in the central hours), yet the CES structure promotes competition between solar and wind, as they belong to a CES branch with an elasticity of 2 (see Appendix A). On the other hand, the demand profile does not change in time, neither does the firm requirement (i.e. peak demand).

A more recent implementation of WITCH includes a time-dependent firm requirement coefficient, which progressively decreases after year 2015, as illustrated in chapter 4: it constitutes the starting point of our work.

2.4.4 Grid

WITCH represents the electricity transmission and distribution grid as a homogeneous, generic capital (no technological distinction) undergoing depreciation, featuring the same cost all over the world and no associated electricity losses. Installed grid capacity is linearly proportional to the installed generation capacity, plus some cost markups for wind and solar PVs, depending on their distance from the load center (they are classified as “far”, “intermediate” and “near” with respect to the load centers). A simple representation of the grid pooling effect, that is the tendency to improve the grid connection over large areas to smooth VRE variability by means of long-distance high voltage (DC or AC) lines or smart controls, is included through a formulation taken from another IAM, REMIND [40].

2.4.5 Storage

Investments in a single type of short-term storage (the one that can deal with intraday VRE output variability) are endogenously accounted for in WITCH, nevertheless storage is not an actual electricity technology, but more a “dummy” technology the model can invest on since it positively contributes to capacity and flexibility equation, without actually entering the CES or and being associated to any economic value in the production function.

Seasonal storage, that could smooth anti-correlations between supply and demand on a seasonal basis [32], is not represented in WITCH, neither demand response.

Chapter 3

Grid and Storage Technologies: State of the Art

In this chapter, we first provide a review of electric grid types, their features, cost and role in accommodating VRE generation. Second, we provide an overview of the main electricity storage technologies, starting from their working principles, performance and cost, moving on to some consideration about their commercial maturity and to the motivations lying behind our modeling choices. This is repeated for both short-term and seasonal storage.

All the data used in the modeling activity are summed up in tables at the end of each section.

3.1 Grid

This section provides a brief description of the electric grid. The first part is devoted to the description of the two types of electric grid that are traditionally distinguished: transmission and distribution grids. The second part deals with the challenges to the grid infrastructure introduced by increasing VRE shares, and the possible ways to overcome them. The final part deals with the choice of typical cost and performance parameters for the technologies we model in this work, and the reasons behind these modeling choices.

3.1.1 Transmission and Distribution grid

Transmission and distribution electric grids are respectively the backbone and the ramifications of electric power systems. Figure 3.1 provides a simplified representation of an energy system where electricity is produced in a centralized way, far from the load centres. After generation, it is transported by the transmission line to a transmission substation, and then it may follow two different paths: either its voltage is stepped down and it directly satisfies industrial demand (typically requiring higher voltage), or it is transported by a lower voltage distribution line serving load centres such as urban areas, where it is consumed for residential or commercial purposes. To get a better understanding of the roles of transmission and distribution system in electric power systems, they will be described separately in the following, highlighting the main

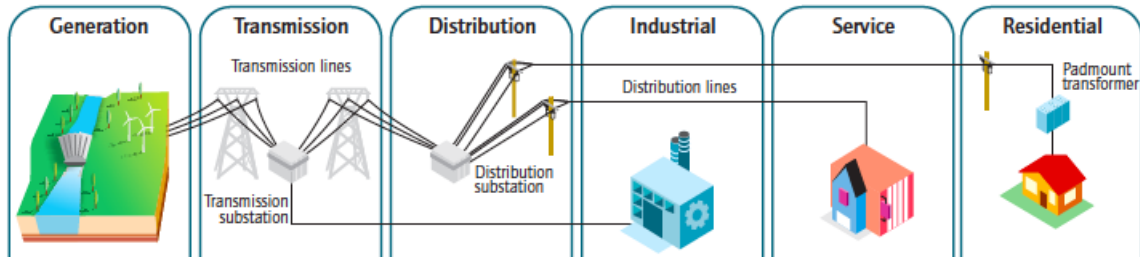


Figure 3.1: Transmission and distribution grid in the energy system. Source: [15]

technical differences between them.

Transmission systems are aimed at carrying electric power over long distances, from power plants to the connection with the distribution system. They are made of power lines, normally attached to high towers or, more rarely, buried underground or below the sea surface, and stations or substations. These latter contain switchgear (circuit breakers and switches to disconnect the line in case of need), measurement instrumentation, communication equipment for metering and remote controlling purposes, and transformers, machines that scale up or down the voltage of the transmitted power [14]. Since power has to be transported over long distances, voltage is kept at very high levels (commonly ranging from 100 kV up to 800 kV, with peaks of 1000 kV in China) This is done because high voltages, at same transmitted power, entail lower current, hence lower Joule losses (proportional to squared current) and smaller diameters for cables, meaning lower costs. High voltage entails also safety hazards, that are prevented through appropriate cable insulation and large clearance from the ground, which in turn affect costs.

Most transmission lines are three-phase alternate current (AC), yet in recent years High Voltage Direct Current (HVDC) lines are becoming an attractive alternative over long distances (more than 600-800 km) because of their lower average losses for long lines and lower right-of-way requirements. As a matter of fact, they need just two cables, yet material savings are counterbalanced by higher initial investment costs, related to the AC-DC conversion equipment. Transformers are used in substations to scale down the voltage and connect transmission network to subtransmission (to connect transmission and distribution, typically shorter and in the order of 100 kV) or directly to distribution lines. From the topologic point of view, transmission lines have a mesh configuration, meaning that there is more than one line connecting two nodes (buses) of the grid, in order to ensure redundancy and satisfy the load even in case of contingency (a power plant or a line goes offline). This configuration, however, makes it difficult to compute exact power flows, increases their interdependency and leads to flows on undesirable paths.

Limits to power flow on a transmission line may be due to three reasons: thermal stability, voltage stability or transient stability. Thermal stability limit is related to thermal operating constraints of power cables: high currents induce heat production (Joule effect) that, in turn, increases the temperature and the resistance losses up to unacceptable limits, that may entail excessive cable dilatation and lack of clearance from the ground. Voltage stability limit depends on the reactance of the line, which induces a voltage drop at the extreme below the security level (typically 95% of the

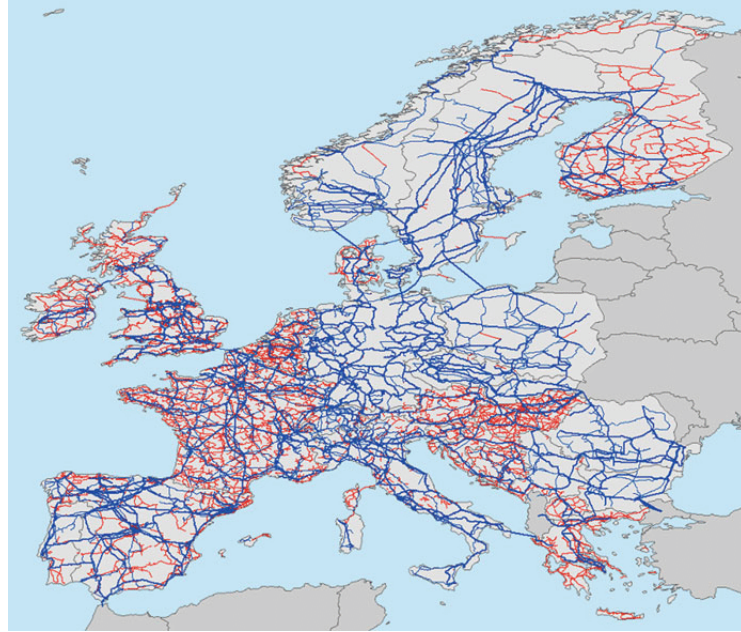


Figure 3.2: European high voltage (220 kV and above) transmission grid. Higher voltage lines in blue, lower voltage lines in red. Source: ENTSO-E

nominal voltage) when power flow trespasses a certain threshold.

The transient stability constraint, finally, is related to steep power flow ramp-ups or downs, causing the generators to fall out of synchronism. Thermal stability limit is usually binding on short lines, while the other two limits impose the maximum power flow. When one or more of these constraints prevent the excess capacity in the lowest-cost generating units from supplying the load a congestion occurs, which may impose stress on the entire grid and obviously entails extra costs for the system.

The purpose of the distribution network, instead, is carrying power from transmission or subtransmission to final users, even though some large industrial consumers directly withdraw electricity from the transmission line and have their own transformers. Distribution cables are either carried on poles or buried underground (the preferred configuration for urban areas). They are different from transmission lines because of their lower voltage level (typically lower than 35 kV), which requires lower ground clearance, and are connected to transmission lines by distribution substations, where a transformer steps down the voltage to the typical primary distribution range of few kV to few tens of kV. They are less automated than transmission lines, hence a lower level of monitoring and control is achievable, to the detriment of line reliability. The lines leaving the substation are called “feeders” and carry three AC phases, that are then divided to supply different load areas in a urban area. Distribution grids are characterized by a radial topology, with only one line connecting the substation and the load. Sometimes the topology is ring-shaped, with two lines linking the same load to the substation, yet one of the two is kept open by a circuit breaker and closed only in case of problems on the other path. Even though distribution networks are designed under the assumption of uni-directional power flows, current spreading in distributed generation technologies is putting pressure on the existing infrastructure and entailed

a re-thinking of existing design practices[15]. Primary distribution transports electricity until the last few hundreds of meters on single phases, then a local transformer, mounted on a pole or buried, steps down the voltage to the secondary distribution level (few hundreds of volts) for general consumption, serving one or multiple customers.

3.1.2 Smart Grids

IEA defines a smart grid as “*an electricity network that uses digital and other advanced technologies to monitor and manage the transport of electricity from all generation sources to meet the varying electricity demands of end-users*” [15]. It is not a single or well defined number of devices, but rather an evolving set of technologies that will spread in different times and modes all around the world, depending on the economical, regulatory and technical context [15] [14], in an evolutionary context.

Technical solutions encompass different technology areas (from material science to ICT) and act at different steps of the electricity supply chain [15], listed in the following:

- Wide-area monitoring and control: it allows to keep power system operation and performance over large areas and in sensitive spots such as interconnections, through Phasor measurement units (PMU) and other sensors. They help optimize power system coordination and behaviour to avoid blackouts and integrate VRE sources through the use of data from system analytics and control technologies. They inform decision making and increase the level of automation in mitigating disturbances.
- ICT integration: the importance of the communication infrastructure, either privately owned by utilities or provided by public carriers, is a powerful instrument to close the time gap in data transmission for real-time operation, especially during outages. Computing power, planning and control software enable two-side information exchange along the electricity supply chain, promoting efficiency and safety at all levels.
- VRE and distributed generation integration: automation and control can help storage management at different levels of the grid (for centralized and decentralized generation) or also avoid disconnection of inverter-based distributed generation in case of sudden fluctuations of voltage or frequency level, which is what would normally happen in traditional grids. This would be particularly dangerous at high shares of distributed VRE generation, and to prevent this from happening Fault-Ride Through (FRT) capability [16] i.e. their ability to remain connected to the grid also in case of fluctuations, is implemented to preserve the grid stability. Moreover, also new relays and protection system algorithms are developed, to allow correct grid management also in presence of distributed generation and bi-directional flows [16].
- Transmission enhancement applications: a number of different applications can improve transmission performance. First there are Flexible AC transmission systems (FACTS) that use power electronics in transmission lines to maximize power transfer capability and defer further infrastructure investment[16]. Then Dynamic Line Rating (DLR), using sensors to monitor the real time carrying capability of a transmission line helps maximize the use of existing capacity without overload risk [15]. Finally, High-temperature Superconductors (HTS) help reduce trans-

mission losses and increase the capacity of existing cables without the necessity to build more [14], even though their market readiness is questionable.

- Distribution grid management: increasing the level of automation where it lacks the most today is instrumental to a more efficient and economic management of distribution grids. Smart sensors, switchers, capacitors and meters at local level can detect outages, automatically reconfigure feeders, optimize reactive power, help preventive maintenance and defer investment decisions.
- Advanced Metering Infrastructure (AMI): smart meters allow bi-directional flow of information between customer and energy provider, in a way that benefits both the parts. On the one hand, the customer can receive more refined price signals and modify its consumption behaviour according to them, detect sources of losses or improve its energy management. The retail energy service, on the other hand, can retrieve more accurate and refined data on energy consumption, monitor power quality, react in real time in case of outages or thefts and manage its revenues through more effective consumption accounting and debt management [15].

Besides “smartening” and updating existing grids, also pooling VRE production over large geographical areas can help mitigate their inherent variability, related to weather conditions [17]. Grid pooling requires further investments for improving grid inter-connections, at national and international level. This benefits the system stability, smoothing VRE generation and reducing gradients in the residual load, so that less flexibility is needed from the non-VRE power fleet. Pooling is in turn favoured by the introduction of ICT and smart control systems at transmission and distribution level [14], which may ease national and international cooperation in balancing operations [17].

3.1.3 Choice of cost and performance parameters for grid

The aim of this subsection is presenting the reasons behind our modeling choices for the grid and describing how the characteristic cost and performance parameters implemented in WITCH have been derived. Firstly, we decided to differentiate the installed grid capacity between transmission and distribution lines. The distinction is very general because the high spatial aggregation of the WITCH model makes impossible to describe in more detail the grid structure in terms of load locations and connections with generation plants. Thus, all the results concerning capacity have to be intended just an approximation of the actual values that are useful to understand the order of magnitude of the needed investments.

Required grid capacity is considered linearly proportional to the installed generation capacity, as it was previously done in WITCH and it is done in other IAMs (see Section 2.4.4). Since in the associated literature, grid capacity is usually expressed in terms of kilometers of lines (together with the line voltages and the MVA capacities of transformation), we decided to adopt this unit of measure. Thus, a first important parameter characterizing the grid and differentiating between transmission and distribution is the constant of proportionality that links the installed grid capacity in km and the installed generation capacity in TW . We called it “grid requirement” and it represents

the numbers of kilometers that have to be installed on average for each TW of generation capacity. Values for the overall installed km of transmission and distribution lines for some regions have been derived from different literature sources: *china* [41] (in 2013 9.8 mln km of distribution and 700'000 km of transmission); *neweuro* [42] (in 2013 1.6 mln km of distribution and 50'000 km of transmission); *oldeuro* [42] (in 2014 7.4 mln km of distribution and 230'000 km of transmission); *te* [41], [43] (approximated with Russian Federation: in 2015 2.2 mln km of distribution and 140'000 km of transmission); *usa* [13], [41] (in 2014 11.4 mln km of distribution and 650'000 km of transmission). The installed total generation capacity for these regions (in the respective years) have been derived from the IEA Database [44]. From these data, the transmission and distribution “grid requirement” for these regions have been calculated. For the other regions, due to a lack of data about the installed grid capacity, the “grid requirement” has been assumed equal to one of the known regions on the basis of geographical configuration and load centers distribution similarities. In table 3.1 the values for all the different WITCH regions can be found. In absence of information about a foreseeable future pattern, we considered the “grid requirement” value constant over time.

	Grid Requirement [km/TW]	
	Transmission	Distribution
cajaz	604'017	10'626'365
china	700'000	9'800'000
easia	604'017	9'800'000
india	604'017	9'800'000
kosau	604'017	10'626'365
laca	604'017	10'626'365
mena	604'017	10'626'365
neweuro	433'629	14'020'658
oldeuro	295'870	9'566'466
sasia	604'017	9'800'000
ssa	700'000	9'800'000
te	257'432	4'057'249
usa	604'017	10'626'365

Table 3.1: Grid requirement values for all the WITCH regions. It stands for the km of transmission or distribution lines required per 1 TW on installed generation capacity on average.

The other relevant parameter distinguishing between the two types of grid is the installation capital cost of the grid lines. It is expressed in $\$/km$ and it has been assumed uniform among the regions, due to lack of data and to the fact that it is already an average value due to high actual dependence of the grid installation costs on the single project characteristics. For the transmission lines the capital costs has been calculated as the sum of two components: the building cost of installation per km of lines and the capital cost of the associated substation per MVA. The values found in the literature have been converted in $\$/km$.

In particular, the average building cost of 1 km of transmission line (629'020 $\$/km$) has been derived from costs values for lines with voltages between 220kV and 400 kV [45].

The cost of each substation (35'950 \$/MVA), instead, has been considered has the median cost of an AC onshore substation [45]. From data about the italian grid [46], we derived the average MVA of substation capacity installed per 1 km of transmission lines (2.181 MVA/km), thus calculating the average costs for substations per 1 km of line. The overall installation capital cost for 1 km of transmission line results to be 707'420 \$/km.

As regards distribution lines, the average installation capital cost for 1 km of line has been derived from the literature and it is equal to 25'000 \$/km [47].

Concerning the thermal losses on grid lines, we represented them as average overall losses on the whole electric system without differentiating among the grid types. We did so for modeling reasons in order to define the losses just as a reduction of the electricity generation actually entering in the calculation of the monetary value of energy and contributing to the creation of the economic output. This results in the differentiation between the electricity generated and the one that is actually consumed (after the losses) and so can participate in the production function.

The regions have been divided in three different clusters with distinct average grid losses according to the World Bank DataBank: developed, developing and under-developed regions. Developed regions present average losses on the grid network equal to the 6% of the overall electricity generation, while developing and under-developed regions 9% and 12%, respectively. [48]. A linear decrease of the losses values over time has been assumed from their observed historical path [13]. For the different group of regions, we assumed distinct reduction paths. In particular, for developed regions losses decrease to the 4% of generation in 2050 and then remains constant. For developing regions they lower to 6% (initial level of developed ones) in 2050 and then keep constant. While under-developed regions losses reach the 6% of generation just in 2100. Table 3.2 summarizes all this information.

	Grid Losses [% Tot Generation]		
	2015	2050	2100
Developed: cajaz, china, kosau, oldeuro, usa	6%	4%	4%
Developing: easia, laca, mena, neweuro, te	9%	6%	6%
Under-developed: india, sasia, ssa	12%	9.5%	6%

Table 3.2: Grid thermal losses as percentage of the overall electricity generation in the different WITCH regions.

Finally, as regards grid “smartening” and upgrades for VRE integration, together with further interconnections to promote VRE pooling, they have all been represented in the model as additional needed investments in grid. No associated installed capacity is defined. In Section 4.3.3 a detailed description of how we modeled this aspect can be found.

3.2 Storage technologies

This section contains an overview of the main electricity storage technologies, that anticipates the motivations of our technology choices while modeling storage in WITCH. The section follows the same subdivision [49] adopted in the IAM we used: on one side we present short-term storage, defined as the technologies that store the energy excess resulting from a demand-supply mismatch on a minute-to-daily scale (e.g. electrochemical batteries for relieving T&D congestions in critical buses) and the same time scale applies to the average amount of time they keep this energy stored before discharge; on the other side, seasonal storage deals with demand-supply mismatch on a seasonal scale (e.g. power-to-gas conversion of excess wind generation during winter, to use the stored fuel during summer when, in some regions, demand is higher).

3.2.1 Functioning principle and applications

Before any further discussion is started, though, it is useful to describe the main components of a general storage device and its working principle [50]. A storage device is made up of:

- Storage medium: this is a means or system through which energy is stored.
- Charging: this unit permits the flow of energy from the electrical network to the storage medium.
- Discharging: it ensures the delivery of the stored energy when demanded.
- Control: it governs the entire storage system. Figure 3.3 illustrates the architecture of a generic storage device.

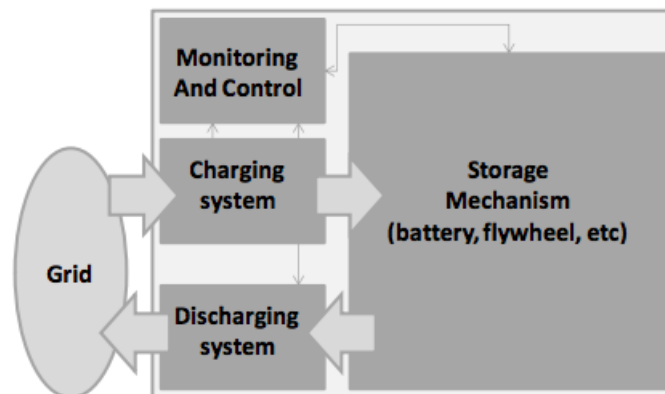


Figure 3.3: Components of an energy storage system. Source: [50]

Due to its capability of accumulating energy, keeping it inside for a variable amount of time (largely depending on the technology type) and then releasing it when needed, storage is suitable for many different applications, other than the already mentioned role in VRE integration (see Chapter 1). Many of these applications can be provided at the same time by a single storage utility. The non-exhaustive list that follows does not include thermal energy storage applications, whose discussion lies beyond the scopes of our work:

- Arbitrage: storing energy at times of low demand (and price) and selling it when

profitable, typically at time of high demand, in two different energy markets (when this happens in the same energy market, it is referred to as storage trade)

- Frequency regulation: ensure the instantaneous balance between energy demand and supply, whose variation induces oscillations in the AC frequency, that must be kept within a security range. It requires a response time of seconds to minute.
- Load following: ensuring the demand-supply balance in normal operating conditions, balancing fluctuations on a time basis of 15 minutes to 24 hours.
- Voltage support: injecting or absorbing reactive power to maintain safe voltage conditions in the electricity grid.
- Black start: helping the electric power system to recover after a black out, by providing the power necessary to restart the traditional units in absence of any other ancillary service available.
- Transmission and distribution (T&D) congestion relief or investment deferral: shifting in time or space an excess of generation (typically by VREs) to avoid congestions in the T&D infrastructure or to defer in time very expensive investments in long-lived assets
- Demand shifting and peak reduction: accumulating energy when actual demand is low or when VRE generation is not fully exploited and releasing it when needed helps shaving the peaks in the residual load curve
- Off-grid applications: storage can support the diffusion of decentralized VRE installations by storing overproduction and reducing or avoiding withdrawals from the grid. This is particularly valuable in islands or areas that lack a grid infrastructure, as storage can ensure their independence from imports of fossil fuels.
- Spinning and non-spinning reserve: compensating for the reserve capacity that is in charge of compensating for rapid and unexpected contingency events (e.g. plant outages, line outages) that may jeopardize the system security. The response time after the outage is the metric to distinguish between spinning (less than 15 minutes) and non-spinning reserves (more than 15 minutes).

These possible applications may pave the way to a potentially profitable use of storage utilities in spot and ancillary services markets [19], and the growing interest towards the introduction of capacity markets in many countries is a further source of optimism [24].

3.2.2 Short-term storage

In answer to our first research question about which storage technologies are more suitable for being included in long-term models, we start providing an overview of the main Short-Term Storage Energy Technologies (STESTs). The aim is better understanding and justifying our modeling choices that will be introduced later.

There are several ways to classify STESTs, from physical working principle [21] (mechanical, electro-chemical, chemical storage etc.) to level of commercial maturity (commercialization, demonstration, resource and development) [20].

We choose to classify them according to the category of applications they belong to, that largely depends on the discharge time of the technology, defined as the amount of time a storage device can continuously provide its rated power to a load, starting from

a full charge condition [19]. The three categories are: power quality, bridging power, energy management. These are the subjects of discussion in the following.

Power quality

It is the necessity to provide sinusoidal power with acceptable voltage and frequency, so as to guarantee a safe operation of the loads and the devices along the entire electricity supply chain [51]. These applications requires a fast response (in terms of milliseconds) and a discharge time in the order of seconds to minutes [23]. The most suitable technologies for this application are listed below.

- **Capacitor:** it offers a direct storage of electricity through two parallel plates separated by a dielectric material. They store electricity at a very fast rate, possessing several thousand charge/discharge cycles without material degradation compared to batteries, and their typical power rating is less than 1 MW. Their main shortcoming is the low energy density, which has enhanced research on a new technology, that of Supercapacitors: they store energy over larger surface areas through an electrolytic solution between two plates, reaching higher values of energy density. The high self-discharge losses, however, limit them to short-time applications [23].

- **Flywheel:** it is an electro-mechanical device where a revertible electric engine converts electrical energy it into kinetic energy of a cylinder, rotating on magnetic bearings in vacuum, to minimize friction losses. It reaches a very high efficiency (90-95%) and a lifetime in the order of several thousands of cycles. This notwithstanding, self-discharge and losses are very high, and limit its applications to short-time and power intensive ones [23].

- **Superconducting Magnetic Energy Storage (SMES):** an innovative technology that converts electrical energy allowing a DC current through a superconducting coil (kept at -269 °C), which induces a magnetic field. This entails extremely high efficiency (up to 98%), just a few milliseconds to switch from discharge to charge and long lifetime (>20 years), yet concerns related to short discharge time, costs and safety still limit its diffusion [23].

Bridging Power

These applications include providing contingency reserves, load following, and other reserves for issues that require fast response and a maximum discharge time in the order of one or few hours, while the typical power rating is 0.01 – 10 MW. Many battery technologies are suitable for these applications, even though the high frequency cycling it requires may reduce their performance and lifetime (and this prevents them from being used in Power Quality applications).

The general working principle of a battery is illustrated in figure 3.4: it is an electro-chemical device made of a number of cells connected in series. Each cell is composed of four main parts: the two electrodes (negative and positive) are separated by an electrolyte and connected through an external circuit. During discharge, the compound that forms the negative electrode undergoes an oxydation reaction (i.e. loses electrons) and generates positive ions. The positive ions travel through the electrolyte and reach the positive electrode, where they undergo a reduction reaction, acquiring an electron (that has travelled through the external circuit) and forming new compounds at the

positive electrode. During discharge, the inverse reaction occurs. This phenomenon induces an electric field in the order of few Volts, and stacking the single cells allows to have battery packs ranging from tens to tens of thousands of Volts. Battery types differ in electrode and electrolyte types and materials, which in turn influences their performance and durability. Some key parameters that characterize battery performance are:

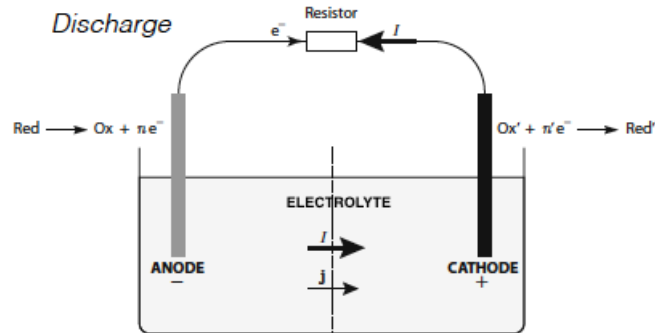


Figure 3.4: Working principle of a battery technology in discharge phase.

round trip efficiency (RTE), state of charge (SOC, the ratio between available battery capacity and nominal battery capacity); nominal voltage between the electrodes at full SOC; lifetime in number of charge-discharge cycles the device can stand; power and energy density in $\frac{W}{kg}$ and $\frac{Wh}{kg}$; energy-to-power ratio, intended as the amount of energy that can be stored by the device per unit of nominal power capacity.

The most widespread technologies for bridging power applications are:

-Lead-acid batteries: they are the oldest and most widespread battery type, advantaged by their low cost. During charge, the electrodes are made of lead (Pb) and lead oxide (PbO₂), while the electrolyte is sulphuric acid (H₂SO₄); during discharge, lead sulphate (PbSO₄) is produced both at anode and cathode, while the electrolyte is water. Lead acid batteries have a good round trip efficiency (70-90%), yet they are limited by low nominal voltage (about 2V), low cycle lifetime (around 2000), toxic sub-products and very low specific power and energy.

-Ni-Cd batteries: the most popular utility-scale nickel-electrode technology, presents drawbacks as regards cycle lifetime (2000-2500), energy density and environmental hazard, due to toxic cadmium-based materials.

-Metal-air batteries: batteries with an open configuration, made of alkali metal anode, aqueous or organic electrolyte, separator (allowing ion reactions) and air cathode. Most of these batteries feature high energy density and are environmentally friendly, but so far they have very low round-trip efficiency and poor recharging capacity [52].

-Lithium-ion batteries (LiB): it is a relatively old technology that has widespread applications in electronics (laptops, tablets, smartphones), Plug-In Hybrid and Full-Electric Vehicles and power grid applications. The negative electrode is made of highly-conductive graphite plates and lithiated carbon (depending on the battery State of Charge), the positive electrode is made of a lithiated metal oxide (such as Manganese, Cobalt or Nickel) and the electrolyte is a lithium salt dissolved in an “organic carbonate” solvent (see figure 3.5). They are closed systems (no external flow or reactants or products) with fixed energy-to-power ratio. The key features of Li-ion batteries,

that distinguish them from the above-mentioned technologies, are higher RTE (about 85%), considerable nominal cell voltage (up to 4.2 V), higher energy and power density ($120\text{-}160 \frac{\text{Wh}}{\text{kg}}$, $200\text{-}300 \frac{\text{W}}{\text{kg}}$) and fairly good cycle lifetime (up to 5000-10000 cycles). On the other hand, the main concerns (especially in power grid applications) regard costs and safety, as internal failures may trigger steep temperature increase and the related fire hazards [53].

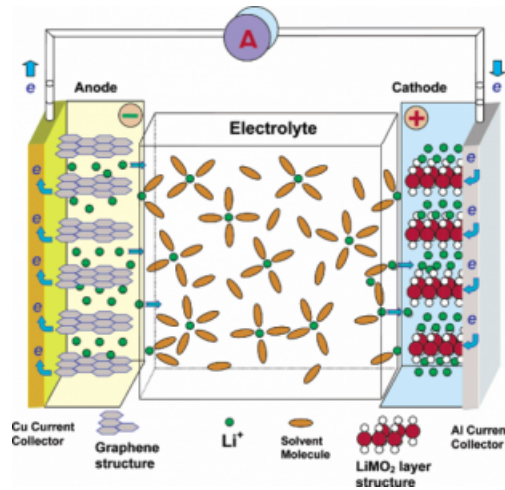


Figure 3.5: Main components of a Li-ion battery. Source: [54]

Energy Management

Storage technologies for energy management should be able to shift power over longer time scales, to provide services such as load leveling or T&D investment deferral. This requires discharge times of several hours and typical applications have a rated power ranging from tens of MW to 1 GW, depending on the technology. The main ones are: **-High energy batteries:** this is the definition for a broad class of batteries that can reach a high energy-to-power ratio, hence the possibility to discharge several hours at their nominal power. On one hand we have high temperature batteries such as Sodium-sulphur batteries (NaS) and sodium-nickel chloride (or ZEBRA) batteries. The first one is a very high power and energy technology, featuring respectively molten sulphur and sodium at the electrodes, separated by a ceramic electrolyte. Ensuring optimal operation requires an external heat source, to keep the battery around 300-350 °C and discharge losses are considerable (around 20% per day). ZEBRA batteries have a similar heat requirement, even though they can operate also at ambient temperature. On the other hand we have Redox Flow Batteries, mainly processing a vanadium-based ionic solution.

Redox Flow Batteries (RFB) have no external heat requirement, moreover energy and power rates can be designed separately, since the ionic vanadium solutions at the electrodes are stored in separate tanks (whose capacity determines the energy characteristics of the battery), while power depends on the number of stacked cell in the “reactor”, the actual device where electro-chemical reactions occur. This requires a pumping system connecting tanks to reactor (which may limit reliability) and requires large volumes, decreasing the energy density of the battery. Moreover, RFB batteries

have not reached considerable commercial application so far [20],[55].

-Liquefied Air Energy Storage (LAES): electricity is used to liquefy air in a cryogenic process; liquid air is then stored in a tank, and brought back to a gaseous state (by exposure to ambient air or with waste heat from an industrial process) and flows through a turbine to produce electricity. LAES systems feature off-the-shelf components with long lifetimes (30 years or more), entailing low technology risk. The main concerns regard the efficiency (about 60%) and the response time (5 minutes from shutdown), lower if compared to batteries, and the current technology maturity level [52].

- Compressed Air Energy Storage (CAES): it is a mechanical storage technology that works converting electricity into air high pressure through a compressor, storing the air in a reservoir (most commonly an underground cavern) and then heating up the air and expanding it in a turbine to generate electricity when needed [23]. There are various plant configurations to realize this seemingly simple process [56]: CAES is classified as diabatic, adiabatic or isothermal, depending on how compression heat is treated and how air is treated before being expanded.

In the diabatic CAES (D-CAES) configuration, air at ambient conditions goes through one or more compression stages (usually intercooled), it is re-cooled before leaving the last compression stage and stored in an underground cavern. In the discharge phase, compressed air is first throttled at a fixed pressure, then it enters a high pressure combustion chamber, where natural gas or oil are burnt to heat it up. Heated air is expanded in a high pressure turbine, then reheated in a second combustion chamber and further expanded in a low pressure turbine. There are two existing and operating D-CAES plants in the world: the first and oldest is in Huntorf (Germany, active since 1978, retro-fitted in 2006) [57], the second in McIntosh/Alabama (USA, active since 1991) [58]. The main technical difference between the two is the exhaust-heat recuper-

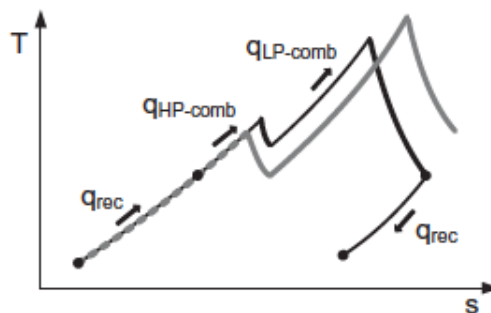


Figure 3.6: Temperature-entropy diagram for the two D-CAES plant: Huntorf (grey) and McIntosh (black). Starting point: air leaving the storage cavern. Source:[59]

ator present only in the American plant (see fig. 3.7), thanks to which the exhausts leaving the low pressure turbine pre-heat the high pressure air before it enters the first combustion chamber, saving fuel. Another clear difference regards the applications of the two plants, as suggested by the two different discharge times: Huntorf has a full-load discharge time of 2 hours and was conceived for reserve power and black-start services, while McIntosh can provide full power for 24 hours at full charge and is mainly designed for load-shifting on a weekly basis. Figure 3.7 illustrates the plant scheme of

McIntosh D-CAES facility. The main disadvantages of the D-CAES configuration are:

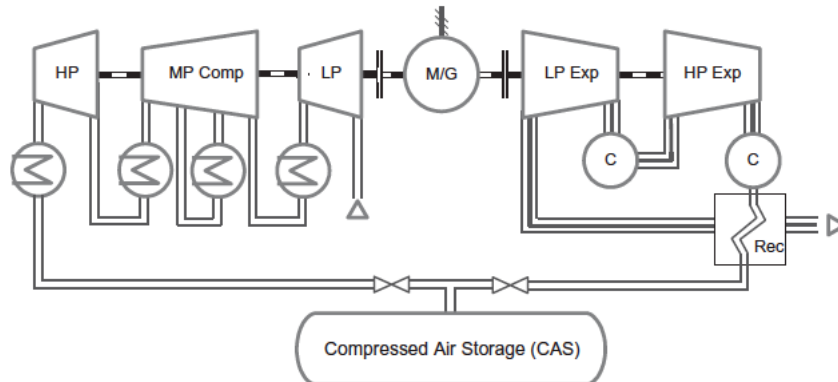


Figure 3.7: Plant scheme of the McIntosh D-CAES facility (1991). Source:[59]

the necessity of an external fuel supply, defining them as a hybrid storage-generation technology, the efficiency penalties this configuration entails and the climate concerns regarding the necessity to emit greenhouse gases in order to power a technology that should help the transition towards cleaner energy solutions.

This concerns fostered research and development activities towards Adiabatic CAES (A-CAES), where the combustion chamber is replaced by a thermal energy storage section using the heat of compression to heat up compressed air before expansion, eliminating the need for fuel supply. We can distinguish between A-CAES without or with energy storage: the former version can be realized just at laboratory scale, due to the fact that even low compression ratios would entail very high air temperatures (about 277°C if air is reversibly compressed at just 10 bar) that salt caverns or similar air storage reservoirs could not withstand. Most of the research is therefore focused on A-CAES with thermal energy storage (TES), even though the storage medium and the proposed plant configurations strongly depend on the maximum air temperature at the compressor outlet.

A more detailed investigation of these technical aspects would be outside the scopes of this work and has already been carried out by Budt et al. ([56]): it highlights pros and cons of high, medium and low temperature applications and concludes that the medium-temperature configuration is the most interesting one at the moment.

Too high temperatures (above 400 degrees Celsius) would in fact require special stress-resistant materials, a complex system engineering and a lot of research to design an electrically-driven compressor, while low temperatures (below 200 degrees) would require an extremely complex plant design with heat exchangers between each of the many compression and expansion stages. Medium-temperature A-CAES appears as good compromise since it can use off-the-shelf compressors and TES media already adopted in other applications, such as molten salt or thermal oil, and even though no commercial applications are available, most of the current research is focused on this alternative [59],[60].

The plant scheme of this configuration (see figure 3.8) shows that during charge air undergoes two (intercooled) compression stages, then is cooled down in the first TES, undergoes a third compression stage, heats up a second TES and is finally stored in the

reservoir. During discharge, compressed air exchanges heat with the two TES systems and is finally expanded in the turbine.

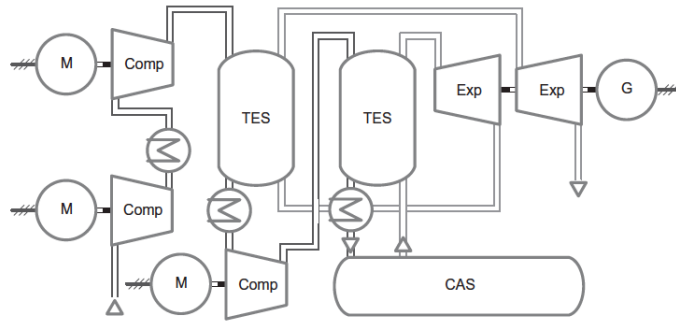


Figure 3.8: Plant scheme of a medium-temperature Adiabatic CAES configuration. Source:[59]

Finally, Isothermal CAES (I-CAES) would require both compression and expansion to be realized at constant (ambient) temperature [61], thus continuously subtracting heat from the former phase (to reduce compression work) and providing the same heat to the latter. Nevertheless, at the moment there is no available machinery able to perform such an operation with acceptable performance, and much of the research in this field is focused on piston machinery (performing a slower compression/expansion, more suitable for heat exchange) and suitable heat exchange processes, though there are only concepts or laboratory-scale applications [62].

As regards the compressed air storage facility, the dominant technology is salt caverns, whose behaviour is known for decades from the storage of natural gas and whose construction is a state-of-the-art procedure [56]. Large-scale storage alternatives are aquifers and high pressure tanks, that are not location-dependent [63].

- **Pumped Hydro Energy Storage (PHES):** PHES is the only commercially-proven large-scale storage technology, with more than 300 plants and almost 100 GW of installed capacity worldwide [64]. Its rise started during the early seventies, when the need for flexible generation to counterbalance base load nuclear power plants or for providing ancillary services drove installations in the United States, Europe and Japan above all. Nevertheless, today a renewed interest in PHES is driven by security-of-supply reasons, by the necessity of more peaking plants in liberalized energy markets and, even more, by the increasing shares of VRE generation [65],[64] and their effects on energy systems, discussed in Chapter 2.

The working principle of this technology is very simple, as it stores electrical energy in the form of hydraulic potential energy, pumping water from lower to higher reservoirs, thus increasing its geodetic height [23] (see fig 3.9). The reservoirs can be upper and lower basins connected by a steep duct, a river interrupted by dams or even a reservoir connected with the sea [66].

As regards the pump-turbine machinery, in the past a fix-speed pump-turbine was the most widespread (e.g. the Francis type connected to a synchronous motor-generator), whereas today variable-speed machinery with asynchronous generator are considered the most appealing technology (fig. 3.10). As a matter of fact, they improve the operating pump-turbine efficiency at many different load levels, the achievable low-regime functioning helps avoid start-and-stops and, in pumping mode, these plants are also

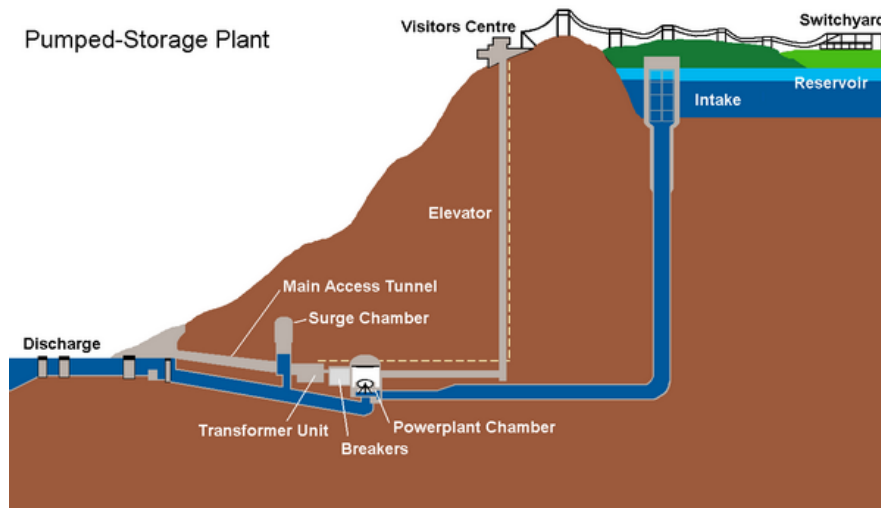


Figure 3.9: PHEs plant layout. Source: Tennessee Valley Authority

suitable for frequency and voltage regulation [67].

Despite being a very mature storage technology with high RTE (varying between 70

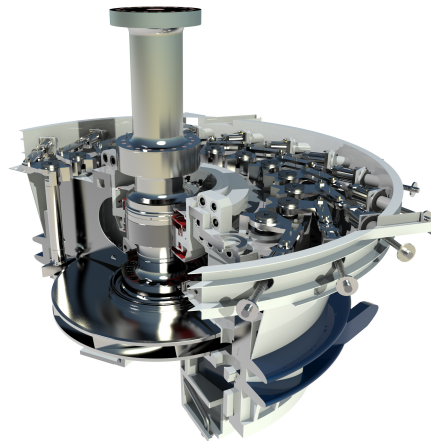


Figure 3.10: Variable speed pump-turbine section 3D rendering. Source: GE Renewable Energy

and 85% [64]), often the largest potential in terms of rated power and storable energy and lower average capital and O&M costs with respect to other storage technologies, a number of drawbacks will probably limit its future application. First and foremost, PHEs is limited by a geographical resource availability constraint [68], as natural basins and sites for new, artificial ones are becoming scarce in most of the regions; then high geographical and project-specificity of each installation, whose cost and construction time may strongly vary depending on the single project; finally, land-use and biodiversity concerns limit its environmental-friendliness and social acceptance [69].

3.2.3 Choice of cost and performance parameters for short-term storage

This subsection brings about the motivations behind our choice to represent three short-term electricity storage technologies: PHEs, A-CAES and Li-ion Batteries. Af-

ter this explanation, cost, performance and market-constraint choices for the selected technologies are introduced, motivated and presented in two tables (3.3, 3.4).

The first criterion for the technology choice is the compatibility with WITCH level of temporal detail and stylized representation of complex phenomena. WITCH has a temporal resolution of one year and 5-year time steps, and the level of time detail is improved by equations that represent short-term dynamics derived from hourly-resolved models (flexibility and capacity coefficient, see sections 2.4 and 4.1). Therefore it is however characterized by the impossibility to capture the second-to-minute dynamics that regulate power quality applications (see 3.2). For this reason, it does not make sense to model technologies such as flywheels, capacitors or SMES.

As regards technologies used in bridging power applications, their characteristic dynamics can be more easily represented, especially for those technologies and uses that entail discharge times close to one hour, such as the provision of power to allow smoother ramp-ups of flexible thermal plants in response to steep residual load variations. Finally, technologies for energy management contribute to satisfy firm capacity requirements, load shifting over periods of several hours and their dynamics can be captured in a schematic way by WITCH, especially with the formulation detailed in section 4.1. Among the storage technologies for bridging power and energy management, the chosen ones have been Li-ion batteries, adiabatic CAES and PHEs for a number of reasons here listed:

- Commercial maturity: figure 3.11 represents the level of maturity and associated capital risk of many storage technologies. As visible, PHEs is a very mature and low-risk technology, while LiB have witnessed the first commercial large-scale utility applications[70]. Adiabatic CAES is at a less advanced stage, but the growing interest towards CAES (that enjoys the second largest installed capacity among e-storage technologies [20]) and the level of maturity of the “mother” technology (diabatic CAES, described in the previous section) may facilitate its deployment. Moreover, some demonstrations of the A-CAES technology are already in place [23] and are regarded as one of the preferable options in a high VRE energy system [71].
- Future perspectives: as said in the previous section, both PHEs and D-CAES are limited in their development mostly by resource availability (the first) and environmental concerns (the second), therefore research is focusing on a-CAES as a potential low-carbon alternative for large scale storage option, especially in view of the increasing share of VRE generation in many regions [23],[22]. Also Lithium-ion batteries enjoy some competitive advantage over other batteries due to their higher efficiency, low-temperature functioning, energy and power density. Moreover, their costs and lifetime concerns are being faced by targeted R&D programmes [72] and may benefit from mass production of EV power units.
- Completeness in storage representation: as visible in figure 3.12, representing LiB, CAES and PHEs allows to cover a wide band of energy capacity and discharge time, providing a satisfactory representation of energy storage applications in general. CAES bridges the gap between PHEs and LiB in terms of discharge time, scalability and dependence on resource availability (constrained by the availability of salt caverns if large-scale solutions are chosen [56]).
- Analogy with other IAMs: the only other ADVANCE IAM (see section 2.3.1)

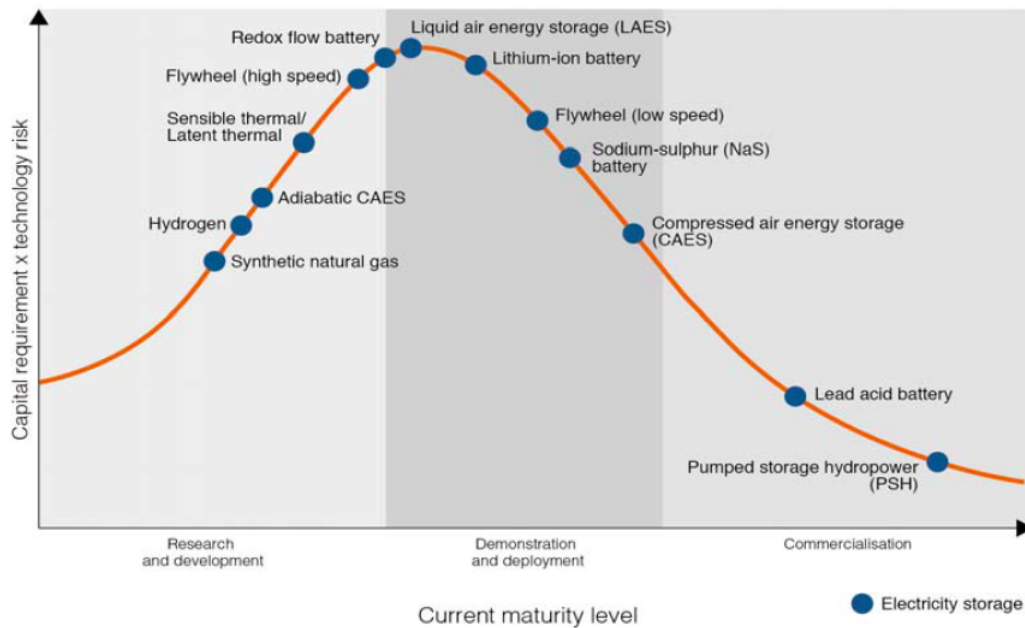


Figure 3.11: Capital x technology risk vs level of commercial maturity for many storage technologies. Source:[20]

that features a detailed short-term storage technology implementation, POLES [24], [33], shows exactly the same technological differentiation, asserting similar motivations for the choice. Moreover, by varying the key performance parameters

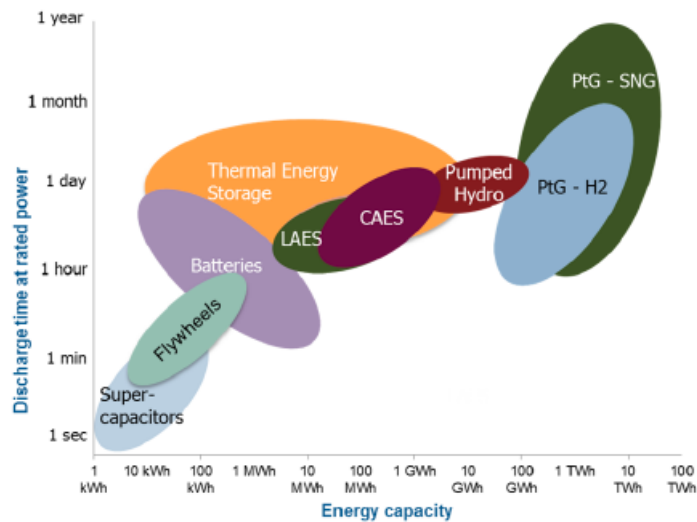


Figure 3.12: Mapping storage technologies according to discharge time at rated power and energy capacity. Source:PwC, (2015), following Sterner et al. (2014)

of Lithium-ion batteries (efficiency, cost, energy-to-power ratio etc.) it is possible to schematically represent other battery technologies such as NaS or RFB. Given this technological choice, the following step is gathering data about costs and performance parameters to feed as initial parameters in WITCH. Regional installed capacity (in GW) at year 2005, 2010 and 2015 come from IRENA 2017 Renewable Capacity Statistics report for Pumped Hydro [73], while data for CAES

and batteries come from DOE Global Energy Storage web Database [74]. All of them are reported in Appendix E. As regard costs, we relied on the extensive literature review provided by Zakery et al. (2015) [75], that presents capital cost divided into energy and power part of each energy storage technology, plus fixed (depending on installed capacity) and variable (depending on stored energy) Operation and Maintenance costs. Each of these cost are organized in ranges: for capital costs we used the median value as medium cost assumption (mid), the value on the first quartile as minimum cost (min), and the value on the third quartile as maximum; this is done to avoid outliers and have a variable yet reliable representation of the cost range. The mid cost is used as default value, while min and max values are used in the sensitivity analysis described in Section 5.3. As regards O&M costs, we chose just the median value to represent them, given the small variability within the range and their lower weight with respect to capital costs. Table 3.3 summarizes all cost assumptions for short-term storage technologies. Costs have been converted to 2005 US Dollars, the money unit in WITCH.

Technology	Energy cost $\frac{\$05}{kWh}$			Power cost $\frac{\$05}{kW}$			O&M cost	
	min	mid	max	min	mid	max	var $\frac{\$05}{kWh}$	fix $\frac{\$05}{kW}$
PHES	41.51	68.85	116.44	424.26	534.63	837.38	0.00032	4.66
CAES	30.38	40.50	47.59	704.74	853.58	939.65	0.0045	3.95
LiB	684.49	804.98	1158.36	403.00	461.81	536.65	0.0030	6.99

Table 3.3: Cost data for short-term storage technologies. Variable O&M costs are intended per unit of energy, while fix ones are per unit of power.

The choice of reliable values for performance parameters stems from an extensive literature review and, in absence of reasonable sources or where considered appropriate, from personal assumptions of the authors. Table 3.4 lists all the performance parameters used for modeling short-term storage. Some of them will be subject of specific sensitivity analyses in Section 5.3.

The first key parameter is the Round Trip Efficiency RTE, defined as the ratio be-

Technology	RTE	Lifetime (yrs)	Lifetime (cyc)	Cycle disch. time
PHES	0.775	55	30000	-
CAES	0.54	35	20000	2.6
LiB	0.85	12.5	3000-6500	2
	Full prod h	E2P ratio	FlexC	CapC
PHES	457-1202	9.8	0.75	1
CAES	1486	7.8	0.75	1
LiB	480-1040	2	1	0.8
	Learning rate	Floor cost		
PHES	0	-		
CAES	5%	half initial cost		
LiB	12%	half initial cost		

Table 3.4: Short-term storage technologies: values of the parameters implemented in WITCH.

tween the energy discharged over the energy charged by the specific storage technology

during a charge-discharge cycle, at the end of which the state of charge of the device must be equal to the initial one. The specific literature provides values between 0.7 and 0.85 for PHEs, hence an intermediate value of 0.775 has been chosen [24], [75]. The same worked for Li-ion batteries, whose RTE range is between 0.8 and 0.9, hence the choice of 0.85 [22],[23]. As regards A-CAES, the choice of a value has been complicated by the absence of real commercially-proven data, yet the value of 0.54 has been chosen for two reasons: first, it represents the lower bound of the efficiency range for medium-temperature adiabatic CAES plants, estimated by the literature review in Budt et al. ([56]) and shown in figure 3.13.

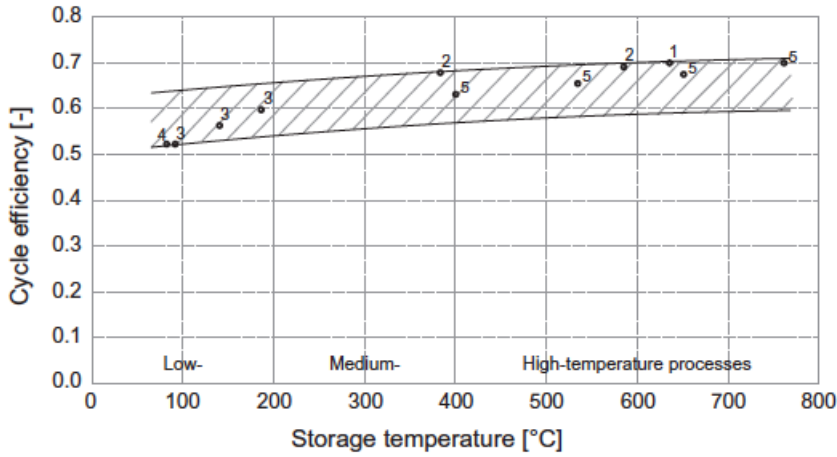


Figure 3.13: Mapping storage technologies according to discharge time at rated power and energy capacity. Source:PwC, (2015), following Sterner et al. (2014)

Second, it is McIntosh plant’s efficiency [58] and, even though it is a D-CAES configuration, represents today’s highest efficiency of a commercial CAES facility, so it appears a conservative assumption. A sensitivity analysis with different values of the RTEs is performed in section 5.3.

Then comes the lifetime, expressed both in number of years and number of cycles. The former is more relevant for PHEs and CAES, as mechanical storage technologies can easily withstand several tens of thousands of cycles (30000 and 20000 cycles respectively), and a useful life of 55 and 35 years, respectively, has been assumed for the two technologies [22],[24]. The latter is particularly relevant for batteries, whose performance is affected severely by the number and severity of charge-discharge cycles, due to its electro-chemical working principle [76]: a value that starts from 3000 cycles and grows linearly to 6500 cycles has been chosen to represent technological progress in this field [22], with a useful life of 12.5 years. To define the hours of full power production (Full prod. h) for CAES and batteries, we used an equivalent metric (see eq. 3.1, defined as the product of the average “Cycle discharge time” times the number of cycles a storage technology can perform in one year, obtained dividing the lifetime in cycles by the lifetime in years (and assuming a constant number of cycles per year).

$$Full_prod_hours_{stor}(t) = \frac{lifetime_cycles_{stor}(t)}{lifetime_years_{stor}} \times Cycle_disch_time_{stor} \quad (3.1)$$

Where the average ‘‘Cycle discharge time’’ values are 2.6 hours for CAES and 2 hours for batteries, from [24].

Full production hours for PHES, instead, are derived from the IRENA 2017 Renewable Capacity Statistics report for Pumped Hydro [73], reported in Appendix E . The available data are the values of installed PHES capacity in MW and the electricity generated by PHES in GWh for the years between 2005 and 2016 in all the countries where this technology is present. From these data, we calculated the annual full production hours dividing the electricity generated by the installed capacity. The found national values have then been averaged (among the countries belonging to the same WITCH region) to compute the regional values for the WITCH 13 regions. After that, we selected the average, the minimum and the maximum values, with the aim of carrying out a sensitivity analysis on this parameter. Note that, within the model, this parameter is maintained constant along the years as an assumption.

Another important parameter is the average energy-to-power ratio, the ratio between energy and power-based installed capacity for each storage technology: it is kept constant as a simplifying assumption, even though it is highly variable for those technologies in which the energy and power capacity can be designed separately according to the expected utilization pattern or the available reservoir (PHES, CAES, RFB etc.), while it is just slightly variable for closed systems such as Li-ion batteries, due to technical reasons. After considering data from existing plants we decided to assume values of 9.8, 7.8 and 2 respectively for PHES, CAES and battery.

The average energy-to-power ratio is used to calculate the initial overall capital costs in terms of $\$/kW$ from the distinct capital costs for the energy and power parts of each short-term storage technology (Table 3.3) as follows:

$$Cost_{tech}(t_0) = Power_Cost_{tech}(t_0) + Energy_Cost_{tech}(t_0) \times avg_EtoP_ratio_{tech} \quad (3.2)$$

As regards the capacity and flexibility coefficients used (see section 2.4.1), since no specific values for the different technologies were available in previous studies, a qualitative reasoning has been necessary. We assume that the two functions that storage can provide in this stylized representation peak load supply (represented by the capacity equation) and flexibility supply (represented by the flexibility equation) are complementary just up to a certain point and then become substitute i.e. they are in competition. We can explain this assuming that storage can supply flexibility and this flexibility requirement can partially coexist with the need of supplying the peak load. But after a certain point, the need to maintain the storage capacity fully charged of energy to cover the peak load can be in contrast with the need of supplying flexibility and vice versa. To differentiate among the different storage technologies, we consider that PHES and CAES are more prone to supplying peak load while batteries are more prone to supplying flexibility. For this reason batteries have a higher flexibility coefficient (1 vs. 0.75 for PHES and CAES), while the other two technologies have a higher capacity coefficient (1 vs. 0.8 for battery). These values will be subject to a sensitivity analysis in section 5.3.

While PHES is considered a mature technology that is going to experience minor-to-none cost reductions in the future [22] (or even cost increases, due to the progressive scarcity of geographical resources [77]), CAES and above all batteries are expected to face considerable cost reductions in the years to come [23], [75]. To capture this trend we decided to use learning curves [78] [79], a schematized representation of technological learning: the more a certain technology is produced, the more the manufacturer acquires experience, improves its technique and reduced production times, all resulting in a higher efficiency and, ultimately, lower cost per production units. Learning curves are a very simple modeling tool that relate the cost of a technology with its cumulative produced (or, as in this case, installed) capacity and typically extrapolate from historical data the exponent that explains this relationship, as seen in equation 3.3 (also called Wright's law):

$$Cost_{tech}(t) = Cost_{tech}(t_0) \times \sum_t \left(\frac{CumulativeInstalledCapacity_{tech}(t)}{CumulativeInstalledCapacity_{tech}(t_0)} \right)^{-b} \quad (3.3)$$

Where t_0 is the initial year, the initial cost is the initial overall capital cost of the technology (in terms of \$/kW) and the exponent b (specific for each technology) can be used to compute the learning rate. The latter is defined as the cost reduction provoked by a doubling of the installed capacity, and calculated as:

$$Learningrate = 1 - 2^{-b} \quad (3.4)$$

Values for the learning rate are respectively 5% for CAES [24] and 12% for utility-scale Li-ion batteries [77]. As a conservative assumption, we set the maximum decrease for the capital costs of LiB and CAES to half the initial cost by defining an associated floor cost. A sensitivity analysis has been carried out to understand the potential of a further lowering of the capital cost.

The last part of this subsection is dedicated to the discussion of the implemented exogenous constraints to investments of short-term storage technologies. As regards CAES and batteries, we implemented market constraints in analogy with what has been done for VRE technologies (see 2.4.1): A-CAES has a maximum annual growth rate of 7.5% (constant in time), while batteries, given their more advanced degree of commercial maturity, can grow of an annual 15% until 2050 and 20% afterwards. The rationale for this numbers is: batteries have the same market growth rates of solar PV, a technology that can be coupled with batteries and will likely foster its development [19], while A-CAES, a less mature technology, is allowed to experience just half this market growth.

Moreover, large scale CAES plants require large compressed air storage, especially underground salt caverns, and this represents a geographical constraint and a potential upper bound to a-CAES installed capacity [56]. Even if some studies assess the potential for salt caverns in specific regions (e.g. [68]), no comprehensive study considers the global potential to our knowledge, thus some qualitative considerations have been done. We started by finding an empirical relation between energy capacity of a CAES plant and volume of the salt cavern. The figures are approximately 283.000 m^3 for

2.86 GWh of storage for McIntosh plant [58], while 310.000 m^3 of salt caverns store 0.64 GWh in Huntorf power plant [57]: this results in an average “energy density“ 6.08 kWh of stored energy per cubic meter of cavern used for existing D-CAES plants.

We then compared this figure to the total amount of global underground natural gas storage capacity expected by a CEDIGAZ study [80], which is approximately 550 billion cubic meters. Of these, based on EIA data for working gas storage facilities in the US [81], we estimated 10% are provided by salt caverns, hence an overall available storage volume for CAES of 55 billion cubic meters worldwide, equivalent to 113.3 TWh of CAES. The regional CAES potential has been found as the weighted average of the global value over the surface areas of the 13 WITCH regions, that gives a potential ranging from 1.20 TWh for *neweuro* to 20.3 TWh for *ssa*. This figure is intended just as a conservative order of magnitude of the upper bound for A-CAES installed capacity as it clearly comes from strong and rough assumptions: the first regards the storage requirement for A-CAES plants (here assumed equal to the one of D-CAES), affecting their “energy density”; the second regards available storage capacity of salt caverns, that is strongly region-dependent and should be the subject of a more detailed study; the third, and broader, regards the storage means, as not only salt caverns but also depleted gas fields, mine shafts and large-scale tanks could potentially store compressed air [56]. We anticipate that this upper bound has never been reached in any of the runs presented in this work, for any region and time step, therefore it has not influenced the results.

Finally, the assessment of market growth potential for PHEs has been supported by a larger amount of data available, hence its higher level of detail. As regards PHEs potential before 2050 for *china*, *usa* and *oldeuro* regions, IEA Technology Roadmap for Hydropower (2012) provides upper bounds for PHEs power capacity potential in China (200 GW), U.S. (139 GW) and Europe (188 GW) in a high-renewables scenario [82].

For all other regions, the upper bound is on the ratio of PHEs installed capacity over total hydroelectric capacity (PHEs plus traditional hydroelectric), that cannot exceed 30% at each time step. This figure comes from historical data on PHEs and hydropower installed capacity worldwide [73], that we have aggregated in regions following WITCH division and analyzed (see Appendix E). It appears that the *kosau* region has by far the highest ratio (around 30%), that has then been chosen as an upper bound. Finally, to avoid unrealistic increases of this PHEs-to-total-hydropower ratio in time, this figure can increase at best 30% every time step for all regions that already have considerable amounts of installed PHEs capacity (see Appendix E), and at best 1000% for regions with initially negligible amounts of PHEs (*ssa*, *sasia*).

3.2.4 Seasonal storage

In answer to our first research question about which storage technologies are more suitable for being included in long-term models, we start providing an overview of the main seasonal electricity storage technologies (SESTs). The aim is better understanding and justifying our modeling choices that will be introduced later.

Seasonal storage originates from the mismatch between seasonal VRE supply and de-

mand pattern [83] that may occur when VRE production is particularly high in a season while yearly load peaks in another one: figure 3.14 represents the (normalised) hourly load throughout a year in the U.S. (black), plotted with the hourly wind (blue) and solar (yellow) production, coming from an hourly dispatching model, as described in [34].

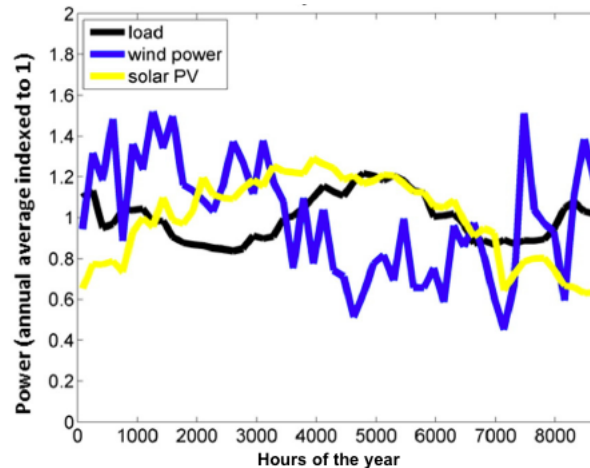


Figure 3.14: Annual time series of weekly averages that illustrate the seasonal correlation of load, wind and solar for U.S.A. Source: [34]

As visible, during winter and early spring (hours 0-3000) wind production is higher than load, while demand peaks during summer (hours 4000-6000), when corresponding wind generation is lower. This entails the opportunity to store the energy excess during winter for a long period of time (months) and re-injecting the stored energy into the grid during summer, to satisfy the peak in yearly demand. This requires storage technologies able to store large amounts of energy with minimum self-discharge (or leakage) rate. For these reasons, the main options for this kind of long-term storage are Pumped Hydro, Compressed Air Energy Storage and conversion to hydrogen, that allow for storage in water basins (PHES), salt caverns and other forms of gas storage (the other two technologies).

PHES and CAES technologies have been widely discussed in section 3.2, while hydrogen production from VRE excess generation and its re-conversion to other energy forms is discussed in the following. In particular, as our work is focused on power-to-power (P2P) storage technologies for VRE integration, we will focus on the possible paths hydrogen can follow to be re-converted into electricity for final use, and not other hydrogen applications such as its use in the transport sector, in industrial processes or in co-generation and tri-generations discussed in the literature [84], [85].

Electrolyser

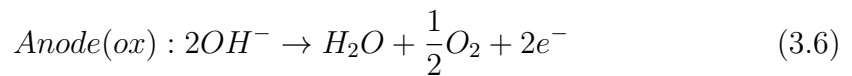
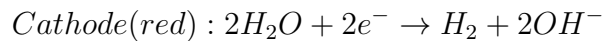
Hydrogen is produced from excess VRE generation via electrolysis, a process that consists in splitting water molecules through the passage of direct current in an appropriate electrolyte, driving the thermodynamically non-spontaneous decomposition of water into its constituent elements: hydrogen and oxygen [86]. The technology performing this transformation is called electrolyser, where the overall water splitting

reaction occurs:



An electrolyser is made up of several cells, assembled in a stack, plus auxiliaries such as a current rectifier, a water demineralization unit, a water pump and a cooling system, a hydrogen purification unit, and instrumentation. Each cell contains two electrodes, where the redox reactions of water splitting and product formation occur, plus an electrolyte that allows the transport of ions from one electrode to the other, separated by a membrane or a diaphragm. Hydrogen and oxygen are produced separately in the two distinct electrodes of the electrolysis cell, the cathode and the anode respectively. The size of a cell is limited by the capacity of the membrane or the diaphragm to withstand the electric current [87]. Cells are therefore stacked to increase hydrogen production. Three water electrolysis technologies can be considered for hydrogen production: Alkaline Electrolysis Cells (AEC), Proton Exchange Membrane Electrolysis Cells (PEM-EC) and Solid Oxide Electrolysis Cells (SOEC).

- **Alkaline electrolyser:** it is the state of the art technology developed for water electrolysis, and currently the only commercially available power-to-gas application [87]. It uses an alkaline solution as electrolyte to transfer hydroxide ions (OH^-) from cathode to anode, in the following reactions:



The reactions are enhanced by catalysts at the electrodes, respectively made of Nickel-Carbon and Nickel-Cobalt-Iron for cathode and anode, presenting the advantage of being cheap and active in this non-acidic environment. The main issue about AEC is the formation of gas product bubbles at both the electrodes, hindering the electrode activity, and hydrogen's tendency to migrate towards the anode (called crossover), where a dangerous contact with oxygen may occur [88]. Two different cell structures are used to address this problem: the first and oldest features two fixed, solid metallic bars constituting the electrodes, divided by a large space (called inter-electrode gap) to discourage hydrogen migration and separated by a diaphragm. This is a cellulose or polymer-made separator with holes allowing the passage of OH^- ions. The second configuration is called *zero-gap* since electrodes, porous in this case, are much closer to each other and separated just by a thin membrane, called Anion Exchange Membrane (AEM), that minimizes hydrogen crossover [88]. This innovative configuration helps reduce gas mixing and ion transport losses as the inter-electrode gap is reduced, yet AEM stability issues still limit its application. Figure 3.15 provides a schematic representation of the two AEM configurations.

Overall, AEC technology features high efficiency (55-65% with still some margins for improvement), cheap materials and long lifetime, yet issues related to gas crossover limit their performance in terms of hydrogen purity, maximum allowed current density and pressurized operation [89].

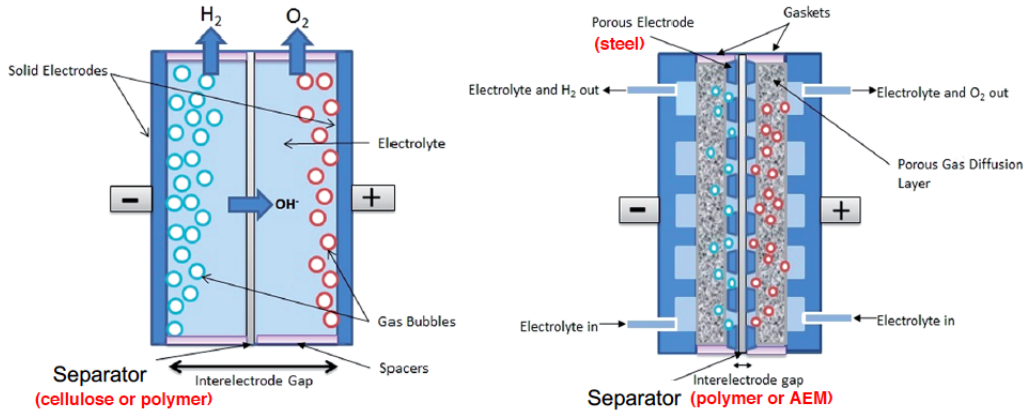
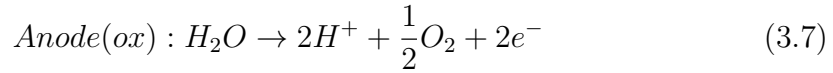
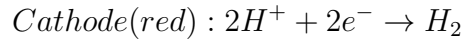


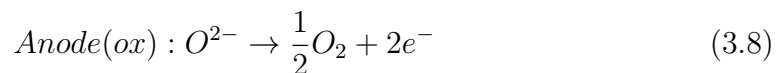
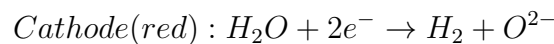
Figure 3.15: Traditional (left) and zero-gap (right) configurations for alkaline electrolyser. Source: [88]

- **PEM electrolyser:** it is a more recent technology that is currently in demonstration phase for large scales (up to 2 MWel per electrolyzer). This technology uses proton transfer polymer membranes simultaneously as electrolyte and separation material between the electrodes [87], in which the following reactions occur:



Since protons are transported in the electrolyte, the cells operates in an acidic environment. This requires the adoption of more expensive catalysts such as iridium oxide on a titanium support for the anode, while Platinum is used at the cathode [90]. Titanium, which is very stable also in acidic environment, is used also for other parts of the cell. Therefore, PEM EC does not show the typical crossover limits of AEC and can potentially achieve higher efficiency, but this comes at higher costs and lifetime is reduced by the adverse working conditions [89], that still limit its deployment and are the current focus of R&D activities [85].

- **Solid Oxide electrolyser:** this technology operates at high temperature (700-800 °C) to minimize the demand for electricity. The necessity for materials to withstand high temperatures led to the use of ceramic materials for electrolyte (solid Yttrium-stabilized Zirconia forming a lattice structure) and electrode materials [87]. Oxide ions are transferred through the electrolyte and the following reactions occur:



The advantages presented by these technologies are: the possibility to reach higher efficiency (up to 90%) exploiting residual heat from other processes, cost reductions and the possibility to perform a CO_2 -based electrolysis to produce syngas [91] or to use solid oxide fuel cells in reverse operation [92]. Nevertheless, this

technology is still at an early stage of development and high uncertainty is still present as regards cost and key performance parameters for large-scale applications [87].

Once hydrogen has been produced, it can follow different paths towards re-conversion to electricity, as illustrated by figure 3.16:

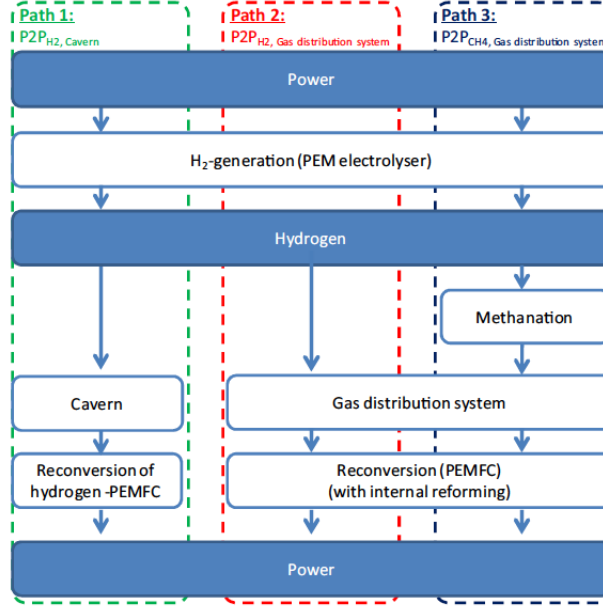
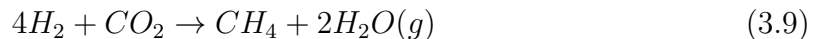


Figure 3.16: Main potential hydrogen storage paths in the energy sector. Source: [68]

As a first option, it can be stored in large natural storage facilities such as salt caverns, that are considered the most suitable geological formation for hydrogen storage from the point of view of safety, technical and economical feasibility [84], and then re-converted to electricity by fuel cells. Other options for hydrogen storage include pressurised tanks, cryogenic vessels or metal hydrides structures [84], [68].

The second option is blending hydrogen with natural gas, therefore using the existing natural gas T&D infrastructure to store the blend, converting it to electricity by means of a gas turbine. This option would certainly decrease storage cost, as natural gas transport and storage infrastructure is already widespread in most developed countries [84],[81], yet IEA mentions gas turbines, compressing stations and compressed-natural-gas storage tanks as the weak points of this supply chain, as they are particularly sensitive to high hydrogen shares [84].

The third option implies a further conversion step for hydrogen: it reacts with carbon monoxide or dioxide in a highly exothermic, catalytic reaction whose products are methane and steam, referred to as methanation [87] and summarised by the reaction:



There are two main kinds of methanation research is currently focusing on, as pointed out by [93]: first is catalytic methanation, a well known industrial process with high efficiency (up to 80%) dating back to 1902 and currently performed in high temperature and pressure adiabatic, fixed-bed reactors [87] that operate continuously. Nevertheless,

P2G applications for VRE integration would require smaller plants and intermittent operation, thus new reactors are under study, such as isothermal and fluidised-bed ones: the main issues for research are temperature control and flexible operation. On the other hand there is biological methanation, where methanogenic microorganisms operate as bio-catalysts [87]. It can occur at low pressure and temperature conditions and the reactor designed would be much simpler, yet issues related to kinetics and volume requirement limit its development [93]. As regards the applications, biological methanation is a better option for small plants and is less sensitive to gas impurities, while catalytic methanation is more efficient and suitable for large scale applications, even though major flexibility issues have to be overcome [93]. After methane production, the following step is burning it in a gas turbine: this introduces a further efficiency loss that penalises this option with respect to the other two.

Fuel cell

The last part of this section is devoted to a deeper discussion of fuel cells, considering their working principle and the main technological options available today. Fuel cells are electrochemical devices that directly convert chemical energy of a fuel (typically, but not only, hydrogen) into electrical energy (and in some cases also heat), without the need for combustion and the negative externalities it entails: pollutant production, dangerous temperatures, GHG emissions. The working principle is the same for all fuel cells, and so is the structure: each cell is made of two electrodes (positive and negative) where redox reactions occur, and they are separated by an electrolyte, that allows ion transport from one electrode to the other. Gas reaches the chemically reactive area (the interface between electrolyte, conductive material and catalyst) by crossing first the flowfield channels and then the gas diffusion layer, with a gasket between them to increase mechanical stability. Figure 3.17 gives a stylized representation of the fuel cell structure: cells are then stacked and connected in series to sum their voltage and provide non-negligible power output [89].

Fuel cells are typically classified based on the electrolyte material: the most relevant ones are Alkaline (AFC), Phosphoric Acid (PAFC), Direct Methanol (DMFC), Molten Carbonate (MCFC), Polymer Electrolyte Membrane (PEMFC) and Solid Oxide fuel cells (SOFC). In the following we choose to discuss just the last two technologies because they have the highest number of installed applications [94], and they seem particularly suitable for VRE integration applications [84]. Moreover, a comprehensive overview of fuel cell technologies is limited by the space constraints this work is subject to and does not represent its central purpose.

- **PEM Fuel cell:** it is the most widespread fuel cell technology by units shipped and installed capacity [94], so the most commercially mature and technologically advanced. It is characterized by a polymeric electrolyser made out of Nafion, which requires water humidification for proper ion transport, and two electrodes where the catalyst particles (Platinum) lay on a carbon support. The working principle is illustrated in figure 3.18: hydrogen reaches the chemically active sites

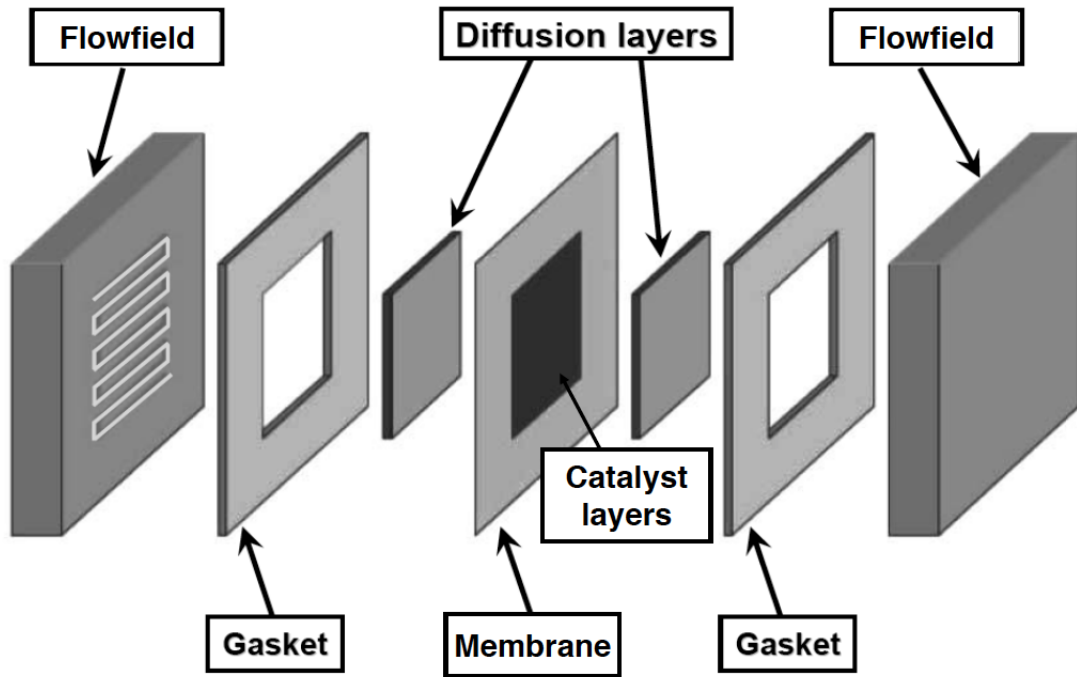
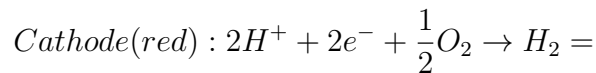
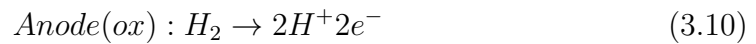


Figure 3.17: Components of a generic fuel cell. Source: [89]

at the negative electrode through the flowfield and the gas diffusion layer, where it oxidises in a catalytic reaction enhanced by Pt particles. Hence H^+ ions are formed and they cross the electrolytic membrane towards the positive electrode, where they react with oxygen from the incoming air flow and electrons that have travelled through the external circuit to produce water in the reduction half-reaction. The characteristic chemical reactions are:



PEM fuel cells work at low temperature, which allow them to perform fast cold start-ups and ramp-ups. They also have high power density (up to 3 kW per cubic decimeter [94]) and their only sub-product is water, which makes them an environmentally-friendly technology [84]. The two main weaknesses of this technology are duration, related to several degradation mechanisms that occur in the cell [95], and its cost, which is influenced by high Pt catalyst loading, and by another aspect that distinguishes Fuel Cells from all the energy technologies based on thermodynamic cycles. As a matter of fact, if Carnot efficiency shows that thermodynamic cycles perform better if they work at higher enthalpy drops, so at higher maximum temperature, which entails higher power produced, for fuel cells the situation is the opposite: the higher the current density in the cell, the higher the voltage losses due to kinetics, ion and electron mass transport [89]. This means that the closer we get to nominal power operation, the lower will be the efficiency, or in other words if high efficiency levels are the goal, the fuel cell must run at partial load, so specific costs per unit of power produced grow, as shown in figure 3.19.

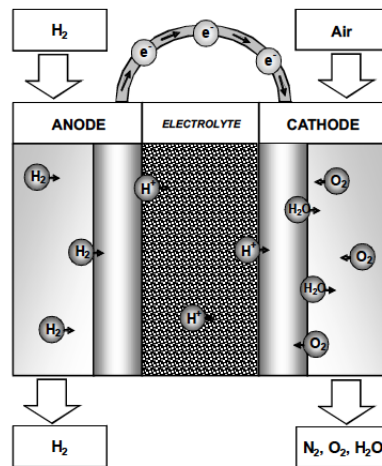


Figure 3.18: Scheme of a PEM fuel cell. Source: [89]

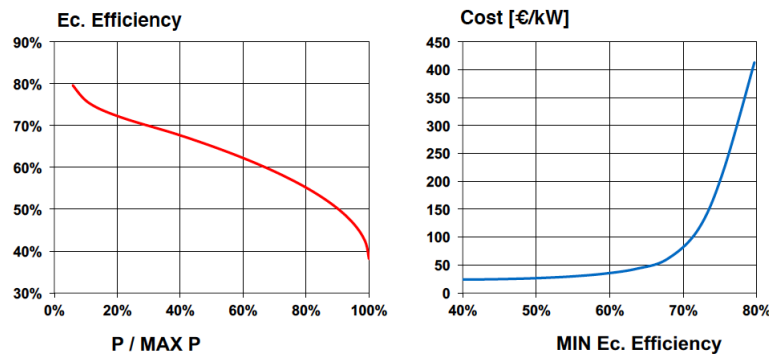


Figure 3.19: PEMFC efficiency as a function of normalized operating power (left). Specific cost per unit of useful power as a function of fuel cell efficiency. Source: [89]

- SO Fuel Cell:** it is a high temperature fuel cell, particularly suitable for stationary applications and combined heat and power (CHP) production. The structure and materials used have already been described when considering Solid Oxide Electrolysers (and so have the characteristic reactions, where products and reactants should be inverted from the electrolyser to the fuel cell configuration). The main difference between the two is the possibility, for SOFC, to perform internal reforming of natural gas or syngas within the system, favoured by high temperatures [96]. For this reason a section of the anode, called “anode support”, is devoted to reforming, while just a smaller layer of anode is the actual active area for oxidation, as visible in figure 3.20. The main advantages of SOFC with respect to PEMFC are the higher kinetics of reaction (enhanced by high temperatures), hence the possibility to use cheaper catalyst, the flexibility with respect to fuel, the combined heat and power or the hybrid configurations [96] that increase the total system efficiency, the fuel flexibility which may exclude the need for electrolysis and the possibility to operate at high pressure. On the other hand, a number of disadvantages are still subject of R&D efforts and limit their diffusion, such as high costs, durability issues (degradation is faster at high temperature and pressure), operational flexibility, which is limited by material dilatation issues, and

sensitivity to carbon formation and sulphur poisoning [97]. However, the recent inclusion of SOFC in the largest deployment program for residential CHP fuel cells, the Japanese ENE-Farm [94], highlights the growing interest towards this technology and the existing opportunities to reduce costs with mass-production.

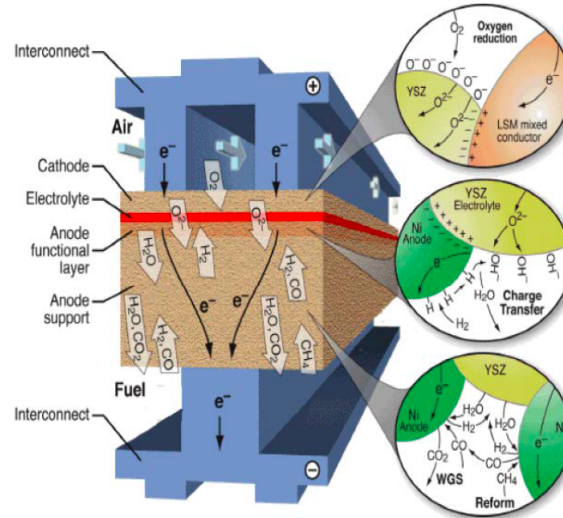


Figure 3.20: Typical components of a SOFC and main reactions occurring in each layer. Source: [96]

3.2.5 Choice of cost and performance parameters for seasonal storage

This subsection illustrates the motivations behind our choice to represent the combination of alkaline electrolyzers and PEMFC as P2P seasonal storage technology. After this explanation, cost, performance and market-constraint choices for the selected technologies are introduced, motivated and presented in three tables. As regards the technology selection, while PHES and CAES are presented as a more favourable option for short-term storage, entailing a high number of charge-discharge cycles, the situation changes for seasonal storage, that requires just a few cycles per year. This low level of cycling makes it more difficult to repay high fixed cost for seasonal storage technologies, typically related to the volume that storing a unit of energy requires [49], [68]. This volume requirement per energy unit stored is roughly calculated in [49], assuming compressed air and hydrogen are stored in underground facilities at typical pressures for the two technologies and water is stored in two equally-sized basins at different heights. It results that the volume requirement for hydrogen storage is 10 times lower compared to compressed air and up to 350 times lower compared to Pumped Hydro. This, combined with the cost decrease that electrolyzer and fuel cell technologies are expected to enjoy in the next decades [77],[84], makes hydrogen production and storage one of the most promising technologies for seasonal storage [68],[49], as suggested by the number of P2G projects launched worldwide and shown in figure 3.21: most of them regard hydrogen applications rather than methanation.

Concerning the choice of the electrolyser, to date the alkaline electrolyser technology is the only commercially mature and the cheapest, while the PEM electrolyser presents the highest margins for cost reduction and also easier operation, yet concerns about

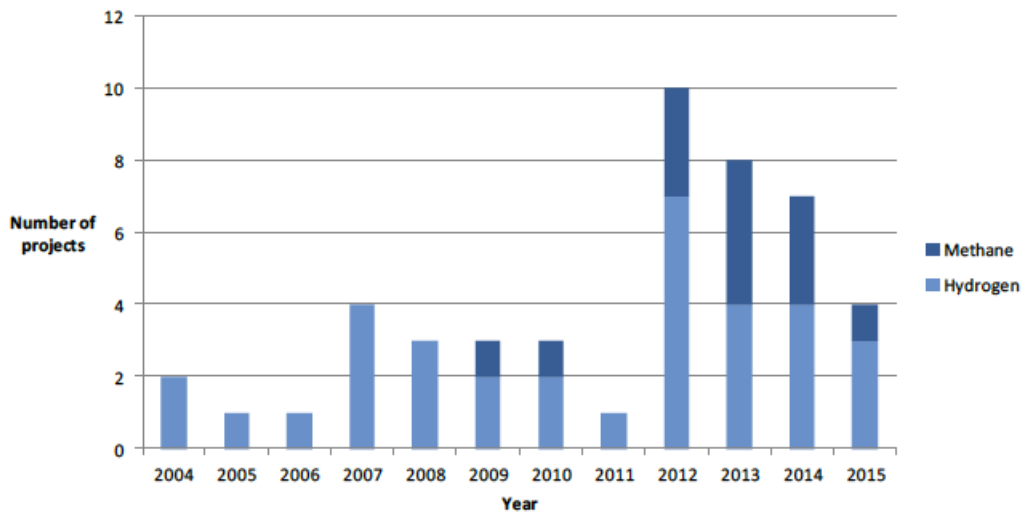


Figure 3.21: Number of pilot and demonstration projects of power-to-gas launched worldwide in the past decade. Source: [87]

its low lifetime and few commercial applications still limit its potential, and SOEC electrolysis is still at an early stage of development [87]. Finally, high-temperature electrolyzers are an attractive technology for low-carbon applications given their potentially higher efficiency and the possibility to convert CO_2 , nevertheless they are at an early development stage and considerable research effort will be required to make them competitive [98]. Given this brief overview, we decided to model the electrolyser technology based on typical performance of the alkaline type.

Among the various conversion paths hydrogen can follow after electrolysis, summed up in figure 3.16, our choice has been direct conversion of hydrogen gas in PEMFC for these reasons: first, it is indicated by IEA Hydrogen Roadmap [84] as the conversion path with the highest power-to-power efficiency if compared with natural gas blending or methanation with subsequent conversion with a gas turbine. Second, electricity from both natural gas blending and methanation entails a higher amount of associated CO_2 emissions: these come from the final combustion in a gas turbine and, unless suitable CCS technologies are deployed to avoid these emissions, represent a clear obstacle if the deployment of seasonal storage is aimed at decarbonizing the power sector and fostering the diffusion of VRE technologies. On the other end, operation of PEMFC entails no carbon emissions as the only byproducts of this device are water and heat, besides a small fraction of unreacted input. Since our goal is understanding to what extent storage may help the diffusion of carbon-free VRE, representing storage technologies that entail GHG emissions during their operation may limit their diffusion in scenarios where limits or prices on emissions are imposed. This could possibly hinder, in turn, the diffusion of VRE, in a dynamic that is exactly the opposite of what we want to investigate. Finally, the technological choice reflects what has been done in POLES by Déspres et al. [33], in analogy with the modeling of short-term storage.

Among all the available technological options for fuel cells, Polymeric Electrolyte fuel

cells are the most commercially mature ones and the most widespread in stationary applications [84]. Their low operating temperature (around 80°C) does not require additional heat sources as for SOFCs and MCFCs, which would have required a more complex modeling, as WITCH does not allow an easy representation of cogeneration technologies.

Furthermore, our modeling paves the way to the implementation of other technologies in the module dedicated to seasonal storage. In fact other types of electrolyzers and fuel cells can be easily modeled by changing the characteristic parameters of fuel cells, and hydrogen could be additionally converted into natural gas with a modest modeling effort.

Having discussed the reasons behind the technology choice, we now deal with the selected cost and performance parameters for alkaline electrolyser and PEMFC. We opted for representing capital cost for the two technologies as power-specific (i.e. in $\frac{\$05}{kW}$) plus a markup for hydrogen storage and transportation, that depends on the actual amount of hydrogen produced via electrolysis. For electrolyser we chose today's cost for a large-scale (10 MW) alkaline electrolyser as reported by Enea Consulting 2016 report on Power to Gas technologies [87], i.e. 1000 €2015 per kW. For fuel cell, we relied on Zakeri's literature review [75], even though making an assumption has been necessary: since Zakeri's costs for fuel cells (in 2015 €per kW) include also electrolyser technology, we have to subtract the electrolyser cost to the three cost values we pick (min, mid and max) to get capital costs for PEM fuel cell. Finally, the markup for hydrogen storage (the storage means being solution-mined salt caverns) and O&M cost both come from [75], and are expressed in €/kWh. All the costs are then converted in \$05 per kW or kWh, as summarised by table 3.5.

Technology	Capital cost $\frac{\$05}{kW_{year}}$			O&M cost $\frac{\$05}{kW}$	Storage cost $\frac{\$05}{kWh}$
	min	mid	max		
Electrolyser	-	997.2	-	-	-
PEM Fuel Cell	625.5	1454.3	2862.9	24.81	-
H_2	-	-	-	-	0.0338

Table 3.5: Cost data for seasonal storage technologies.

The performance parameters for alkaline electrolyser come from [87] (efficiency and lifetime) and [77] (learning rate, same for both the technologies). As far as lifetime is concerned, it is a weighted average on capital cost between the cell stack, accounting for 30% of the total capital cost and having a lifetime of 60000 hours, and the rest of the system, accounting for 70% of the capital cost with a lifetime of 20 years. The equation used to compute the electrolyser lifetime is then:

$$lifetime_{electr} = 0.7 \times lifetime_{system} + 0.3 \times \frac{lifetime_{stack}}{fullproductionh_{electr}} \quad (3.11)$$

resulting approximately in 21 years of lifetime for the electrolyser. As regards PEM Fuel Cells, 50% efficiency is assumed coming from 2020 U.S. Department of Energy (DOE)

targets for stationary Fuel Cells [85] (where “*more of 45%*” is specified). Lifetime is computed dividing the expected life hours (60000 h, from the same source) by the yearly full production hours (2465 h derived from [75]), yielding approximately 24 years. Capacity and flexibility coefficient, respectively 1 and 0.9, comes from our assumptions, and so do floor costs, assumed as half the initial cost for both technologies. Table 3.6 summarizes all the parameters discussed above.

Technology	Efficiency	Lifetime (yrs)	Full prod h	
Electrolyser	0.70	21	(see Section 4.4.2)	
PEM Fuel Cell	0.50	24	2465	
	FlexC	CapC	Learning rate	Floor cost
Electrolyser	-	-	18%	half initial cost
PEM Fuel Cell	0.9	1	18%	half initial cost

Table 3.6: Seasonal storage technologies: values of the parameters implemented in WITCH.

Chapter 4

WITCH Model Advancement

This chapter aims at explaining the advancement in the representation of VRE technologies integration within the WITCH model reached through our contribution. The chapter is structured as follows. Firstly, the pre-existing VRE integration formulation in WITCH is described, since it constituted the starting point of our work. Then, our new interpretation of the flexibility coefficient curves of VRE technologies is introduced. After that, our new formulation of the electric grid in WITCH is described. Finally, our new formulation of short-term and seasonal electricity storage in WITCH is presented.

4.1 Pre-existing VRE integration modelling

Within the general effort of the IAMs development teams towards a complete modelling of the VRE integration characteristics, also in the WITCH model some pre-existing, already implemented features have been encountered at the beginning of our work.

In particular, the pre-existing WITCH model advancements can be divided in two subsequent development steps:

- The first one belonged to the first wave of IAMs models improvements and included the implementation of the system integration features already described in Chapter 2 [36].
- The second one, which coincided with the starting point of our work, has been carried out by Samuel Carrara, the co-supervisor of our thesis, in the first months of 2017, within his Marie Skłodowska-Curie grant-awarded research activity. It followed the latest progress in the VRE system integration modelling, allowed by the development of the RLDCs and presented in [37]. Modifications have been implemented along three main directions, aimed at improving the features described in Section 2.4: the capacity constraint equation, the definition of the VRE curtailment concept and the flexibility constraint equation.

In the following Sections, the outcomes of the above mentioned second step of development are explained in detail. The reason for this explanation is that having a clear

understanding of the pre-existing formulations is necessary to comprehend how they interact with and compare to the model advancements we introduced.

4.1.1 Capacity Constraint Equation

Starting from the capacity constraint equation in the form of eq. 2.3, some updates have been implemented from the findings of RLDCs-based work described in [37]. As regards this study, it is based on the previous development of the RLDCs. In particular, typical RLDCs have been derived for each region and for different shares of VRE generation (and for each share RLDCs for different mix of PV and wind plants) [32]. From the specific RLDCs, some parameters have been calculated in order to characterize the peculiarities of each region in terms of coupling between potential VREs generation and local load. These parameters are described in the following.

First of all, as regards the firm capacity requirement, which represents the capacity required to meet the peak load as a multiple of the annual average load, it is expected that it will vary across regions and over time as electricity demand changes with development. The evolution of firm capacity requirement over time for the different regions is calculated using a method proposed by [99]: approximating the ratio between the annual peak load and the annual average load from the projected shares of residential and industrial electricity demands and adding a margin of 20% to cover contingency events. So, with this new formulation, *firm_req* has become a function of regions and time (values for the different WITCH regions can be seen in Appendix D).

Moreover, the RLDCs for the different regions have been used to quantify how the Capacity Values (CVs) of PV and wind power plants change with increasing generation shares of these technologies [37]. The capacity value of a technology is defined as its contribution to the firm capacity requirement and so its ability to cover the peak load. The capacity value of the single VRE technology is calculated as the fraction of the technology capacity that contributes to covering peak load. To express CV as a function of VRE share, it has been derived from several different RLDCs, featuring an increasing VRE share. The overall analytic formulation of the capacity constraint equation (eq. 4.1) is the same as the previous one (eq. 2.3), with the difference that the updated implementation identifies unique capacity values for the single VRE technology ($jel|VRE$) in the different regions as a function of its generation share (before considering curtailment): $CV(jel|VRE, t, n) = f(SHARE_EL_BC(jel|VRE, t, n))$. Therefore, the main improvement with respect to the previous implementation is the complete differentiation across regions, based on the regional RLDCs.

$$\begin{aligned} \sum_{jel|non-VRE} K_EL(jel, t, n) + \sum_{jel|VRE} K_EL(jel, t, n) \times CF(jel, t, n) \\ \times CV(jel, t, n) + K_EL_{storage}(t, n) \times CC_{storage} \\ \geq firm_req(n) \times \frac{Q_EL_TOT(t, n)}{yearly_hours} \end{aligned} \quad (4.1)$$

In Fig.4.1 it is visible how the capacity value of wind and PV technologies decreases with an increasing generation share of these technologies. It is worth highlighting how the capacity value of PV technology starts at a much higher level than the wind one at low generation shares, but then it presents a much steeper decrease. This is due to the fact that solar PV generation is well-aligned with peak load at low VRE deployment, but provides very little capacity value beyond a 30% share, while the behaviour of wind plants is more uniform.

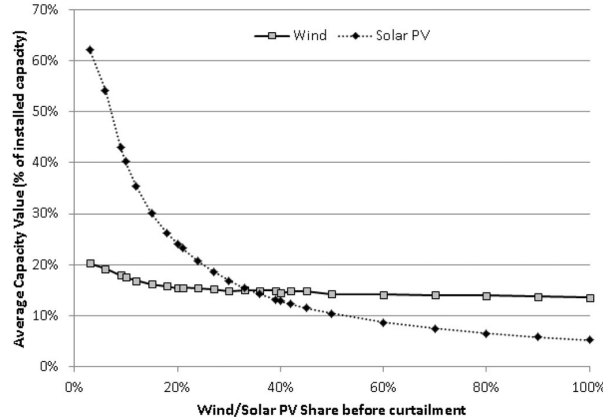


Figure 4.1: Average capacity value of VRE technologies as a function of their generation share before curtailment for the case of USA [37].

4.1.2 VRE Curtailment

Since VRE generation is intermittent and non-dispatchable, a wide deployment of these energy sources may mean a significant curtailment, especially when coupled with inflexible base load generation. Curtailment represents potentially useful electricity produced by VRE technologies that is actually wasted, because this generation would occur in period of not high enough load.

One important feature of the RLDCs is the ability to represent the curtailed generation at the different shares of generation by VRE technologies. Curtailment can be defined as the amount of negative residual load, or VRE oversupply, in a given RLDC (Fig. 2.3). A negative residual load indicates that VRE generation alone exceeds electricity demand. The average total curtailment is split into two different components:

- **SHORT-TERM CURTAILMENT:** the portion that can be addressed with short-term (<24 h) storage and is due to the daily mismatch between VRE production and electricity demand.
- **SEASONAL CURTAILMENT:** the portion that can be handled with seasonal storage and is caused by the seasonal mismatch of high VRE production and high electric load. The portion of seasonal curtailment has been calculated in [37] in the following way. The authors used two estimates of curtailment (developed by Denholm & Hand [100]), respectively with no storage and with 24 hours of storage for the Electricity Reliability Council of Texas (ERCOT) region, in the

USA. Starting from these estimates, they quantified the seasonal fraction of total curtailment for each VRE share as the fraction of total curtailment that is still present in the Denholm & Hand system with 24 hours of storage. Therefore, in this perspective, seasonal curtailment is defined simply as the fraction that cannot be handled with short-term storage. A limitation of this formulation is that, for lack of regional data, the split between short-term and seasonal curtailments, found by Denholm & Hand specifically for the ERCOT region and for a 70/30 wind/solar mix, has been applied for all the world regions and for all the possible wind/solar mixes.

The resulting seasonal fraction of total curtailment for all the regions increases from 15% at 50% VRE share to 35% at 100% VRE share.

In the MESSAGE model, total curtailment is defined from the regional RLDCs as a function of the VRE generation share before curtailment in that region. It is modeled equal to zero until a certain VRE share around 40-50 % (specific of the region) and then increases with the generation share [37]. In Fig.4.2 the behaviour of the total curtailment (sum of short-term and seasonal) is shown for the USA case. In MESSAGE this curve is approximated with a stepwise function presenting growing uniform values in 10% wide VREs shares bins [37].

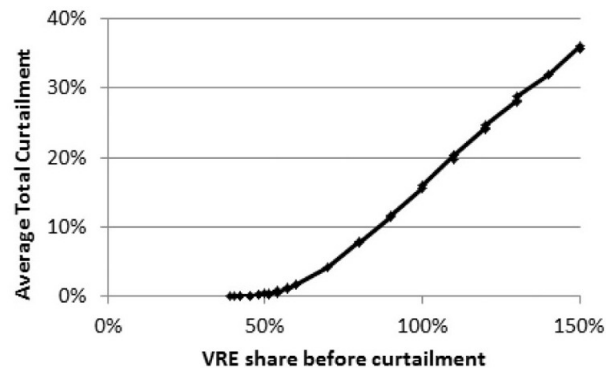


Figure 4.2: Average total curtailment as a function of the VRE share before curtailment in MESSAGE, for the USA case [37].

In the WITCH model, a similar representation of curtailment has been implemented, with the difference of using a second degree function, starting from VRE share equal to zero. The reason behind this choice is twofold: the first one is the numerical structure of the model, which does not allow an easy representation of discontinuous functions or functions with discontinuous first derivative, as the one used in MESSAGE; the second one is related to the fact that considering curtailment equal to zero up to VRE shares around 40-50% appears unrealistic and not able to represent what is actually happening in systems with lower VRE shares [101]. In Fig.4.3 the behaviour of WITCH short-term and seasonal curtailment is shown for the USA case. In Appendix D the WITCH values of short-term and seasonal curtailment as a percentage of VRE generation before curtailment could be seen for all regions.

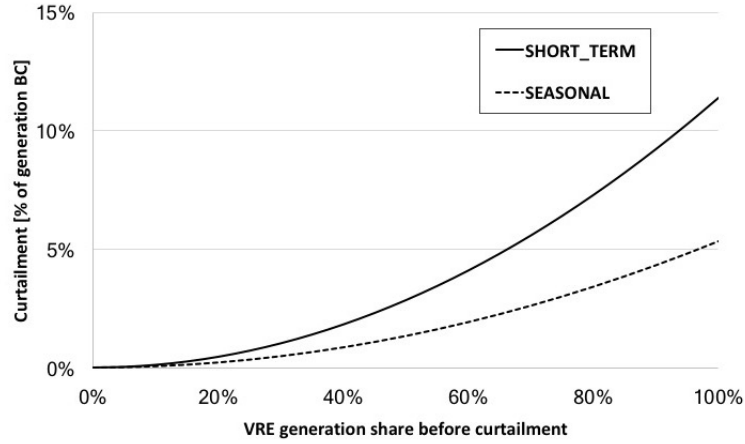


Figure 4.3: Short-term and seasonal curtailment representation in WITCH as a function of the VRE share before curtailment for the USA.

VREs generation Q_{EL} after considering curtailment is calculated in the WITCH model as the difference between production before curtailment Q_{EL_BC} and the curtailed fraction of generation Q_{EL_CURT} (defined for all j_vre technology):

$$Q_{EL}(j_vre, t, n) = Q_{EL_BC}(j_vre, t, n) - \sum_{curt_type} Q_{EL_CURT}(j_vre, curt_type, t, n) \quad (4.2)$$

Where Q_{EL_CURT} are the curtailed fractions (short-term and seasonal).

4.1.3 Flexibility Constraint Equation

As regards the flexibility constraint equation, the development of the WITCH model has followed three main guidelines set by the recent improvements in the MESSAGE model [37]:

- The differentiation of the load flexibility coefficient among the different regions
- Improved representation of flexible operation in thermo-electric power plants
- Better definition of flexibility coefficients for VRE technologies

Flexibility Coefficient of Load

The flexibility coefficient of load represents the flexible fraction of total generation that must be supplied to meet fluctuations and uncertainty in demand. It is derived, for each region, from the load duration curve with no VRE deployment and so, not being influenced by the supply system structure, it represents the need for flexibility proper of the load [37]. Table 4.1 provides the values of the flexibility coefficient of load for the 13 regions of the WITCH model. In particular, for all the regions except *india* and *sasia*, its absolute value has increased with respect to the previous formulation (it was -0.1 for all the regions).

	cajaz	china	easia	india	kosau	laca	mena
<i>FC_load</i>	-0.17	-0.13	-0.13	-0.05	-0.17	-0.18	-0.18
	neweuro	oldeuro	sasia	ssa	te	usa	
<i>FC_load</i>	-0.20	-0.20	-0.05	-0.12	-0.20	-0.19	

Table 4.1: Flexibility coefficient of load for the 13 regions of the WITCH model [37].

Flexible Operation of Thermoelectric Power Plants

Most thermo-electric power plant technologies can be managed to provide some operating reserve to the system. However, entering a flexible operation mode can cause significant impacts on O&M costs, efficiency and capacity factor [102],[103]. In the MESSAGE model the representation of thermo-electric power plants has been updated to take into account two different modes of operation: baseload and flexible [37]. In this formulation the flexible operation provides a fraction of generation as operating reserve, but comes with penalization in terms of higher O&M costs, lower efficiency and lower capacity factor.

Since in WITCH, due to its numerical structure, a continuous representation is needed, the MESSAGE approach has been partially modified to be integrated within the model. In WITCH, the annual generation of a particular technology jel is defined by the following equation:

$$Q_{EL}(jel, t, n) \leq K_{EL}(jel, t, n) \times CF(jel) \times yearly_hours \quad (4.3)$$

Where K_{EL} is the installed full nameplate capacity of the technology in that year. The capacity factor used in equation 4.3 is defined as the typical maximum achievable capacity factor for each technology. Thus, the model is able to optimize the actual generation between zero and the maximum possible value, given the installed capacity. The representation of the flexible operation of thermo-electric power plants is introduced adding the following equation:

$$Q_{EL}(jel, t, n) = K_{EL}(jel, t, n) \times CF_{REAL}(jel) \times yearly_hours \quad (4.4)$$

Where $CF_{REAL}(jel)$ is defined as the actual capacity factor of the particular technology jel at the period t , resulting from the optimized solution. Starting from the definition of this new variable, the ratio between $CF_{REAL}(jel)$ and the maximum achievable capacity factor $CF(jel)$ is used to derive the impacts of the operation mode on O&M costs, thermal efficiency and flexibility coefficient of the thermoelectric power plants.

The implemented formulation is the following. The 40% of the maximum achievable capacity factor $CF(jel)$ is set as the minimum load at which usually thermoelectric power plants are able to work [102]. In WITCH there is a further approximation of reality, because the model considers the overall installed capacity of a particular

technology in each region, and there is not a representation of each single power plant. At the minimum load, the increase of O&M costs is derived from [37] and the thermal efficiency reduction is determined from [102]. Besides introducing the latter two forms of penalization, the flexible operation mode has the positive effect of increasing the Flexibility Coefficient (FC) of the technology. The FC increment for the different thermo-electric technologies derived from [37] is set in correspondence of the minimum load. Then, the actual variation of these three parameters (O&M increase, efficiency reduction and FC increment) is described as a linear function of the ratio between $CF_REAL(jel)$ and the maximum achievable capacity factor $CF(jel)$. In particular, the variation are set equal to zero when $CF_REAL(jel) = CF(jel)$ and so their ratio is 1 and equal to the above mentioned values (derived from literature) when the ratio is equal to 40%¹.

We analyzed the impact of this new formulation and we got some interesting insights. Without the definition of CF_REAL , the optimization results were such that in some time steps some installed capacity of non-VRE technologies was not producing at full capacity factor, or even not producing at all. This could be explained by the fact that the optimal solution included installing some non-VRE capacity at a certain point to meet the demand or satisfy the capacity or flexibility constraint equations and then, when more favourable ways of meeting the objective were reached, the capacity was just exploited less, because there were not associated penalties.

With the new formulation, including CF_REAL , the results are different to what may be expected. The model never exploits non-VRE capacity at lower capacity factor than the maximum possible one, because it appears that the higher O&M costs, lower efficiency and lost production are not economically justified by the possible higher flexibility coefficient². This behaviour is explicable through its perfect foresight characteristics, so that the model is able to optimize the amount of non-VRE installed capacity to avoid that in the subsequent time steps is used at lower capacity factor than the maximum possible. The general impact on the energy system is a moderate change in the overall generation of non-VRE technologies, together with a decrease in their installed capacity with respect to the case with the old formulation, because the installed capacity is used always at the highest capacity factor.

VRE Flexibility Coefficient

In the last updates of MESSAGE model, a series of RLDCs for the different regions with increasing VRE shares has been used to estimate how the flexible fraction of non-VRE generation varies with increasing VRE deployment [37]. The flexibility coefficient of VRE technologies is defined as the additional amount of generation by flexible

¹Since in WITCH a continuous formulation is needed, for values below the defined minimum load $CF_REAL(jel) = 40\% \times CF(jel)$, the variations of the parameters listed above continue increasing linearly till $CF_REAL(jel) = 0$.

²As it will better discussed in the results section, this is related to the fact that the capacity constraint equation influences the optimization solution more than the flexibility constraint one, especially in the first half of the century and in non-strict climate policy scenarios. Therefore it is easier to satisfy the flexibility constraint equation and it is not required to make the non-VRE technologies work with higher flexibility coefficient

non-VRE technologies (in kWh) required for 1 additional kWh produced by VRE represents. This formulation is used in the flexibility constraint equation. It stands for the supplementary flexibility required by the system due to an extra kWh of VRE production.

In MESSAGE it is defined the marginal variation of the VRE flexibility coefficients (Marginal flexibility coefficients MFCs) that assumes different values in three different ranges of VRE generation shares. In table 4.2 the values employed in MESSAGE for the USA are shown. In table D.3 in appendix D the values adapted to all the 13 regions of WITCH are listed.

VRE share BC	Marginal VRE FC
0 - 15%	-0.03
15 - 50%	-0.39
>50%	0.29

Table 4.2: Marginal Flexibility Coefficients of VRE technologies for different ranges of VRE shares before curtailment for USA [37].

These values have been implemented in WITCH by our co-supervisor Samuel Carrara, with a continuous formulation in full coherence with the MESSAGE formulation. In particular, the VRE flexibility coefficient corresponding to a particular share of VRE has been defined as the weighted mean of the marginal VRE flexibility coefficients derived from [37]. The following example aims at clarifying the formulation.

Let's consider USA VRE MFCs from table 4.2 and an overall generation of 100 TWh. With a VRE share before curtailment of 10%, the VRE flexibility coefficient to be used in the flexibility constraint equation is just equal to:

$$\frac{10\% \times 100 \text{ TWh} \times (-0.03)}{10\% \times 100 \text{ TWh}} = -0.03$$

In correspondence of a VRE share of 30%, instead, it is equal to:

$$\frac{(15\% \times (-0.03) + 15\% \times (-0.39)) \times 100 \text{ TWh}}{30\% \times 100 \text{ TWh}} = -0.204$$

This negative value means that, with a VRE share of 30%, for each TWh produced by VRE technologies there is the need for 0.204 TWh generated by non-VRE flexible power plants.

Finally, with a 100% VRE share, instead, it is:

$$\frac{(15\% \times (-0.03) + 35\% \times (-0.39) + 50\% \times (0.29)) \times 100 \text{ TWh}}{100\% \times 100 \text{ TWh}} = 0.003$$

This operation has been repeated for all VRE shares between 0 and 120% and the resulting values have been then interpolated with a 3rd degree polynomial curve, ensuring compatibility with the numerical structure of the WITCH model. Increasing the polynomial degree of the fitting function would increase both fit accuracy and model

complexity. Given this trade-off, a third-order polynomial has been considered a good choice³. In the graph of Fig. 4.4 the two curves for the USA case can be seen: the dotted one representing the original values calculated from the MFC values and the solid one being the derived 3rd degree polynomial curve.

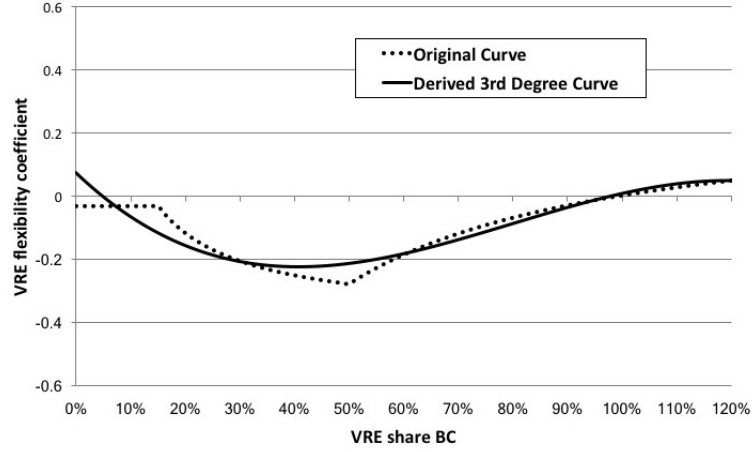


Figure 4.4: VRE Flexibility Coefficient curve derived from marginal VRE flexibility coefficient values in [37] for the USA case.

Our work started from these flexibility coefficient curves and we tried to give them a more technical interpretation to explain the obtained behaviour. The results of our analysis and the consequent effect on the curves implementation within the WITCH model are explained in detail in the following Section 4.2.

To conclude, the formulation of the flexibility constraint equation resulting from the updates described in this section is the following:

$$\begin{aligned}
 & \sum_{jel|non_VRE} Q_EL(jel, t, n) \times FC_non_VRE(jel) + \\
 & \sum_{jel|VRE} Q_EL(jel, t, n) \times FC_VRE(jel) + \\
 & K_EL_storage(t, n) \times CF_storage \times yearly_hours \times FC_storage \\
 & + FC_load(n) \times Q_EL_TOT(t, n) \geq 0 \quad (4.5)
 \end{aligned}$$

Where, with respect to equation 2.4, FC_load is now different across regions; FC_non_VRE is a function of the actual capacity factor of the non-VRE technology jel : $FC_non_VRE(jel|non_VRE) = f(CF_REAL(jel))$; FC_VRE is a function of the VRE share before curtailment $FC_VRE(jel|VRE) = f(SHARE_EL_VRE_BC(t, n))$, as shown in Fig.4.4.

³The fitting curve for all the WITCH regions presents a coefficient of determination R^2 higher than 0.88

4.1.4 Pre-existing Electric Grid Formulation

As it has already been introduced in section 2.4.4, in its pre-existing WITCH formulation electric grid capacity K_EL_GRID was expressed in $TW - equivalent$ and was linearly proportional to the installed generation capacity. Moreover, the equation to calculate the installed electric grid capacity featured two additional grid stock requirements, specifically defined for VRE technologies. The first one represents the additional grid required to connect solar and wind plants located far from load centers or shores. In this sense, it should be remembered that, in WITCH, solar and wind plants are differentiated by distance from load centers ("near", "intermediate" and "far" plants) with additional transmission costs $transm_cost$ (equation 4.6) defined accordingly. The second one represented an early attempt to take into consideration the grid pooling effect, by considering the necessity of building a wider grid interconnection for the integration of VREs (curtailment reduction, dispatchability increase, etc.) [36]. The latter term was defined for each VRE technology and increased exponentially with the generation share $SHARE_EL$ of the single VRE with an exponent b equal to 1.55 [40]. Therefore, the equation to calculate the installed grid capacity from installed generation capacity had the following shape:

$$\begin{aligned}
 K_EL_GRID(t, n) = & \sum_{jel|non.VRE} K_EL(jel, t, n) \\
 & + \sum_{jel|VRE} \sum_{distance} K_EL_D(jel, t, n, distance) \times \frac{transm_cost(jel, distance)}{grid_cost} \\
 & + \sum_{jel|VRE} K_EL(jel, t, n) \times (1 + SHARE_EL(jel, t, n)^b) \quad (4.6)
 \end{aligned}$$

Where $K_EL(jel, t, n) = \sum_{distance} K_EL_D(jel, t, n, distance) \forall jel|VRE$.

The adopted grid investment cost $grid_cost$ was equal to 400 \$/kW and had been obtained averaging costs over lengths and capacities of transmission lines[36].

The second equation modeling the electric grid was the capital stock equation. This equation, for every region and time step, accounted for the aging and the consequent retirement of the existing grid capacity and the capacity addition due to the yearly investments in grid.

The main weaknesses of this formulation were the lack of a distinction between transmission and distribution lines, the absence of a representation of thermal losses on the lines and the coarse description of the grid pooling effect. Our work has been directed towards solving these issues.

4.1.5 Pre-existing Electric Storage Formulation

As anticipated in section 2.4.5, in its pre-existing formulation, electric storage was not an actual generation technology, but more a "dummy" technology the model can invest on since it positively contributes to capacity and flexibility equation. Storage had no

associated input and output electricity and so it was not characterized by a round-trip efficiency. Storage stood just as an alternative way of providing the capacity and flexibility needed by the power system. Its investment cost was characterized by an exponential decay between 6000 \$05/kW in 2005 and 550 \$05/kW:

$$inv_cost_{storage} = \max(inv_cost_{storage}(t = 1) \times t^{-0.8}; 550) \quad (4.7)$$

With t representing a five years timestep and $t = 1$ set at 2005. The associated O&M costs were null.

The installed storage capacity was able to provide a contribution within the capacity constraint equation 2.3 through a Capacity Coefficient (CC) equal to 0.85. Moreover, it was involved in flexibility constraint equation 4.5 assuming 2000 yearly full production hours, to obtain the fictitious TWh generated by the storage, with a flexibility coefficient FC equal to 1. Thus, investing in storage capacity represented just a measure to install high capacities of VRE, characterized by a low contribution to meeting the peak load and by a negative flexibility coefficient.

However, this previous formulation had some clear limitations due to the insufficient description of the operation of storage technologies. In particular, the absence of an electricity input from the other generation technologies and of an electricity output to the grid, associated to an efficiency loss, represented the main weakness. The development of a more detailed formulation of electric storage in WITCH has been at the core of our work and it will be described in section 4.4.

4.2 New Interpretation of VRE Flexibility Coefficient

Our analysis of flexibility coefficient for VRE technologies started from the curves described in section 4.1.3. The shape of these curve led us to make some reflection upon the technical and physical meaning behind them. Our investigation has been focused on two particular aspects:

- First of all, looking at the MFC values from [37] and available in table D.3 in appendix D, it could be noticed that for some regions the value in the first VRE shares range is positive⁴, apparently meaning that VRE could provide flexibility. The involved regions are *mena*, *neweuro*, *oldeuro* and *ssa*. Looking at the data about the electricity generation mix between 2005 and 2015 for these regions from IEA Statistics [44], it has been possible to highlight that these regions are currently characterized by a high share of generation provided by non-VRE flexible generation. This in contrast with other regions, whose electricity mix is dominated by baseload technologies. Thus, since the RLDCs from which these values have been derived are built for the current electricity mix of the different

⁴Here we are referring just to the signs of the MFC values in table D.3 in appendix D, not to the fact that, interpolating the original values, for example in the USA case in Fig.4.4, the resulting curve assumes positive values at very low VRE shares. We accepted this approximation as a consequence of the needed interpolation because, happening just at very low VRE shares, its impact is negligible.

regions, it could be concluded that the positive value of the coefficient at low VRE shares (0-15%) comes from the higher available flexibility of the power system. Therefore this means that it is or has been possible to install low shares of VRE without increasing the production from non-VRE flexible power plants. To allow a better understanding of this statement, it is reminded that the VRE flexibility coefficient represents the additional required non-VRE flexible technologies generation for each extra TWh of VRE production.

- The second point is linked to the fact that, for all the regions, the marginal flexibility coefficient for VRE becomes positive in the third VRE deployment bin. This leads to an increase in the VRE flexibility coefficient that starts becoming less negative from the beginning of the third bin (corresponding to a VRE share of 50%) and going on with increasing VRE share, as it could be clearly seen in Fig.4.4. This behaviour is the result of how the VRE MFCs have been calculated in [37]. We had the possibility, thanks of a direct contact with the authors of this study, to analyze in detail the calculations behind those values and this allowed us to reach a broader understanding of this issue.

4.2.1 Behind the Calculation of VRE Marginal Flexibility Coefficients

The VRE MFC in a certain range of VRE shares has been calculated as the average marginal increase of non-VRE flexible generators production per 1 kWh growth in VRE generation. Thus, what happens is that through the first and the second bins the growth of VRE production goes together with a higher generation from non-VRE flexible power plants, to the detriment of baseload plants generation. But with the beginning of the third VRE shares bin, a further increase in VRE production must imply also an absolute decrease of non-VRE flexible generation. This simply because the sum of the production shares of all the technologies is 100% and to have a further increase of VRE share, the share of flexible generators have to decrease too. Nonetheless, this should not mean that the VRE, alone, are capable of requiring less flexibility, because the need for flexibility is intrinsically dependent on the nature of the VRE technologies and on their reliance on an intermittent natural energy source. To conclude, we think that the shape of the curve resulting from VRE MFCs (Fig. 4.4) could not represent the flexibility coefficients of VRE technologies alone, but there should be another contribution that allows the VRE technologies to ask for less flexibility at high shares. A personal communication with Nils Johnson, the corresponding author of [37], clarified that, in the MESSAGE model, the contribution of grid upgrades to the integration of VREs is not explicitly modeled, but it is intrinsically included in the existing formulation. Thus, we concluded that a contribution related to the “smartening” and pooling of the grid is the one that allows the VREs to require less flexibility per unit of electricity generated, i.e. their flexibility coefficient becomes less negative. This contribution becomes significant at VREs shares higher than 50% (that corresponds to the third MESSAGE deployment bin) because higher VREs shares are not likely to be achieved without the above mentioned interventions on the grid.

4.2.2 Flexibility Coefficient Curve as Sum of Two Contributions

Our solution to this issue is that the VRE flexibility coefficients curve in Fig. 4.4 is the results of the sum of two different contributions:

- A curve representing the flexibility coefficient proper of VRE technologies, as they are installed and interact with the rest of the power system. This contribution has been modeled as a 3rd degree polynomial curve function of the VRE share before curtailment⁵ that behaves as the overall FC curve in the first two VRE shares bins and then remains constant at the value assumed in correspondence of the beginning of the third bin.
- A curve representing the contribution of grid pooling, that stands for the whole set of technology options (described in Section 3.1.2) into which investments could be made in order to increase the electric grid connection and reliability and allow high shares of VRE generation. This contribution has been modeled as a 2nd degree positive polynomial curve function of the VRE share before curtailment, starting from a value of 0 with a null VRE share and then increase reaching significant values at the beginning of the third VRE shares bin. To find this curve, a difference between the curve interpolated from the original MFCs values and the curve of VRE alone FC above mentioned has been performed. Then, the obtained values have been interpolated with a 2nd degree positive polynomial curve, starting from the origin and reaching the actual value for a VRE share of 100%. The effect of grid pooling is represented with the grid pooling coefficient POOLING that assumes the values of the curve and whose meaning and use will be explained in section 4.3.

In Fig. 4.5 the curves representing the two different contributions and the overall resulting FC curve could be seen for the USA case.

In Fig. 4.6, instead, it could be seen a comparison between the 3rd degree polynomial curve of the overall VRE FC that we implemented in WITCH and that results from the sum of the two above mentioned contributions, and the VRE FC 3rd degree polynomial curve derived from the original MFCs values and also visible in Fig. 4.4. The comparison highlights that the implemented curves constitute a good approximation of the originally interpolated ones. In appendix D the polynomial coefficients used in the WITCH model for representing the different curves described in this section can be found.

4.3 New Electric Grid Modeling

Our work on the electric grid modeling in WITCH has proceeded along four directions:

- Better definition of installed grid capacity.

⁵Here it is intended the share of electricity generation of all the VRE technologies as a whole, considered before taking into account the short-term and seasonal curtailment

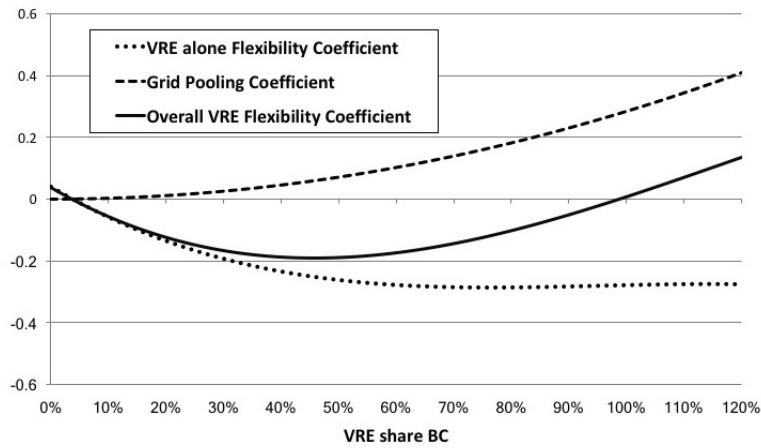


Figure 4.5: VRE alone FC 3^{rd} degree polynomial curve, grid pooling coefficient 2^{nd} degree polynomial curve and overall VRE FC curve resulting from the sum of the other two curves, all function of the VRE share before curtailment, for the USA case.

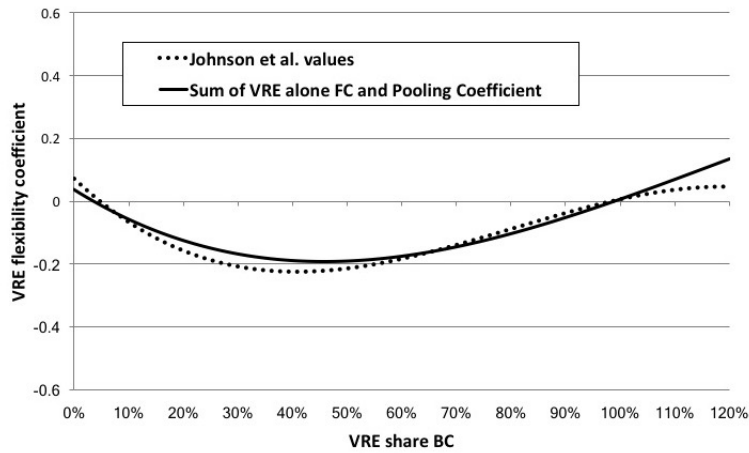


Figure 4.6: Comparison between the overall VRE FC 3^{rd} degree polynomial curve implemented in WITCH and 3^{rd} degree polynomial curve interpolated from the original MFCs values taken from Johnson et al. [37].

- Distinction between two different types of electric grid: transmission and distribution lines, characterized by different extensions and investment costs.
- Refinement of the grid pooling modeling.
- Introduction of losses on electric grid lines to differentiate between electricity input to the the grid and the output to the demand.

4.3.1 Better Definition of Installed Grid Capacity

Installed grid capacity is still considered linearly proportional to the installed generation capacity. Nevertheless, we introduced the conversion factor grid requirement *grid_req* expressed as km of installed grid per TeraWatt (TW) of installed generation capacity, to translate the installed grid capacity into *km*, instead of TW. The reason behind this choice is that the *km* are a measurement unit we found broadly used in

the related literature and with respect to which it is much easier to derive literature data on the grid investment costs.

4.3.2 Distinction between Transmission and Distribution Lines

We decided to introduce just a general distinction among transmission and distribution lines, because a more detailed differentiation, based on the different lines voltages, would have been outside the scope of an IAM as the WITCH model. Moreover, the representation of grid has to be based on strong approximations in a model without a detailed geographical representation of load locations and grid extensions.

The distinction among transmission and distribution lines pursues the objective of highlighting the specific investments required in the two different types of grid, based on the fact that different types of VRE technologies (depending on the distance from load centers) and of storage technologies ask for different types of grid. Moreover, as it has already been introduced in Section 3.1.1, the differentiation between the two type of lines has been implemented through some specific parameters, assuming different values for transmission and distribution lines. The differences, already motivated in Chapter 3, can be summed up as in the following:

- Different lifetime: 60 years for transmission and 50 years for distribution lines. This corresponds in WITCH to a yearly depreciation rate δ_{grid} (see Chapter 2) of 0.024 for transmission and 0.027 for distribution lines.
- Distinct grid requirement : different values have been used for different region, as it is explained in Section 3.1.1. For transmission lines, the ranges of values is between around 200'000 and 700'000 km/TW . While for distribution lines the ranges of values is between around 4 *mln* and 14 *mln* km/TW . The higher values for distribution lines are due to the fact that these are usually much shorter than transmission line, but the distribution grid is much more widespread.
- Different grid investment costs: around 700'000 \$2005/ km for transmission lines and 25'000 \$2005/ km for distribution lines.
- All non-VRE generation technologies requires both transmission and distribution lines, while for VRE technologies we applied some distinctions based on distance from load centers. Solar and wind capacity with *intermediate* or *far* distance necessitates both transmission and distribution since the electricity they produce need to be firstly transmitted to the load centers and then distributed. Besides, for far VRE plants markup is set by multiplying the transmission grid requirement by a factor of 4 (assumed as the ratio between mean distance of “far” VRE plants and “average” VRE plants), to consider the additional grid needed to connect solar and wind plants very far from the load centers, often characterized by geographical obstacles and difficulties. On the other hand, solar and wind capacity characterized by *near* distance (<50 km) requires just distribution line because they are close to the electricity consumption points and they can also represent

VRE capacity at the residential level.

- About storage capacity, we assumed that PHES and CAES technologies just require transmission lines because they are usually used as centralized electric storage systems connected to the high voltage lines. Conversely we assumed that batteries and fuel cells only need distribution lines because they are widely thought as distributed electric storage systems.

As a result, we wrote the following equations describing the electric grid. The capital stock equation eq. 4.8 has the same shape as in the pre-existing formulation but now it is differentiated for the two grid types (the exponent 5 is related to the WITCH time steps length that is 5 years). Eq. 4.9 represents the definition of installed transmission grid capacity from installed generation and storage capacity, while eq. 4.10 is the analogous for distribution grid capacity. In eq. 4.9 and eq. 4.10 the new formulation of the installed capacities K_STOR and K_FUEL_CELL of electric storage technologies (in TW) is introduced, please refer to Section 4.4 to fully understand its meaning.

$$K_EL_GRID(grid_type, t + 1, n) = K_EL_GRID(grid_type, t, n) \times (1 - \delta_grid)^5 + 5 \times \frac{I_GRID(grid_type, t, n)}{grid_inv_cost(grid_type)} \quad (4.8)$$

$$K_EL_GRID_{transmission}(t, n) = grid_req_{transmission} \times \left[\sum_{jel|non.VRE} K_EL(jel, t, n) + \sum_{jel|VRE_{intermediate}} K_EL(jel, t, n) + 4 \times \sum_{jel|VRE_{far}} K_EL(jel, t, n) + K_STOR_{phes}(t, n) + K_STOR_{caes}(t, n) \right] \quad (4.9)$$

$$K_EL_GRID_{distribution}(t, n) = grid_req_{distribution} \times \left[\sum_{jel|non.VRE} K_EL(jel, t, n) + \sum_{jel|VRE_{near}} K_EL(jel, t, n) + K_STOR_{batteries}(t, n) + K_FUEL_CELL(t, n) \right] \quad (4.10)$$

4.3.3 Refinement of the Grid Pooling modeling

In introducing a way to represent the concept of grid smartening and pooling (for simplicity, in the following it will be referred to as just "pooling"), our objective has not been to represent it in a detailed way: we are aware that developing the grid in order to reach a higher integration of VRE technologies, by reducing volatility and

increasing dispatchability, requires a wide set of solutions. After having investigated these solutions from a technical view-point in Section 3.1.2, here we aim at explaining how this has been translated into the WITCH model. First of all, it should be pointed out that we decided to represent grid pooling as additional investments, that are required to upgrade the existing grid or build more connections. Therefore, there is not an installed capacity associated to pooling. Because of the variegate nature of the actual grid smartening and pooling solutions, in our view, representing only its economic values is a good approximation in a model like the WITCH one.

This additional amount of investments that need to be performed in order to implement grid pooling and integrate VRE into the grid has been considered proportional to the sum of the investments I_GRID in transmission and distribution lines. The rationale behind it is that the more transmission and distribution lines are built, the more investments will be require to smarten and connect them at international level. So, it works as an investments markup. In particular, the factor of proportionality is the variable $POOLING$ that is represented by the 2^{nd} degree positive polynomial curve function of the VRE share before curtailment introduced in Section 4.2.2. Thus, the variable $POOLING$ grows quadratically with the VRE share before curtailment (Fig. 4.7 for the USA case). In table 4.3 the values assumed for the different regions in correspondence of VRE shares before curtailment equal to 30%, 50% and 100% could be seen.

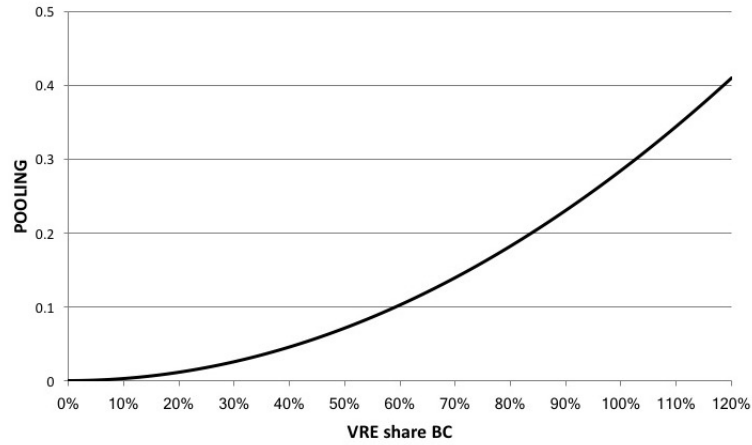


Figure 4.7: $POOLING$ quadratic behaviour as a function of $SHARE_EL_VRE_BC$ for the USA case.

Therefore, the investments in pooling are defined as follows:

$$I_GRID_POOLING(t, n) = pooling_req \times POOLING(t, n) \times \sum_{grid.type} I_GRID(t, n) \quad (4.11)$$

Where $POOLING = f(SHARE_EL_VRE_BC(t, n))$ and the “pooling requirement” coefficient $pooling_req$ has a default value of 1. It has been defined to perform a sensitivity analysis on the link between investments in pooling and the overall investments in grid (see Section 5.3).

Polynom coefficient	POOLING						
	cajaz	china	easia	india	kosau	laca	mena
30%	0.042	0.033	0.032	0.046	0.042	0.033	0.010
50%	0.117	0.093	0.088	0.127	0.117	0.092	0.028
100%	0.467	0.372	0.353	0.509	0.467	0.369	0.111
	neweuro	oldeuro	sasia	ssa	te	usa	
30%	0.029	0.015	0.046	0.014	0.015	0.026	
50%	0.080	0.043	0.127	0.038	0.040	0.071	
100%	0.322	0.171	0.509	0.151	0.162	0.285	

Table 4.3: POOLING values in correspondence of three different VRE share BC for all the WITCH regions.

4.3.4 Grid Losses

The lack of a description of thermal losses on electric lines can be considered a weakness of the previous formulation of the electric grid, because these losses constitute a non-negligible fraction of the electricity generation all around the world [48]. Introducing them allows to add the distinction between the electricity generated that is the input into the electric grid and the electricity that can actually be consumed.

To understand our modeling choice, it is useful to recall the broader scope of the WITCH model, that is to get the overall generation by the energy sector and convert it into its economic value, that will enter the utility function together with capital and labour (see 2.2). This conversion is done through the energy factor productivity, a parameter that translates the TWh of electricity produced into its monetary value in \$05. Therefore, we decided to represent the grid thermal losses just as a portion of the economic value of electricity that is lost. This is done by subtracting the portion $transm_distrib_loss \times Q_{EL}$, that is lost on the grid lines, from the calculation of the monetary value of electricity Q .

As it has already been introduced in Section 3.1.1, the parameter $transm_distrib_loss$ has distinct values for developed, developing and underdeveloped regions and decreases linearly over time (Table 3.2).

4.4 New Electric Storage Formulation

Our objective, in modeling electric storage in the WITCH model, has been introducing a new formulation that allows to represent the general operation of storage, in terms of input (charge) and output (discharge) electricity and related losses, due to non-unitary round-trip efficiency. However, we are aware that this formulation must include some strong assumptions and approximations, due to the impossibility of representing the actual charge-discharge cycles and geographical locations of storage technologies, because of the high temporal and geographical aggregation of WITCH. Thus, in doing the needed assumptions, we always tried to rely on our engineering and technical background, along with solid literature references, in order to guarantee the technical consistence of the model formulation and of the consequent results.

More precisely, about our electric storage modeling choices, we decided to model two different types of storage with different input sources and uses, as it has been described in Chapter 3:

- **Short-Term Storage:** it represents the storage technologies used for daily shifting of electricity generation to meet peak load, that does not happen in coincidence with high VRE production, or to exploit daily differences in electricity prices. In our formulation it can receive electricity input from three different types of sources: non-VRE power plants, VRE short-term curtailment (described in Section 4.1.2) and non-curtailed VRE generation.
- **Seasonal Storage:** it stands for the set of technologies used to implement a shifting of generation between different seasons. It could be particularly exploited in regions where there is a decoupling of high electricity demand and high VRE generation among different seasons. In our formulation, it can receive input from just one source: VRE seasonal curtailment (again described in Section 4.1.2).

4.4.1 Short-Term Storage

In Section 3.2.3, the choices we made in terms of short-term storage technologies to be modeled are presented. In particular, we selected Li-ion batteries, adiabatic CAES and PHES for several reasons, among which commercial maturity and future perspectives of these technologies. These technologies have been introduced in the WITCH model through some characteristic parameters, whose values are listed in table 3.4.

As regards the installed capacity, the storage technologies have been considered from both the dimensions that characterize storage: the power conversion system and the energy reservoir. Accordingly, two different capacities have been defined for short-term storage technologies: K_STOR that is the installed power capacity (in TW) and K_STOR_RES that is the installed energy capacity (in TWh). For each technology, we considered an investment cost per unit of TW installed for the power conversion system and an investment cost per unit of TWh installed for the energy reservoir. Thus, the overall investment cost in short-term storage I_STOR includes both the investment in power and energy capacities.

Lacking the possibility to model the ratio installed storage TWh/TW as based on optimization of charge-discharge cycles (due to temporal and geographical aggregation of the WITCH model), we fixed the ratio between installed K_STOR and K_STOR_RES of each technology through the parameter avg_EtoP_ratio (average energy-to-power ratio). The value chosen for this parameter is based on historical data for PHES, while it has been derived from the assumed avg_disch_hcycle (average discharging hours per cycle) for CAES and LiB (as it has been described in Section 3.2.3). The following equation defines the link between the two installed capacities of storage technologies:

$$K_STOR_RES(j_stor, t, n) = avg_EtoP_ratio(j_stor) \times K_STOR(j_stor, t, n) \quad (4.12)$$

Regarding the overall investment cost, as it is explained in Section 3.2.3, it has been derived through the sum of the two distinct cost components, for the power and energy capacity of the technology. It has been expressed in terms of installed power by converting the cost in TWh through the *avg_EtoP_ratio* specific of each technology. Moreover, for LiB and CAES, the overall capital cost decreases with growing cumulative installed power capacity, through Learning by Doing, and therefore it is a function of time.

Consequently, for each short-term storage technology *j_stor*, a capital stock equation has been defined:

$$K_STOR(j_stor, t + 1, n) = K_STOR(j_stor, t, n) \times (1 - \delta_stor(j_stor))^5 + 5 \times \frac{I_STOR(j_stor, t, n)}{INV_COST_STOR(j_stor, t)} \quad (4.13)$$

The short-term storage technologies can receive electricity as input from three different sources: non-VRE thermal power plants, VRE short-term curtailment and non-curtailed VRE generation. The first two ones can supply a fraction of installed storage capacity called *K_STOR_CURT*⁶, while the latter can supply the second fraction of storage capacity called *K_STOR_PEAK*. Thus, the overall installed capacity of each short-term storage technology *j_stor* and the overall yearly investments in it are defined as follows:

$$K_STOR(j_stor, t, n) = K_STOR_CURT(j_stor, t, n) + K_STOR_PEAK(j_stor, t, n) \quad (4.14)$$

$$I_STOR(j_stor, t, n) = I_STOR_CURT(j_stor, t, n) + I_STOR_PEAK(j_stor, t, n) \quad (4.15)$$

Non-VRE Technologies Input to Storage

All non-VRE plants can feed electricity into short-term storage *K_STOR_CURT* capacity, except for the hydro and CSP⁷. Our research objective was to study the effect of storage technologies on VRE integration, so the contribution of non-VRE technologies

⁶This name has been chosen because the aim of our research is highlighting the interaction between storage technologies and VRE integration, as it will be clarified in the following paragraph, when talking about the contribution of non-VRE power plants to storage input.

⁷CSP is modeled in WITCH as already provided with its own storage capacity, that is not explicitly represented. In fact it is a dispatchable technology, participating in the capacity constraint equation with its whole installed capacity

could have represented an interference with what we aimed at observing. Thus, we decided to fix the contribution of non-VRE technologies to storage to the initial starting level. For PHES, we did so by fixing the share of non-VRE plants generation that feeds PHES to the initial 2015 value. While for CAES and LiB, we fixed the upper bound of the input to the initial 2015 value (the small initial installed capacity of CAES and LiB has been modeled as fed just by non-VRE power plants, for simplicity).

Despite the fact we considered the non-VRE power plants contribution just as an interference and we decided to apply the above mentioned restrictions, we decided to model their role mainly for two reasons:

- To define the electricity input to the initial installed capacity of PHES in the years between 2005 and 2015. We thought that considering the initial PHES capacity just fed by non-VRE generation plants represents a conservative and realistic assumption (in the perspective of considering the effect of storage on VRE integration) because what happens in the real electric systems is that PHES plants usually store electricity when its price is low and this is usually related to base-load plants production during hours of low demand, and they resell it when price rises. Moreover, also the initial installed capacities of CAES and LiB are considered just to be fed by non-VRE power plants. However, these initial capacities are much smaller than the PHES one, so this assumption has a negligible impact on the results.
- To allow a possible future study of the potential impact of deploying storage technologies for non-VRE power plants, by letting them free to feed their production to storage.

The input electricity to storage from the j_{el} non-VRE technologies Q_{EL_STORED} has been defined by dividing the overall generation Q_{EL} of the j_{el} technology in a stored and a non-stored fractions:

$$Q_{EL_{non-VRE}}(j_{el}, t, n) = \sum_{j_{stor}} Q_{EL_STORED}(j_{el}, j_{stor}, t, n) + Q_{EL_NON_STORED}(j_{el}, t, n) \quad (4.16)$$

The losses in storage technologies related to non-VRE input are considered by subtracting the value of losses from the non-VRE j_{el} technologies overall generation entering in the calculation of the monetary value of energy.

Short-Term VRE Curtailment Input to Storage

The energy input to storage technologies from short-term VRE curtailment has been defined through the following equation that, instead of the input, involves the output from storage:

$$\sum_{j_stor} \frac{Q_OUT_STOR_CURT(j_vre, j_stor, t, n)}{\eta_{stor}(j_stor)} \leq Q_EL_CURT_{short-term}(j_vre, t, n) \quad (4.17)$$

This equation is defined for each VRE technology j_vre . $Q_OUT_STOR_CURT$ is the output electricity from the single storage technology that derives from short-term VRE curtailment. It is divided by the round-trip efficiency of each storage technology η_{stor} to obtain the electricity input. Then, the sum of the inputs in each storage technology from a particular VRE technology has to be lower or equal than the short-term curtailed fraction of generation of VRE technology .

Finally equation 4.18 links each j_stor technology electricity output with its installed capacity K_STOR_CURT . This relationship is ruled by the parameter $full_prod_hours$ that stands for the annual full production hours during which the j_stor technology can produce. Using the equal sign, we assume that the storage is always used at its full potential. In our view, since there is not the possibility to model the optimization of actual charging-discharging cycles, this represents a good approximation. In the equation the two sources of electricity for the K_STOR_CURT capacity can be seen in terms of electricity outputs: the non-VRE stored production Q_EL_STORED , translated into the output from the j_stor technology through its round-trip efficiency, and the $Q_OUT_STOR_CURT$.

$$\begin{aligned} \sum_{j_el} Q_EL_STORED(j_el, j_stor, t, n) \times \eta_{stor}(j_stor) \\ + \sum_{j_vre} Q_OUT_STOR_CURT(j_vre, j_stor, t, n) = \\ K_STOR_CURT(j_stor, t, n) \times full_prod_hours(j_stor, t, n) \quad (4.18) \end{aligned}$$

Non-Curtailed VRE Generation Input to Storage

The development of the model has proceeded step by step. First of all, we implemented the input to storage from VREs short-term curtailment and we had a look at the results. Keeping in mind that curtailment is a quadratic function of the VRE share BC (Section 4.1.2) and that the capacity value CV of wind and solar plants decreases with the VRE share BC (Fig. 4.1), we found out that considering just the short-term curtailment as input to storage hinders the installation of VREs. This because meeting the firm capacity and flexibility requirements turn out to be the most binding constraint in VREs integration in the WITCH model. Nevertheless, the storage capacity that can be installed just using as input the short-term curtailment results to be insufficient to balance the need for flexibility and capacity , due to a higher overall generation ⁸ or to

⁸It is worth recalling that the peak load used in the capacity constraint equation is proportional to the average annual load, so to the annual generation through the firm requirement parameter

a reduction of non-VRE flexible power plants production.

As a consequence, to allow the VREs to exploit more the storage technologies and so foster their integration, counterbalancing their low capacity value, we decided to model a second source of electricity input to storage. This is defined as a fraction of the non-curtailed VREs generation going as input to the storage capacity K_STOR_PEAK . An upper bound on the exploitable portion is set through the parameter $fraction_vre_stored$, and the default value we chose for this parameter is 20%. The reason for this choice lies in the temporally and spatially refined model for the scheduling and operation of a wind farm with storage in a market configuration, presented in [104]. This model can also be applied to different regions, VRE and storage technologies [104]. The simulations conducted with the model show that, using real data from the Norwegian region, about 18% of wind generation is stored and then discharged to follow the market scheduling and ensure reliable supply. The figure has then been rounded to 20% for simplicity. The limitations of the research from which we derived this assumption impose further analyses to understand its impact and its robustness. We therefore performed a broad sensitivity analysis on its value to get insights on its influence on the installation of storage capacity and on VREs generation. The results of this analysis can be seen in Section 5.3.4.

Because of how the VREs generation is defined in the model (distinction between curtailed and non-curtailed fractions), in order to define properly this electricity input to storage and its contribution to the overall VREs production, entering in the calculation of the monetary value of energy, we had to define a proper short-term storage capacity K_STOR_PEAK . The following equation defines the link between this storage capacity and the fraction of non-curtailed VRE generation that could be fed into it.

$$\begin{aligned} \sum_{j_stor} \frac{K_STOR_PEAK(j_stor, j_vre, t, n) \times full_prod_hours(j_stor, t, n)}{\eta_{stor}(j_stor)} \\ \leq fraction_vre_stored \times (Q_EN_BC(j_vre, t, n) \\ - \sum_{curt_type} Q_EN_C(j_vre, curt_type, t, n)) \quad (4.19) \end{aligned}$$

4.4.2 Seasonal Storage

Seasonal storage can receive electricity input just from one source: seasonal curtailment of VRE generation (see Section 4.1.2). In particular, it is worth recalling that seasonal curtailment is a quadratic function of VRE share BC (see table D.2 in Appendix D for the fraction of curtailment values at different VRE shares).

As introduced in Section 3.2.5, we have modeled seasonal storage with the production and further consumption of hydrogen. The reason behind this choice is that hydrogen can be considered a good solution in terms of long-term storable and dispatchable energy carrier and because the implemented technologies are already in their commercial phase. In particular, hydrogen is produced through a generic electrolyzer technology that is fed by the electricity input from seasonal VRE curtailment. Then, hydrogen

is stored and transported and we considered the economic impact of this operations through an overall storage and transport cost per unit of kWh of hydrogen produced. Finally, hydrogen represents the fuel input into a generic fuel cell technology modeled as a Polymeric Electrolyte Membrane Fuel Cell (PEMFC).

Hydrogen Production

First of all, the maximum hydrogen production Q_ELH2 in terms of TWh in each time step and in each region is defined by the seasonal curtailed fraction of VREs generation⁹ reduced through the assumed efficiency of the electrolyzer technology (refer to Section 3.2.5 for the values used for the different parameters characterizing seasonal storage technologies).

$$Q_ELH2(j_vre, t, n) \leq Q_EN_C_{seasonal}(j_vre, t, n) \times \eta_electrolyzer \quad (4.20)$$

After that, in equation 4.21 the hydrogen production is linked to the installed electrolyzer capacity K_ELH2 (in TW). In particular, the hydrogen production has to be lower than the product between the electrolyzer installed capacity and an average number of annual operating hours, that is directly related to an average number of full production hours ($avg_CF(j_vre) \times yearly_hours$) of the single j_vre . In particular, the annual operating hours that the electrolyzer can dedicate to the input from a particular j_vre is derived from the average number of full production hours of this j_vre multiplied by the share of the overall VREs seasonal curtailment represented by this specific j_vre technology. We are aware that this is an approximation, but in our opinion it is a consistent way to define the real annual operating hours of the electrolyzer technology and from it derive the installed capacity K_ELH2 through the hydrogen production $Q_ELH2(j_vre, t, n)$ (which derives from equation 4.20). The reason behind this modeling choice is that the installed electrolyzer capacity should not be derived from its hydrogen production through some annual operating hours defined *a priori*. On the contrary, the electrolyzer can work just in the hours when there is available electricity from VREs seasonal curtailment.

$$Q_ELH2(j_vre, t, n) \leq K_ELH2(t, n) \times avg_full_prod_hours_{VRE}(j_vre, n) \times \frac{Q_EN_C_{seasonal}(j_vre, t, n)}{\sum_{j_vre} Q_EN_C_{seasonal}(j_vre, t, n)} \quad (4.21)$$

The last equation is the capital stock equation that links installed capacity and investments for the electrolyzer technology:

$$K_ELH2(t + 1, n) = K_ELH2(t, n) \times (1 - \delta_electrolyzer)^5 + 5 \times \frac{I_ELH2(t, n)}{INV_COST_ELH2} \quad (4.22)$$

⁹ Note that in our formulation Q_ELH2 is also a function of the VRE technology j_vre since in equation 4.21 the operating hours of the electrolyzer are defined through an average capacity factor of VRE technologies.

Fuel Cells Capacity and Generation

The first equation modeling the fuel cell technology links its electricity generation Q_FUEL_CELL ¹⁰ to the available amount of exploitable energy in terms of TWh of hydrogen Q_ELH2 through the efficiency of the fuel cell.

$$Q_FUEL_CELL(j_vre, t, n) = Q_ELH2(j_vre, t, n) \times \eta_{fuel_cell} \quad (4.23)$$

The second equation expresses the relationship between the fuel cell technology annual generation Q_FUEL_CELL and its installed capacity K_FUEL_CELL ¹¹ in TW, through the parameter $full_prod_hours_{fuel_cell}$ indicating the annual full production hours that characterize fuel cell technology operation.

$$Q_FUEL_CELL(j_vre, t, n) \leq K_FUEL_CELL(t, n) \times full_prod_hours_{fuel_cell} \quad (4.24)$$

Finally, the last equation is the capital stock equation for the fuel cell technology in the usual form.

$$K_FUEL_CELL(t + 1, n) = K_FUEL_CELL(t, n) \times (1 - \delta_{fuel_cell})^5 + 5 \times \frac{I_FUEL_CELL(t, n)}{INV_COST_FUEL_CELL} \quad (4.25)$$

4.4.3 Effect of New Formulation on Pre-Existing Equations

The effects of the new formulation of electric storage is particularly visible on three pre-existing equations in WITCH:

- The definition of VREs generation Q_EL after considering curtailment
- The capacity constraint equation
- The flexibility constraint equation

Definition of VREs Generation After Curtailment

The VREs generation after considering curtailment, Q_EL , is the one that enters in the calculation of the monetary value of energy, to consider its effect on the utility function. Thus, the positive effect of the additional contributions of short-term and

¹⁰Since, as explained in note 9, Q_ELH2 is a function of the VRE technology j_vre whose seasonal curtailment is feeded to the electrolyzer, also Q_FUEL_CELL has to be a function of j_vre in the model.

¹¹In the model code we called the capacity of the seasonal storage related generation capacity $K_STOR_SEASONAL$, function of the $j_stor_seasonal$ technology to allow the possibility of adding easily an alternative solution. Here, since we implemented just the fuel cell technology, we call it K_FUEL_CELL .

seasonal curtailment fractions that are stored and then produced have to be taken into consideration¹². Along with the negative effect of the losses related to the non-curtailed portion of VRE generation that is stored. The resulting equation has the following aspect (defined $\forall j_vre$ technology):

$$\begin{aligned}
Q_{EL}(j_vre, t, n) &= Q_{EL_BC}(j_vre, t, n) \\
&- \sum_{curt_type} Q_{EL_CURT}(j_vre, curt_type, t, n) \\
&+ \sum_{j_stor} Q_{OUT_STOR_CURT}(j_vre, j_stor, t, n) \\
&- \sum_{j_stor} K_{STOR_PEAK}(j_vre, j_stor, t, n) \\
&\quad \times full_prod_hours(j_stor, t, n) \times \left(\frac{1}{\eta_{stor}(j_stor)} - 1 \right) \\
&+ Q_{FUEL_CELL}(j_vre, t, n)
\end{aligned} \tag{4.26}$$

Capacity Constraint Equation

As compared to equation 4.1, the new formulation of the capacity constraint equation presents differences in the definition of termes referring to capacities of storage technologies. First of all, there is the contribution of installed capacity of every short-term storage technology K_{STOR} , each multiplied by its capacity coefficient $CC_{stor}(j_stor)$ (1 for PHES and CAES, 0.8 for LiB). Then, the component related to the installed fuel cell technology capacity K_{FUEL_CELL} is visible with a capacity coefficient CC_{fuel_cell} of 1. Again, the positive contributions of generation plants and storage technologies have to be greater or equal than the product of firm requirement and annual average load for each time step and region.

$$\begin{aligned}
&\sum_{jel|non_VRE} K_{EL}(jel, t, n) + \sum_{jel|VRE} K_{EL}(jel, t, n) \times CF(jel, t, n) \times CV(jel, t, n) \\
&+ \sum_{j_stor} K_{STOR}(j_stor, t, n) \times CC_{stor}(j_stor) \\
&+ K_{FUEL_CELL}(t, n) \times CC_{fuel_cell} \\
&\geq firm_req(n) \times \frac{Q_{EL_TOT}(t, n) - LOSS(t, n)}{yearly_hours}
\end{aligned} \tag{4.27}$$

Where:

¹²These contributions are taken into account as output from the storage technologies so that the entailed losses are already accounted

$$LOSS(t, n) = \sum_{jel|non-VRE} \sum_{j_stor} Q_EL_STORED(jel, j_stor, t, n) \times (1 - \eta_{stor}(j_stor))$$

The $LOSS$ is subtracted from the overall electricity generation $Q_EL_TOT(t, n)$ to consider the losses in storage related to input from non-VRE technologies.

Flexibility Constraint Equation

The flexibility equation is the one that presents the addition of the highest number of terms (compare with equation 4.5). Firstly, we can focus on the first term between square brackets, that is multiplied by FC_VRE (second, third and fourth rows of equation 4.28). Here, the overall generation of a single VRE technology after considering curtailment Q_EL has to be reduced by the fractions that are actually produced by short-term storage technologies, the first and second term, and by fuel cell technology, the third one. This because in the calculation of the Q_EL of the j_vre technology, these terms were included (equation 4.26) to have the right value entering the calculation of the monetary value of energy.

Then, the second term between square brackets, that is all multiplied by FC_{stor} (fifth, sixth and seventh rows of equation 4.28) represents the contribution of short-term storage technologies. For each short-term storage technology j_stor , all the three storage outputs (each one related to a different input source) are multiplied by the proper flexibility coefficient FC_{stor} (0.75 for PHES and CAES, 1 for LiB). The last new term is the one related to the fuel cell technology: its annual generation multiplied by a flexibility coefficient FC_{fuel_cell} equal to 0.9. Finally, the term related to the flexibility requirement of load appears.

$$\begin{aligned}
& \sum_{jel|non-VRE} Q_{EL_NON_STORED}(jel, t, n) \times FC_{non-VRE}(jel) \\
& + \sum_{jel|VRE} \left[Q_{EL}(jel, t, n) - \sum_{j_stor} \left(Q_{OUT_STOR_CURT}(j_vre, j_stor, t, n) \right. \right. \\
& \quad \left. \left. - \frac{K_{STOR_PEAK}(j_stor, t, n) \times full_prod_hours(j_stor, t, n)}{\eta_{stor}(j_stor)} \right) \right. \\
& \quad \left. - Q_{FUEL_CELL}(j_vre, t, n) \right] \times FC_{VRE}(jel) \\
& + \sum_{j_stor} \left[\sum_{j_vre} \left(Q_{OUT_STOR_CURT}(j_vre, j_stor, t, n) \right. \right. \\
& \quad \left. \left. + K_{STOR_PEAK}(j_vre, j_stor, t, n) \right. \right. \\
& \quad \quad \left. \left. \times full_prod_hours(j_stor, t, n) \right) \right. \\
& \quad \left. + \sum_{jel|non-VRE} Q_{EL_STORED}(jel, j_stor, t, n) \right] \times FC_{stor}(j_stor) \\
& + Q_{FUEL_CELL}(j_vre, t, n) \times FC_{fuel_cell} \\
& + FC_{load}(n) \times (Q_{EL_TOT}(t, n) - LOSS(t, n)) \geq \mathbf{0}
\end{aligned} \tag{4.28}$$

Chapter 5

Results and robustness analysis

In this chapter the results of our analysis will be presented. Firstly, a policy analysis is carried out to see the role of VREs together with the one of electric storage and grid in different climate change mitigation policies. In particular, some scenarios with a significant push towards VREs installation are assessed to study the impact of electric storage and grid in this sense. Then, a comparison of WITCH results with the old editions of the model is performed to understand better the effect of our new formulation on the WITCH model itself. After that, a deeper look at the impact of storage and grid modeling on VRE system integration is taken. Then, several sensitivity analyses are carried out to identify the main parameters that drive the installation of storage and grid. Finally, a comparison of the WITCH results with the ones of other IAMs and other more detailed models is presented.

5.1 Policy analysis

In this chapter, we present the results of model runs with the new features discussed in chapter 4, under different climate policy assumptions. These results should not be seen as an attempt to predict accurately transformations and configurations of future energy systems. As a matter of fact, they come from an optimization process, whose outcome is the welfare-maximizing organization of the energy sector, influenced by the external economic stimuli we select in the form of policy scenarios. Therefore, they should be rather seen as an economically-optimal scenario that can be used to inform policy-makers on how to allocate resources and stimulate the diffusion of low-carbon energy technologies if emission targets are to be met.

As regards the climate policies represented in the results, we investigate three scenarios:

- Business as usual (BAU): no effort is put in place to mitigate climate change, so no carbon mitigation policy is implemented.
- Carbon Tax (CTAX): there is a global effort to mitigate climate change, yet there is no precise target about the maximum end-of-the-century temperature increase allowed. A carbon tax on CO_2 emissions is established, starting in 2020 from $30 \frac{\$}{tonCO_2}$ ¹ and growing as shown in figure 5.1 reaching a value of around 460

¹It should be recalled that all the monetary values in WITCH are expressed in \$2005. From now on, in this chapter the specification of the year will be omitted.

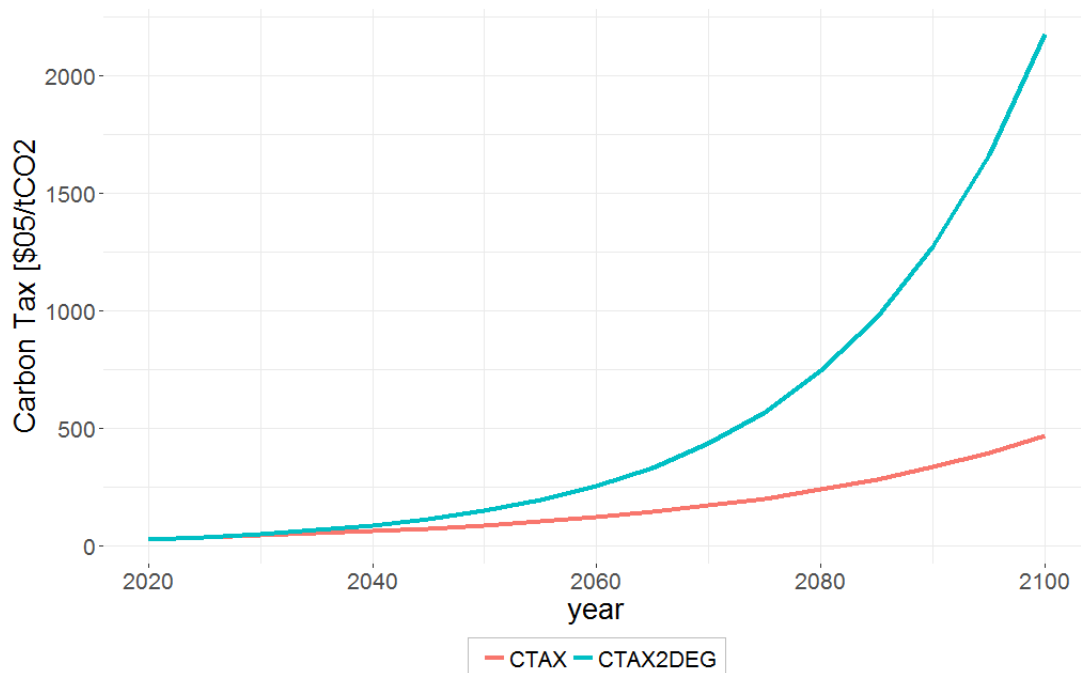


Figure 5.1: Carbon tax and carbon tax for 2 degrees: growth in time.

\$/tonCO₂ in 2100.

- Carbon Tax for meeting the 2 degrees objective (CTAX2DEG): not only is a global price on emissions set, but it is also designed (see fig. 5.1) to limit the temperature increase with respect to pre-industrial era to 2°C by the end of the 21st century. This is the minimum objective set by the Paris Agreement, even though the aim is staying “well below” this threshold, keeping temperature increase as close as possible to 1.5 °C [4].

5.1.1 Policy impact on Electricity Generation

As we can see in figure 5.2, representing global electricity generation over time by technology class, the policy scenario adopted has a strong impact on the global energy mix. For the sake of clarity, this graph represents VRE electricity supply after it has been stored, so a fraction of the VRE generation (both the curtailed part that is recovered via storage and the non-curtailed part that is stored at moments of low demand) has been lost due to the non-unitary storage efficiency.

Electricity generation technologies have been grouped into seven macro categories or classes, described in table 5.1.

As regards the total electricity generation, it is similar among the three different policy scenarios. In particular, it is a bit higher in the CTAX2DEG and a bit lower in the CTAX with respect to the BAU scenario.

Considering the BAU scenario, the first observation is that energy production increases in time, approximately a five-fold increase between 2015 and 2100. Fossil fuels plus nuclear power plants represent the majority of electricity production throughout the century, even though their weight in the overall mix gradually decreases in time (from

Category	Technologies
ccs	Coal IGCC, Biomass IGCC, Gas Combined Cycle with CCS, Pulverized Coal Steam Turbine with CCS, Coal Oxy-fuel Combustion Plant
coal	Pulverized Coal Steam Turbine
gas	Gas Combined Cycle
hydro	Hydro-Power Plant
nuclear	Nuclear Power Plant
oil	Oil Combustion Turbine
other_ren	CSP, Pulverized Biomass Steam Turbine
pv	PV
wind	Wind Onshore and Offshore

Table 5.1: Generation technologies included in each macro category.

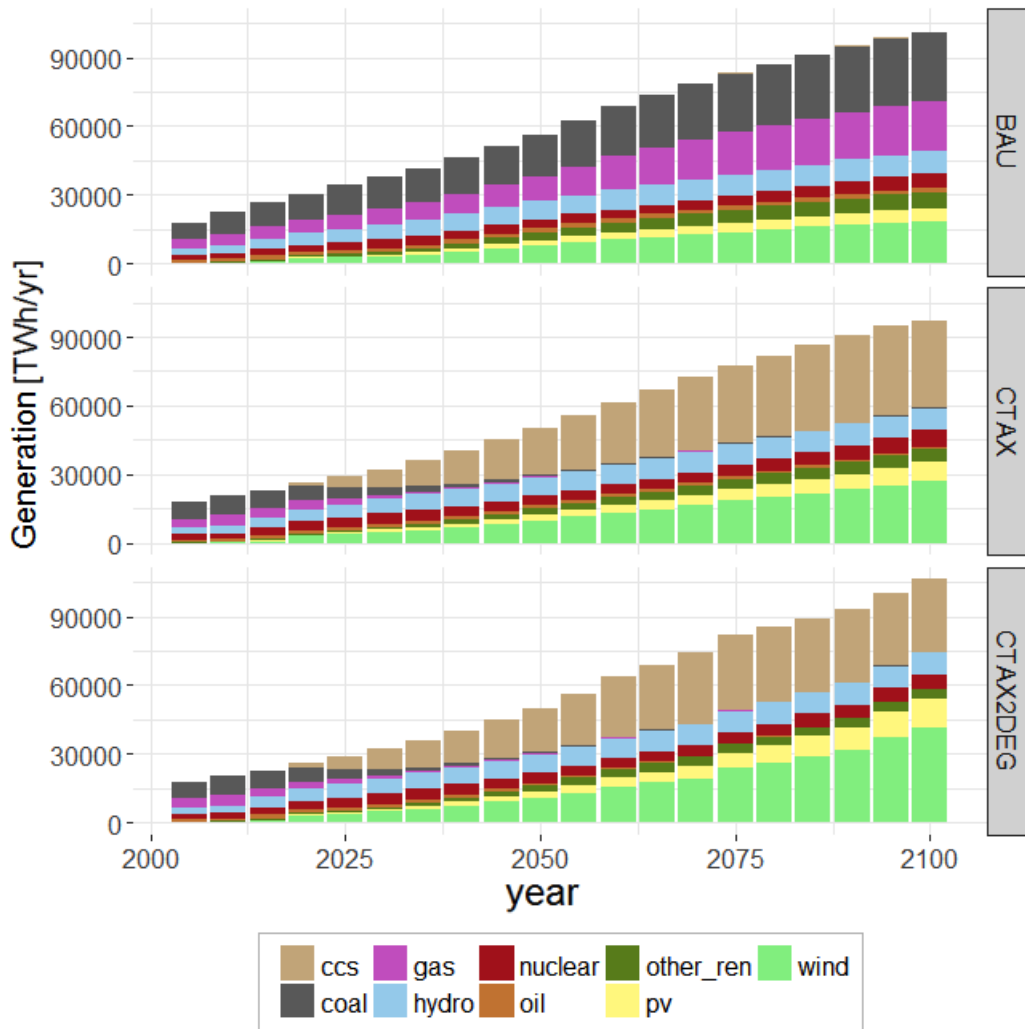


Figure 5.2: Electricity generation (after storage) by technology type in BAU, CTAX and CTAX2DEG policy scenarios.

62% in 2015 to 54.1% in 2050 and 53.1% in 2100). VRE generation represents a non-negligible share of total generation, growing in time from 9.5% in 2020 to 18.5% in 2050 and 24% in 2100.

The CTAX scenario witnesses a progressive phase-out of coal and gas power plants from 2020 on, and they end up representing just 5.5% of the energy mix already in 2050 being replaced by CCS plants², that become the dominant technology (40% in 2050 and approximately constant share until the end of the century). VRE technologies grow more rapidly than in BAU (25% in 2050) and represent more than one third of total generation by the end of the century (37% approximately).

Finally, the CTAX2DEG scenario boosts both VREs and CCS with a faster carbon tax growth, accelerating the phase-out of fossil-based plants (4.2% in 2050 and less than 1% in 2080) and favouring VREs over CCS throughout the century, reversing the trend seen in the CTAX scenario: VRE represent 29.1% of total generation versus 37.8% for CCS in 2050, while the situation is inverted in 2100, with a significant 51.0% of wind and PV plants (after curtailment and storage losses) versus 29.8% for CCS.

As regards local VRE generation, figure 5.3 shows VRE production in all the 13 regions modeled by WITCH at the end of the 21st century: the regions with higher VRE generation are *china*, *mena*, *oldeuro*, *usa* and *india*, and in Paragraph 5.1.2 it is shown how this is related to storage technology diffusion.

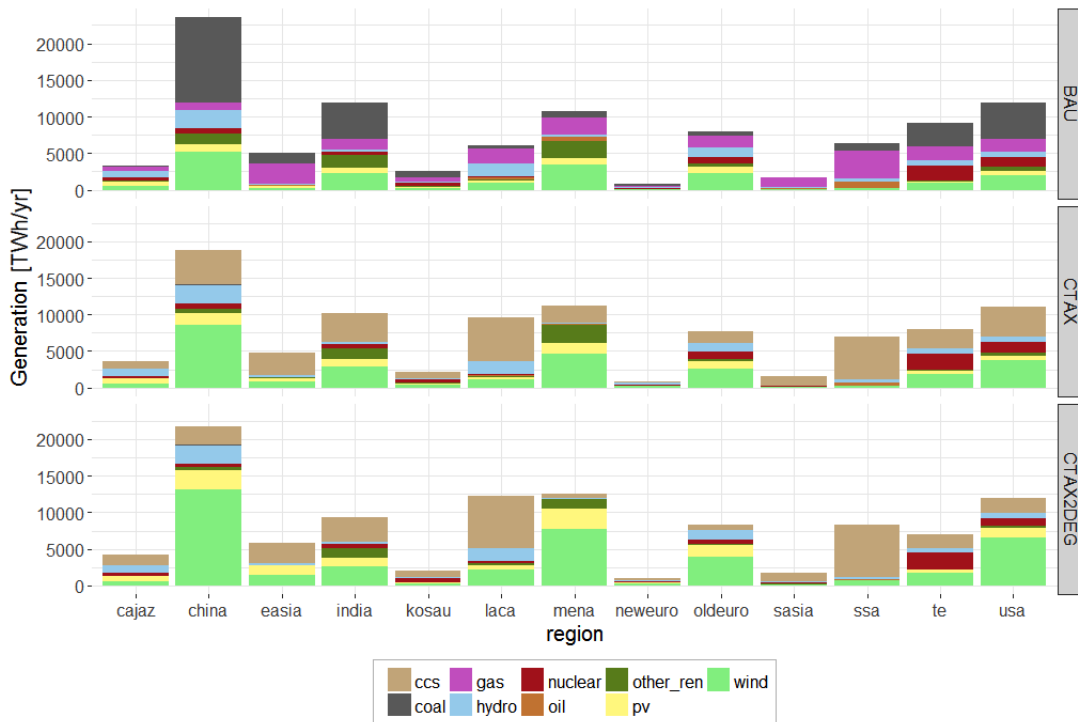


Figure 5.3: Regional electricity generation by technology type in BAU, CTAX and CTAX2DEG policy scenarios in 2100.

5.1.2 Policy impact on Grid and Storage

This Subsection investigates how the above mentioned climate policies impact on investments in electric grid and electricity storage capacity. Grid investments are affected

²Along this chapter, with CCS plants we refer to fossil fuels based CCS plants (Table 5.1), while biomass based CCS plant is included in the *other_ren* category.

by the different policy scenarios, that in turn influence the electricity mix and the corresponding need for investments in transmission and distribution lines, plus grid pooling (see section 4.3). Figure 5.4 shows yearly grid investments (in $\frac{T\$}{year}$), distinguished by type for BAU, CTAX and CTAX2DEG scenarios.

The two main trends that stand out observing the graph are: 1) grid investments increase in time in all the scenarios and they double (BAU and CTAX) or even treble (CTAX2DEG) from 2015 to 2100; 2) grid investment change remarkably across scenarios, and increase with increasing value of carbon tax. More precisely, investments in transmission grid decrease from BAU to CTAX and CTAX2DEG, while investments in distribution grid and pooling behave the other way around, with a remarkable growth for pooling investments, going from 4.8 $\frac{bln\$}{year}$ in CTAX to 17,3 $\frac{bln\$}{year}$ in CTAX2DEG for the period 2095-2100, reflecting the VRE share increase from the former scenario to the latter (36% vs 51% in 2100).

The increase in distribution grid investments with respect to the CTAX case and the stagnation of transmission grid investments indicate that most of the installed VRE capacity in the CTAX2DEG policy scenario is of the *near* type, as it does not require transmission grid investments but only distribution, so it is clearly favoured by this modeling choice (see section 4.3.2). On the other hand, since the unitary cost per km

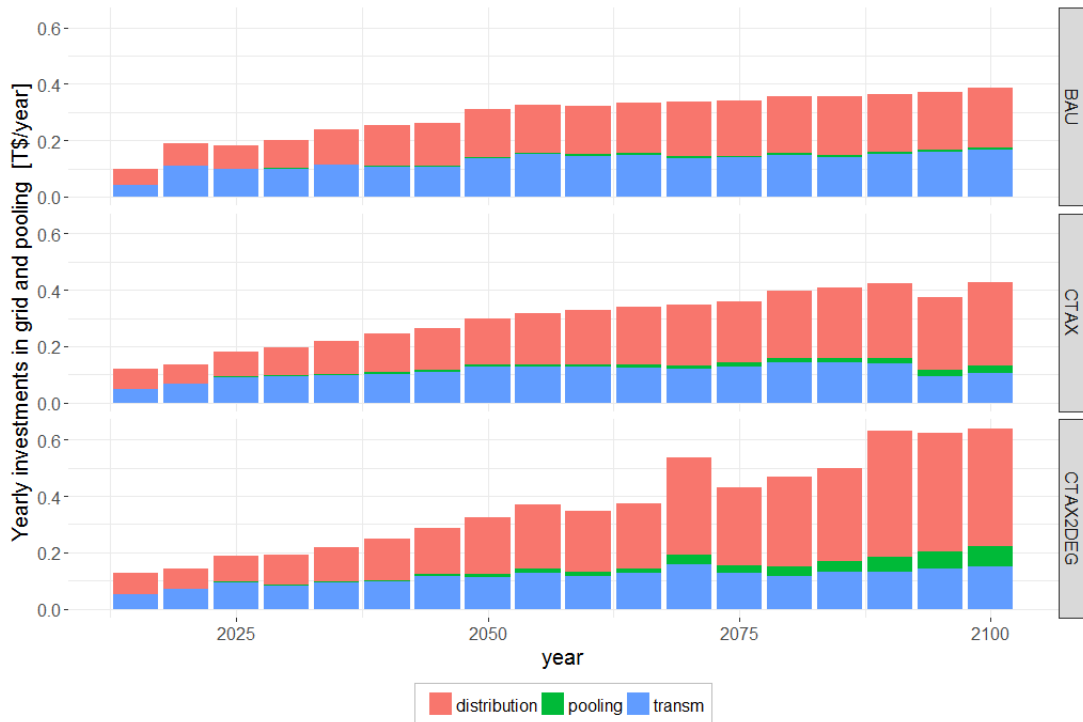


Figure 5.4: Yearly investments in grid and pooling [$\frac{T\$}{year}$] in BAU, CTAX and CTAX2DEG policy scenarios.

of transmission lines is much higher, though the investments are of comparable orders of magnitude, the installed capacity in kilometers is strongly unbalanced. Figure 5.5 shows that the global length of distribution lines is larger than that of transmission by a factor of 33 for BAU (7.9 million km of transmission versus 263 million km for distribution in 2100) up to a factor of 60 for CTAX2DEG (6.98 million km versus 422.3 million km in 2100). These shares are in line with data from the European

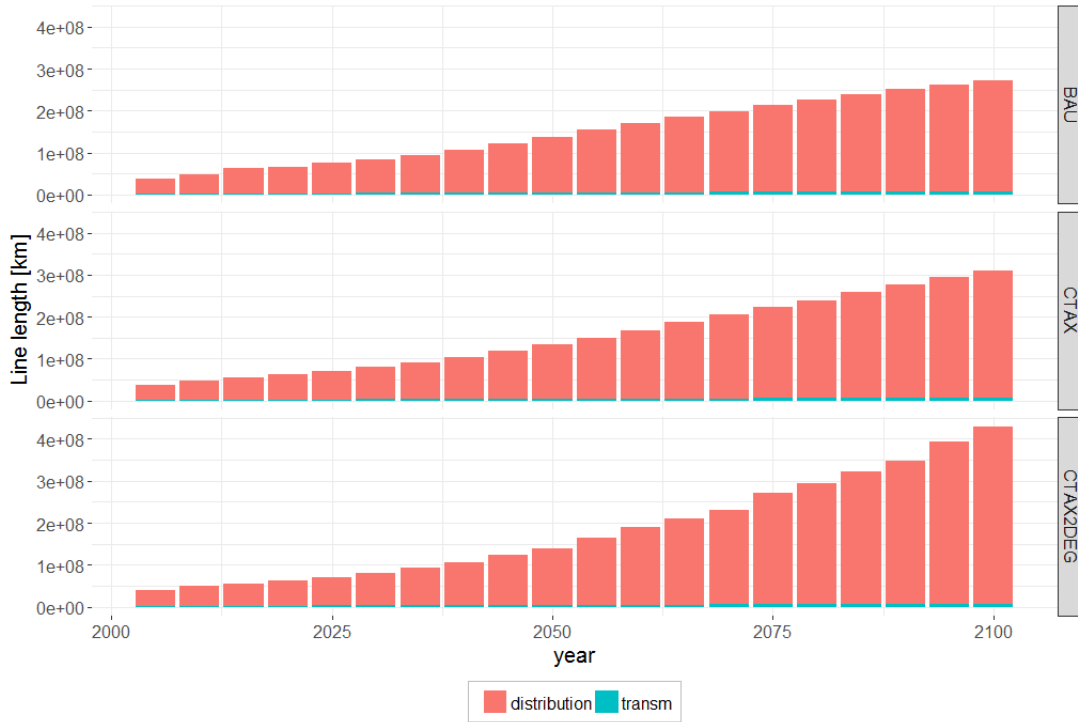


Figure 5.5: Installed grid length [km] for transmission and distribution grid in BAU, CTAX and CTAX2DEG policy scenarios.

Union, indicating that today transmission lines represent 3% of the total power line distance [13], exactly the same value found for global installed grid length in 2100 for the BAU scenario: a 97/3 ratio in favour of distribution lines. This figure is reduced to 2.3% in the CTAX scenario and to 1.7% in CTAX2DEG, but these seem reasonable values for two main reasons: first, Europe is a developed region and presents abundant interconnections between the different countries, this means the transmission line (requiring long-term investments and international coordination for management) is more developed there than in most developing countries, so the 97/3 ratio is probably an overestimation of the global average. Second, the diffusion of VRE technologies and decentralized generation may require more distribution lines and less transmission, especially if decentralized technologies such as residential PV will be predominant. This will further drive down the above mentioned 97/3 ratio. Moreover, IEA indicates that global transmission and distribution length will grow up to 93 million km in 2035 [13], and WITCH indicates 93.2 (BAU), 91.7 (CTAX) and 92.2 km (CTAX2DEG), which seems a very good approximation.

Moving to storage analysis, figure 5.6 shows the evolution in time of short-term storage installed energy capacity, divided by technology and subject to the three different policy scenarios. The first thing to observe is that storage capacity grows with increasing carbon tax and with the share of VRE generation. If before 2050 the capacity share of PHEs and CAES dominates, batteries become widespread in the three scenarios after 2050, reaching PHEs capacity in CTAX scenario, overtaking PHEs and almost reaching CAES in CTAX2DEG. In presence of a carbon tax, CAES is the most installed technology in 2100 (10.7 TWh in CTAX, 14.3 TWh in CTAX2DEG), followed

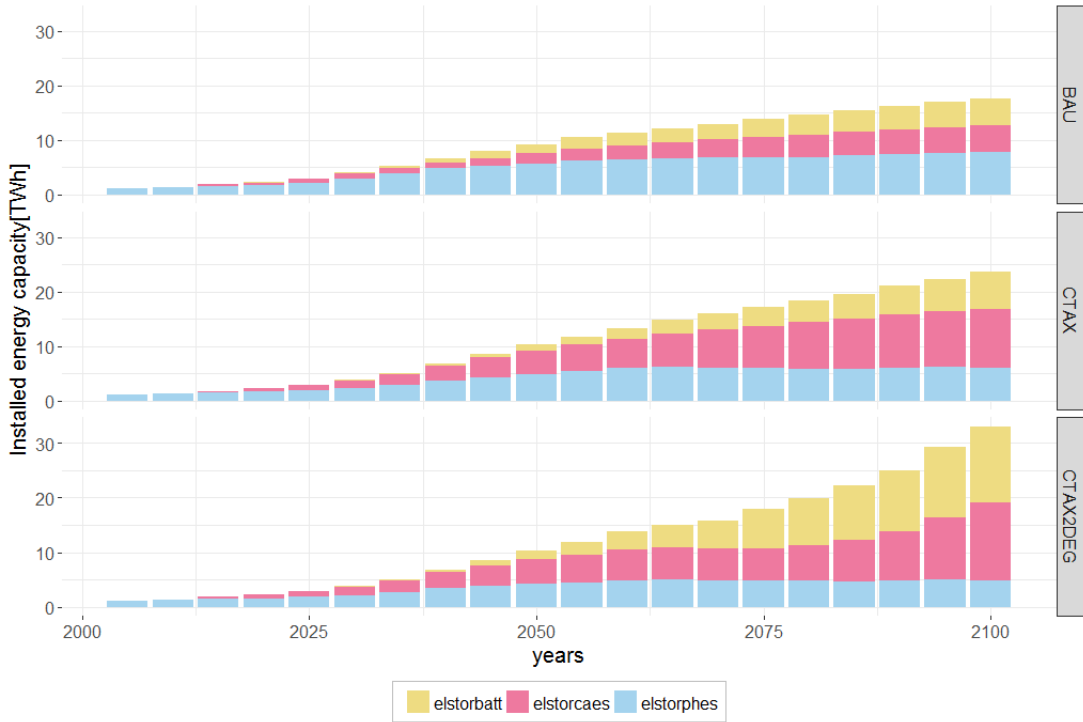


Figure 5.6: Global short-term storage installed energy capacity [TWh] by technology type in BAU, CTAX and CTAX2DEG policy scenarios in 2100.

by batteries (6.9 TWh in CTAX, 13.8 TWh in CTAX2DEG) and PHES (6.0 TWh in CTAX, 4.9 TWh in CTAX2DEG) that is a more interesting option in BAU and progressively loses share when carbon tax increases. This trends depend on two main reasons: first, while Batteries and CAES are subject to learning-by-doing (see Sub-section 3.2.3), that allows a cost decrease with increasing installed capacity, PHES is considered already a mature technology and cannot experience cost decrease: this may undermine its competitiveness with respect to other storage technologies in the long run. Second, PHES capacity expansion is constrained by traditional hydro, which has in turn strict exogenous limitations on its growth, i.e. imposed *a priori* in the model, and this is found to be binding for some regions.

The picture radically changes if we look at installed power capacity [TW] (figure 5.7): batteries represent by far the majority of the storage mix in all scenarios (around 7.2 TW in 2100 for CTAX2DEG policy), followed by CAES (1.8 TW) and PHES (0.5 TW). This is due to the fact that batteries have a much lower energy-to-power ratio (2 hours), versus 7.8 hours for CAES and 9.8 hours for PHES), so, according to our modeling (see Section 4.4), batteries require a much larger installed power capacity compared to the other technologies if they are to store the same amount of energy.

Global yearly investments in short-term storage experience a considerable growth in time, particularly in presence of a carbon tax: in the 2°C scenario, they raise from 14.4 billion \$ in 2020 to 57.1 bln\$ in 2050, up to 203 bln\$ at the end of the century: the latter value has the same investments in transmission plus grid smartening and pooling.

As regards seasonal storage, that is to say electrolysers and fuel cells, the installed capacity of the latter is much lower than the short-term technologies, reaching, in 2100,

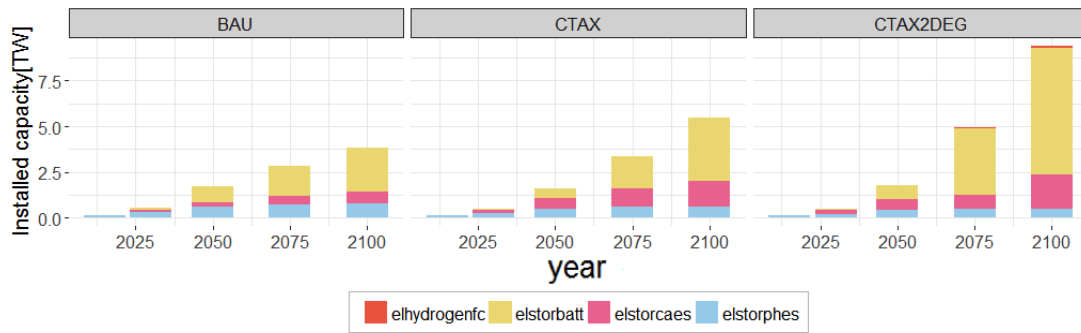


Figure 5.7: Global storage installed power capacity [TW] by technology type in BAU, CTAX and CTAX2DEG policy scenarios.

49 GW with CTAX policy and almost 127 GW with CTAX2DEG, while the installed capacity is negligible in the BAU scenario (see figure 5.8). This is due, first, to the fact that hydrogen production from VRE can exploit just the seasonal curtailment, while short-term storage can be charged also by a fraction of non-curtailed VRE generation (see section 4.4). Second, hydrogen production requires investments in two devices, electrolyser and fuel cell, and this may economically penalize seasonal storage with respect to short-term one.

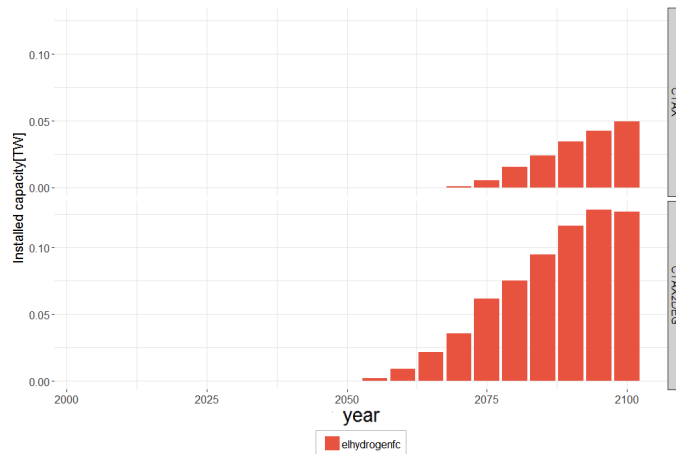


Figure 5.8: Global fuel cells installed capacity [TW] in CTAX and CTAX2DEG policy scenarios.

To understand the rationale behind low fuel cell installed capacity, it is useful to examine the destination of short-term and seasonal curtailment, i.e. the proportion between the amount of curtailed VRE output that is stored and converted into useful energy and the amount that is just wasted and is not injected into the grid. Figure 5.9 shows the total amount of seasonal and short-term curtailment available in the three scenarios and depicts in blue the amount actually stored, while in red the wasted fraction. This graph underlines two important facts: first, seasonal curtailment is always lower than short-term curtailment at same VRE share³, and this limits the diffusion of hydrogen storage with respect to other short-term storage options. Second,

³It is useful to recall that the seasonal curtailment has been calculated as a fraction of total curtailment in [37]. The same behaviour has been applied to all the regions. In particular, the seasonal fraction of total curtailment increases from 15% at 50% VRE share to 35% at 100% VRE share.



Figure 5.9: Seasonal and short-term curtailment destination in time for BAU, CTAX and CTAX2DEG policy scenarios. Stored curtailment in blue, wasted curtailment in red.

if short-term curtailment is totally stored and converted into useful electric energy, on the opposite seasonal curtailment is never stored before 2050, while after 2050 just a fraction of it (approximately half) is converted into hydrogen only in CTAX and CTAX2DEG scenarios. This means that the most significant obstacle to diffusion of hydrogen storage is its high investment costs and not the limits to the storable resource. Moreover, modeling an energy input to hydrogen storage from non-curtailed VRE production would be useless, because if seasonal storage does not manage to saturate all the available curtailment, which comes “for free” as energy that would be otherwise wasted, for sure it will not store VRE generation, as this would also bring about an energy loss due to non-unitary efficiency of electrolysers and fuel cells.

Finally, observing regional storage installed capacity is instrumental in capturing the dynamics that regulate choice among different storage technologies and increase of installed capacity with VRE share. Figure 5.10 shows regional installed energy capacity of short-term storage in 2100, divided by technology type. It has to be compared with figure 5.3, showing regional generation mix: regions with higher VRE shares in their energy mix also show large storage capacity, they are *china*, *mena*, *oldeuro*, *usa* and *india*. The only exception is represented by *laca*, taking advantage of its high hydro potential to install a considerable amount of PHES, the highest amount all over the world.

As regards the share of single short-term storage technologies, it is visible that, among the regions with the highest storage capacity, *oldeuro* and *usa* install more batteries in the CTAX2DEG scenario, *china* is more balanced between CAES and batteries, while *mena* prefers CAES.

The reason probably lies in the amount of firm capacity available in the three regions, and in the respective capacity factors of batteries (0.8) and CAES (1). Looking at figure 5.3, we can see that while *china* and *usa* feature considerable amounts of firm capacity (namely CCS and hydro for *china*, CCS and nuclear for *usa*), in *mena* just a small share of traditional biomass and CSP is present, while the rest of the demand is satisfied by VRE generation. This latter are strongly penalized in the capacity constraint equation (see chapter 4), so their presence requires capacity backup: this is guaranteed by the installation of large amounts of CAES, which has a higher capacity factor and therefore can contribute more effectively to meeting this requirement. Moreover, the higher share of batteries in *oldeuro* and *usa* is due to the fact that these two regions have lower VRE shares (around 70%) in 2100 with respect to *china* (80%) and *mena* (94%), hence higher non-VRE firm capacity, and can avoid high shares of CAES for the above explained reasons.

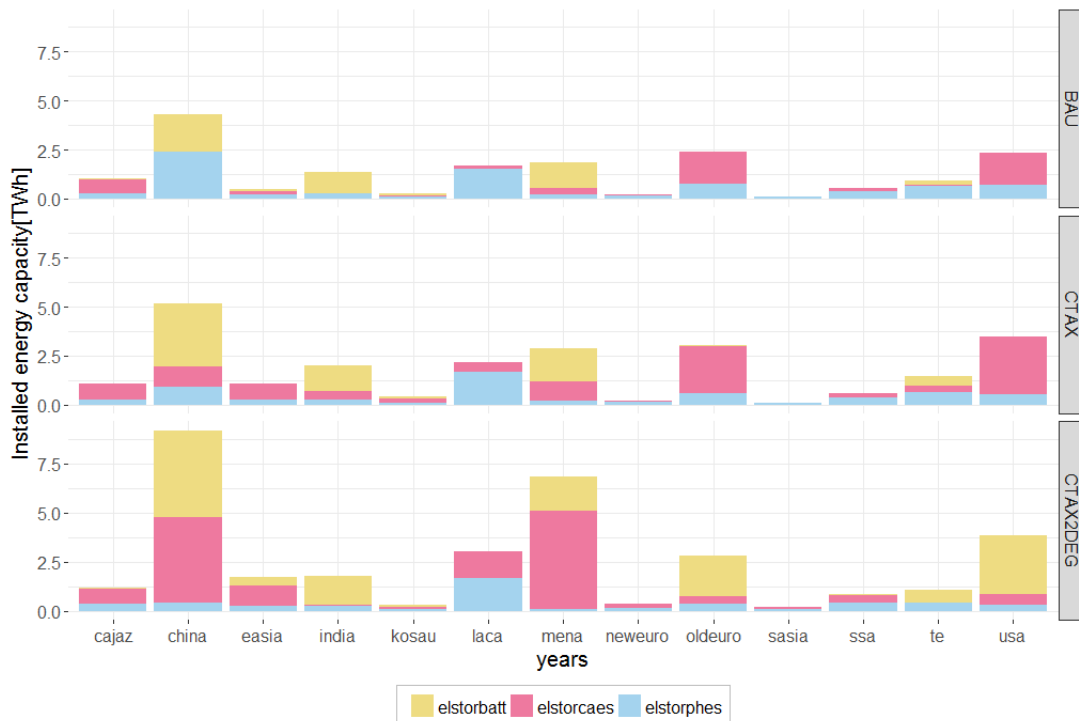


Figure 5.10: Regional storage installed energy capacity by technology type in BAU, CTAX and CTAX2DEG policy scenarios in 2100.

5.1.3 Policy impact on GHG Emissions and Economy

Introducing a price for carbon dioxide emissions entails not only a shift in the electricity mix, but also a significant reduction in GHG emissions if the price is high enough. It is indeed interesting to look at global GHG emissions in CO_2 -equivalent per year across the three different scenarios, in figure 5.11. While in BAU scenario emissions peak just around 2085, when growing prices for fossil fuels make investing in renewables a competitive option, in CTAX and CTAX2DEG emissions decrease already in 2020 and the decrease proceeds at different rates, depending on the value of the carbon tax: the more stringent the tax, the faster the emission decrease. The 2°C scenarios, in

particular, imposes zero global GHG emissions by the end of the century.

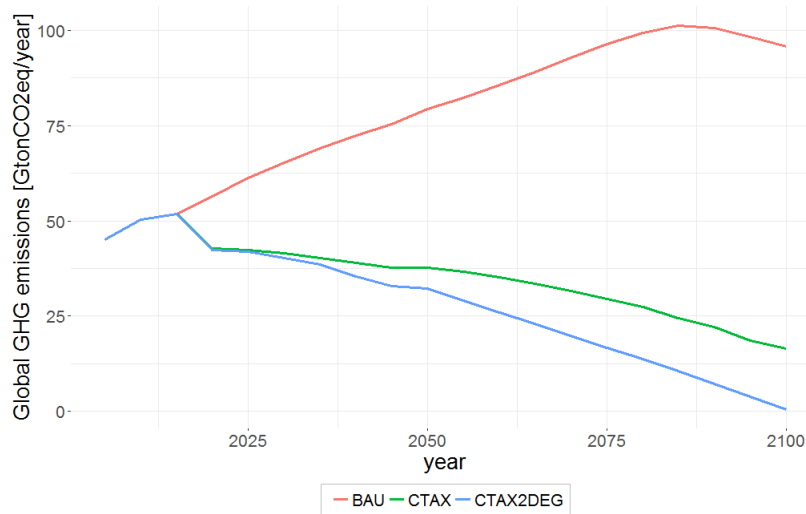


Figure 5.11: Global equivalent CO_2 emissions [Gton] in BAU, CTAX and CTAX2DEG policy scenarios.

Assessing the cost of climate policies is a non-trivial task, and a metric often used to do so is the undiscounted Gross Domestic Product (GDP) loss with respect to the BAU scenario, taken as a reference. As visible in figure 5.12, CTAX policy entails an undiscounted GDP loss of about 4 percentage points by the end of the century, while CTAX2DEG impact on economic growth is more than double, at 9.8 percentage point by the end of the century.

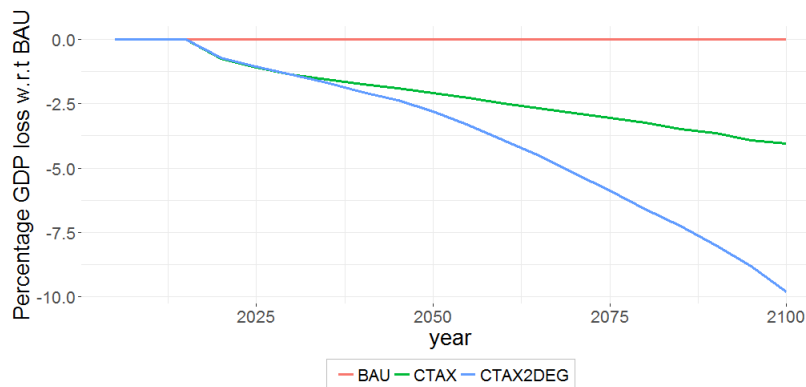


Figure 5.12: Undiscounted GDP loss with respect to BAU scenario for CTAX and CTAX2DEG policies.

5.1.4 Policy impact and technology substitution: towards 100% renewable scenarios

The scope of this part is understanding how the model behaves when very high shares of VRE generation are reached (above 60%) and 100% renewable electricity scenarios

are approached. The attention will be focused, in particular, on grid investments and storage installed capacity, as they are the object of our modeling work.

As seen in paragraph 5.1.1, global VRE generation share (after storage and curtailment) does not go beyond 51%, even in presence of a high carbon tax, since the model considers other low carbon technologies such as nuclear, hydro and above all CCS more convenient to cover the remaining share (see fig.5.2). The solution to overcome this barrier and reach high VRE shares is forcing the model not to install any CCS and nuclear after 2015, depicting a “Technology substitution” scenario in which these two technologies, for a number of reasons (related to profitability, safety or public opinion issues), are disregarded all over the world and receive no further investments. Figure 5.13 represents the new electricity mix under the same policy conditions presented at the beginning of the chapter, named CTAX_NOCCS and CTAX2DEG_NOCCS to distinguish them from the case where investments can also benefit nuclear and CCS technologies (CTAX and CTAX2DEG). As visible, the lack of other low carbon technological options redirects investments towards wind and solar, that together account respectively for 63.0% (CTAX_NOCCS) and 83.5% (CTAX2DEG_NOCCS) of total electricity supply after storage in 2100. This demonstrates that the model can achieve very high shares of VRE in the electricity mix when adequately stimulated from the economical and technological point of view. Moreover, gas is never completely phased-out in the CTAX_NOCCS scenario and represents the only relevant fossil-based technology after 2060, with hydro and other renewables completing the picture.

The CTAX2DEG_NOCCS scenario, instead, entails just a very small share of gas generation after 2060, as it is replaced by wind and solar. Nuclear plants represent a small share (around 2%, decreasing in time) even when no further investments are allowed, because of their non-negligible initial installed capacity and their long lifetime, that entails a very slow depreciation of their capital⁴. Most importantly, it is shown that a practically 100% renewables scenario can be achieved in CTAX2DEG_NOCCS.

These changes in the electricity mix deeply affect investments in grid, as visible in figure 5.14: if no major changes are noticeable in the CTAX scenario, in the 2°C scenario overall investments increase if no new nuclear and CCS are allowed, especially because both pooling and distribution are linked to the amount of installed VRE capacity, that increases considerably with respect to the case without nuclear and CCS.

To understand why also transmission investments grow, it is necessary to compare also the installed energy capacity of short term storage (figure 5.15). It can be noticed that, while in CTAX just a small additional investment in batteries (to the detriment of PHES) is necessary to accommodate the larger share of renewables in absence of CCS and nuclear, in the CTAX2DEG scenario CAES is subject to massive investments and its installed capacity witnesses almost a four-fold increase (from 14 to 52 TWh) in the Technological Substitution case. This is mainly due to the fact that VRE technologies, especially when their share is high (hence their capacity value is low, see section 4.1.1), are not able to provide firm capacity and require some other technology, with high capacity coefficient, to cover peak demand. The model finds installing CAES capacity as the most convenient option, as it has the highest capacity coefficient together with

⁴This derives from how the depreciation is defined in the WITCH model: exponential depreciation of the capital stock.

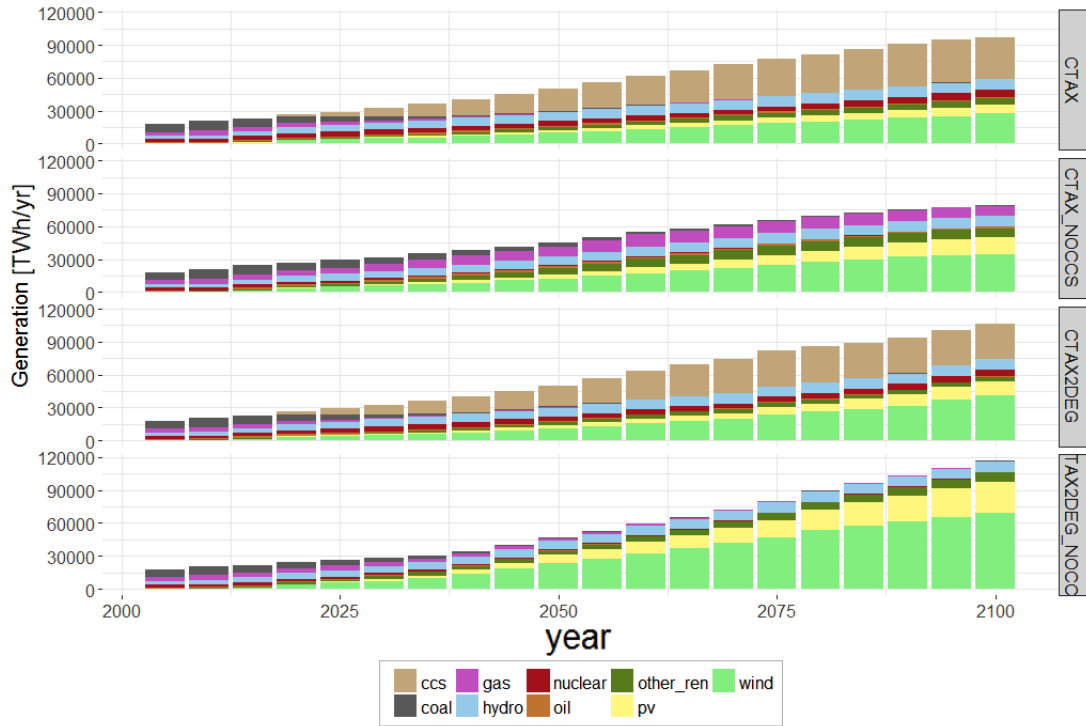


Figure 5.13: Electricity generation (after storage) by technology type in CTAX and CTAX2DEG policy scenarios, with and without the possibility to invest in nuclear and CCS.

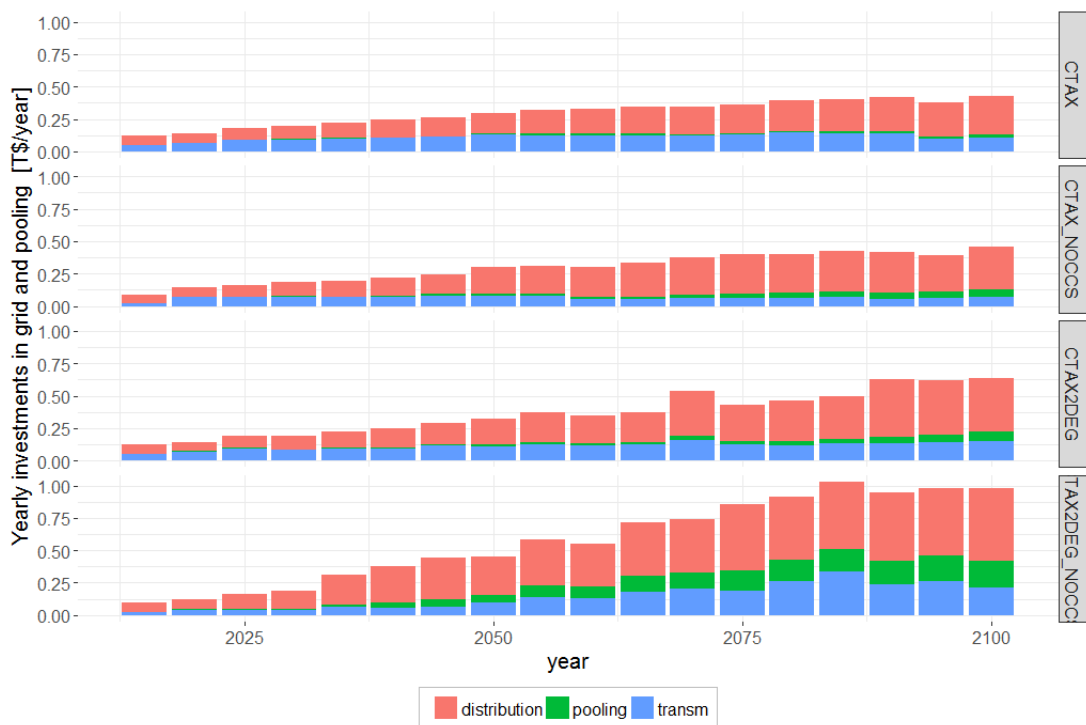


Figure 5.14: Investments in electric grid divided by type in CTAX and CTAX2DEG policy scenarios, with and without the possibility to invest in nuclear and CCS.

PHES (both 1) and its cost is subject to learning: the more it is installed, the more it becomes economically attractive.

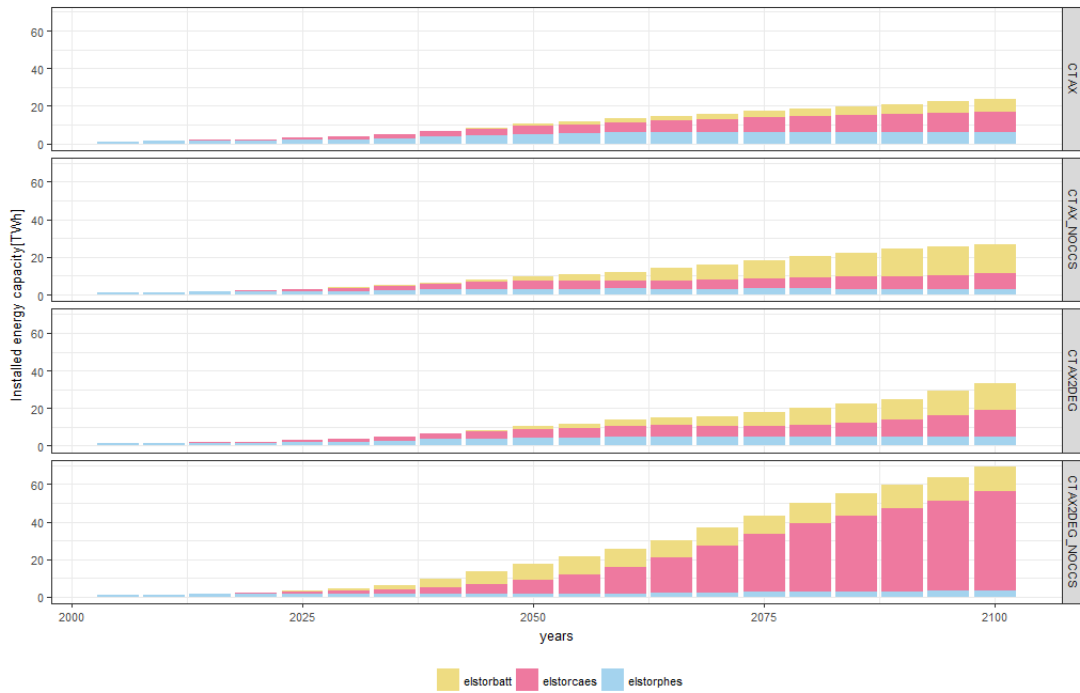


Figure 5.15: Short-term storage technologies installed capacities in CTAX and CTAX2DEG policy scenarios, without the possibility to invest in nuclear and CCS.

Since CAES capacity requires investments in transmission grid, an increase in them is noticeable with respect to the base CTAX2DEG case. Moreover, it is shown that storage, with the ability of satisfying the peak demand (high capacity coefficient), is pivotal for achieving a 100% renewable scenario as CTAX2DEG_NOCCS. Finally, it is interesting to observe the economic impact of installing large shares of VRE technologies instead of CCS and nuclear plants. To do this, we compute the GDP loss of the two “Technological substitution” scenarios with respect to the BAU scenario of the base case. The undiscounted GDP loss for the CTAX_NOCCS is around 4.9

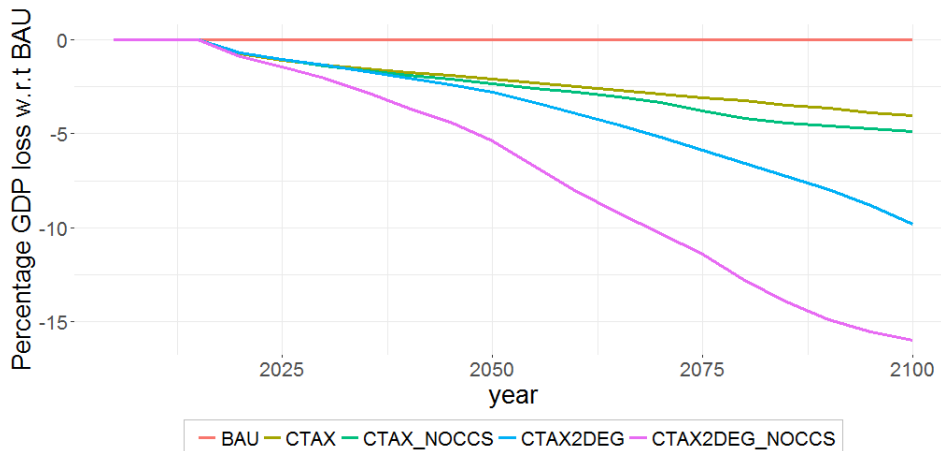


Figure 5.16: Undiscounted GDP loss of CTAX_NOCCS and CTAX2DEG_NOCCS scenarios with respect to BAU of the base case.

percentage points, almost one point more than the base CTAX, while a much larger difference arise with the 2°C target: 16% undiscounted GDP loss, 6 points more than the corresponding base case. This indicated that, at same temperature increase target, achieving the target with a 100% renewable scenario has a more negative impact on global economic growth than doing it also with other non-renewable options, such as CCS and nuclear technologies.

5.2 Impact of Storage and Grid modeling on VRE System Integration

5.2.1 Impact of Storage presence

To start, it is worth having a look at the general impact that the presence of storage have on the VREs deployment. In Fig. 5.17 it can be seen the electricity generation mix in 2030, 2050 and 2100 for the CTAX and CTAX2DEG scenario with and without the possibility of installing storage. It is clearly visible that, without the installation of storage capacity, it is not possible to reach high shares of VRE generation in 2100. In fact, while with the possibility of installing the storage world VRE shares (after curtailment) of 37% and 51% are respectively reached in the CTAX and in the CTAX2DEG scenarios, in the case without the storage the role of VREs is strongly affected (19% in CTAX and 20% in CTAX2DEG shares). In particular, as it is better highlighted in Figure 5.18, in the scenarios without the installation of storage, world VRE shares just below the 20% are reached in 2100. Moreover, it is evident that, even with an higher carbon tax (CTAX2DEG) to meet the stricter climate action objective, the deployment of VREs does not increase sensibly. This makes clear that, even with a stronger economic stimulus towards carbon free technologies, without storage, a higher VRE share cannot be achieved. Going back to Fig. 5.17, an other interesting aspect that can be noticed is that, in the case without storage, in the CTAX scenario the VRE generation reduction is counterbalanced by an increment of the shares of other technologies (CCS and other renewables). On the other hand, in the CTAX2DEG scenario this increase is not enough to offset the decrease of VRE production and a significant decrease of the overall generation takes place. In particular, in the case without storage, in 2100 the world VRE generation decreases by 19% from 106'000 TWh to 86'000 TWh. This has an effect on the economic output since, as it is shown in Figure 5.19, the world GDP losses associated to the two different carbon tax growth paths are bigger in the case without storage, especially in the CTAX2DEG scenario. More specifically, in this latter scenario the world undiscounted GDP losses in 2100 increase from 9.8% in the case with storage to 10.4% in the one without storage. This 0.6% increment represents an additional world undiscounted GDP loss of around 1.8 T\$ with respect to the BAU scenario.

5.2.2 Impact on VRE and Electricity LCOE

In this section, the effect of the storage and pooling-related VRE integration costs are evaluated in terms of Levelized Cost of Electricity (LCOE). In figures 5.20 and 5.21 the PV and Wind Onshore LCOE trend over time can be seen for the CTAX2DEG

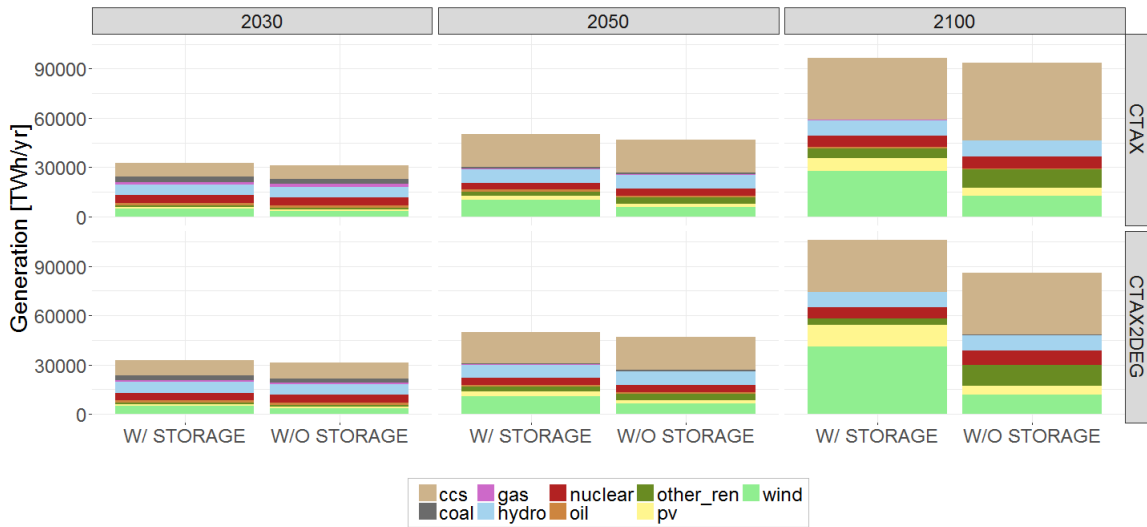


Figure 5.17: Comparison of the electricity generation mix in some relevant years between the cases with and without storage technologies in the model.

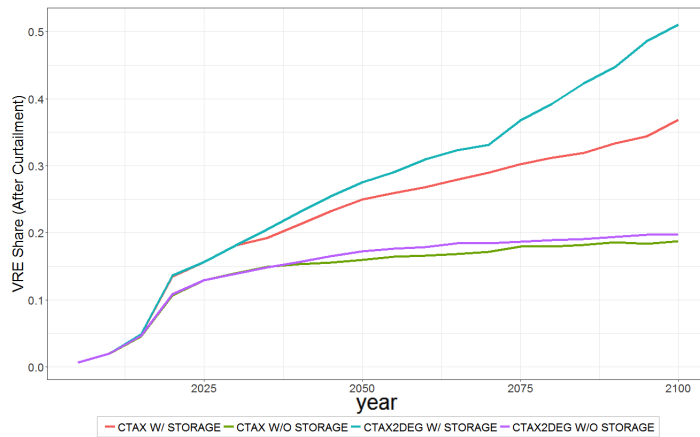


Figure 5.18: Comparison of the world VRE share (after curtailment) over the years between the cases with and without storage technologies in the model.

scenario. The results for two WITCH regions (*oldeuro* and *usa*) are shown. The first curve (only-VRE) represents the LCOE evaluated according to the usual definition, taking into account all the technology related costs (capital and O&M in the case of VREs). It decreases over time thanks to the reduction of the capital costs of the technologies via learning effect.

The second curve (w/ Storage and Pooling) includes the contribution of the investments in storage technologies and grid pooling. These costs have been allocated to the MWh produced by the VRE assuming that they are incurred to integrate VREs. The costs are attributed to the different VREs based on the single VREs shares. The storage technologies capital costs have been depreciated through the depreciation rate deriving from their specific lifetime. On the other hand, investments in pooling, that are not

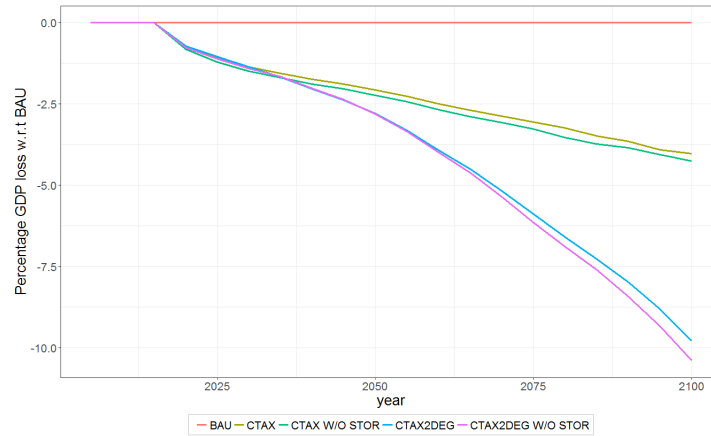


Figure 5.19: Comparison of the world undiscounted GDP losses in the CTAX and CTAX2DEG scenarios (with respect to the BAU scenario) between the cases with and without storage technologies in the model.

associated to a capital stock that depreciates in time, have been discounted together with VREs capital costs. Moreover, also storage O&M have been considered as incurred annually. In figures 5.20 and 5.21 the effect of these additional costs can be seen. In particular, for *oldeuro* both PV and wind onshore LCOE increments vary between 1 \$/MWh in 2050 and 3 \$/MWh in 2100. Before 2050 the increment is lower than 1 \$/MWh. With respect to the only-VRE value this means an increment of 1.5% in 2050 and 7% in 2100 for the PV. Whereas the wind plants experience a larger percentage increase: 4% in 2050 and 17% in 2100. For *usa* the percentage increments are similar for PV and a bit lower for wind plants (2% in 2050 and 14% in 2100).

The third curve (w/ System Integration Constraints) represents the value assumed by the VREs LCOE if also the shadow costs related to the flexibility and capacity constraint equations are taken into account. These shadow costs are derived from the “marginal” values of the two equations, defined as the the variation that the objective value would experience in correspondence of a unitary variation of the constraint. Since these two equations are binding the optimal solution, they entail a limitation of the objective function. Since the VRE technologies provide a negative (flexibility coefficient) or limited (capacity value) contribution to these equations (see Section 4.1.3), a corresponding cost can be associated to their penetration in the electricity mix: this cost should be intended as the consequence of additional flexibility and firm capacity requirement introduced by VRE diffusion. The definition of the new LCOE, including these integration cost components, comes from previous work made on the WITCH model [36]. In particular, the LCOE contributions from the flexibility and the capacity constraints are computed as the ratio between the marginal of the constraint equation and the marginal of the final good consumption equation. The ratio is then multiplied by the relevant flexibility coefficient for the flexibility constraint. Whereas, it is multiplied by the complementary of the relevant capacity value and divided by the yearly hours (in order to obtain values in dollars per watt-hour) for the capacity constraint. From the two figures, it can be noticed that the effect of these contributions is strong and, especially, after 2060 it grows steeply doubling the value of the LCOE with respect to the two previous formulations. In particular, for *oldeuro* the percentage increment with respect to the only-VRE case is 20% in 2050 and 120% in 2100 for the

PV. While for the wind plants it is 45% in 2050 and almost 300% in 2100. This means that the integration of VREs has a significant effect in terms of stress put on the energy system.

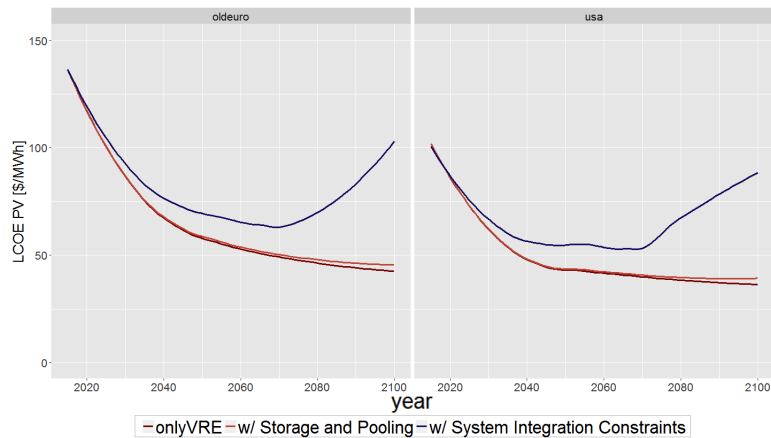


Figure 5.20: PV LCOE [\$/MWh] trend in CTAX2DEG scenario in *oldeuro* and *usa* regions. Three different definitions: “only VRE” includes only the technology related costs, “w/ Storage and Pooling” involves the addition of the costs related to storage technologies and grid pooling, “w/ System Integration Constraints” takes into account also the effect of the shadow cost of the constraint equations.

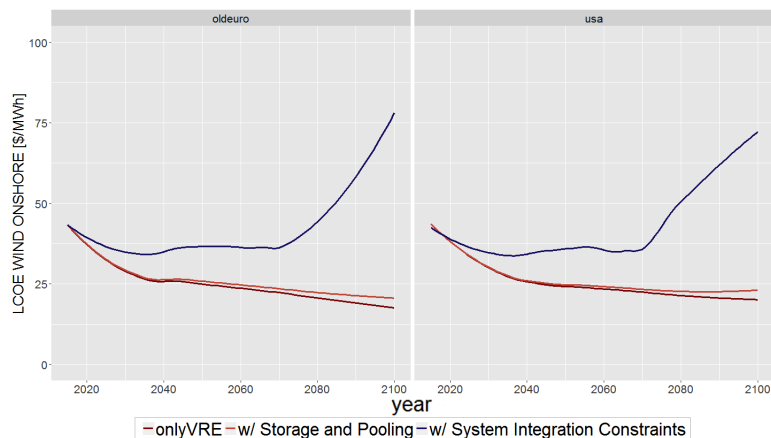


Figure 5.21: Wind Onshore LCOE [\$/MWh] trend in CTAX2DEG scenario in *oldeuro* and *usa* regions. Three different definitions: “only VRE” includes only the technology related costs, “w/ Storage and Pooling” involves the addition of the costs related to storage technologies and grid pooling, “w/ System Integration Constraints” takes into account also the effect of the shadow cost of the constraint equations.

5.2.3 Interdependence of electricity storage and grid

Existing studies that aim at establishing the cost-optimal configuration of electric power systems to achieve low carbon scenarios give contradictory indications about the interdependence between electricity storage and grid [105], [106]. Some claim that the two complement each other, meaning that the installation of a unit of storage requires also an addition of grid capacity. Others present them as substitutes, meaning that installing storage reduces to some extent the need for further grid, and vice versa. Many of the phenomena that literature identifies as key drivers of the two behaviours [105] are either indirectly represented in WITCH (correlation between load and VRE

generation, via RLDC) or not represented at all (frequency and timing of transmission congestion, exact location of storage).

Nevertheless, this analysis aims at identifying, if any, signals of interdependence between these two components of the power system, which may be of interest in view of further studies.

Figure 5.22 represents investments in electric grid (by grid type) and short-term storage technologies in the three main policy scenarios (BAU, CTAX, CTAX2DEG). They are not in the same scale, as investments in storage are approximately one order of magnitude lower than grid investments. It has therefore been necessary to multiply the former by 10 to visualize all the investments on the same graph. As a consequence, the sum of the investments shown in the bar plot does not have an economic sense. The purpose of the figure is instead identifying growth trends in investments and correlations among them. In particular, the BAU scenario shows no correlation between grid and storage investments, whereas in CTAX and, more clearly, in CTAX2DEG distribution and overall storage investments grow together. This suggests the existence of a complementarity between the two. Further analyses on installed capacities (here not reported for lack of space), both at world and regional level, highlight that a positive correlation between battery plus CAES installation and distribution grid does exist, while no relations with transmission have been found.

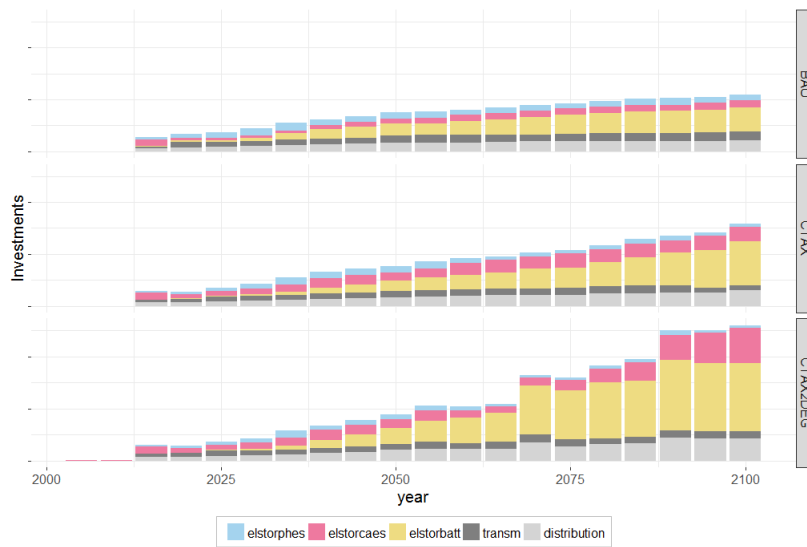


Figure 5.22: Global investments in transmission and distribution grid and short-term storage technologies (the latter multiplied by 10).

5.2.4 Impact of flexibility and firm capacity constraints

This section aims at understanding if flexibility and capacity constraints actually have an impact on the model solution and, if yes, its variation over time. A useful instrument to evaluate the impact of a constraint in a constrained optimization problem, like the one represented in WITCH, is the “marginal” value of that constraint. This is defined as the the rate of change of the constrained optimum with respect to the constraint (and mathematically equal to the derivative of the objective function with respect to the constraint, evaluated in the optimum point). This quantity describes how the the

optimal value increases or decreases due to a one-unit change in the constraint: if the “marginal” value is zero, it means the constraint is not influencing the optimal solution, it is not binding.

Considering the “marginal” values of flexibility and capacity constraints (not shown here for a matter of space availability), some interesting trends emerge. As regards BAU, initially capacity constraint is very binding in all regions, but its “marginal” value decreases in time (even though it is always not null until 2100). The flexibility constraint is instead either very low and decreasing in time or non-binding.

Concerning CTAX, similar trends are observed. The main differences are slightly lower marginals for the capacity constraint, which goes to zero after the first half of the century in many regions, and much higher values for flexibility marginals, meaning this constraint is more relevant, even if decreasing in time.

Finally, as regards CTAX2DEG, the observed marginals for capacity constraints are very similar to those in CTAX scenario, but more regions show null marginals towards the end of the century. On the contrary, the flexibility constraint becomes more stringent than in CTAX2DEG and, interestingly, its marginals increase in time, with the highest values reached in 2100. To sum up, the capacity constraint always decreases in time (most likely because also the firm requirement does the same, see Section 4.1.1). Moreover, increasing the carbon tax progressively raises the importance of the flexibility requirement, to the point that in the 2°C scenario its influence on the objective function increases in time.

5.3 Sensitivity analyses

In this session we investigate the impact on the results of some important parameters, describing cost and performance of grid and storage technologies. This is aimed, on the one hand, at checking the robustness of the assumptions made in sections 3.1.3, 3.2.3 and 3.2.5, where the choice of parameters is presented and motivated. On the other hand, at identifying the parameters whose variation is pivotal for the development and the diffusion of some technologies, especially as regards electricity storage.

The last part of this section is devoted to a sensitivity analysis on the amount of VRE non-curtailed production that can be stored by short-term storage technologies, as this constitutes the fundamental assumptions behind the diffusion of storage and VRE sources, described in section 4.4.1.

5.3.1 Sensitivity on Grid parameters

The parameters chosen for this sensitivity analysis are: grid cost [T\$/km] (both transmission and distribution), grid requirement [km/TW] (both transmission and distribution) and pooling investments, described by equation 4.11. What is interesting to evaluate is their impact on average yearly investments in grid (transmission, distribution and pooling) in the 2015-2100 period. The goal is to understand how much the existing assumptions affect the results and the effect of their potential inaccuracy. Table 5.2 shows the values used in the sensitivity and the way to visualize them in the graph. Figure 5.23 shows the results of the analysis. The results show that the impact of grid cost and grid requirement on average grid investments is much higher

than that of pooling requirement: changing the first two by plus or minus 25% entails an increase/decrease of investments of 20 – 23%, while a $\pm 25\%$ in pooling investment requirement affect global investments by just 1%. However, in the case of the sensitivity on the grid cost these lower/higher average investments are not reflected in a significant change in the installed grid capacity: variations are lower than 3%. On the other hand, in the case of the sensitivity on the grid requirement the different average investments lead to a variation in the installed grid capacity. But this percentage variation is very close to the 25% of the grid requirement parameter (grid capacity increases/decreases by around 22%). Thus, we can conclude that in both the cases the change in grid investments and capacity is related almost exclusively to the variation of the grid parameters values and not to a modification in the overall generation capacity. This means that the overall generation capacity is inelastic to variations up to 25% of grid cost and requirement.

Point shape	Grid cost	Grid requirement	Pooling requirement
■	default x1.25	default x1.25	default x1.25
—	default	default	default (1)
×	default x0.75	default x0.75	default x0.75

Table 5.2: Legend for sensitivity analysis on grid parameters.

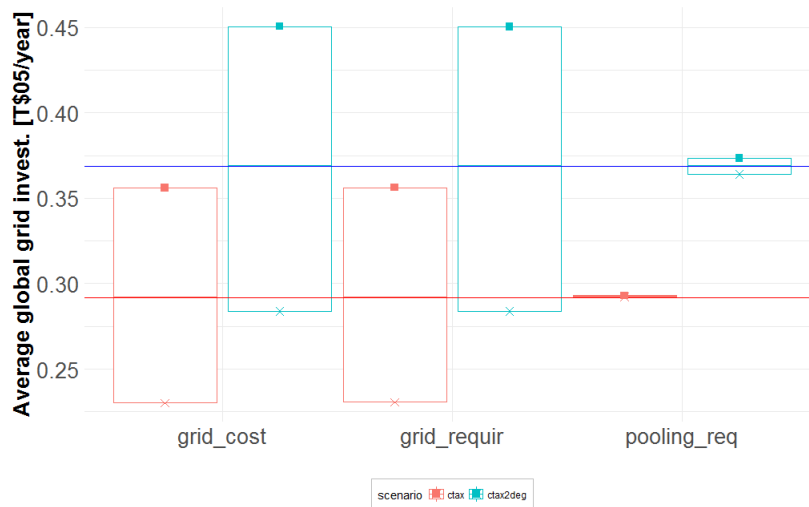


Figure 5.23: Sensitivity analysis on average 2015-2100 investments in grid [T\$/year], for CTAX (red) and CTAX2DEG (blue) scenarios: effect of the main parameters. Horizontal lines represent the results with the parameters default values.

5.3.2 Sensitivity on Storage parameters

The short-term storage parameters that will be subject to sensitivity are: capacity coefficient, flexibility coefficient, floor cost, learning rate, storage cost and storage efficiency (the last three just for CAES and batteries). The parameters used in the sensitivity analysis are listed in table 5.3.

An important observation has to be done before further sensitivity analyses are discussed. The charts that follow are not intended to represent the relative impact of

varying each parameter with respect to the other ones, because the percentage variation of each parameter compared to the default value is not the same across parameters. In some cases, such as with CAES efficiency, it would not make sense to have it decrease with respect to the default value (as happens with costs), that already comes from a conservative assumption. Furthermore, it is our opinion that, when data from literature are available, such as in the case of costs (the min, mid and max values come from [75]) and efficiency, it is sensible to use the ranges of variation suggested by the literature rather than imposing some undocumented relative variations, to keep the analogy with other parameters. The following charts are indeed aimed at condensing a considerable amount of information in just one image (mainly for reasons of space) and, when reasonable, compare the effect of varying different parameters on the same variable of interest.

Point shape	Cap.Coeff	Flex. Coeff.	Floor Cost
■	0.9(PHES, CAES) 0.7(batt)	0.7(PHES, CAES) 0.95(batt)	$\frac{1}{3}$ initial cost
—	default	default	default ($\frac{1}{2}$ initial cost)
×	0.5(PHES, CAES) 0.3(batt)	0.25(PHES, CAES) 0.50(batt)	$\frac{1}{4}$ initial cost
Point shape	Learning rate	Storage cost	Stor. efficiency
■	default x1.5	min	0.7(CAES) 0.95(batt)
—	default	default (mid)	default
×	default x0.5	max	0.6(CAES) 0.90(batt)

Table 5.3: Legend for sensitivity analysis on storage parameters.

Figure 5.24 shows how sensitivity on the above mentioned parameters influences VRE share of generation before curtailment in 2100. Looking at the effect of capacity and flexibility coefficients, we can see that their decrease has a relevant negative impact on share, especially in the CTAX2DEG scenario. This indicates that, especially at high shares of wind and solar, short-term storage plays a pivotal role in balancing the need for firm capacity and flexible generation of VRE sources: if storage contribution decreases (since coefficients are lowered), the model does not find convenient to install VRE and shifts towards other, more flexible, low-carbon options such as CCS and other renewables. In particular, we notice that, in the 2°C scenario, cutting the flexibility coefficient of 0.50 implies a loss of 25 percentage points in VRE share of generation: a much larger loss compared to cutting the capacity coefficient of the same quantity in the same policy scenario.

This is probably due to the fact that, while capacity coefficient of VRE sources is low but still positive, their flexibility coefficient is instead negative (see Section 4.1.3). The model is not able to satisfy the flexibility constraint maintaining the same VRE share as in the default case because it needs to install other generation technologies, more flexible.

The impact of a floor cost decrease is relevant especially in the CTAX scenario, meaning that with lower carbon tax the competitiveness of storage with respect to other

technologies (which triggers the installation of more VRE capacity) strongly depends on how much its costs are reduced, while higher carbon taxes (CTAX2DEG) increase its competitiveness, notwithstanding the minimum cost achievable. As regards the learning rate, while an increase has just a minor effect on VRE share, a decrease reasonably drives the share down, as it slows down the storage cost reduction. Increasing and decreasing storage costs (using min and max values from [75]) entails the opposite trend for VRE share (it grows when cost go down and vice versa). Finally storage efficiency, overall, has a very small influence, apart from the “high” efficiency case in CTAX2DEG, where share before curtailment is reduced: this happens because higher storage efficiency means lower storage losses, hence the net VRE generation after curtailment increases. Then the net VRE generation remains constant with respect to the default case.

Figure 5.25 shows the effect of the same parameters discussed above on average storage installed capacity between 2015 and 2100: the effect of the single parameters is similar to what observed for VRE share before curtailment, since what happens at storage installed capacity is directly reflected on VRE diffusion. This proves the complementary nature of these two technologies.



Figure 5.24: Sensitivity analysis on 2100 VRE generation share before curtailment, for CTAX (red) and CTAX2DEG (blue) scenarios: effect of the storage main parameters. Horizontal lines represent the results with the parameters default values.

5.3.3 Sensitivity on CAES and battery technologies

Since these two technologies have not reached full commercial maturity (A-CAES is actually at an earlier stage than batteries), it is interesting to see how technological breakthroughs, design choices and cost decrease may affect their future deployment. In particular, we study the influence of Energy-to-Power ratio EtoP, Round Trip Efficiency (RTE) and Full Production Hours (FPH), described in Section 3.2.3, assuming the values described in tables 5.4 and 5.5. Results for these analyses are obtained running the model with just one modification at time (e.g. one run just changing CAES RTE to 0.6, one run just changing battery EtoP Ratio to 4). As regards floor costs, instead, they are varied together for the two technologies, to investigate if they would favour

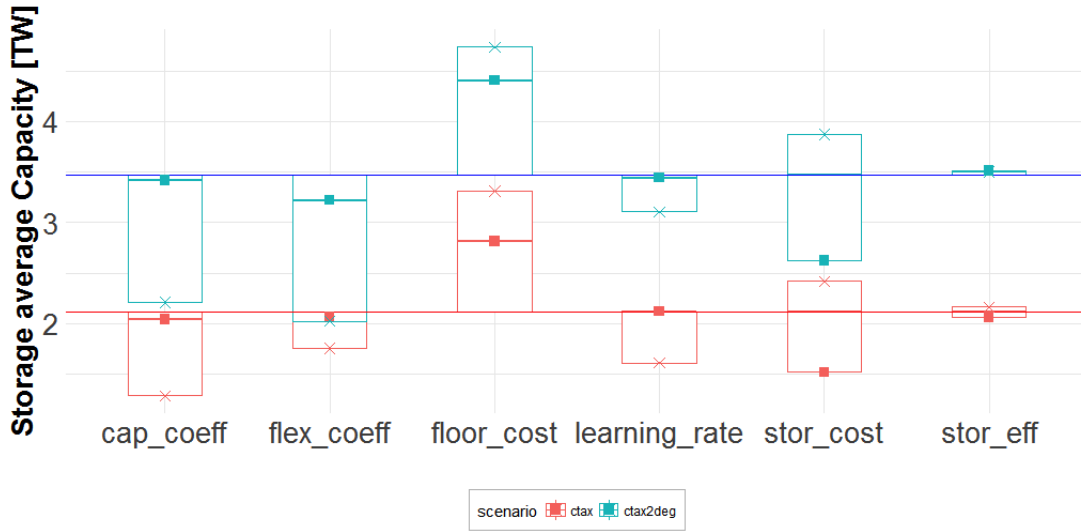


Figure 5.25: Sensitivity analysis on average 2015-2100 storage installed power capacity [TW], for CTAX (red) and CTAX2DEG (blue) scenarios: effect of the storage main parameters. Horizontal lines represent the results with the parameters default values.

one over the other.

Point shape	EtoP ratio	RTE	Floor cost	FPH
■	26	0.7	$\frac{1}{4}$ initial cost	2058
—	default (2.6)	default (0.54)	default ($\frac{1}{2}$ initial cost)	default (1486)
×	13	0.6	$\frac{1}{3}$ initial cost	914

Table 5.4: Legenda for sensitivity analysis on CAES parameters.

Point shape	EtoP ratio	RTE	Floor cost	FPH
■	4	0.95	$\frac{1}{4}$ initial cost	720-1560
—	default (2)	default (0.85)	default ($\frac{1}{2}$ initial cost)	default (480-1040)
×	3	0.9	$\frac{1}{3}$ initial cost	240-520

Table 5.5: Legenda for sensitivity analysis on battery parameters.

The main finding for the analysis on CAES is its strong positive correlation with its efficiency: the more it increases, the more capacity is installed. As regards FPH, an increase entails the need for lower power capacity installed, as more energy can be stored and discharged during the year at same nominal power. A decrease in FPH leads to the opposite.

Batteries, on the other side, show the same behaviour concerning the effect of Efficiency (with a lower impact, as the default value, 0.85, is already high) and FPH. An interesting finding, when comparing the two technologies, derives from the effect of Floor Cost: a decrease of the minimum cost achievable by the two technologies penalizes CAES, as batteries have a higher learning rate and are able to reach the minimum cost by 2050, while CAES costs decrease more slowly, undermining its competitiveness with respect to batteries.

EtoP ratio deserves a separate discussion, as its effect on storage power capacity

strongly depends on the assumptions made about the kind of variables used in learning equation (see 3.3). As a matter of fact, considering learning equation as a function of cumulative power capacity, increasing EtoP ratio is seen just as an extra cost by the model, as it entails higher investments on energy capacity with no benefits in return (these results are not presented in any of the figures, for reasons of space). Instead,

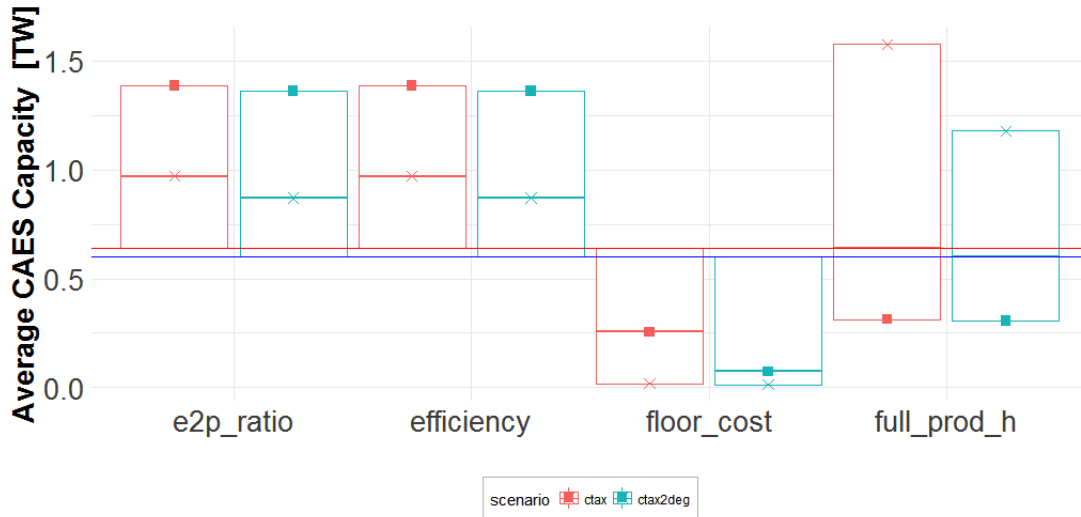


Figure 5.26: Sensitivity analysis on average 2015-2100 CAES installed capacity [TW], for CTAX (red) and CTAX2DEG (blue) scenarios: effect of the storage main parameters. Horizontal lines represent the effect of default values.

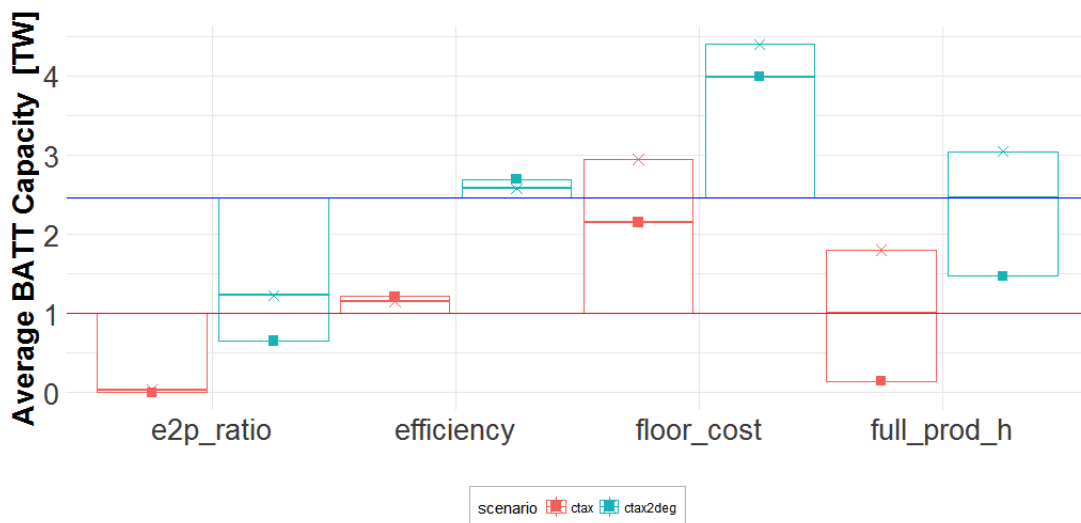


Figure 5.27: Sensitivity analysis on average 2015-2100 battery installed capacity [TW], for CTAX (red) and CTAX2DEG (blue) scenarios: effect of the storage main parameters. Horizontal lines represent the effect of default values.

if we consider learning equation as a function of cumulative energy capacity (keeping the same learning parameters as done in [77] for batteries and [24] for A-CAES), increasing EtoP ratio has a double effect: first, it increases energy investments per unit of power (negative effect), but it also increases the cumulative energy capacity in learning equation, driving down storage costs more rapidly at same installed power capacity (positive effect). This is visible looking at figure 5.26 and 5.27, where we present the results of this second configuration, the one with energy-based learning

(while in the rest of the runs power-based learning is the default option). The 5-fold and 10-fold increase in CAES EtoP Ratio has a positive effect on its diffusion, as costs are reduced more rapidly, while the 1.5 and 2-fold increase experienced by batteries is not enough to make them more economically attractive, and their higher energy cost limit their diffusion. This dynamics highlight a limitation of our storage modeling, typical of IAMs with high temporal aggregation [33], concerning the impossibility to fully represent benefits of a larger energy storage capacity.

For the sake of completeness, it must be said that also a sensitivity analysis on PHEs full production hours has been performed, considering the min, mid and max values listed in Appendix E. The observed results are very similar: global power capacity remains very close to 500 GW, the value obtained in the mid case, in the CTAX2DEG scenario, decreasing to 477 GW in the max case. This suggests that the influence of Full Production Hours on PHEs deployment is minor.

5.3.4 Fraction of VREs Non-Curtailed as Input to Short-Term Storage

In this chapter we present quantitative analyses and qualitative reflections regarding the choice of the value for the parameter *fraction_vre_stored* defined in Section 4.4.1. This parameter represents the maximum fraction of non-curtailed VRE generation that the model can store in short-term storage capacity *K_STOR_PEAK* in order to shift the VRE production in time and meet the peak load. We described the reasons behind our choice of 20% as default value in Section 4.4.1. Here, we want to show some results on the effect of the chosen value and of its variation.

First, it is interesting to have a look at how much of this allowed fraction of storable generation is actually used. In figure 5.28, the amount of non-curtailed VRE production that is stored in the CTAX scenario can be seen. In the graph, the black lines on each bar stand for the default value of 20% of generation. It can be highlighted that, after 2040, the allowed storable fraction of VREs production is mostly used and, after 2080, it is completely used. Therefore, it is worth analyzing how this storable fraction of VRE generation is exploited with lower or higher values of *fraction_vre_stored*, from 5% to 50%. As visible in figure 5.29, for values lower than 20% the storable amount of non-curtailed VRE generation is saturated well before. The saturation factor reaches 1 already in 2050 for both CTAX and CTAX2DEG scenarios. On the contrary, full saturation is never reached with values of 30% and 50%.

This qualitatively indicates that the 20% value is neither too binding (as it is not saturated before 2080) nor too loose (as for 30% and 50% values, never exploited fully), so the empirical evidence seems to confirm that this value represents a balanced choice in terms of influence on storage input from VRE generation.

Further insights about the impact of this parameter on the electricity mix are given by figure 5.30 and 5.31, representing global electricity generation and short-term storage installed capacity as functions of the chosen *fraction_vre_stored*. Looking at them together allows a better understanding of the investment decision dynamics in WITCH, in relation to the parameter of interest.

The two graphs underline the fact that a small *fraction_vre_stored* value (5% and 10%) depresses both the overall energy generation and the share of VRE in the mix.

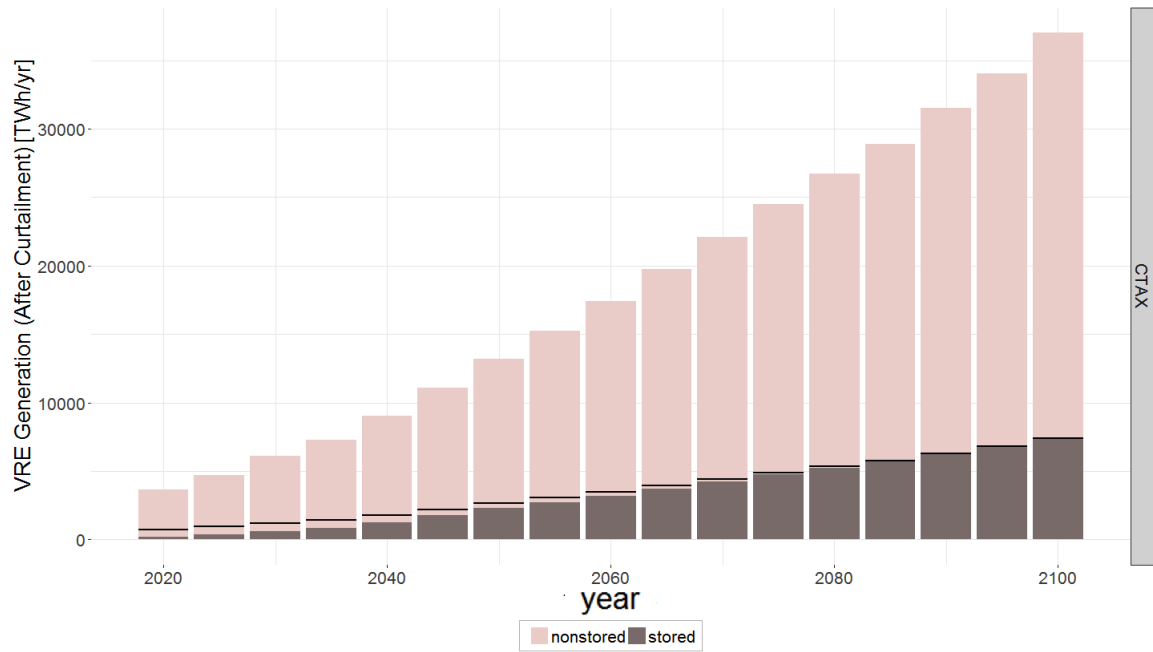


Figure 5.28: Destination of the world non-curtailed VRE generation along the years. The non stored portion meets directly the demand, while the stored one is fed to the storage capacity K_{STOR_PEAK} .

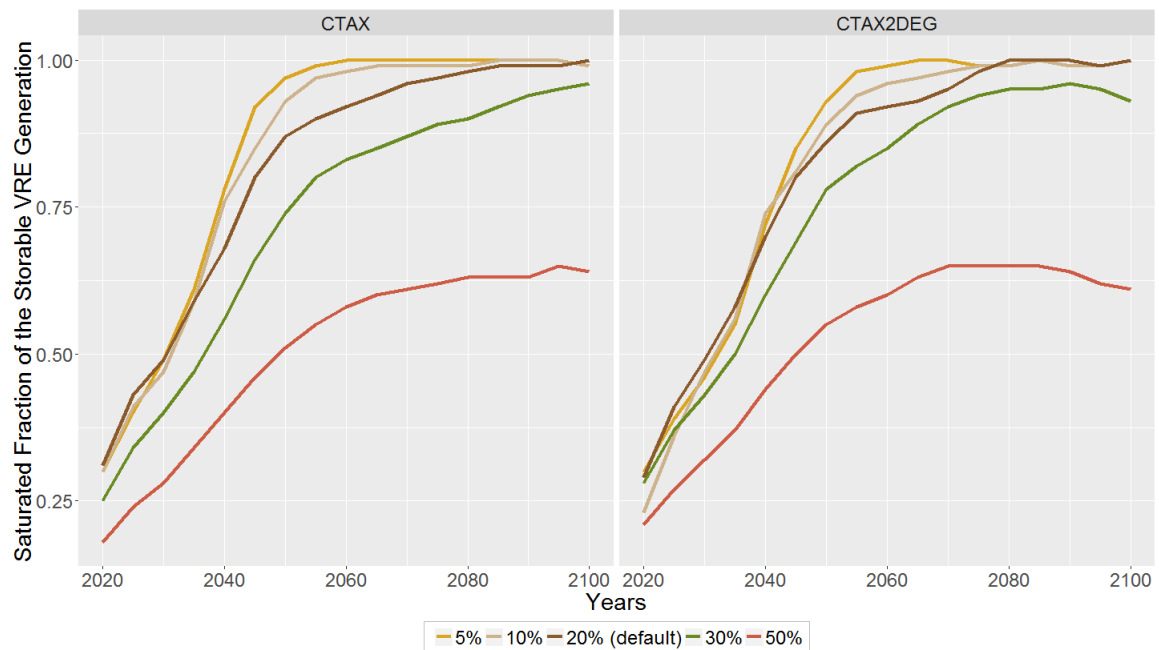


Figure 5.29: Saturation level of the storable fraction of VRE non-curtailed generation for five different values of the allowed storable fraction.

This is probably due to the fact that the amount of storage that can be installed per unit of VRE capacity is too small to compensate for the request of flexibility and firm capacity new VRE brings about.

At the same time, such a small storage requirement does not allow learning-induced cost reductions, hence CAES and batteries do not reach competitiveness compared to PHES, that is the dominant storage technology at the beginning. These two dynamics

trigger a negative feedback loop in the investment choices, so that the model finds optimal to reduce overall generation to respect the flexibility and capacity constraints and relies on other low carbon technologies than VREs, able to contribute more in the two equations. At *fraction_vre_stored* equal to 30% and 50% we see that storage

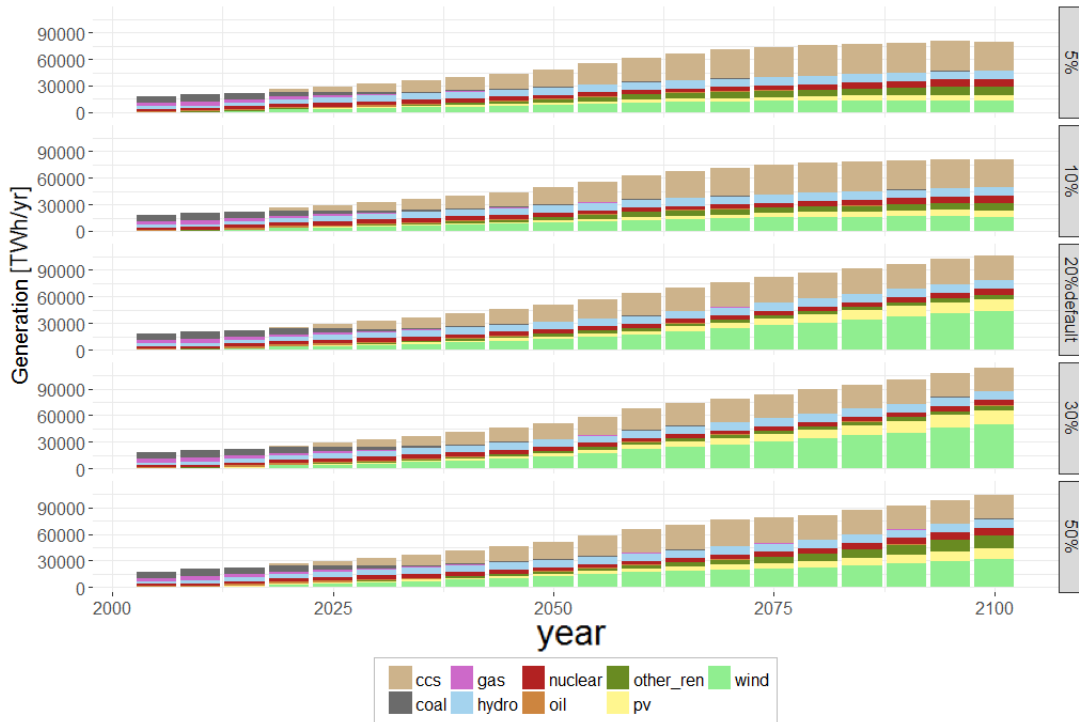


Figure 5.30: Global electricity generation [TWh/year] by technology type in CTAX2DEG scenario, as a function of *fraction_vre_stored* value.

installed capacity almost doubles and almost only CAES is chosen. Our explanation of this behaviour is that, maintaining the same VRE generation, the amount of storage that can be installed increases, and when high amount of storage are allowed the optimal choice is CAES: it is able to reach its floor cost (while this does not happen with 20%) and becomes more competitive than batteries, and has a higher capacity factor to compensate for the increasing firm capacity request of VREs. When the parameter is at 50%, the model tends to install such a high quantity of storage per unit of VRE generation that this undermines the economical competitiveness of VRE themselves, and other renewables, such as traditional biomass and BECCS, are preferred.

Therefore, the 20% value appears *ex post* as a good trade-off between too low values, that would prevent VREs and storage from spreading (since wind and solar lack firm capacity support) and too high values, that would represent an economical burden for VREs rather than a technology enabler. Moreover, it ensures a balance between the three short-term storage technologies in terms of competitiveness and installed capacity, while lower values restrict the choice to the only already existing capacity, PHES, and higher values would enhance only CAES. In particular, the discontinuity from a balanced storage mix to a CAES-dominated scenario lies in the range between 20% and 30%, which makes this interval of values a critical area in the space of possible solutions, that would require further investigation.

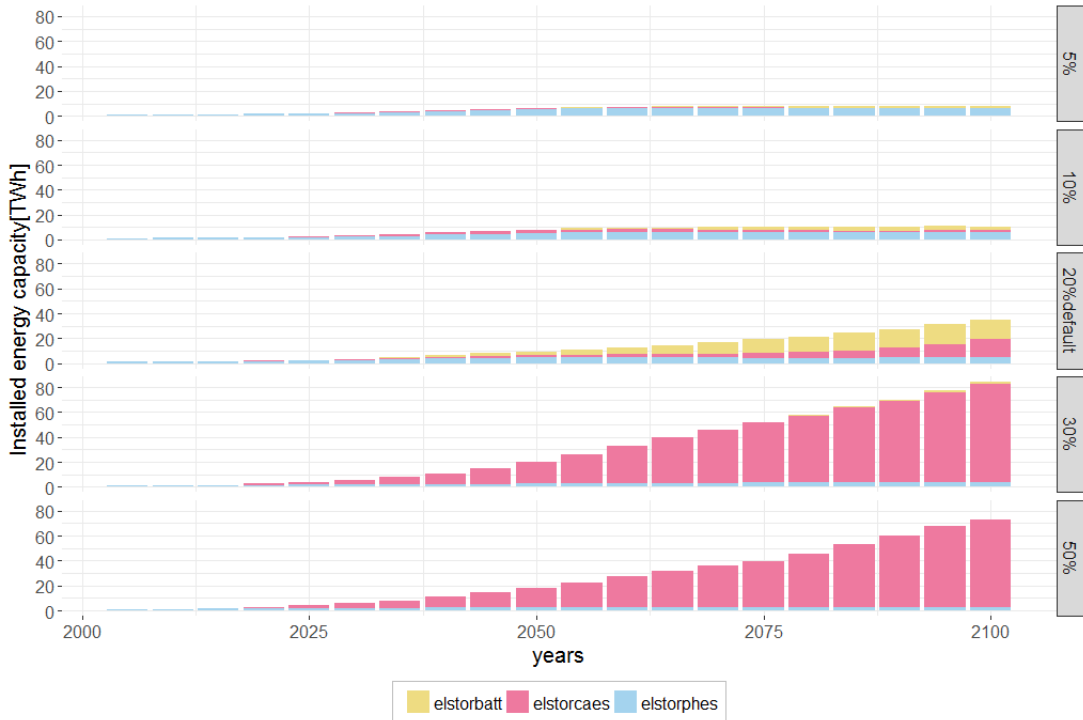


Figure 5.31: Global short-term storage installed capacity by type in CTAX2DEG scenario, as a function of *fraction_vre_stored* value.

5.4 Comparison with previous WITCH modeling

As described in Section 4.1, our work started from some pre-existing implementations of VRE integration characteristics. In our opinion, highlighting how the results obtained with the our new formulation differ from the ones of the previous WITCH versions is relevant, as it shows the impact on the model results in terms of VRE technologies integration. Thus, we decided to devote this section to such a comparison. In order to do so, we selected four main WITCH model versions to be compared. These versions represent how the model has evolved in time, incorporating a more accurate representations of VRE system integration at each step, starting from the MASTER edition to conclude with our final version, +STORAGE. The main characteristics of each edition are summed up below:

- MASTER: This was the model edition on which our thesis co-supervisor Samuel Carrara started working to implement the new VRE integration features. In particular, it was the edition of the model considered in the ADVANCE project [17]. Section 2.4 describes what this model edition included. To sum up: the flexibility and capacity constraint equation were already implemented, but just in their first form (equations 2.3 and 2.4); the old formulation of the grid was in place (equation 4.6); storage was intended just as a “dummy” technology that provides positive contribution in the flexibility and capacity constraint equations; VRE curtailment was not represented.
- SYST_INT: This was the model edition from which our work started. The up-

dates with respect to the MASTER edition are broadly described in section 4.1. In particular, the new formulation of VRE curtailment and VRE capacity values based on RLDCs were introduced; the first implementation of the RLDCs based VRE flexibility coefficient was included (Section 4.1.3) and the flexible operation of non-VRE power plants was represented.

- **+GRID:** This edition is the result of the first part of our work. It includes the new interpretation of VRE flexibility coefficients (Section 4.2 and the new representation of electric grid. In this edition storage was still implemented as in the old formulation.
- **+STORAGE:** This edition is the final outcome of our work. With respect to +GRID edition the new formulation of short-term and seasonal storage technologies have been inserted.

The comparison among the different WITCH model editions will be focused on some key aspects: the electricity generation mix, the generation plants installed capacity mix, the installed storage capacity and the investments in grid. Most of these comparisons are made on two different scenarios (with and without the inclusion of nuclear and CCS power plants) and on three different policies (BAU, CTAX and CTAX2DEG). Thus, in each graph the results for 24 cases (2 scenarios x 3 policies x 4 WITCH model editions) can be seen. The three different columns of graphs boxes correspond to the policies, while the two rows of boxes correspond to the two scenarios (nukeccs_ON and nukeccs_OFF, indicating respectively the scenarios with and without the installation of new nuclear and ccs power plants).

First of all, in Fig. 5.32 the global electricity generation mix in 2100 is shown. Focusing our attention on the results for the MASTER and SYST_INT editions, it is clear how the effect of the implemented VRE integration features is a reduction of VRE technologies generation. In the BAU and CTAX (nukeccs_ON) cases this is balanced by an increased generation of the other technologies. While in the CTAX2DEG (nukeccs_ON), and CTAX_NOCCS and CTAX2DEGX_NOCCS (without investments in nuclear and CCS), this corresponds to an inflection of the overall generation, respectively because the more stringent climate change objective has to be met and because the CCS technologies are not available.

Then, we can focus our attention on the comparison between the SYST_INT and +GRID editions. In all the cases, the VRE generation increases, with the production of the other technologies staying almost constant. This is due to the introduction of the new grid formulation, in particular to the differentiation between distribution and transmission lines, and to the fact that WITCH models two different types of PV (“near” and “far” from the load centre) and three different types of onshore wind (“near”, “intermediate” and “far”), as said in Section 4.3. In the previous formulation, all the VRE capacity required the same associated installed capacity of grid, with an additional markup based on the classification by distance of solar and wind power plants. This representation was not able to completely capture the fact that near PV and wind capacities, especially PV at residential and commercial level, require a lower absolute amount of grid capacity since they usually need just distribution capacities

or local interconnections for stand-alone systems. The differentiation we introduced between transmission and distribution lines allows to represent better this lower grid capacity requirement by near VRE plants, so this promotes their installation. The overall result is an important increase in the VRE electricity generation. In the meantime, the absolute generation of the other technologies remains almost constant. Thus, an increment of the overall generation can be seen.

Finally, we could compare the two steps of our work: +GRID and +STORAGE. It can be easily seen that, in all the cases, VRE generation is considerably reduced with the overall production of other technologies remaining almost constant. This corresponds to a decrease of the overall generation and, in particular, to an important inflection of the VRE share. From the shown results, it can be concluded that including the new, more detailed description of storage (with the associated efficiency losses) hinders VRE deployment with respect to the previous implementation (MASTER and SYST_INT cases). It is worth noting that this happens even if, between 2015 and 2100, the cost for the “dummy” storage technology was higher than in our representation. Thus, adding the key features of storage technologies related to the input and output of electricity strongly offsets this lower average cost.

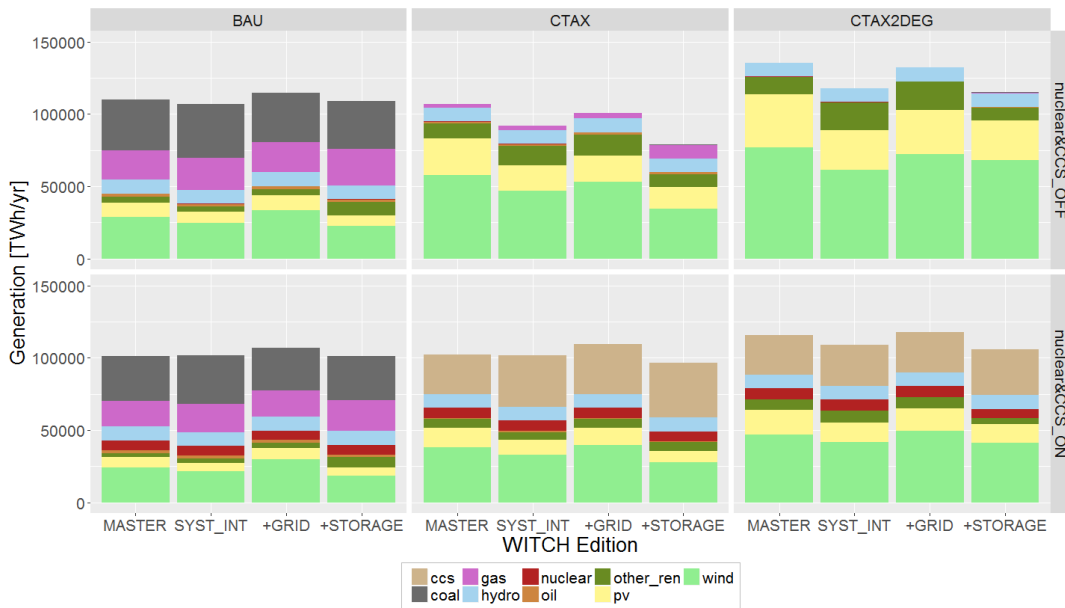


Figure 5.32: Electricity generation (after storage) by technology type in 2100 for the comparison between WITCH model editions.

Looking more specifically at the effect of the new storage formulation on its installation, in Fig. 5.33 the overall installed capacities of storage in all the different cases can be seen (for +STORAGE it is the sum of the installed capacities of all the short term storage technologies and of fuel cells). It is worth highlighting that in the model editions with the old formulation, a much higher capacity of storage was installed even in the BAU scenarios. A great difference can be seen also in the CTAX with nuclear and CCS technologies activated. The reason is that in the previous editions, even if on average the cost of storage was lower, it did not entail losses and it was provided with a higher flexibility coefficient. On the other hand, when the growth of the CTAX is faster to meet the 2°C objective, storage becomes a more favorable option and the

installed capacity in +GRID is approximately as large as in previous editions. In Fig. B.1 in Appendix B the overall installed capacity of storage for all the comparison cases can be seen as part of the installed generation capacities mix.

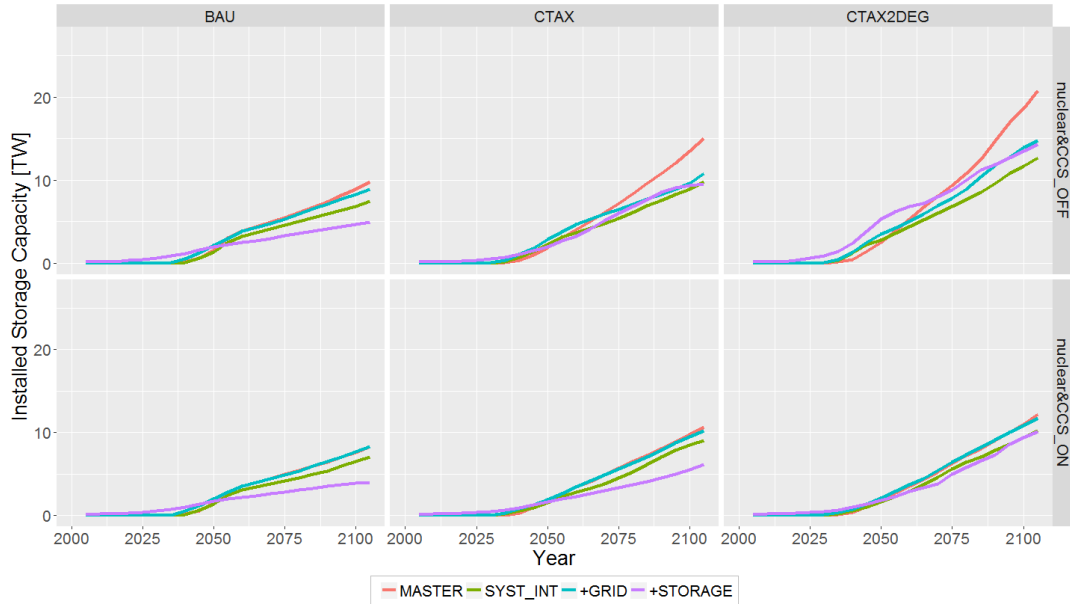


Figure 5.33: Installed overall storage capacity along the years for the comparison between WITCH model editions.

To conclude, it is interesting to have a look at the overall investments in grid in the different model editions. In Fig. 5.34 the comparison between the four considered model editions for the CTAX and CTAX2DEG with nuclear and CCS technologies activated can be seen. It is clear how the new formulation implies lower total investments in grid after 2060, even if, as can be seen in Fig. B.1 in Appendix B, the total installed generation capacity is higher in the +GRID edition in both CTAX and CTAX2DEG and it is at the same level for the +STORAGE one in the CTAX2DEG case (while it is lower in the CTAX one). As we mentioned above, this is related to the fact that on average the grid cost is more favourable for VRE technologies because “near” ones just need distribution. In fact, the increment of installed capacity happens in this type of VRE capacities.

Moreover, it can be noticed that in the CTAX2DEG the investments in grid for the +STORAGE edition is higher than the ones for +GRID. The reason is that, in this case, a significant amount of storage capacity is installed in both the editions, but while with the previous formulation of grid a grid capacity installation relative to storage was not considered, with the latest version also storage capacities require grid capacity and so investments.

5.5 Comparison with other Models

The aim of this section is comparing WITCH results, especially those concerning VRE sources, electric grid and storage, with other models. The models chosen for the comparison are of two types. The first ones belong to the same model class of WITCH,

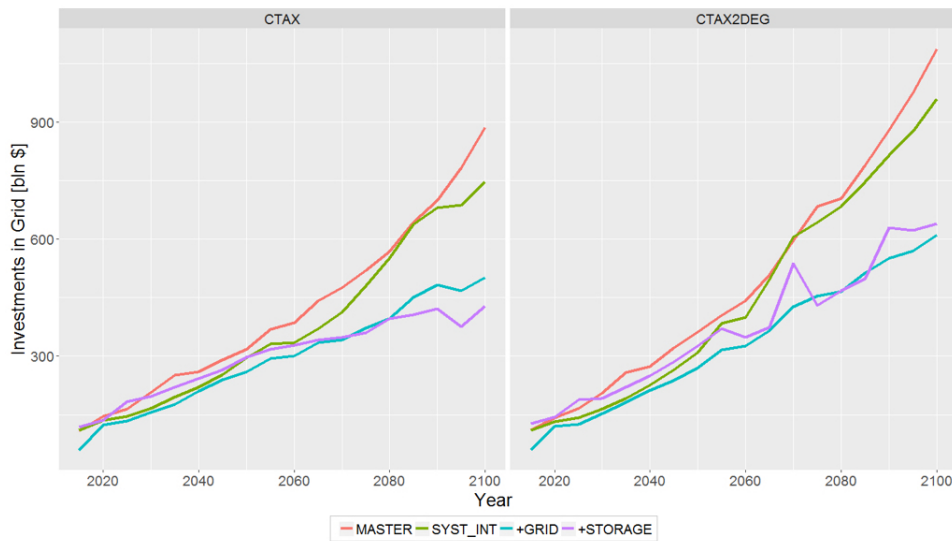


Figure 5.34: Overall yearly investments in grid for the comparison between WITCH model editions.

sharing features, modeling choices and objectives, as the case of ADVANCE IAMs [17]. The second ones feature a more refined representation of the power sector on a spatial and temporal basis (as the case of EUCAD [33] and SWITCH [107]) and can be instrumental to validate the accuracy of our assumptions and results.

5.5.1 ADVANCE IAMs

The ADVANCE modeling framework, already discussed in Section 2.3.1, is a set of 6 models (AIM, IMAGE, MESSAGE, POLES, REMIND and WITCH itself) that share similar features in terms of temporal and spatial aggregation, objective function, accuracy in the representation of the energy sector and scope [17]. Their main features are presented in table A.3, in Appendix A.

Over the last years, the six modeling teams have performed a joint effort aimed at a better representation of challenges and dynamics introduced by the system integration of VRE sources in energy systems [17], [36], [37]. In particular, POLES is the only other ADVANCE IAM to represent endogenous investments in short-term storage with technological differentiation, featuring exactly the same technologies modeled in our work (PHES, A-CAES, battery) plus seasonal hydrogen storage [24]. POLES introduces a more refined representation of the correlation between VRE production and load: its investment are based on combinatorial RLDCs formed from 54 days: 2 seasons \times 3 demand levels (high/med/low) \times 3 solar levels (high/med/low) \times 3 wind levels (high/med/low). Moreover, it couples its long term investment planning model with European Union Commitment and Dispatch model (EUCAD) [33], that features hourly resolution and the different VRE-load matching conditions of 12 representative days throughout the year [24]. This allows POLES to incorporate, in its long-term investments decision, the typical short-term dynamics that characterize VRE integration and short-term storage, as described in Section 2.3. Therefore, POLES results on VRE share and storage are taken as a benchmark in this comparison, especially those for EU countries.

All the results shown below are obtained running the same policy scenario on all the six IAMs: a carbon tax starting from $30 \frac{\$05}{\text{tonCO}_2}$ in 2020 and increasing of 5% a year (called CTAX30).

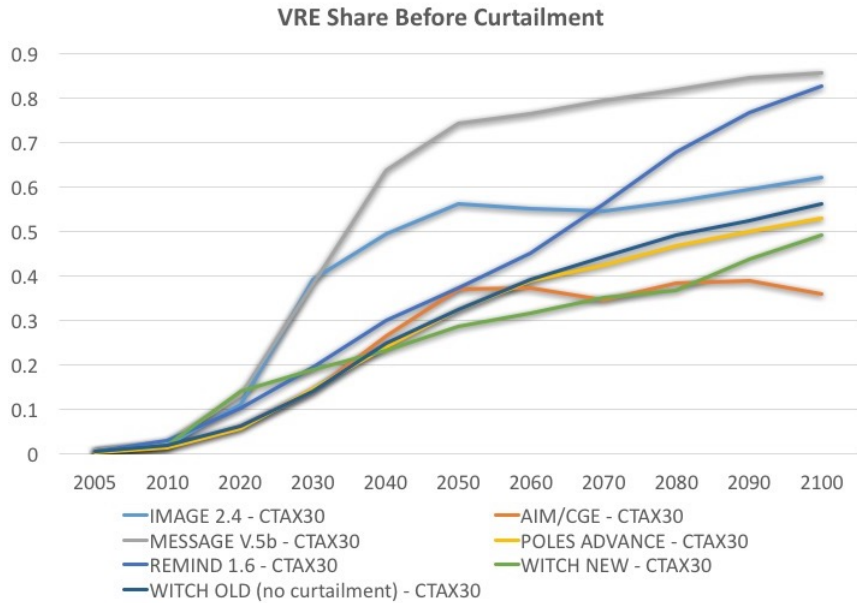


Figure 5.35: Global VRE share of electricity generation before curtailment (if modeled) in a CTAX30 policy scenario for the six ADVANCE IAMs. Source: ADVANCE database and own data.

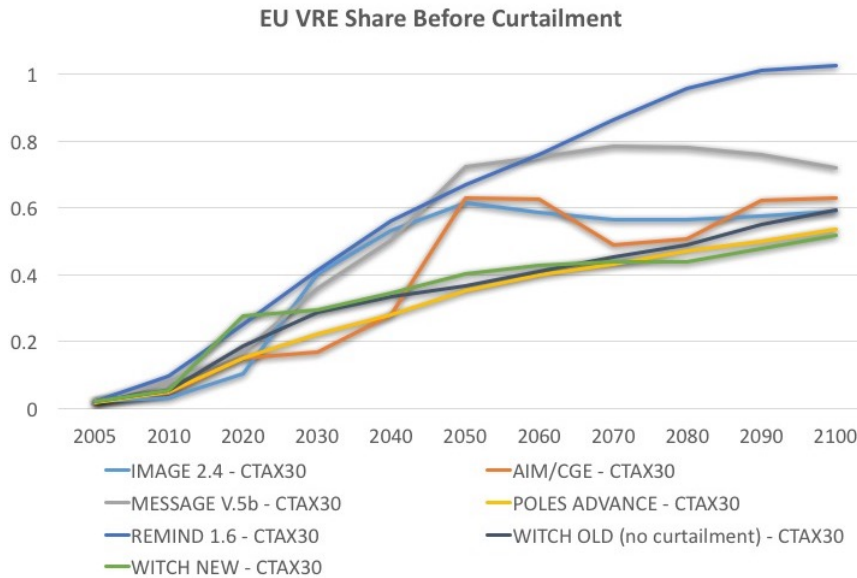


Figure 5.36: EU VRE share of electricity generation before curtailment (if modeled) in a CTAX30 policy scenario for the six ADVANCE IAMs. Source: ADVANCE database and own data.

Figure 5.35 represents the VRE share of electricity generation before curtailment. We choose to present VRE production before curtailment because curtailed energy is treated differently (wasted or recovered) across different models, and this makes any comparison of generation after curtailment hardly reliable. We can see that the new WITCH version and POLES follow very similar paths until 2040, then they diverge

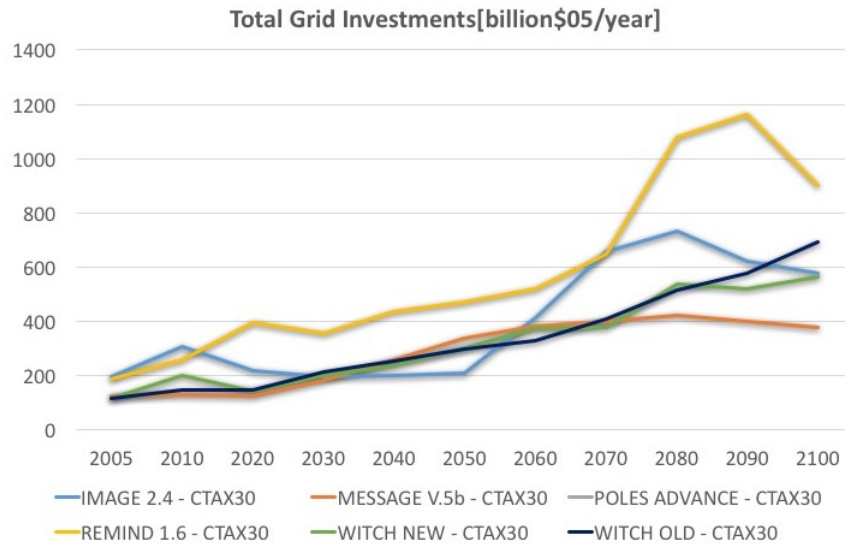


Figure 5.37: Global, total investments in grid [$\frac{bln\$}{year}$] in CTAX2DEG scenario, as a function of $fraction_vre_stored$ value. Source: ADVANCE database and own data.

towards the middle of the century but end up featuring similar shares in 2100: 52% for POLES, 49% for WITCH. This suggests that the following results on storage can be compared not only in absolute sense, but also in view of analogous VRE investment and generation choices for the two models. Considering also other models, we can see that the values we obtained lie closer to the lower bound of the interval defined by AIM (36%) than to the upper bound, represented by MESSAGE (85%). Moreover, looking at old WITCH results (corresponding to the MASTER version discussed in Subsection 5.4) the previous version seems to compare even better to POLES than the new one. Nevertheless, it should be said that old WITCH version does not feature curtailment explicitly, so the VRE share it provides is, most likely, underestimated, and hard to be compared with the other models in the graph.

Looking only at figure 5.36, representing the VRE share in EU countries (where investment decisions are supported by EUCAD), we can see that new WITCH and POLES show similar results especially in the second half of the 21st century, at high shares. In this case, new WITCH results compare to POLES better than old WITCH version after 2060.

As regards global grid investments (figure 5.37), a comparison with POLES is not possible as no grid is represented in this model, nevertheless WITCH values compare very well with results from IMAGE and MESSAGE (both featuring differentiation between transmission and distribution lines and investments in pooling [17]). The results we obtain are also comparable with the old WITCH implementation, that tends to overestimate investments in the last two decades.

Finally, as regards global short-term storage installed capacity in GW (figure 5.38), we can see that POLES and new WITCH follow very similar trajectories, with just a slight deviation between 2050 and 2090, when also VRE shares diverge. The same reasoning applies to storage capacity installed in the 27 EU countries (figure 5.39, that is chosen because of the temporally and spatially detailed EUCAD dispatch model). In particular, the two trajectories are coupled until 2050, very similar until 2090 and slightly

more divergent, yet comparable, in 2100. This important finding appears to corroborate and validate the results obtained in our new WITCH version, and the importance of this finding increases if we consider that WITCH does not feature any coupling with dispatch models. So its investment decisions are only based on the stylized representation of VRE integration challenges, grid and storage investments described in Chapter 4. If we examine data from the old WITCH version, we can note that storage capacity is systematically underestimated in the first half of the century and then overestimated in the second half. This might be due to the fact that the only function of storage in the old implementation was providing flexibility and capacity (no input from VREs or efficiency loss was modeled) and its initial cost was very high yet decreasing exponentially in time. The model therefore found storage a convenient option to help VRE integration just after a certain cost threshold, reached around 2050, and after that threshold storage was installed in very high quantities because no negative effects on generation (such as efficiency losses) were associated to its installation.

Compared to the starting point of our modeling work, in 2100 WITCH now features a slightly lower amount of VRE generation (49% share vs. 56% with previous modeling) but also a lower need for storage capacity (green vs. dark blue line in figure 5.39): for EU countries circa 738 GW of short term storage, growing to 746 GW if we consider also seasonal storage (fuel cells) *versus* the previously installed 1094 GW of generic *storage technology*.

To conclude, looking at the evolution of the WITCH model itself, we can summarize the effect of a better representation of VREs system integration dynamics on VREs installation and share. Firstly, the upgrade from a pre-MASTER model configuration (see Appendix A), with no capacity and flexibility constraint, simplified grid representation and just cost markups on VREs to represent storage and curtailment, to the one we called MASTER in Section 5.4, determined a substantial increase in VRE share (as it is described in [17], that performs a comparison between ADVANCE IAMs versions with and without VREs system integration). On the contrary, the more accurate representation of electric grid and storage for VREs integration that we introduced has the effect of reducing the overall share of wind and solar generation, since it takes better into account the associated challenges, but also of decreasing the storage capacity needed.

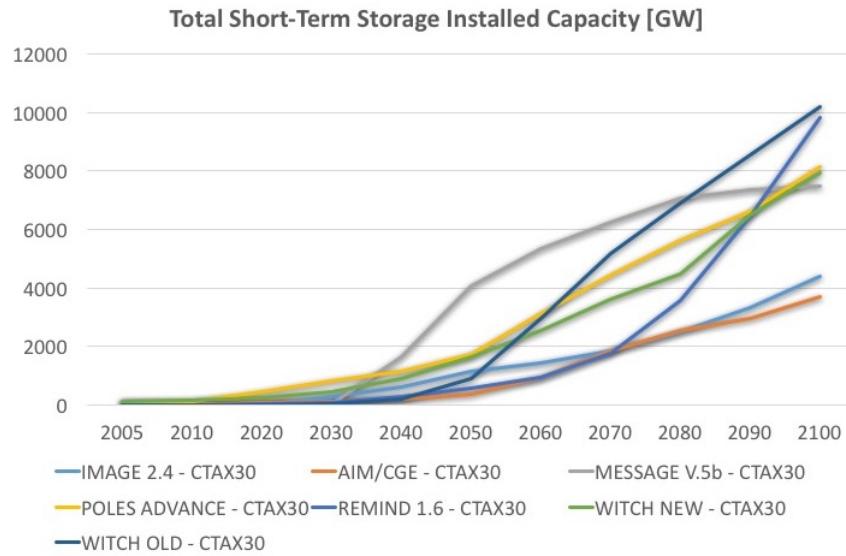


Figure 5.38: Global short-term storage installed capacity by type in CTAX2DEG scenario, as a function of *fraction_vre_stored* value. Source: ADVANCE database and own data.

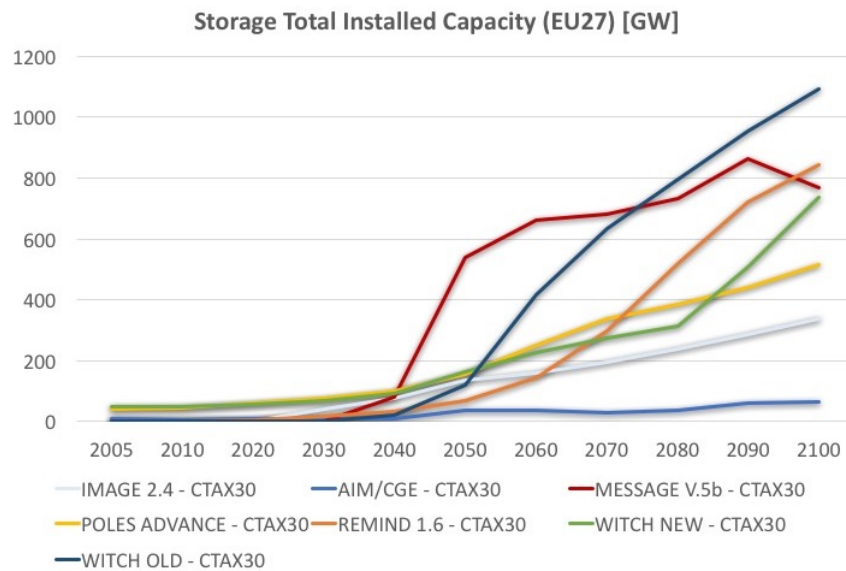


Figure 5.39: EU short-term storage installed capacity by type in CTAX2DEG scenario, as a function of *fraction_vre_stored* value. Source: ADVANCE database and own data.

5.5.2 SWITCH China

SWITCH (Solar and Wind energy Integrated with Transmission and Conventional sources) is a linear programming model used to investigate the least cost energy system design to meet specific performance and environmental objectives [107]. It has been developed by the Renewable & Appropriate Energy Laboratory (RAEL) at the University of California, Berkeley. Its objective function is to minimize the cost of producing and transporting electricity through the construction and retirement of several power generation plants, storage technologies, and transmission grid options between the present day and future target dates according to projected demand. In particular, as regards the grid, SWITCH optimizes both its long-term investments and its short-

term operation through the optimization of the hourly generation and transmission dispatch. As regards SWITCH temporal dimension, for each month of the year, two characterizing days are considered: the peak and median load days. For each day six characterizing hours are included. Concerning the geospatial definition of the Chinese power sector in the study, the mainland China is divided into 31 load areas connected by transmission lines. Thanks to its high temporal and spatial resolution, its prediction about the development of the investment in grid projects can be considered a reliable term of comparison.

As a consequence, we performed an evaluation of the consistence of our results about grid related investments through a SWITCH based study. We chose to use the SWITCH model as term of comparison because the co-supervisor of our thesis Samuel Carrara is at the moment developing his research at the University of California, Berkeley. To conduct our analysis, we referred to an article about a SWITCH study of the Chinese power system [108] and its supplementary material. Thanks to the help of our co-supervisor, we contacted directly the authors of the article. They provided us with the full set of the results data that are not fully available in the article. The aim of this study was to investigate different possible paths for decarbonizing the Chinese power sector in the 2015-2055 time span. In particular, we focused our attention on the SWITCH-China IPCC scenario that involves an overall power sector carbon emission target of 80% below the 1990 level baseline in 2050, as proposed in the 2°C scenario suggested by the IPCC. We chose this scenario because it is the one that sees the highest installation of VREs capacity and our objective in the comparison was specifically testing the behaviour of our formulation with high shares of VREs. The SWITCH results include the extension planning of the transmission lines between China load areas and the related investments. On the other hand, the distribution related investments are represented just in an approximated way. The distribution network in each area is built to serve the peak load of 2010. In the future, the peak load is assumed to be a liner function of the demand, and so are the related investments. Finally, the results include also the electricity production mix and the generation and storage technologies installed capacities in each timestep.

In Figure 5.40 a comparison of the overall annual grid investments in transmission and distribution as a function of the VRE share⁵ between WITCH and SWITCH results can be seen. Three different WITCH scenarios are represented. The WITCH CTAX100 into which a constant carbon tax of 100 \$2011/tonCO₂ is applied from 2020⁶. It is shown because in this scenario the Chinese power sector CO₂ emissions approximately follow the assumption of the SWITCH IPCC scenario. But, since a carbon tax of 100 \$/tonCO₂ is not enough in an integrated assessment model like WITCH to significantly transform the generation mix, only a VRE share of 36% can be reached.

Therefore, to investigate the WITCH results behaviour with higher shares of VREs,

⁵The grid annual investments in correspondence of a particular VRE share are the ones evaluated in the same years that VRE share is registered, so they are the investments that have effect on the grid capacity in the following time period. The SWITCH-China results we were provided were averaged on ten years spans between 2015 and 2055. So, we did the same averaging WITCH results on ten years spans.

⁶Monetary values in SWITCH are expressed in \$2010, they have been converted in \$2005 to be comparable with WITCH values

also the CTAX and CTAX2DEG scenarios are displayed. It could be noticed that the trend of overall grid investment as a function of the VRE share is similar. The SWITCH IPCC and the WITCH CTAX2DEG curves are partially diverging at VRE shares higher than 60%. Due to the limited amount of data available from the SWITCH-China study, it has not been possible to compare better the behaviour at VRE shares higher than 60%.

However, the order of magnitude of the investments is similar. They increase from 18 bln\$/yr at a 16% VRE share to 99 bln\$/yr at a 66% VRE for the SWITCH IPCC scenario. While, they grow from 55 bln\$/yr at a 13% VRE share to 175 bln\$/yr at a 73% VRE for the WITCH CTAX2DEG scenario. The higher WITCH values can be explained by the fact that the distribution related costs are described in more detail than for SWITCH, in which they just grow linearly with the demand. Moreover, the larger difference at higher share of renewable can be attributed to the grid pooling additional investments required in WITCH, that at the distribution level cannot be captured by SWITCH due to its not detailed formulation. Finally, it should be highlighted that, while in the SWITCH IPCC scenario the 66% VRE share is reached already in 2050, in the CTAX2DEG the highest share is obtained only in 2100.

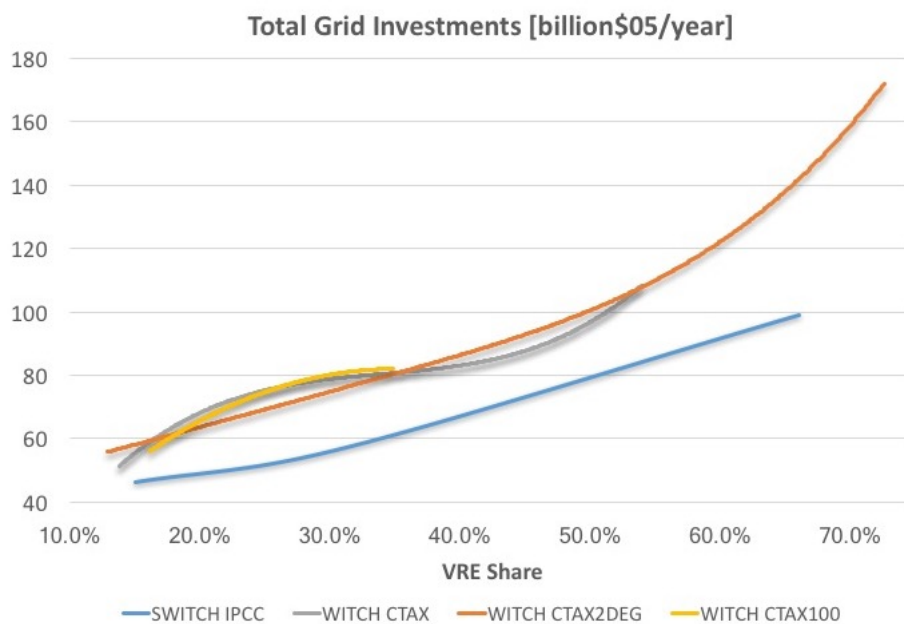


Figure 5.40: Comparison of total investments in grid trend as a function of the VRE share (after curtailment for WITCH) for China between the SWITCH IPCC Scenario [108] and three WITCH scenarios.

In Figure 5.41 we also included a comparison between the two models of the behaviour of the ratio between the installed capacity of storage technologies and of VREs, both in GW. The graph highlights that the general trend with growing VRE share is similar for the SWITCH IPCC and the CTAX2DEG scenarios. On the contrary, the behaviour of the WITCH CTAX100 and CTAX, at shares lower than 40%, appear to be really different. This could be explained by the fact that when in WITCH the carbon tax is not high enough (CTAX100 and CTAX before reaching 30% share), it does not foster the installation of high shares of VREs. The model, however, tries to push in this direction installing more storage capacity per unit of VRE capacity.

The higher capacity installation of storage in WITCH with respect to SWITCH can be explained focusing what is the function of storage technologies in SWITCH. In SWITCH, electric storage contributes to meeting the load and providing operating reserve and capacity reserve margin. Thus, it can store VREs production in order to shift it and meet the load. On the other hand, storage cannot exploit VREs curtailment that is just wasted [108]. Therefore, the installed capacity K_STOR_CURT that can store the VREs curtailment⁷ in WITCH is missing in SWITCH. As a consequence, it probably makes more sense to compare only the K_STOR_PEAK storage capacity installed in WITCH to supply the peak load with the SWITCH storage capacity. In Figure 5.42, this second curve WITCH “CTAX2DEG (Only K_STOR_PEAK)” is represented for the CTAX2DEG scenario. We are here considering just the SWITCH IPCC and the WITCH CTAX2DEG scenarios because in the latter one the highest VREs share is reached. It can be noted that the gap between the SWITCH and WITCH curves has been reduced considering just the storage capacity type that is modeled also in SWITCH. Moreover, a further observation can be added. In SWITCH, an other dispatchable technology whose main aim is providing operating reserve is represented: the combustion gas turbine (CGT). The CGT, on the contrary, is missing in WITCH. Thus, it could be stated that a portion of the operating reserve required with growing VREs share in SWITCH is provided by the CGT instead that by storage. To validate this conclusion, in Fig. 5.42 a fourth curve representing the behaviour of the ratio between the sum of storage and CGT capacities and VREs one in SWITCH can be seen “SWITCH IPCC (Storage + CGT)”. This ratio starts at much higher values than the WITCH storage one at low VREs shares. But this can be explained considering that in 2015 a certain capacity of CGT was already installed in China [109] and at low VREs shares CGT is however a cleaner solution than coal power plants. Then, at high VREs shares it can be noticed how the WITCH CTAX2DEG (Only K_STOR_PEAK) and SWITCH IPCC (Storage + CGT) curves converge, meaning that the storage capacity K_STOR_PEAK is well representing the overall dispatchable capacity requirement per unit of installed VREs capacity.

To conclude, other differences between WITCH and SWITCH that can clarify why there is a gap between the installed storage capacity in the two models and why the CGT is partially preferred in SWITCH are the following. The storage capacity shown in Fig. 5.41 for SWITCH belongs just to NaS batteries with a round-trip efficiency of 76.7%. Moreover, in SWITCH the capacity of Pumped Hydro is maintained constant at the initial value, while CAES is not considered in the results at our disposal. Thus, modeling the use of LiB with higher efficiency may make the battery technology more convenient because it would entail lower losses. Besides, the possibility of PHES future projects (since it presents still a big potential in China) and the introduction also of the CAES choice should be taken into account because they may foster the installation of storage capacity.

⁷Note that here we are referring just to the short-term storage capacity K_STOR_CURT that is fed by short-term storage curtailment because seasonal storage is totally missing in SWITCH.

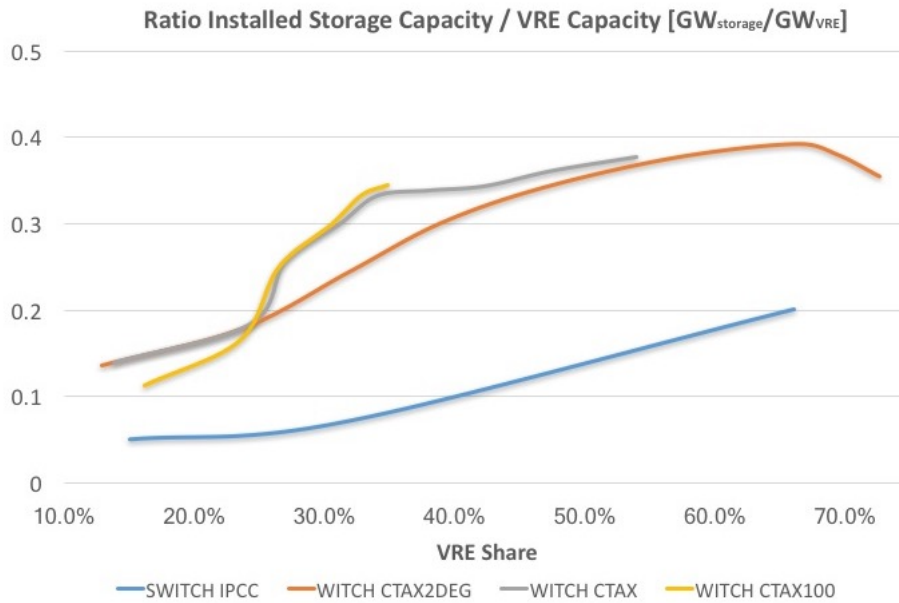


Figure 5.41: Comparison of the trend of the ratio between the installed capacity of storage in GW and the installed capacity of VRE in GW as a function of the VRE share (after curtailment for WITCH) for China between the SWITCH IPCC Scenario [108] and three WITCH scenarios.

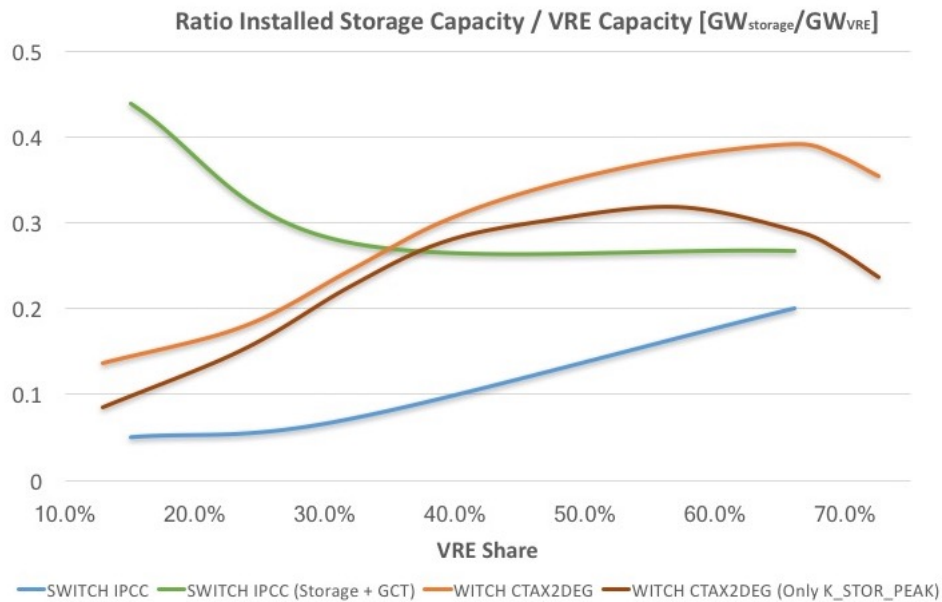


Figure 5.42: Comparison of the trend of the ratio between the installed capacity of storage in GW and the installed capacity of VRE in GW as a function of the VRE share (after curtailment for WITCH) for China. The comparison is made between the SWITCH IPCC scenario [108] with and without considering the installed capacity of CGT, and the WITCH CTAX2DEG scenario counting the overall storage capacity and only the *K_STOR_PEAK* one.

Chapter 6

Conclusions and future work

In this chapter, we summarize the main results achieved in our work and the main conclusions we can draw from them, answering to the questions that motivated our research. The questions are reported in the following:

1. Among the main electricity storage technologies, which ones are more suitable for being included in long-term models?
2. What is the effect of different climate policy scenarios on the diffusion of VRE technologies and on grid and storage technologies?
3. How do grid and storage technologies affect the electricity generation mix? How does this impact on economic growth and costs, in the context of VRE system integration?
4. Which of their cost and performance parameters have the strongest impact on VRE diffusion and on grid and storage investments?
5. What are the effects on results of the new, more accurate representation of grid and storage if compared to previous versions of the model?

Main questions discussion

1. As regards short-term storage, after a comprehensive review of the state of the art, the three technologies modeled are Pumped Hydro Energy Storage (PHES), Adiabatic Compressed Air Storage (A-CAES) and Lithium-ion batteries. The criteria behind this choice, supported by the literature, are: compatibility with the level of temporal detail captured by WITCH (that can hardly represent the impact of storage technologies with average discharge time in the order of seconds, or minutes), technological and commercial maturity of the technologies, their potential for future development, their ability to complement each other in terms of performance and technology type. Moreover, the modeling of Li-ion batteries is very flexible and can be potentially adapted to represent also other battery technologies.

As regards seasonal storage, the only technological solution modelled is the conversion of seasonal curtailment into hydrogen via alkaline electrolyser and its subsequent re-conversion into electricity via Polymeric Electrolyte Membrane Fuel Cells (PEMFCs). The reasons for this choice are analogous to those presented for short-term storage.

2. Increasing the value of a global carbon tax to achieve increasingly ambitious temperature reduction targets has a positive effect both on the deployment of VRE technologies and of electricity storage technologies if compared to the Business As Usual (BAU) scenario, where no price on carbon emissions is set. As a matter of fact, while VRE technologies represent in 2100 just 24% of global net generation in the BAU scenario, dominated by fossil fuels, the figure increases to 37% if a default carbon tax is applied (CTAX) starting from 2020. The other carbon tax effect is stimulating the phase-out of fossil-based plants around 2050 and boost CCS options, that become the dominant technologies. If the tax is raised to achieve the 2°C target indicated by the Paris Agreement (CTAX2DEG), this boosts VRE diffusion even further as they become the most widespread technology option, with 51% of global net electricity generation.

As regards yearly grid investments, they increase in time in all the scenarios from 2015 to 2100. Moreover, they change remarkably across scenarios, and grow with increasing value of carbon tax: investments in transmission grid decrease from BAU to CTAX and CTAX2DEG, while investments in distribution, smartening and pooling of the grid behave the other way around, with a considerable growth for investments in grid pooling and smartening: they grow from 4.8 $\frac{\text{bln}\$}{\text{year}}$ in CTAX to 17,3 $\frac{\text{bln}\$}{\text{year}}$ in CTAX2DEG for the period 2095-2100. Investments in transmission and distribution, however, lines are an order of magnitude larger than the ones in pooling and smartening. Global distribution lines in 2100 represent 97% of the global grid line length in the BAU scenario, and this figure raises respectively to 97.7% and 98.3% in the CTAX and in the 2°C scenario, meaning distributed VRE generation is favoured.

Concerning storage capacity, it grows with increasing carbon tax and with the share of VRE generation. PHES is the dominant technology in the BAU scenario, while the introduction of a carbon tax benefits CAES and batteries, that leverage on cost reductions from learning effect to become the dominant technologies. Considering the energy capacity, CAES is the dominant option in CTAX and CTAX2DEG, followed by batteries, while if we consider the power capacity, a proxy for the number of single installation required, batteries are the most widespread technologies in both the scenarios, due to their lower energy-to-power ratio. Overall, A-CAES is the preferred short-term storage option in regions with very high VRE shares, due to its higher capability to provide firm capacity compared to batteries. Global yearly investments in short-term storage experience a considerable growth in time, particularly in presence of a carbon tax: in the 2°C scenario, they raise from 14.4 billion \$ in 2020 to 57.1 bln\$ in 2050, up to 203 bln\$ at the end of the century: the latter value has the same order of magnitude of investments in transmission plus grid smartening and pooling.

Seasonal storage deployment is almost an order of magnitude lower than short-term one in the most favourable CTAX2DEG scenario, slowed mostly by the high investment costs of electrolysers and fuel cells. Maximum yearly investments in electrolysers and fuel cells amount approximately to 14 bln\$ in 2100, for the 2°C scenario.

Interestingly, the model is able to reach a 100% renewable scenario if no in-

vestments towards nuclear and CCS are allowed (simulating social or political obstacles to the adoption of these technologies) and a 2°C target via carbon tax is imposed. This scenario entails a four-fold increase in installed CAES capacity, becoming the dominant storage option and responding to the high firm capacity and flexibility requirements of this electricity mix. This fully renewable scenario, however, requires higher expenditures in the energy sector than the normal 2°C scenario and this reflects on global economic growth, with an undiscounted GDP loss of 16 percentage points with respect to BAU in 2100 (the loss in case of CCS and nuclear availability is lower, around 10%).

3. WITCH results indicate that without the installation of storage capacity, it is not possible to reach high shares of VRE generation. In a counter-factual scenario in which storage technologies are not present in the model, the role of VREs is considerably undermined: world net VRE shares arrive at best just around 20% in 2100, even in presence of a high carbon tax aimed at achieving the 2°C target. The model compensates the limitation on VRE installing more biomass plants, CSP and CCS and decreasing global generation. This, in turn, affects economic growth, entailing, for the CTAX2DEG scenario, an additional 0.6% undiscounted GDP loss in 2100 with respect to BAU, equivalent to 1.8 trillion \$ of 2005. Regarding the effect of grid, VRE plants that are closer to load centers are favoured as they only necessitate distribution line investments and no transmission line.

As regards the system integration requirements in WITCH, it can be said that, in the first years, the requirement of firm capacity has more influence on VRE and storage investment options than the flexibility requirement, in all the scenarios. On the other hand, increasing the carbon tax entails a growing influence of the flexibility requirement, also in time.

Concerning the translation of storage and grid installation into integration costs, we have investigated the effect on the LCOE of VREs technologies. Taking Europe as an example, the impact becomes visible in 2050 with a LCOE increment of 1.5% for PV and 4% for wind plants. In 2100 the largest increase occurs: 7% for PV and 17% for wind plants. Taking into account also the effect on LCOE of the shadow costs related to the VRE additional flexibility and firm capacity requirement, their impact on integration costs is much larger: LCOE of wind is increased by half in 2050 and almost tripled in 2100. This signifies that the integration of VREs has a significant effect in terms of stress it puts on the energy system. Finally, results indicate that if a price on emissions is present, distribution grid and short-term storage (especially CAES and Li-ion battery) complement each other from an economic point of view, meaning investments in both of them are necessary to increase VRE generation.

4. The sensitivity analysis on grid cost and grid requirement per unit of generation capacity installed shows that these parameters hold a great influence on average grid investments. However, they do not show a significant impact on the installed generation capacity. Concerning the pooling requirement coefficient, the analysis suggests that the choice of its value, even if subject to uncertainty, does not affect results in a relevant way.

As regards the effect of varying storage parameters, decreasing the capability of storage to provide flexibility and firm capacity (through the correspondent coefficients) dramatically affects both VRE share and storage investments. This confirms that, on the one hand, the satisfaction of flexibility and firm capacity requirements plays a central role in the diffusion of VRE technologies, and on the other hand storage is instrumental in providing this flexibility and firm capacity to the system, benefiting wind and solar installations. The costs of short-term storage technologies, both the initial and the minimum one (floor cost) they can achieve through learning-induced cost reduction, are other two important drivers of VRE share growth and overall storage investments, while varying learning rate and storage efficiency (especially increasing them) does not influence much these two global variables. On the other hand, looking at the impact of storage parameters on the single technologies, efficiency improvements may considerably enhance the diffusion of CAES, and higher values of Full Production Hours for both CAES and batteries technologies could play an important role as well, while their impact on PHES is minor. The effect of energy-to-power ratio, instead, strongly depends on the formulation of the learning equation, and further research on this topic is needed to assess its influence.

5. Considering the differences between our new formulation and our starting point, already featuring a detailed description of system integration but with a simplified grid and storage description, the main effect of the more detailed representation of electric grid introduced in our work is an overall increase in VRE generation with respect to the previous grid modeling, in all the policy scenarios. This is due to the fact that “near” VRE technologies require only investments in distribution line, and this decreases their integration cost with respect to the previous WITCH implementation, where a generic electricity transportation line was represented. This, in turn, enhances the installation of “near” wind and solar plant, whose relative share in the VRE mix increases with respect to previous results.

On the other side, the new storage modeling has the opposite effect on VREs, whose global generation decrease in all policy scenarios (while other technologies are not affected by these change). This is mainly due to the fact that we introduced an efficiency loss due to storage, previously absent, that penalizes net wind and solar generation. The combined effect of grid and storage yields different results according to the policy scenario considered. For null or low levels of carbon tax, the new formulation entails a lower penetration of VRE technologies, while if the tax is raised to meet the 2° target, wind and solar generation are approximately equal in the two cases, and the new version allows to reach even higher shares in case nuclear and CCS options are not available. This suggests that, with the new formulation, the model is more responsive to price signals and technology availability options.

If we compare our new WITCH version with the old MASTER, featuring a less detailed representation of system integration, grid and storage, it is clear that the overall effect of modeling VRE system integration challenges, together with detailed electric grid and storage formulations, compensates for the previous underestimation of VRE integration costs and entails a reduction of the global net VRE share of 4 percentage point in the CTAX2DEG scenario: 55% for the MAS-

TER version, 51% with the new modeling.

Finally, WITCH results for VRE share, grid investments and storage capacity have undergone comparison with other models. Within the ADVANCE IAM modeling framework, a group of six models (including WITCH) that feature similar structure, level of aggregation and purpose, WITCH results for VRE share and storage installed capacity (all obtained under the same carbon tax policy scenario) place themselves near the ones from POLES. This is the only other ADVANCE IAM to feature a detailed technological representation of short-term and seasonal storage technologies, the same technological choice for them and also a better representation of VRE supply-load matching throughout the year, considered a very important piece of information for representing the typical dynamics of VRE integration, grid and storage investments. Moreover, storage results for the EU countries are analogous for the two models. Considering that investment and generation decisions for EU countries in POLES rely on a temporally and spatially detailed unit commitment and dispatch model (EUCAD), a matching between our and POLES' results represents an important *ex post* validation of our work.

As regards global grid investments, not present in POLES, they are in line with two out of the three IAMs considered in this comparison.

A further comparison has been performed with the SWITCH model application to the Chinese power sector. Thanks to its higher temporal and spatial resolution, its prediction about the development of the investment in grid projects can be considered a reliable term of comparison. Comparing the high VREs penetration scenario with the WITCH CTAX2DEG one, we found that the order of magnitude of the investments is the same, even if investments are higher in the WITCH scenario. The higher WITCH values can be explained by the fact that in our new formulation the distribution-related costs are described more in detail, moreover investments related to grid smartening and pooling are included.

Furthermore, we tried to draw a comparison between the two models about the ratio between the installed capacity of storage per installed unit of VRE capacity. As a result, we observed that the storage capacity installed in WITCH to shift the VRE generation and supply the peak load is comparable to the overall capacity of storage and CGT that is installed in SWITCH specifically to meet the peak demand. Thus, this allowed us to validate the formulation we introduced regarding the storage capacity fed by non-curtailed VREs generation.

Scientific contributions provided

To summarize the outcomes of our work, we believe that this thesis contributes to the climate change mitigation literature in two different yet intertwined ways.

The first contribution regards the energy modelling for climate change, in particular the IAMs field. The improvements we introduce in WITCH make it, to our knowledge, the only Integrated Assessment Model in the ADVANCE modeling framework, and one of the few worldwide, to introduce technological differentiation for both grid and storage technologies and endogenous global investments in short-term and seasonal storage that are driven by VRE-share dependent capacity and flexibility coefficients.

This is expected to provide a more realistic representation of the role played by electric grid and storage in VRE system integration. From the policy-making perspective, the technological differentiation we introduced, the results obtained running the model with different policy scenarios and the sensitivity analyses on key cost and performance parameters represent, in our view, a good source of information to design climate policies aimed at increasing VREs penetration while minimizing the correlated integration cost.

Further developments

Besides the contribution provided by our work, we believe that further research developments would complete the analysis and deepen the understanding about the influence grid and storage technologies on VRE system integration in a climate mitigation context. Future work should follow two different directions: the first is a continuation of the modeling work, aimed at deepening some representations introduced in this work and represent possible links with other parts of the model. The second direction regards the other research themes that can be addressed with the current version of the model but were not developed in our work. Some topics related to the first direction of future work are:

- (i) A more detailed representation of battery technologies, introducing further technological differentiation to understand how other promising electro-chemical energy storage technologies such as Sodium-Sulphur and Redox Flow batteries can contribute to VRE integration. In this sense, investigating a cross-learning option between utility-scale and electric vehicle Li-ion batteries (maybe through a spillover of one technology in the learning equation of the other) would complete the picture.
- (ii) A more accurate representation of CAES geographical potential on a regional basis, based on a comprehensive review of resource availability, aimed at highlighting the cost-effective storage options for compressed air at global level.
- (iii) The modeling of Hydrogen as a secondary energy source, allowed to compete with other fuels on a global market, and its supply chain. Its introduction in other sectors, such as transportation and combined heat and power applications, would certainly shed light on the potential of this promising energy vector in low carbon scenarios.
- (iv) An explicit representation of Demand Response and its role in mitigating the flexibility and firm capacity requirement introduced by increasing VRE generation, considering also the facilitating function of investments in grid smartening and storage.
- (v) The introduction of Vehicle-to-Grid (V2G) options, considered a major option to smooth residual load variability in a context of high penetration of electric vehicles. It would be interesting to understand if V2G and electricity storage would substitute or complement each other.

As regards the second direction, further result analyses may address:

- (i) The relationship between storage and other technologies providing firm capacity, such as traditional fossil fuel plants, CCS technologies and traditional hydro. This theme has been considered only marginally, with particular attention to CCS

plants. Investigating the complementarity or substitutability of these technologies would provide useful insights to policy makers.

- (ii) The impact of the new grid technologies on VRE mix (wind vs. solar) and on the choice of distance from load centres for the single wind and solar technologies. This topic has only been partially addressed in the results section, even though the choice between wind and solar technologies is influenced by a very low value of elasticity (2) in the CES node shared by VREs. Studying how an increasing share of VRE installations would be driven by a trade-off between lower costs and decreasing social acceptance seems a potentially insightful exercise.

Appendix A

WITCH model description and other ADVANCE IAMs

WITCH model description

This section provides a more detailed description of the economy and energy modules featured in the WITCH model.

A.1 The Economy

A.1.1 Welfare function

In WITCH, the discounted utility W of each coalition is maximized by a social planner, clt . Utility for every region and at every time step is based on a constant relative risk aversion (CRRA) utility function, depending on *per capita* consumption. For different coalitions, the non-cooperative solution, and it can take different formulations based on the set of coalitions in the scenario clt .

A.1.2 Utility function

If WITCH scenarios are run in a non-cooperative mode, each region n acts on its own, maximising its welfare, so each region corresponds to a coalition. For each region n and time period t , regional utility is computed as:

$$W(n) = \sum_t l(t, n) \frac{\left(\frac{C(t, n)}{l(t, n)}\right)^{1-\eta} - 1}{1 - \eta} \beta^t.$$

Where C is overall consumption, l is population, η is relative risk aversion and β , the pure time preference discount factor, is derived with the discounting rule:

$$\beta = (1 + \rho)^{-\Delta_t}$$

$\Delta_t = 5$ is the number of years covered by one time step and ρ the discount rate.

A.1.3 Consumption

Total consumption C is calculated with the budget constraint equation, where from net output Y we subtract several different types of investment, and O&M costs (source: WITCH documentation [25]):

- investments in final good, I_{FG} ,
- energy technology investments j , I_j
- investments in research and development j , (R&D), $I_{RD,j}$,
- investments in extraction sector, $I_{OUT,f}$
- investments in electric grid, I_{GRID}
- operation and maintenance costs of power plants j , $oem(j)$ and
- fuel extraction costs f , $oem_ex(f)$.
- investments in adaptation ($I(PRADA, t, n)$, $I(SCAP, t, n)$, $I(RADA, t, n)$)

$$\begin{aligned}
C(t, n) = & Y(t, n) \\
& - I_{FG}(t, n) \\
& - \sum_j (I_{RD,j}(t, n) + I_j(t, n) + (oem_j(t, n) * K_j(t, n))) \\
& - \sum_f (I_{OUT,f}(t, n) + (oem_ex_f * Q_{OUT,f}(t, n))) \\
& - I_{GRID}(t, n) \\
& - I(PRADA, t, n) - I(SCAP, t, n) - I(RADA, t, n)
\end{aligned}$$

where

- j are the different energy technologies
- f are the different fossil fuels

A.1.4 Output

The economic production is very aggregated. The output of each region is a single good, used for consumption or investments. The final good Y production is computed by a nested CES function combining capital (K), labour (L) and energy services (ES). The first t are aggregated using a Cobb-Douglas production function. The damage function $\Omega(t, n)$ represents the fact that, due to the effects of climate change on human activities, a share of output is lost. Also the costs of fossil fuels, C_f costs related to mitigation of GHG emissions $C_{ghg}(t, n)$ (carbon tax, reduced deforestation etc.) are subtracted from net output. Regional production in time is thus obtained as:

$$\begin{aligned}
Y(t, n) = & \frac{tfp0(n) (\alpha(n) (tfp_y(t, n) K_{FG}(t, n)^{\beta(n)} l(t, n)^{(1-\beta(n))})^\rho + (1 - \alpha(n)) ES^\rho(t, n))^{\frac{1}{\rho}}}{\Omega(t, n)} \\
& - \sum_f C_f(t, n) \\
& - \sum_{ghg} C_{ghg}(t, n),
\end{aligned}$$

where $\alpha(n)$ and ρ are the CES parameters. The parameter ρ is derived as $\rho = \frac{f-1}{f}$, with f being the elasticity of substitution. $\beta(n)$ is the coefficient of the capital-labour aggregate. Labour l is equal to the population, assuming no unemployment. Finally, the parameter $tfp(n)$, concerning total factor productivity, are calibrated in static or dynamic way by the model.

A.1.5 Energy Services

Energy services ES come from both physical energy input and a stock of R&D in energy efficiency. This allows energy efficiency to be improved endogenously. investing in energy R&D. It substitutes physical primary energy consumption. Energy services ES are thus a CES function of the amount of energy consumed, EN , and a stock of R&D, $RDEN$, :

$$ES(t, n) = \phi_{ES}(n) (\alpha_{ES}(n)RDEN(t, n)^{\rho_{ES}} + (1 - \alpha_{ES}(n))tfpn(t, n)EN(t, n)^{\rho_{ES}})^{\frac{1}{\rho_{ES}}}$$

CES parameters $\phi_{ES}(n)$, $\alpha_{ES}(n)$, and ρ_{ES} depend on quantities and prices in 2005, the base year . Energy consumed for production of output is a CES function of electricity and non-electric energy. Electric energy is generated by different technological options, while non-electric energy entails the use of oil,coal, gas, biomass, and a backstop technology for residential consumption, transportation and industry. The CES function is: ρ_{EN} .

$$EN(t, n) = (\alpha_{EN}(n)EL(t, n)^{\rho_{EN}} + (1 - \alpha_{EN}(n))NEL(t, n)^{\rho_{EN}})^{\frac{1}{\rho_{EN}}}$$

Where both electric and non-electric parts are further decomposed into several options using CES and linear production functions.

A.2 The Energy sector

The energy sector, is divided in electric sector, and transportation sector, and an aggregated non-electric sector. These are the primary and secondary energy forms (source: WITCH documentation [25]):

Primary Energy	Secondary Energy
Coal	Electricity
Oil	
Gas	
Uranium	
Bioenergy	

The following power plant technologies are included:

Power plant
Coal with and without CCS
Oil without CCS

 Power plant

Gas with and without CCS

Wind onshore and offshore

Solar PV and CSP

Nuclear LWR and advanced

Bioenergy with and without CCS

Hydro power

A.2.1 Energy supply

A comprehensive range of technology options allows electricity generation and energy final use. The key techno-economical parameters featured are: investment, and operation and maintenance costs, lifetime, yearly full production hours and efficiency.

The following figure shows the central nested CES structure of the economy-energy system. The number in each node is the elasticity of substitution between the options below that node.

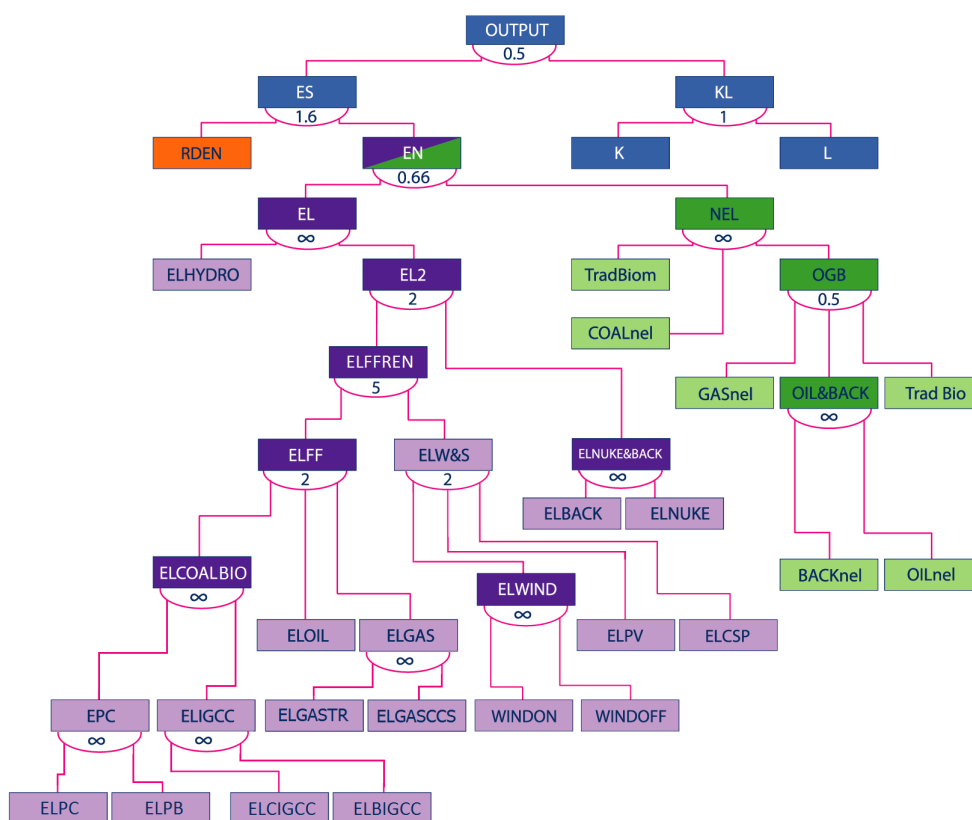


Figure A.1: CES Production Function of WITCH

A.2.2 Electric energy technology sectors

Electricity is generated by several different traditional fossil fuel-based and carbon-free technologies, already shown in the table above.

The electricity generation cost is computed endogenously and includes capital, O&M and fuel costs. For nuclear power WITCH includes also waste management costs.

A.2.3 Capital accumulation for electric energy technology sectors

The stock of capital of electricity generation technologies is computed as:

$$K_j(t+1, n) = K_j(t, n) (1 - \delta_j(t+1, n))^{\Delta t} + \Delta t \times \frac{I_j(t, n)}{SC_j(t, n)}, \forall j \in \mathcal{J}_{inv},$$

where \mathcal{J}_{inv} is the group of generation technologies in which the model can invest. Less mature technologies can undergo endogenous technical change: solar and wind experience Learning-by-Doing, while investment costs SC for backstop technologies depend on a Two Factor Learning Curve: they are function of cumulative installed capacity and stock of R&D knowledge.

A.2.4 Additional constraints in the electric sector

The electricity production EL is upper-bounded by the capital stock multiplied by the full production hours μ :

$$EL_j(t, n) \leq \mu_j(t, n) \times KEL_j(t, n)$$

Technologies that require fuel have their production capacity, Q_j equal to the primary energy consumed times the fuel rate of the technology ξ :

$$Q_j(t, n) = \sum_f \xi_{j,f}(t, n) \times Q_{j,f}(t, n)$$

Other ADVANCE IAMs

This section summarizes the main features of the five IAMs that, together with WITCH, represent the ADVANCE modeling framework [17]-

<i>AIM/CGE</i>	Electricity is a uniform good, technologies compete on LCOE in a multinomial logit Short-term storage and curtailment exogenous functions of wind and solar share, parameterized based on ADVANCE RLDCs
<i>IMAGE</i>	Investment based on ADVANCE RLDC (20 load bands) Technologies compete on LCOE in a MNL Capacity and energy backup requirements lead to LCOE markups for wind and solar Exogenous curtailment derived from ADVANCE RLDC Exogenous short-term storage facilitates integration Investment on 10 time slices, technologies compete on LCOE in a MNL Exogenous fix backup for VRE Exogenous curtailment and spinning reserve
<i>MESSAGE</i>	Electricity is a uniform good, technologies compete linearly on LCOE basis Capacity equation with ADVANCE RLDC-derived parameters Flexibility equation with ADVANCE RLDC-derived parameters Storage investments driven by capacity & flexibility equation Exogenous curtailment derived from ADVANCE RLDC Endogenous hydrogen storage investments Electricity is a uniform good, technologies compete linearly on LCOE basis Generic capacity equation Flexibility equation with fixed parameters Generic exogenous curtailment
<i>POLES</i>	Investment based on combinatorial RLDC formed from 54 days: 2 seasons \times 3 demand levels (high/med/low) \times 3 solar levels (high/med/low) \times 3 wind levels (high/med/low) Technologies compete on LCOE in MNL Additional “technology diffusion” markups for wind/solar Dispatch within EU calculated in dispatch model EUCAD between POLES investment calculations, on 12 hourly representative days from new cluster analysis Endogenous within-day storage investment, technological differentiation (PHES, A-CAES, battery) Investment on 24 2 h–time slices: 2 days (winter/summer) Investment based on LCOE, using a multinomial logit function Hard upper bounds on wind and solar share (region-specific) Additional cost markups for wind and solar
<i>REMIND</i>	Investment based on ADVANCE RLDC, implemented via 4 load boxes with wind/solar-share-dependent heights Technologies compete linearly on load-band LCOE Introduced peak capacity equation based on ADVANCE RLDC Exogenous curtailment and short-term storage capacities based on ADVANCE RLDC Grid cost markups updated based on REMIX results Endogenous hydrogen storage investments Electricity is a uniform good, technologies compete linearly on LCOE basis Integration cost markup for wind and solar to represent curtailment and storage costs Grid cost markups

Table A.3: Main characteristics of the five IAMs that, together with WITCH, represent the ADVANCE modeling framework. Source: [17]

Appendix B

Additional Graphs



Figure B.1: Installed capacity in TW by technology type (included storage) in 2100 for the comparison between WITCH model editions. Source: own graph.

Appendix C

RLDC approach for system integration

Figure C.1 shows how the well-known concept of Load Duration Curve (LDC) is derived. The load curve, i.e. the time series of power demand for one year, is sorted from the highest to the lowest values. The y-axis of an LDC indicates the minimum capacity necessary to supply total annual electricity demand, which is represented by the area below the curve. If VRE technologies are added to the system, the power they generate at each timestep can be subtracted from the load at that same time to derive the time series that represents the residual load that must be supplied by the rest of the system (Fig. C.2 on the left). The Residual Load Duration Curve (RLDC) is then derived by ranking this residual load curve in descending order. In particular, the area between the LDC and the RLDC stands for the electricity generation from VREs. Note that the information about the temporal distribution of VRE supply is lost because the shape of the area between the LDC and RLDC is not able to indicate it.

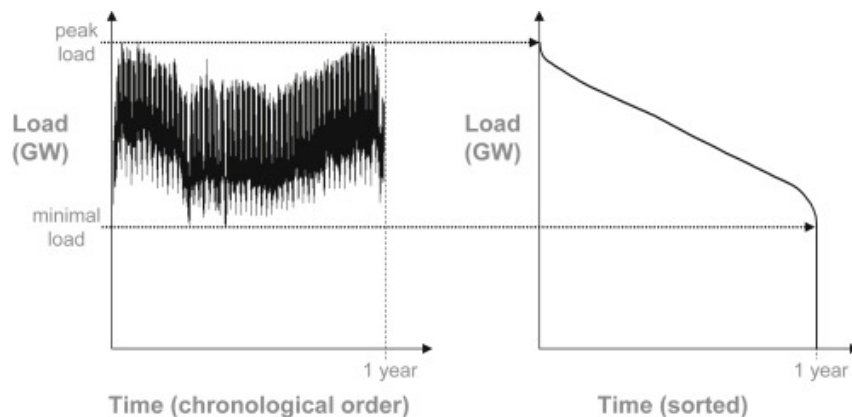


Figure C.1: The Load Duration Curve (LDC) (right) is derived by ranking the load curve points (left) in descending order. Source: [9]

Figure C.3 illustrates the pieces of information about three major challenges related to VREs integration that the RLDCs are able to capture:

- Low capacity credit: VREs contribute providing energy to the system, but they

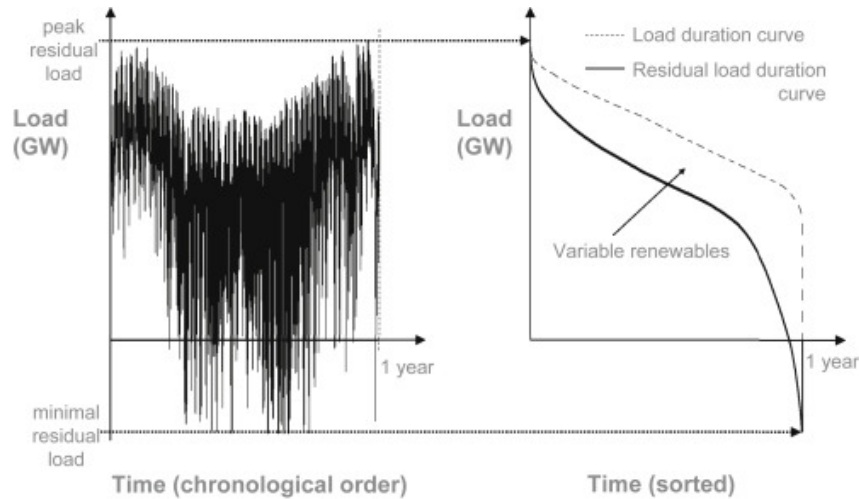


Figure C.2: The residual load curve time series (left) is obtained by subtracting the time series of VRE from the time series of the electric load. The RLDC (right) is obtained by ranking the residual load curve points in descending order. Source: [9]

only slightly lower the requirement for total generation capacity to meet the peak load. This is especially true at high VREs shares, due to their relatively low capacity value.

- Reduced full-load hours: with increasing penetration of VRE technologies, the annual full-load hours of the dispatchable power plants needed to meet the residual load will be reduced.
- Over-production of VREs: there is a series of hours in which total VRE generation exceeds the demand, thus production must be curtailed if it cannot be stored or transmitted. Curtailed portion increases with growing VREs shares.

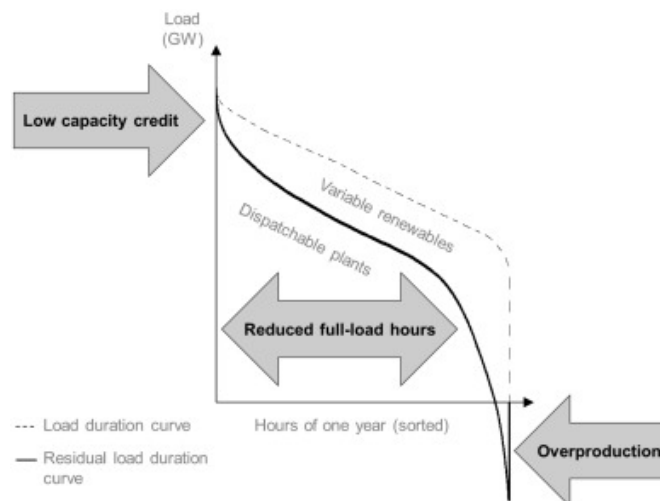


Figure C.3: RLDCs are able to represent three main challenges of the integration of VREs. Source: [9]

RLDCs have been derived for several countries for growing VREs shares and for each VRE share with different mixes of PV and wind plants. In particular, figure C.4 shows the RLDCs derived for Germany and US Indiana [9].

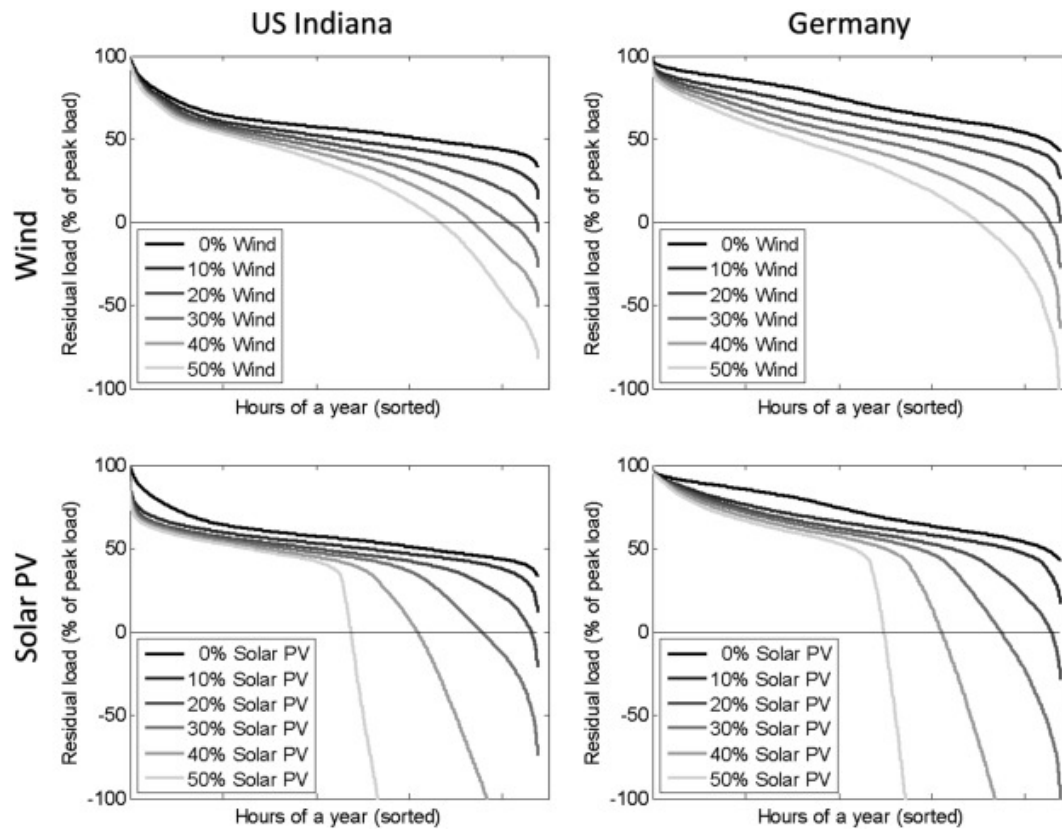


Figure C.4: Installed capacity in TW by technology type (included storage) in 2100 for the comparison between WITCH model editions. Source: [9]

Appendix D

VRE System Integration: Additional Material

The first three tables include values already implemented in the WITCH model at the beginning of our work. Tables D.4, D.5 and D.6 include coefficient values that we derived in our research work.

	Firm requirement [Multiple of annual average load]						
	cajaz	china	easia	india	kosau	laca	mena
2010	1.94	1.46	1.62	1.59	1.521	1.61	1.86
2020	1.85	1.5	1.71	1.63	1.521	1.67	1.83
2030	1.78	1.54	1.69	1.63	1.521	1.69	1.79
2040	1.73	1.58	1.68	1.65	1.521	1.71	1.77
2050	1.7	1.61	1.68	1.68	1.521	1.73	1.75
2060	1.68	1.62	1.67	1.68	1.521	1.71	1.73
2070	1.67	1.62	1.66	1.68	1.521	1.7	1.72
2080	1.66	1.63	1.65	1.68	1.521	1.69	1.72
2090	1.66	1.63	1.65	1.69	1.521	1.69	1.72
2100	1.66	1.64	1.64	1.69	1.521	1.68	1.73
	neweuro	oldeuro	sasia	ssa	te	usa	
2010	1.9	1.79	1.59	1.58	1.74	1.87	
2020	1.81	1.75	1.63	1.64	1.68	1.81	
2030	1.77	1.74	1.63	1.65	1.69	1.8	
2040	1.75	1.72	1.65	1.65	1.7	1.79	
2050	1.76	1.71	1.68	1.66	1.72	1.78	
2060	1.74	1.69	1.68	1.62	1.7	1.77	
2070	1.73	1.68	1.68	1.62	1.68	1.77	
2080	1.72	1.67	1.68	1.62	1.67	1.76	
2090	1.7	1.66	1.69	1.61	1.66	1.76	
2100	1.7	1.65	1.69	1.6	1.64	1.75	

Table D.1: Firm requirement values for the different WITCH regions. It represents the peak load to be supplied as a multiple of the annual average load (equation 4.1). Values derived from [37] and then adapted to WITCH.

VRE SHARE BC	Short-Term Curtailment [% VRE Generation BC]						
	cajaz	china	easia	india	kosau	laca	mena
30%	6.0%	3.0%	3.0%	6.9%	6.0%	3.7%	1.9%
50%	10.0%	5.1%	5.1%	11.5%	10.0%	6.2%	3.1%
100%	20.0%	10.1%	10.1%	23.1%	20.0%	12.4%	6.2%
VRE SHARE BC	neweuro	oldeuro	sasia	ssa	te	usa	
	cajaz	china	easia	india	kosau	laca	mena
30%	3.4%	3.0%	6.9%	2.1%	3.0%	3.4%	
50%	5.6%	5.0%	11.5%	3.5%	5.0%	5.7%	
100%	11.2%	9.9%	23.1%	6.9%	10.0%	11.4%	
VRE SHARE BC	Seasonal Curtailment [% VRE Generation BC]						
	cajaz	china	easia	india	kosau	laca	mena
30%	2.8%	1.5%	1.5%	3.3%	2.8%	1.9%	1.0%
50%	4.7%	2.6%	2.5%	5.5%	4.7%	3.1%	1.7%
100%	9.3%	5.2%	5.0%	11.0%	9.3%	6.2%	3.3%
VRE SHARE BC	neweuro	oldeuro	sasia	ssa	te	usa	
	cajaz	china	easia	india	kosau	laca	mena
30%	1.7%	1.5%	3.3%	1.1%	1.5%	1.6%	
50%	2.9%	2.5%	5.5%	1.8%	2.6%	2.7%	
100%	5.8%	5.1%	11.0%	3.6%	5.1%	5.4%	

Table D.2: Short-term and seasonal curtailment values in WITCH as percentage of VRE generation before curtailment for the 13 WITCH regions

VRE share BC	Marginal VRE Flexibility Coefficient						
	cajaz	china	easia	india	kosau	laca	mena
0 - 15%	-0.35	-0.21	-0.21	-0.65	-0.35	-0.24	0.07
15 - 50%	-0.67	-0.53	-0.49	-0.86	-0.67	-0.48	-0.14 ^a
>50%	0.36	0.31	0.3	0.22	0.36	0.33	0.24 ^a
VRE share BC	neweuro	oldeuro	sasia	ssa	te	usa	
	cajaz	china	easia	india	kosau	laca	mena
0 - 15%	0.06	0.16	-0.65	0.05	0.14	-0.03	
15 - 50%	-0.48	-0.39 ^a	-0.86	-0.29 ^a	-0.35 ^a	-0.39	
>50%	0.33	0.29 ^a	0.22	0.25 ^a	0.28 ^a	0.29	

^a Second deployment bin is 15-60% and third bin is >60%.

Table D.3: Marginal Flexibility Coefficients of VRE technologies for different ranges of VRE shares before curtailment, derived from [37] and adapted to WITCH regions

Polynom coefficient	3rd Degree Polynom: $y = a * X^3 + b * X^2 + c * X + d$						
	cajaz	china	easia	india	kosau	laca	mena
a	-0.369	-0.369	-0.323	-0.242	-0.369	-0.277	-0.242
b	1.056	1.056	0.924	0.693	1.056	0.792	0.693
c	-0.968	-0.968	-0.847	-0.635	-0.968	-0.726	-0.635
d	-0.289	-0.149	-0.157	-0.610	-0.289	-0.194	0.110
	neweuro	oldeuro	sasia	ssa	te	usa	
a	-0.623	-0.635	-0.242	-0.392	-0.565	-0.415	
b	1.783	1.816	0.693	1.122	1.618	1.188	
c	-1.633	-1.664	-0.635	-1.028	-1.482	-1.089	
d	0.163	0.265	-0.610	0.115	0.233	0.039	

Table D.4: Coefficients of the 3rd degree polynomial curves representing the flexibility coefficients of the VRE technologies alone for the different WITCH regions.

Polynom coefficient	2nd Degree Polynom: $y = a * X^2$						
	cajaz	china	easia	india	kosau	laca	mena
a	0.467	0.372	0.353	0.509	0.467	0.369	0.111
	neweuro	oldeuro	sasia	ssa	te	usa	
a	0.322	0.171	0.509	0.151	0.162	0.285	

Table D.5: Coefficients of the 2nd degree polynomial curves representing the grid pooling coefficients for the different WITCH regions

Polynom coefficient	3rd Degree Polynom: $y = a * X^3 + b * X^2 + c * X + d$						
	cajaz	china	easia	india	kosau	laca	mena
a	-0.369	-0.369	-0.323	-0.242	-0.369	-0.277	-0.242
b	1.523	1.428	1.277	1.203	1.523	1.161	0.804
c	-0.968	-0.968	-0.847	-0.635	-0.968	-0.726	-0.635
d	-0.289	-0.149	-0.157	-0.610	-0.289	-0.194	0.110
	neweuro	oldeuro	sasia	ssa	te	usa	
a	-0.623	-0.635	-0.242	-0.392	-0.565	-0.415	
b	2.104	1.987	1.203	1.274	1.779	1.473	
c	-1.633	-1.664	-0.635	-1.028	-1.482	-1.089	
d	0.163	0.265	-0.610	0.115	0.233	0.039	

Table D.6: Coefficients of the 3rd degree polynomial curves representing the overall flexibility coefficients of the VRE technologies, including the effect of grid pooling

Appendix E

Datasheets

	Initial PHES Installed Capacity [GW]		
	2005	2010	2015
cajaz	25.7	25.8	27.1
china	11.5	17.9	23
easia	1.8	1.8	1.7
india	4.1	4.8	4.8
kosau	6.7	6.7	7.5
laca	1	1	1
mena	0.7	0.7	1.7
neweuro	5.9	6.2	6.5
oldeuro	41.2	42.3	44.2
sasia	0.1	0.1	0.1
ssa	0.1	0.1	0.1
te	2.6	3.1	3.4
usa	21.9	30.8	31.2

Table E.1: PHES Initial installed capacity. Data gathered at national level from IRENA Renewable Energy Statistics [73] and then aggregated at regional level for the implementation in WITCH.

	PHES Full Production Hours [h/yr]		
	min	mid	max
cajaz	409.2	457.2	519.5
china	533.6	682.5	820.0
easia	369.6	659.2	1024.6
india	1034.1	1043.8	1121.9
kosau	849.5	1060.9	1252.9
laca	552.4	678.6	838.8
mena	286.6	637.7	956.9
neweuro	440.5	666.4	896.8
oldeuro	584.3	808.5	1117.3
sasia	1034.1	1043.8	1121.9
ssa	286.6	637.7	956.9
te	672.9	1202.8	1758.9
usa	621.3	830.7	1184.6

Table E.2: PHES full production hours. Data for the installed capacity and annual generation gathered at national level from IRENA Renewable Energy Statistics [73] and then averaged at regional level for the implementation in WITCH. For each region the annual minimum, average and maximum values (between 2005 and 2015) of PHES full production hours have been selected to perform a sensitivity analysis.

	Initial 2015 Installed Capacity [MW]	
	CAES	Li-B
cajaz	1	119
china	0	45
easia	0	50
india	0	0
kosau	0	396
laca	0	59
mena	0	0
neweuro	0	0
oldeuro	853	205
sasia	0	0
ssa	0	1
te	0	3
usa	440	562

Table E.3: CAES and Li-B initial installed capacity in 2015. Data gathered at national level from **insereire reference** and then aggregated at regional level for the implementation in WITCH.

Appendix F

GAMS code

Due to space limits, it has not been possible to report here the full GAMS code we introduced in WITCH. The modules on which we intervened are: *mod grid*, *mod storage*, *mod storage seasonal*, that we have written from scratch, and *core energy*, *core economy*, *mod systint*, already present in the module, to which we added the features described in Section 4.4.3. We have written approximately 1900 new lines of WITCH code.

These WITCH modules are available at this link:

https://www.dropbox.com/sh/o5m2g8rj5ailo2s/AAC6W3A9nWE_V0V14CqQpZQsa?dl=0

All the data analyses have been performed with the help of R and Excel software.

Bibliography

1. Crowley, T. J. Causes of climate change over the past 1000 years. *Science* **289**, 270–277 (2000).
2. IPCC. *Climate Change 2014: Synthesis Report. Contribution of Working Groups I, II and III to the Fifth Assessment Report of the Intergovernmental Panel on Climate Change*. tech. rep. (2014).
3. Clarke, L. & Kejun, J. IPCC WG3 Ch6: assessing transformation pathways. *Climate Change 2014: Mitigation of Climate Change* (2014).
4. Rogelj, J. *et al.* Paris Agreement climate proposals need a boost to keep warming well below 2 C. *Nature* **534**, 631–639 (2016).
5. Stern, N. *The Stern Review on the Economic Effects of Climate Change*. tech. rep. (2006).
6. Krey, V. & Clarke, L. Role of renewable energy in climate mitigation: a synthesis of recent scenarios. *Climate Policy* **11**, 1–28 (2011).
7. Luderer, G. *et al.* The economics of decarbonizing the energy system: results and insights from the RECIPE model intercomparison. *Climate Change* **114**(1), 9–37 (Sept. 2012).
8. Krey, V., Luderer, G., Clarke, L. & Kriegler, E. Getting from here to there — energy technology transformation pathways in the EMF27 scenarios. *Climate Change* **123**, 369–382 (Oct. 2014).
9. Ueckerdt, F., Brecha, R. & Luderer, G. Analyzing major challenges of wind and solar variability in power systems. *Renewable Energy* **81**, 1–10 (Sept. 2015).
10. Hirth, L., Ueckerdt, F. & Edenhofer, O. Integration costs revisited – An economic framework for wind and solar variability. *Renewable Energy* **74**, 925–939 (Feb. 2015).
11. Terna. *RAPPORTO PUBBLICO DELLA SPERIMENTAZIONE – PROGETTI STORAGE ENERGY INTENSIVE* tech. rep. (Apr. 2017).
12. Mohd, A., Ortjohann, E., Schmelter, A., Hamsic, N. & Morton, D. *Challenges in integrating distributed energy storage systems into future smart grid in Industrial Electronics, 2008. ISIE 2008. IEEE International Symposium on* (2008), 1627–1632.
13. IEA. *Energy Technology System Analysis Programme (ETSAP). Technology Brief E12* tech. rep. (2014).
14. Massachusetts Institute of Technology (MIT). *The Future of Electric Grid: a multidisciplinary study* tech. rep. (2011).
15. IEA. *Technology Roadmap: Smart Grids* tech. rep. (2011).

16. IEA-ETSAP. *Renewable Energy Integration in Power Grids. Technology Brief E15* tech. rep. (2013).
17. Pietzcker, R. C. *et al.* System Integration of Wind and Solar Power in Integrated Assessment Models: A Cross-Model Evaluation of New Approaches. *Energy Economics* **64**, 583–599 (May 2016).
18. McKinsey & Company. *Battery storage: The next disruptive technology in the power sector - Report* tech. rep. (June 2017).
19. Denholm, P., Ela, E., Kirby, B. & Milligan, M. *Role of Energy Storage with Renewable Electricity Generation* tech. rep. (DOE - NREL, Jan. 2010).
20. IEA. *Technology Roadmap: Energy Storage* tech. rep. (Jan. 2014).
21. IRENA. *Renewables and electricity storage: A technology roadmap for REmap 2030* (June 2015).
22. 32 Companies and organisations supported by the European Commission. *COMMERCIALISATION OF ENERGY STORAGE IN EUROPE. A fact-based analysis of the implications of projected and development of the European electric power system and towards 2030 and beyond for the role and commercial and viability of energy storage.* 2015.
23. Akinyele, D. & Rayudu, R. Review of energy storage technologies for sustainable power networks. *Sustainable Energy Technologies and Assessments* **8**, 74–91 (2014).
24. Després, J. *Modelling the long-term deployment of electricity storage in the global energy system* Thesis (Université Grenoble Alpes, Sept. 2015).
25. Fondazione ENI Enrico Mattei. *WITCH Model* <http://www.witchmodel.org/model/>.
26. CIESIN. *Thematic Guide to Integrated Assessment Modeling of Climate Change* <http://sedac.ciesin.columbia.edu/mva/iamcc.tg/mva-questions.html>. 1995.
27. Edmonds, J. *et al.* Integrated Assessment of Climate Change: An Overview and Comparison of Approaches and Results. *Climate Change 1995 - Social and Economic Dimensions of Climate Change*. 366–392 (Jan. 1996).
28. IPCC. *IPCC Working Group III: Mitigation. Top-Down and Bottom-Up Models* <http://www.ipcc.ch/ipccreports/tar/wg3/index.php?idp=310>.
29. Bosetti, V., Massetti, E. & Tavoni, M. The WITCH Model. Structure, Baseline, Solutions. *Nota di Lavoro, Fondazione Eni Enrico Mattei* **10.2007** (2007).
30. Arrow, K. J., Chenery, H., Minhas, B. S. & Solow, R. M. Capital-labor substitution and economic efficiency. *The Review of Economics and Statistics*, 225–250 (1961).
31. Henningsen, A. & Henningsen, G. Econometric Estimation of the "Constant Elasticity of Substitution" Function in R: Package micEconCES (2011).
32. Ueckerdt, F. *et al.* Representing power sector variability and the integration of variable renewables in long-term energy-economy models using residual load duration curves. *Energy* **90**, 1799–1814 (Oct. 2015).
33. Després, J. *et al.* Storage as a flexibility option in power systems with high shares of variable renewable energy sources: a POLES-based analysis. *Energy Economics* **64**, 638–650 (2017).

34. Ueckerdt, F. *et al.* Decarbonizing Global Power Supply under Region-Specific Consideration of Challenges and Options of Integrating Variable Renewables in the REMIND Model. *Energy Economics* **64**, 665–684 (May 2017).
35. Sullivan, P., Krey, V. & Riahi, K. Impacts of considering electric sector variability and reliability in the MESSAGE model. *Energy Strategy Reviews* **1**, 157–163 (2013).
36. Carrara, S. & Marangoni, G. Including System Integration of Variable Renewable Energies in a Constant Elasticity of Substitution Framework: The Case of the WITCH Model. *Energy Economics* **64**, 612–626 (May 2017).
37. Johnson, N. *et al.* A reduced-form approach for representing the impacts of wind and solar PV deployment on the structure and operation of the electricity system. *Energy Economics* **64**, 651–664 (2017).
38. European Commission. *EU Research Funding 2007-2013: 7th Framework Programme* https://ec.europa.eu/research/fp7/index_en.cfm.
39. Sioshansi, R. & Short, W. Evaluating the impacts of real-time pricing on the usage of wind generation. *Power Systems, IEEE Transactions* **24**, 516–524 (2009).
40. Luderer, G. *et al.* *Description of the REMIND model* Nov. 2015.
41. Siemens. *Connecting Possibilities - Scenarios for Optimizing Energy Systems* tech. rep. Accessed: 2017-09-16 (2013).
42. Eurelectric. *Power Distribution in Europe - Facts & Figures* tech. rep. Accessed: 2017-09-16 (2013).
43. Cigre. *The Electric Power System - Russian Federation* tech. rep. Accessed: 2017-09-17 (2015).
44. IEA. *IEA Statistics* <https://www.iea.org/statistics>. Accessed: 2017-11-10.
45. ACER. *Electricity Infrastructure - Report on unit investment cost indicators and corresponding reference values for electricity and gas infrastructure* Aug. 2015.
46. Terna. *La Rete di Trasmissione Nazionale (RTN) - Consistenza impianti* tech. rep. Accessed: 2017-09-15 (2014). <http://integrated.terna-reports.it/2013/it/overview/business-gestione-capitali/consistenza-impianti-rete-nazionale#start>.
47. Energy Sector Management Assistance Program (ESMAP). *Sub-Saharan Africa: Introducing Low-cost Methods in Electricity Distribution Networks* tech. rep. (Oct. 2006).
48. World Bank. *World Bank DataBank: Electric power transmission and distribution losses (% of output)* <https://data.worldbank.org/indicator/EG.ELC.LOSS.ZS>.
49. Converse, A. O. Seasonal Energy Storage in a Renewable Energy System. *Proceedings of the IEEE* **100** (2012).
50. Quanta Technology. *Electric energy storage systems* tech. rep. (2013), 1–12.
51. Bollen, M. H. J. *Understanding Power Quality Problems-Voltage Sags and Interruptions*. *IEEE Press, New York* (2001).
52. Ding, Y. *et al.* Liquid air energy storage. *Storing Energy: with Special Reference to Renewable Energy Sources*, 167 (2016).

53. Yang, H., Bang, H., Amine, K. & Prakash, J. Investigations of the exothermic reactions of natural graphite anode for Li-ion batteries during thermal runaway. *Journal of the Electrochemical Society* **152**, A73–A79 (2005).
54. Stanford Chidsey Lab. *Anode Passivation in Li-ion batteries* <https://chidseylab.stanford.edu/anode-passivation-lithium-ion-batteries>.
55. Alotto, P., Guarnieri, M. & Moro, F. Redox flow batteries for the storage of renewable energy: A review. *Renewable and Sustainable Energy Reviews* **29**, 325–335 (2014).
56. Budt, M., Wolf, D., Span, R. & Yan, J. A review on compressed air energy storage: Basic principles, past milestones and recent developments. *Applied Energy* **170**, 250–268 (2016).
57. Mattick, W., Haddenhorst, H. G., Weber, O. & Stys, Z. S. *Proceedings American Power Conference (United States)* in. **37** (1975).
58. Pollak, R. *History of first U.S. Compressed Air Energy Storage (CAES) plant (110MW 26h); volume 2: Construction; Palo Alto* tech. rep. (1994).
59. Wolf, D. *Methods for Design and Application of Adiabatic Compressed Air Energy: Storage Based on Dynamic Modeling* (Laufen, 2011).
60. Freund S. Schainker R., M. R. *Commercial concepts for adiabatic compressed air energy storage in 7th Renewable Energy Storage Conference. Berlin, Germany: Eurosolar* (2012).
61. Lemoufuet-Gatsi, S. Investigation and optimisation of hybrid electricity storage systems based on compressed air and supercapacitors (2006).
62. Qin, C. & Loth, E. Liquid piston compression efficiency with droplet heat transfer. *Applied Energy* **114**, 539–550 (2014).
63. Yamashita, Y. & Takano, K. *Practical tests for a New Urban CAES Tank. Report of Obayashi Corporation* tech. rep. (July 1998), 55–57.
64. Deane, J. P., Gallachóir, B. & McKeogh, E. Techno-economic review of existing and new pumped hydro energy storage plant. *Renewable and Sustainable Energy Reviews* **14**, 1293–1302 (2010).
65. Rehman, S., Al-Hadhrami, L. & Alam, M. M. Pumped hydro energy storage system: A technological review. *Renewable and Sustainable Energy Reviews* **44**, 586–598 (2015).
66. Fujihara, T., Imano, H. & Oshima, K. Development of pump turbine for seawater pumped-storage power plant. *Hitachi Review* **47**, 199–202 (1998).
67. Electricity Storage Association. *Variable speed pumped hydroelectric storage*. tech. rep. (2014).
68. Klumpp, F. Comparison of pumped hydro, hydrogen storage and compressed air energy storage for integrating high shares of renewable energies—potential, cost-comparison and ranking. *Journal of Energy Storage* **8**, 119–128 (2016).
69. Chen, H. *et al.* Progress in electrical energy storage system: A critical review. *Progress in Natural Science* **19**, 291–312 (2009).
70. The Guardian. *Tesla to build World's biggest lithium ion battery in South Australia* <https://www.theguardian.com/australia-news/2017/jul/07/tesla-to-build-worlds-biggest-lithium-ion-battery-in-south-australia>. July 2017.

71. Pickard, W. F., Shen, A. Q. & Hansing, N. J. Parking the power: Strategies and physical limitations for bulk energy storage in supply–demand matching on a grid whose input power is provided by intermittent sources. *Renewable and Sustainable Energy Reviews* **13**, 1934–1945 (2009).
72. European Commission. *Declaration of Intent: "Become competitive in the global battery sector to drive e-mobility forward"*. European Commission, SET-Plan ACTION n 7 tech. rep. (July 2016).
73. IRENA. *Renewable Energy Statistics 2017* (2017).
74. U.S. Department of Energy. *DOE Global Energy Storage Database - website* http://www.energystorageexchange.org/projects/data_visualization. Accessed: 2017-07-15. 2017.
75. Zakeri, B. & Syri, S. Electrical energy storage systems: A comparative life cycle cost analysis. *Renewable and Sustainable Energy Reviews* **42**, 569–596 (2015).
76. Wang, J. *et al.* Degradation of lithium ion batteries employing graphite negatives and nickel–cobalt–manganese oxide+ spinel manganese oxide positives: Part 1, aging mechanisms and life estimation. *Journal of Power Sources* **269**, 937–948 (2014).
77. Schmidt, O., Hawkes, A., Gambhir, A. & Staffell, I. The future cost of electrical energy storage based on experience rates. *Nature Energy* **2**, nenergy2017110 (2017).
78. McDonald, A. & Schrattenholzer, L. Learning rates for energy technologies. *Energy policy* **29**, 255–261 (2001).
79. Kittner, N., Lill, F. & Kammen, D. M. Energy storage deployment and innovation for the clean energy transition. *Nature Energy* **2**, nenergy2017125 (2017).
80. CEDIGAZ. *The Underground Gas Storage & LNG Storage Market in the World* <http://www.cedigaz.org/documents/2016/UGS%202016/Leaflet.pdf>. 2016.
81. EIA. *Underground Natural Gas Storage Capacity* https://www.eia.gov/dnav/ng/ng_stor_cap_dcu_nus_a.htm.
82. IEA. *Technology Roadmap: Hydropower* tech. rep. (2012).
83. Converse, A. O. The impact of large-scale energy storage requirements on the choice between electricity and hydrogen as the major energy carrier in a non-fossil renewables–only scenario. *Energy Policy* **34**, 3374–3376 (2006).
84. IEA. *Technology Roadmap: Hydrogen and Fuel Cells* tech. rep. (2015).
85. U.S. Department of Energy. *Fuel Cell Technologies Office Multi-Year Research, Development, and Demonstration (MYRD&D) Plan* tech. rep. (2016), 25–27.
86. Barbir, F. PEM electrolysis for production of hydrogen from renewable energy sources. *Solar energy* **78**, 661–669 (2005).
87. ENEA Consulting. *The potential of Power-to-gas. Technology review* tech. rep. (Jan. 2016).
88. Phillips, R. & Dunnill, C. W. Zero gap alkaline electrolysis cell design for renewable energy storage as hydrogen gas. *RSC Advances* **6**, 100643–100651 (2016).
89. Casalegno, S. *Notes from the course Master "Electrochemical Energy Conversion and Storage" - Lesson 11: Electrolyser Technology* 2017.

90. Carmo, M., Fritz, D. L., Mergel, J. & Stolten, D. A comprehensive review on PEM water electrolysis. *International journal of hydrogen energy* **38**, 4901–4934 (2013).
91. Ebbesen, S. D., Knibbe, R. & Mogensen, M. Co-electrolysis of steam and carbon dioxide in solid oxide cells. *Journal of The Electrochemical Society* **159**, F482–F489 (2012).
92. Ferrero, D., Lanzini, A., Leone, P. & Santarelli, M. Reversible operation of solid oxide cells under electrolysis and fuel cell modes: Experimental study and model validation. *Chemical Engineering Journal* **274**, 143–155 (2015).
93. Götz, M. *et al.* Renewable Power-to-Gas: A technological and economic review. *Renewable Energy* **85**, 1371–1390 (2016).
94. E4Tech. *The Fuel Cell Industry Review 2016* tech. rep. (2016), 28–29.
95. Burlatsky, S. F., Atrazhev, V., Cipollini, N., Condit, D. & Erikhman, N. Aspects of PEMFC degradation. *ECS Transactions* **1**, 239–246 (2006).
96. Campanari, S. *Notes from the course Master "Electrochemical Energy Conversion and Storage" - Lesson 16: High temperature fuelcells–MCFC, SOFC and SOEC* 2017.
97. Koh, J., Yoo, Y., Park, J. & Lim, H. C. Carbon deposition and cell performance of Ni-YSZ anode support SOFC with methane fuel. *Solid State Ionics* **149**, 157–166 (2002).
98. Ni, M., Leung, M. K. & Leung, D. Y. Technological development of hydrogen production by solid oxide electrolyzer cell (SOEC). *International Journal of Hydrogen Energy* **33**, 2337–2354 (2008).
99. Heinen, S., Elzinga, D., Kim, S.-K. & Ikeda, Y. Impact of Smart Grid Technologies on Peak Load to 2050 (Jan. 2011).
100. Denholm, P. & Hand, M. Grid flexibility and storage required to achieve very high penetration of variable renewable electricity. *Energy Policy* **39**, 1817–1830 (2011).
101. Yasuda, Y. *et al.* *International comparison of wind and solar curtailment ratio* in (Energynautics, 2015).
102. Kumar, N., Besuner, P., Lefton, S., Agan, D. & Hilleman, D. *Power Plant Cycling Costs* tech. rep. (USDOE Office of Electricity Delivery and Energy Reliability, July 2012).
103. Debra, L. *et al.* *The Western Wind and Solar Integration Study Phase 2* tech. rep. (USDOE Office of Energy Efficiency and Renewable Energy (EERE), Wind Program (EE-4W) (Wind Program Corporate), Sept. 2013).
104. Korpaas, M., Holen, A. & Hildrum, R. Operation and sizing of energy storage for wind power plants in a market system. *International Journal of Electrical Power & Energy Systems* **25**, 599–606 (2003).
105. Neetzow, P., Pechan, A. & Eisenack, K. *Interdependence of electricity storage and transmission capacities* in *Working Paper for EAERE annual conference 2017* (May 2017).
106. Denholm, P. & Sioshansi, R. The value of compressed air energy storage with wind in transmission-constrained electric power systems. *Energy Policy* **37**, 3149–3158 (2009).
107. Renewable & Appropriate Energy Laboratory UC Berkeley. *SWITCH — A capacity expansion model for the electricity sector* <https://rael.berkeley.edu/project/switch/>.

108. He, G. *et al.* SWITCH-China: A Systems Approach to Decarbonizing China's Power System. *Environmental science & technology* **50**, 5467 (July 2016).
109. Power Engineering International. *Unlocking China's gas turbine potential* <http://www.powerengineeringint.com/articles/print/volume-23/issue-4/features/opinion-china-turbine-market/unlocking-china-s-gas-potential.html>. Accessed: 2017-11-10. 2015.